The development of an efficient tyre testing procedure to gather data for the parameterisation of Magic Formula 6.1 tyre models

Smith, Gregory

Award date:
2018

Awarding institution:
Coventry University

The development of an efficient tyre testing procedure to gather data for the parameterisation of Magic Formula 6.1 tyre models

Gregory Smith

PhD

January 2018

The development of an efficient tyre testing procedure to gather data for the parameterisation of Magic Formula 6.1 tyre models

Gregory Smith

PhD

January 2018

A thesis submitted in partial fulfilment of the University's requirements for the Degree of Doctor of Philosophy

Abstract

This thesis describes an efficient tyre test procedure that can be used by automotive manufacturers to gather the data required to parameterise empirical tyre models used in the computer simulation of vehicle dynamics. The new test procedure builds on established methodologies developed as alternatives to traditional Square Matrix testing. The new process is designed to reduce the duration of expensive tyre tests without compromising the accuracy of the generated tyre model parameters.

The process is demonstrated by a programme of tyre testing carried out using major tyre testing facilities in the United Stated of America. Testing has been carried out at using the Calspan TIRF (TIre Research Facility) tyre testing rig in Buffalo, NY; as well as the SoVaMotion flat-trac facility in Alton, VA. It is shown here how the new test procedure can be used more efficiently to parameterise all components for the well-known Magic Formula tyre model, for load cases including free-rolling, longitudinal and combined slip conditions; as well as inflation pressure interpolation for both steady state and transient manoeuvres. This is achieved using a 'cruise' type procedure which is more representative of the loading conditions exerted on the tyre whilst driving a real vehicle. During the test, an innovative new sweep shape is used to minimise both mechanical hysteresis and temperature variation during each test sweep, while an automated logic approach is used to manage the tyre temperature throughout the procedures. Graph Sweeps are introduced at the start and end of the test, allowing a judgement to be made as to the influence of tyre wear on data obtained throughout the test. Finally, the new test procedure is compared with the more traditional Square Matrix style of testing and a 73% reduction in overall test duration is demonstrated.

The development of accurate and representative tyre models remains a significant challenge as vehicle manufacturers target increased use of virtual prototypes and simulation. The presented work contributes to this by improving the efficiency of the expensive tyre testing required to parameterise the models. This has been achieved through the introduction of a novel tyre test process that has been developed and proven during this study.

Acknowledgements

The author would like to thank the following:

Jaguar Land Rover Limited, Whitley, UK; for funding the research and facilitating the technical development; particularly Mateo Happyrock for providing on-site technical support and practical ideas.

Prof. Mike Blundell, Coventry University, Coventry, UK; for supporting the project with both administrative and practical advice as well as on-site technical support at test facilities.

Henning Olsson, Calspan Corporation, Buffalo, NY; for general technical assistance and advice on how to get the best from the Calspan rig and use it in the most efficient way.

Mrs. H.H. Bunni-Smith, for helping with, proof reading and general support.

Finally, Miss Maddelyn Stapleton-Smith and Miss Matilda Stapleton-Smith for being awesome!

Author's Publications

Smith, G. and Blundell, M. (2016). A new efficient free-rolling tyre-testing procedure for the parameterisation of vehicle dynamics tyre models. Proceedings of the Institution of Mechanical Engineers, Part D: Journal of Automobile Engineering, Vol 231, Issue 10. pp.1435–1448.

Smith, G. (2014) Advanced tire CAE. Tire Technology International 2014 Annual Showcase, pp.48.

Smith, G. (2015 - Current). Regular Column: Gregory Smith. Tire Technology International.

Smith, G. (2016). GS2MF - An innovative and highly efficient flat trac test procedure to gather data for the parameterisation of MF-Tyre 6.1 tyre models. In: Tire Technology Expo 2016. Cologne, Germany. (Winner, Tire Tech International 2016 Young Scientist Award)

Author's Patents

Smith, G. and Olsson, H. (2015). Adjusting a tyre vertical load based on its slip angle such as the simulate the weight shift of a physical vehicle. GB1519907.8

Smith, G., Olsson, H. and Gladstone, M. (2015). Varying the slip angle or slip ratio rate of change so as to minimise both mechanical and thermal hysteresis during tyre testing. GB1519909.4

Smith, G. and Olsson, H. (2015). Increasing tyre load at high slip angles in order to test a tyre under extreme loading conditions while minimising tyre wear. GB1519912.8

Smith, G., Olsson, H. and Gladstone, M. (2015). The use and inclusion of identical comparison test sweeps to judge the change in tyre performance as a result of testing. GB1519913.6

Table of Contents

Lists of Figures, Tables and Equations

The referencing of figures, tables and equations includes the chapter number within the naming convention. The chapter number is included first, then a hyphen, followed by a letter corresponding to the particular figure within the given chapter. For example, within chapter 2.1.4 on friction there are two different figures, these are 2.1.4-A and 2.1.4-B.
The only exception to this are figures preceding the introduction, these are labelled 1, 2, 3 etcetera accordingly.

List of Figures

Figure 2.2.2-D. Schematic combined with a photograph showing the layout and internal test surface (in this case covered with snow) of the Karlsruhe internal drum rig. (Greßler, Gauterin, Hartmann and Wies, 2007)

Figure 2.2.2-E. One quarter of the track at the Camber Ridge facility Charlotte, NY. (Camber Ridge, 2017)

Figure 2.2.2-F. Camber Ridge Genesis Machine Charlotte, NY. (Camber Ridge, 2017)

Figure 2.2.2-G. Comparison of longitudinal force measurements from the sand paper surface of the Calspan rig (Y axis, labelled CFx) with exactly equivalent measurements (identical load case and test procedure) from the paved road surface used with the UMTRI rig (X Axis, labelled UFx). (M'gineering History of Tire Characterizing, 2016)

Figure 2.2.3-A. Calspan rig, Buffalo NY, photographed circa 1973. (original source unknown, photograph provided by M'gineering LLC, Akron OH, 2017)

Figure 2.2.3-B. Calspan rig, Buffalo, NY, photographed in 2016. (Photograph provided by Calspan Cooperation, Buffalo, NY 2017)

Figure 2.2.3-C. MTS 'Flat-Trac 1', photographed in 1980. (original source unknown, photograph provided by M'gineering LLC, Akron OH, 2017)

Figure 2.2.3-D. Rendered CAD drawing of the MTS Flat-Trac LTRe rig. (GM Corporate Newsroom, 2012).

Figure 3.2.1-A. Data Comparison of Calspan Un-Coupled, Calspan Coupled and SoVaMotion Coupled, for Overturning Moment, MXW (Nm) versus Slip Angle, SLIPANGL (°).

Figure 3.4-A. Tyre tread temperature, TRDTEMPC (°C) versus Runtime, RUNTIME (s). Repeated Graph Sweeps without a warmup, also showing the 45°C baseline temperature.

Figure 3.4-B. Warmup profiles when using a single and double block of warmup sweeps, also shows the baseline temperature.

Figure 3.4-C. Comparison between sweeps immediately after the warmup with sweep further along the test procedure.

Figure 3.5-A. Tyre temperature during a full test and the thermal logic regulated baseline temperature which is active between 2,450 and 6,000s.

Figure 3.6.1-A. 'FreeRolling' sweeps at 10 and 4°/s.

Figure 3.6.1-B. Lateral force versus slip angle coloured by runtime for a constant rate free rolling sweep conducted at 30°/s.

Figure 3.6.1-C. Sketch showing the typical shape of a thermal hysteresis loop when the tyre begins the sweep close to its optimal temperature and overheats as a result of the test.

Figure 3.6.1-D. Sketch showing the typical shape of a thermal hysteresis loop when the tyre begins the sweep at a cool temperature and warms towards its optimal temperature as a result of the testing.

Figure 3.6.1-E. Comparison between a constant rate sweep and variable rate sweep.

Figure 3.6.2-A. Lateral force versus slip angle for the five identical sweeps tested repeatedly throughout the test procedure.

Figure 3.6.2-B. Comparison of constant rate sweeps close to zero slip angle.

Figure 3.6.2-C. Tyre outer surface temperature versus runtime for the free rolling constant rate sweeps.

Figure 3.6.2-D. Accumulative sliding energy (AcSldEny) versus runtime for each of the 'FreeRolling' constant rate sweeps.

Figure 3.6.2-E. Correlation between peak temperatures during each sweep compared to the total sliding energy.

Figure 3.6.2-F. Lateral force versus slip angle for free rolling variable rate sweeps set to different 'high rates'.

Figure 3.6.2-G. Relaxation length versus slip angle for a tyre at three different vertical loads. (Rill, 2006)

Figure 3.6.2-H. Tyre tread surface temperature versus time for free rolling variable rate sweeps using different 'high rates'.

Figure 3.6.2-I. Lateral force versus slip angle close to zero for free rolling variable rate sweeps each set to a different 'low rate' ranging from 2 to 8°/s.

Figure 3.6.2-J. Lateral force versus slip angle comparing different 'thresholds' used in free rolling variable rate sweeps.

Figure 3.6.2-K. Longitudinal force versus slip ratio for the five identical sweeps tested repeatedly throughout the test procedure.

Figure 3.6.2-L. Longitudinal Force FX (N) versus slip ratio LONGSLIP (-) for 'BrkDrv' constant rate sweeps at different slip rates, zoomed into slip stiffness section.

Figure 3.6.2-M. Longitudinal Force FX (N) versus slip ratio LONGSLIP (-) for 'BrkDrv' constant rate sweeps at different slip rates.

Figure 3.6.2-N. 'TRDTEMP3' (tyre outer surface central tread temperature) versus runtime for the 'BrkDrv' constant rate sweeps.

Figure 3.6.2-O. Longitudinal force versus longitudinal slip for 'BrkDrv' variable rate sweeps set to different 'high rates'.

Figure 3.6.2-P. Tyre tread surface temperature versus time for 'BrkDrv' variable rate sweeps using different 'high rates'.

Figure 3.6.2-Q. Longitudinal force versus slip ratio close to zero for 'BrkDrv' variable rate sweeps each set to a different 'low rate'.

Figure 3.6.2-R. Longitudinal force versus slip ratio comparing different 'thresholds' used in 'BrkDrv' variable rate sweeps.

Figure 3.6.2-S. Longitudinal slip versus zeroed runtime (all sweeps starting from 0s) for 'BrkDrv' sweeps at different 'thresholds'.

Figure 3.6.2-T. Lateral force versus slip angle for the fastest and slowest free rolling constant rate sweeps, along with the variable rate sweep at a reduced slip angle range of -5 to +5°.

Figure 3.6.2-U. Lateral force versus slip angle for the fastest and slowest free rolling constant rate sweeps, along with the variable rate sweep.

Figure 3.6.2-V. Tyre temperature versus time for all free rolling constant rate sweeps compared to the optimised variable rate sweep.

Figure 3.6.2-W. Longitudinal force versus slip ratio for the 'BrkDrv' constant rate sweeps, along with the optimal variable rate sweep and Graph Sweep.

Figure 3.6.2-X. Comparison of the optimised variable rate sweep compared to the nearest two Graph Sweeps within the test sequence.

Figure 3.6.2-Y. Longitudinal force versus slip ratio close to zero for the 'BrkDrv' variable rate sweep compared to the constant rate sweeps.

Figure 3.6.2-Z. Tyre temperature versus time for all 'BrkDrv' constant rate sweeps compared the optimised variable rate sweep.

Figure 3.7-A. Vertical load, FZW (N) versus slip angle, SLIPANGL (°) for the three asymmetric load sweeps covering the typical range of vehicle lateral weight shift conditions.

Table 3.7-B. Two examples where camber is dependent on slip angle and where camber is independent of slip angle.

Figure 3.8-A. Vertical load sweep shape, coloured by sliding power (W).

Figure 3.8-B. Vertical load sweep used to gather data in extreme load case.

Figure 3.9-A. Graph sweeps 1 and 2, shows little change in the tyre's lateral force performance.

Figure 3.9-B. Graph sweeps 1 and 2 show little change in the tyre's radius.

Figure 4.1.3-A. Results from running the heating sweep section of the 'GS2MF FreeRolling' test procedure.

Figure 4.1.5-A. The result from running the first third (one inflation pressure) of the On-Centre and Rolling Radius sweep section of the 'GS2MF FreeRolling' test procedure.

Figure 4.1.6-A. Results from running the first force and moment section of the 'GS2MF FreeRolling' test procedure.

Figure 4.1.7-A. Results from running the second force and moment section of the 'GS2MF FreeRolling' test procedure.

Figure 4.1.9-A. Results from running the Graph Sweep 1 and 2 sections of the 'GS2MF FreeRolling' test procedure.

Figure 4.2-A. Overview of the 'GS2MF BrkDrv' test procedure divided into sections. The initial warmup and the cool down data between each sweep has been removed.

Figure 4.2.3-A. Longitudinal force versus slip ratio for the GS2MF BrkDrv, Pure Long A data section.

Figure 4.2.4-A. Longitudinal force versus slip ratio for the GS2MF BrkDrv, Pure Long B data section.

Figure 4.2.5-A. Comparison between two otherwise identical longitudinal sweeps; one is a pure longitudinal sweep conducted at zero slip angle and the other is a combined sweep conducted at 8.5° of slip angle.

Figure 4.2.5-B. Friction ellipse of two otherwise identical longitudinal sweeps; one is a pure longitudinal sweep conducted at zero slip angle and the other is a combined sweep conducted at 8.5° of slip angle.

Figure 4.2.6-A. A comparison of pure longitudinal camber sensitivity at +/-3° and +/-5° of camber.

Figure 4.2.7-A. Friction ellipse of the tyre under combined testing with and without camber.

Figure 5.1.2-E. Comparison of 'GS2MF BrkDrv' GraphSweep1 and GraphSweep2, for Radius, DSTWOWHC (m) versus Zeroed RUNTIME (s).

Figure 5.1.2-F. Comparison of 'GS2MF BrkDrv' GraphSweep1 and GraphSweep2, for Central Tread Temperature, TRDTEMPC (C) versus Zeroed RUNTIME (s).

Figure 5.1.2-G. Temperature profile of 'GS2MF FreeRolling' data, Central Tread Temperature, TRDTEMPC (C) versus RUNTIME (s) along with the target baseline temperature.

Figure 5.1.2-H. Temperature profile of 'GS2MF BrkDrv' Data, Central Tread Temperature, TRDTEMPC (C) versus RUNTIME (s) along with the target baseline temperature.

Figure 5.1.4-A. Vertical Load, FZW (N) versus Loaded Radius, DSTWOWHC (m); coloured by Inflation Pressure, P. Data is from 'GS2MF FreeRolling' Rolling Radius section divided into separate inflation pressures, linear fits are applied independently to each pressure and extrapolated to FZW = 0 where they converge on the Unloaded Radius of 0.3938m.

Figure 5.2.1-A. Model (Final_v9) and 'FreeRolling' Data (FreeRolling_10Hz) for Lateral Force, FY (kN) versus Slip Angle, SA (°); coloured by Vertical Load, FZ (N).

Figure 5.2.1-B. Model (Final_v9) and 'FreeRolling' Data (FreeRolling_10Hz) for Lateral Force, FY (kN) versus Slip Angle, SA (°); coloured by Camber Angle, IA (°).

Figure 5.2.1-C. Model (Final_v9) and 'FreeRolling' Data (FreeRolling_10Hz) for Lateral Force, FY (N) versus Slip Angle, SA (°); coloured by Inflation Pressure, P (bar).

Figure 5.2.2-A. Model (Final_v9) and 'FreeRolling' Data (FreeRolling_10Hz) for Aligning Torque, MZ (N-mm) versus Slip Angle, SA (°); coloured by Vertical Load, FZ (N).

Figure 5.2.2-B. Model (Final_v9) and 'FreeRolling' Data (FreeRolling_10Hz) for Aligning Torque, MZ (N-mm) versus Slip Angle, SA (°); coloured by Camber Angle, IA (°).

Figure 5.2.2-C. Model (Final_v9) and 'FreeRolling' Data (FreeRolling_10Hz) for Aligning Torque, MZ (N-mm) versus Slip Angle, SA (°); coloured by Inflation Pressure, P (bar).

Figure 5.2.3-A. Model (Final_v9) and 'BrkDrv' Data (BrakeDrive_10Hz) for Longitudinal Force, FX (N) versus Slip Ratio, SR (-); coloured by Vertical Load, FZ (kN).

Figure 5.2.3-B. Model (Final_v9) and 'BrkDrv' Data (BrakeDrive_10Hz) for Longitudinal Force, FX (N) versus Slip Ratio, SR (-); coloured by Inflation Pressure, P (bar).

Figure 5.2.4-A. Model (Final_v9) and 'BrkDrv' Data (BrakeDrive_10Hz) for Longitudinal Force, FX (N) versus Lateral Force, FY (N); coloured by Vertical Load, FZ (kN).

Figure 5.2.4-B. Model (Final_v9) and 'BrkDrv' Data (BrakeDrive_10Hz) for Longitudinal Force, FX (N) versus Lateral Force, FY (N); coloured by Slip Angle, SA (°).

Figure 5.2.5-A. Model (Final_v10) and 'BrkDrv' Data (BrakeDrive_100Hz) for Combined MZ (N-m) versus Slip Ratio, SR (-); coloured by slip angle, SA (°).

Figure 5.2.6-A. Model (Final_v10) and 'BrkDrv' Data (BrakeDrive_100Hz) for Overturning Moment MX (N-m) versus Slip Ratio, SR (-); coloured by Slip Angle, SA (°).

Figure 5.2.6-B. Model (Final_v10) and 'FreeRolling' Data (FreeRolling_10Hz) for Overturning Moment MX (N-m) versus Slip Angle, SA (°); coloured by Vertical Load, FZ (N).

Figure 5.2.8-A. Model (Final_v10) and 'FreeRolling' Data (Radius) for Effective Rolling Radius, Re (mm) versus Vertical Load, FZ (N); coloured by Inflation Pressure, P (bar).

Figure 5.2.9-A. Model (Final_v10) and Static Longitudinal Data (Static Long) for Longitudinal Stiffness, Cx (kN/m) versus Vertical Load, FZ (N); coloured by Inflation Pressure, P (bar).

Figure 5.2.9-B. Model (Final_v10) and StepSteer Data (StepSteer_Cy_63.2perc) for Lateral Stiffness, Cy (kN/m) versus Vertical Load, FZ (N); coloured by Inflation Pressure, P (bar).

Figure 5.3.1-A. Model Comparison of GS2MF Model and SquareMatrix Model, for Lateral Force, FY (N) versus Slip Angle, SA (°); Showing load sensitivity.

Figure 5.3.1-B. Model Comparison of GS2MF Model and SquareMatrix Model, for Lateral Force, FY (N) versus Slip Angle, SA (°); Showing camber sensitivity.

List of Tables

List of Equations

Equation 2.1.3-B. Tyre deflection used in the MF-Tyre 6.1 tyre model.
(TNO Equation Manual, 2010)

Equation 2.1.3-C. Tyre deflection used in the MF-Tyre 6.1 tyre model.
(TNO Equation Manual, 2010)

Equation 2.4.2-A, Magic Formula equation in its general form.
(Bakker, Pacejka and Lidner, 1989)

Equation 3.12.1-A. Time constant equation for an increasing single order system.
(Laptak, 2006)

Equation 5.2.9-A. Longitudinal relaxation length equation. Where σ_x is the longitudinal relaxation length, K_{xk} is the slip stiffness and C_x is the longitudinal stiffness (Besselink, Schmeitz and Pacejka, 2010).

Equation 5.2.9-B. Lateral relaxation length equation. Where σy is the lateral relaxation length, $K_{y\alpha}$ is the cornering stiffness and C_y is the lateral stiffness (Besselink, Schmeitz and Pacejka, 2010).

Nomenclature

TYDEX Standard

Unless otherwise stated all plots within the thesis conform to the channels names, units and axis system defined in the TYDEX (TYre Data EXchange) standard (van Oosten, Unrau, Riedel and Bakker, 1999). This is a very effective and widely used standard for the transfer of tyre test data and tyre models. One characteristic of the standard is the lack of subscripts used in the naming convention (FX rather than F_X). This facilitates the use of the correct name when data is transferred using text files (.txt or .tdx) which do not support the use of subscripts.
In chapter '5.0 GS2MF Fitting' of this thesis, the tyre model fitting software OptimumTire (Developed by OptimumG, Denver, CO) is used, and plots generated by this software are included. OptimumTire uses its own internal channel naming convention and there is no option to overwrite this within the software. Therefore, plots generated using OptimumTire conform to a different (non-TYDEX) convention. Details of relevant channels from the TYDEX convention, as well as their equivalent channels in OptimumTire, along with abbreviations, units and descriptions are shown in Table 1.

Table 1. Details of relevant TYDEX channel names, with equivalent OptimumTire channel names, including abbreviations, units and descriptions (van Oosten, Unrau, Riedel and Bakker, 1999).

In some cases, the letters 'deg' are used as a symbol of degrees of angle or degrees of temperature. This is used when software limitations prohibit the inclusion of the degrees symbol '°' in legends or axis labels.

Deviations from TYDEX Standard

In some cases, relevant data channels are important but are not explicitly specified in the TYDEX standard. This includes tyre temperature, where the TYDEX standard only includes a single channel for tyre tread surface temperature (TRDTEMP); however, additional temperature channels are required such as: central tyre surface temperatures, as well as inside, outside and sidewall temperature channels. The inside and outside channels are named with respect to the flat-trac rig used for the testing, where inside is closest to the drive motor (right side of the tyre when rolling forwards) and outside is furthest away from the drive motor (left side of the tyre when rolling forwards). These additional channels are detailed in Table 2.

Table 2. Additions made to the TYDEX convention to facilitate extra tyre tread surface temperature channels. (van Oosten, Unrau, Riedel and Bakker, 1999)

An additional convention is also employed which facilitates the need to 'zero' the test data. This is where a new data channel is created by subtracting the minimum value within an existing data channel from each value in that same data channel; the new data channel is appended with 'Zeroed ' followed by the original channel name. For example, a zeroed time channel is named 'Zeroed RUNTIME' by appending 'Zeroed ' to the beginning of 'RUNTIME', shown in the Table 3. The purpose of this is to allow different subsections of test data, which occur at different runtimes, to be directly overlaid and compared on the same axis.

Channel Name	Channel Description
Zeroed RUNTIME	Used when the plotted data channel (Zeroed RUNTIME) is equal to the original data channel (RUNTIME) minus the minimum value within the original data channel.

Table 3. Naming convention used when zeroing a data channel.

Axis System

Throughout the thesis, the TYDEX-W axis system is used, as stated in the TYDEX convention. (van Oosten, Unrau, Riedel and Bakker, 1999). This is detailed in Table 4.

(van Oosten, Unrau, Riedel and Bakker, 1999).

The TYDEX-W axis system is visualised in Figure 1, where the contact patch centred axis system can be seen.

Figure 1. Visualisation of the TYDEX-W axis system as stated in the TYDEX Standard. (van Oosten, Unrau, Riedel and Bakker, 1999)

Calculated Channels

Some of the required data channels cannot be directly measured during the testing and instead are calculated afterwards in post-processing carried out by the testing facility prior to the data being delivered. The additional calculated channels are detailed below.

Slip Ratio

The calculation for slip ratio is not trivial and there are various approaches. Once of which is shown in Equation 1.

$$Slip\ Ratio = -\frac{Vx - W\ \times\ Re}{Vx}$$

Equation 1. Slip ratio defined using effective radius.

In Equation 1, *Re* is the effective rolling radius, this is not directly measurable as it is dependent on the tyre's vertical stiffness. Therefore, in order to use this slip ratio definition during rig testing, the tyre's vertical stiffness must first be modelled. To do this, vertical stiffness testing must be carried out before any longitudinal tests can be run; the results from this testing must then be parameterised into a model and fed back into the rig's control system. The rig can then use this radius model, along with measured inflation pressure and vertical load, to predict the effective Rolling Radius at the given load case and then use this to calculate the slip ratio. This approach places a significant constraint on the sequencing of the testing, with vertical stiffness tests being required before any longitudinal testing can commence. It also means the accuracy of the longitudinal physical testing itself is dependent on the accuracy of the vertical stiffness model. With the longitudinal test data being used to parametrise the MF-Tyre 6.1 tyre model, this means the resulting tyre model is effectively a model of a model. Which can significantly reduce the overall accuracy of the resulting tyre model. Furthermore, if an error is made in the vertical stiffness testing and modelling this could result in the longitudinal test data being meaningless.

Due to the problems with this approach, the TIRF facility operated by Calspan Corporation, Buffalo, NY; use a different method to calculate slip ratio. This is shown with the alternative slip ratio definition in Equation 2.

$$\text{Slip Ratio (SR)} = \left[\left(\frac{\text{VX1}}{\text{W1}}\right) \times \left(\frac{\text{W}}{\text{VX}}\right)\right] - 1$$

Where: VX1 is VX (forward velocity) at the free rolling condition.
W1 is W (rotational velocity) at the free rolling condition.

Equation 2. Slip ratio defined using free rolling condition.

The equation effectively defines slip ratio as the amount by which the instantaneous ratio of VX and W deviate from the same ratio during a known free rolling condition at the same load case.

In practice, this definition required the rig to load the tyre to the desired load case, with vertical load, inflation pressure, forward velocity, slip angle and camber angle all constant, while the tyre is still free rolling. Under this load case the free rolling values of VX and W are recorded as VX1 and W1 respectively. A longitudinal slip sweep is then triggered, during which the instantaneous values of VX and W are measured, while the VX1 and W1 values are also known. Hence the equation can be solved and slip ratio can be calculated. This method removes the constraint of having to run vertical stiffness tests prior to longitudinal tests and removes the need for an effective radius model. However, it does place a lesser constraint on the testing. That is the fact that once the free rolling values of VX1 and W1 are recorded the tyre's load case must remain constant throughout the longitudinal sweep. However, this is a far less problematic constraint and as such this method is used.

Sliding Power and Energy

When assessing a test procedure, it is often useful the investigate the sliding power and total sliding energy of the test tyre, as these can be related to the temperature build up and tyre wear.

$$\mathrm{PY(Lateral)} = \mathrm{FY} \times \mathrm{VX} \sin \mathrm{SA}$$

$$\mathrm{PX(Longitudinal)} = \mathrm{FX} \times \mathrm{SR} \times \mathrm{VX} \cos \mathrm{SA}$$

$$\mathrm{SldPower\ (Sliding\ Power)} = \sqrt{(\mathrm{PX}^2 + \mathrm{PY}^2)}$$

Equations 3-A, B and C. Calculating slider power from measured forces and velocities.

Equations 3-A shows the calculation of the tyre's lateral sliding power using VX (Trajectory velocity) and SA (Slip Angle) to calculate the lateral velocity, which is then multiplied by the lateral force to determine the lateral sliding power. Equations 3-B calculates the longitudinal sliding power in an equivariant method to Equations 3-A, however in this case SR (Slip Ratio) is added. With the lateral and longitudinal sliding power known, the resultant sliding power is then calculated using Equations 3-C. Finally, the MATLAB 2016a function 'cumtrapz' (cumulative trapezoid numerical integration) is used to calculate the total energy using the sliding power and runtime channels (MathWorks MATLAB, 2017). The output of 'cumtrapz' is a channel that shows the accumulation of sliding energy through the test, with the last value being the total sliding energy.

Glossary of Terms

GS2MF

Gregory Smith 2 (to) Magic Formula. This is the name given to the tyre test procedure that is the subject of this thesis.

RSAT

Residual self-aligning torque. The torque about the vertical axis developed by the rolling tyre when operating at a slip angle at which no lateral force is generated.

RCF

Residual cornering force. The lateral force produced by the rolling tyre when operating at a slip angle at which no self-aligning torque is generated.

Slip Angle

The angle between the wheel hub and the direction of travel. In a test rig, this is the angle between the wheel hub and the road belt.

Slip Ratio

The ratio between the tyre's rotational and longitudinal velocity.

Hysteresis

This is a variation in either a force or moment observed at otherwise identical load cases brought on by external influences. Common manifestations of this are: variation in on-centre lateral force caused by the direction and speed of a change in slip angle, variation in on-centre longitudinal and lateral force brought on by tyre wear, variation in tyre grip under identical load cases brought on by changes to the tyre surface temperature.

Variable Rate Sweep

A variable rate sweep is one where the rate of change of slip angle or slip ratio is not constant. In such a sweep, the slip rate when close to zero slip (zero slip angle for lateral or zero slip ratio for longitudinal testing) is lower than the rate when further away from zero slip.

Variable Rate Low Rate, High Rate and Threshold.

During a variable rate sweep, the 'low rate' is the rate of change of slip when close to zero slip. The 'high rate' is the rate of change of slip when further away from zero. The 'threshold' is slip position where the transition between the 'low and high rate' occurs.

FreeRolling (Free Rolling)

A test where the tyre's slip ratio is either maintained at zero (such as at the SoVaMotion test facility), or the drive motor is disconnected such that no drive torque can be applied to the tyre and slip ratio is assumed to be zero (such as at the Calspan test facility).

BrkDrv (Braking and Driving)

A test where the tyre's slip ratio deviates from zero.

StaticLong (Static Longitudinal)

A test where the tyre is dragged longitudinally across a test surface while unable to rotate.

GS2MF FreeRolling

The 'FreeRolling' portion of the GS2MF test procedure, which is one of the three separate test procedures that make up GS2MF.

GS2MF BrkDrv

The 'BrkDrv' portion of the GS2MF test procedure, which is one of the three separate test procedures that make up GS2MF.

GS2MF StaticLong

The 'StaticLong' portion of the GS2MF test procedure, which is one of the three separate test procedures that make up GS2MF.

Flash Temperature

This is when a very high temperature is recorded on the tyre's surface that cools very quickly, often having minimal effect on tyre performance. It occurs as a result of the laser measuring system only being able to record temperatures from the outer most surface of the rubber. This surface has minimal depth and close to zero mass, meaning it can change temperature very quickly.

1.0 Introduction

1.1 Background

1.1.1 CAE Driven Vehicle Design Process

In the automotive sector, modern product development processes have continued to move further towards the use of CAE (Computer Aided Engineering). This is where complete vehicle models are built and used extensively to design and develop all aspects of the vehicle. Full vehicle CAE models are an assembly of component parts, not dissimilar to the assembly of a physical vehicle. A model is built of the basic chassis, then a model of the engine is added along with models of the drive train, suspension, net effect of the aerodynamics, mass distribution and electrical systems, amongst many others, along with a model of the tyres. All together this forms a model of the entire vehicle which can then be used to simulate all kinds of every day driving scenarios, extreme manoeuvres, accident avoidance or racing laps. Having simulated any given test, the vehicle's design can then be changed very quickly and inexpensively in CAE and the test can be run again. Doing so means vehicle development can be conducted very efficiently.

The continued move towards CAE is driven by several factors, the most commonly cited of which is the significant cost saving that comes from a reduction in the need for prototype vehicles. These prototypes are extremely expensive to build as they are required in the vehicle design phase which occurs long before the full-scale manufacturing facility is up and running. So, instead they must be completely handmade which requires a significant investment of time, money and man hours. Furthermore, the building and modifying of prototype vehicles can rarely keep up with the pace of the development and the rate at which the vehicle design changes. This means testing is often carried out using prototype vehicles that are not representative of the latest design iteration, hence introducing additional causes for error. The intention of a CAE driven product creation system is to use CAE for as much of the vehicle design process as possible and then only use prototype vehicles to validate the final design. If successful this means there is no need for prototype vehicles up until the very last stage of the design process, with all preceding development work being carried out using CAE. This significantly reduces the total number of prototypes required, while also moving the 'need date' of the prototypes closer to manufacturing 'start date'. At this time, the factories will have begun the retooling process and at least some of the prototype vehicle components can be sourced from the new manufacturing capability. This reduces the number of components that need to be handmade; therefore, it is not just the total number of prototypes that is reduced but the cost of building each one is also lower.

A second major reason for the use of CAE is the consistency and repeatability of the test results. Whenever a vehicle is tested in the real world, it is influenced by numerous environmental conditions which cannot be controlled. For example, if the vehicle was tested in the morning when the air temperature was cool and then the test was repeated later in the day during warmer weather, the results of the testing could be different. This is because various aspects of the vehicles performance could change due to the temperature variation. However, during a CAE simulation the same test can be run multiple times and every time the results will be identical. This means small changes can be made to the vehicle before repeating a test and any change observed in the vehicles behaviour can only come from the changes made to the vehicles design, as there are no uncontrolled outside influences. This significantly helps with the development and fine tuning of a vehicle's design.

A third driver towards the use of CAE within the vehicle design processes, which is often overlooked, is safety. A multitude of physical tests need to be conducted on a new vehicle before it can be declared safe and then sold to the public. Some of these tests, such as high-speed stability and double lane changes, can be very dangerous. Particularly when these tests are being run for the very first time on a new prototype vehicle. During these manoeuvres, it is impossible to know for sure if the car will rollover or not, leading to a significant safety risk. However, by using CAE these manoeuvres can first be run in the computer simulation where rollovers can occur without any risk at all. The vehicle design can then be continually improved until the vehicle remains stable. The learning from these CAE simulations can then be carried over into the prototype vehicle and the physical test can be conducted more safely, as the risk of roll over is reduced due to the CAE testing. This is an approach that is also heavily used in the aeronautical industry. Where extensive simulation and testing is carried out using computer simulation before the first prototype plane is built and flown. This is because it's imperative that the plane can fly and land safely before it even takes to the sky.

1.1.2 The Role of the Tyre Model

A car only contacts the road via its tyres. This means that anything that happens in the vehicles such as advanced suspension systems, improved drive technology, the skill of the driver all must be transferred to the road via the tyres. As such the tyres influence the resulting performance of almost every driving system on the car. The same is true in CAE, where the different components of the vehicle model have various degrees of influences over the full car. However, the net result of all their effects is transferred to the road via the tyre model, which then estimates the forces and moments that cause the car to move across the road. Due to this, the tyre model heavily influences the performance of the full vehicle simulation. If the vehicle model features a poor engine model, then braking simulations could still be accurate. If the

braking model is poor, then accelerating and handling simulation could remain accurate. However, if the tyre model is of poor quality, almost every type of full vehicle simulation will be affected. For this reason, the tyre model can be considered as one of the most important components of a full vehicle simulation.

Knowing the importance of the tyre model as part of the vehicle simulation process, vehicle manufacturers invest significantly in the development and delivery of tyre modelling technology. For full vehicle simulation, FEA (Finite Element Analysis) based tyre models require far too much computational overhead to be practicable for this application. Full vehicle simulation is often conducted on driving simulators which include a human-in-the-loop. During these simulations, the tyre models and vehicle models need to run in real time. Therefore, a computationally simpler approach is employed by means of empirical tyre models.

Empirical tyre models can be thought of as a model of the tyre's performance, rather than a model of the tyre itself. This is because empirical models do not contain any physical information pertaining to the tyre. Instead the physical tyre is tested, data is obtained and an empirical model is produced that mathematically represents that test data. The most commonly used empirical tyre models are the various versions of the so called 'Magic Formula'. This was first published in 1987 by Hans. B. Pacejka and his associates and has been continually developed ever since (Bakker, Nyborg and Pacejka, 1987). The model's popularity has occurred due to its high accuracy, expandability and the fact that the model's equations are entirely open source making it easy to interact with the vehicle model. The specific version of the tyre model used throughout this project is MF-Tyre 6.1 (Besselink, Schmeitz and Pacejka, 2010).

To obtain an MF-Tyre 6.1 tyre model a physical tyre must first be tested on a rig. This is a costly process, as tyre rigs are expensive to use and a significant amount of rig time is required to fully test a tyre. Therefore, the exact method of testing is of importance and forms the basis of this thesis. Once the tyre is tested the resulting data is passed into a model fitting process. This typically consists of a complex optimisation algorithm that adjust the coefficients of the MF-Tyre 6.1 tyre model such that it represents the test data as accurately as possible. This generates a unique list of coefficients which represent the tested tyre. The list of coefficients is then saved as a text file which can be integrated into the full vehicle simulation. With the list of coefficients and the load conditions simulated by the vehicle model, the tyre model's equations can then be solved to predict the tyre's force and moment outputs. These forces and moments are then fed back into the vehicle model to determine how it moved across the road. This enables the simulation of complex vehicle manoeuvres.

1.2 Aim and Objectives

Aim:

To develop a novel process to improve the efficiency of expensive tyre testing procedures. This will be achieved without compromising the functionality of the tyre model parameter sets generated to populate empirical tyre models used in vehicle dynamics simulations.

Objectives:

1. To reduce the number of tyre test rig hours required to gather data to fully populate the widely-used MF-Tyre 6.1 tyre model. Currently, 10 hours of rig time are required based on applying a Square Matrix test procedure. The aim of this study is to investigate a novel approach which could reduce this by up to six hours.
2. To reduce the number of physical tyres required for testing down from 10 to four, which is a crucial milestone as this represents one vehicle-set. Using less than four tyres will still usually require one vehicle-set so there is minimal benefit from doing this, the exception being vehicles with a front-rear split fitment. If five tyres are needed for testing there is little additional cost associated with using eight, as anywhere from five to eight represents two vehicle sets. Any remaining tyres within the vehicle-set are likely to be scrapped.
3. To make the testing more representative of real world operation and to link closely with the load cases to which the tyre will be subjected when fitted to a vehicle. This will involve, for example, linking the test loads to the tyre's load rating, improving and extending on existing methodologies such as those currently used by Michelin. (Buisson, 2006).
4. To formalise a system for managing the significant contribution of tyre temperature. The existing tyre model in this study is not sensitive to tyre temperature and hence temperature needs to be as consistent as possible throughout the testing. Currently there is no formalised approach to manage this within the Square Matrix test procedure.

1.3 Structure of Thesis

The thesis is separated into six main chapters. The first is an introduction that covers the background to the GS2MF test procedure, how it is intended to be used and why it has been developed. Also detailed is the wider use of tyre modelling as part of full vehicle simulation and the reasons behind it. Chapter two is the literature research which attempts to concisely bring together all relevant literature on the subject, including the authors own published works. This chapter highlights the distinct lack of published material specifically on flat-trac tyre test procedures and concludes that publishing such research would significantly add value to the scientific community. Chapter three details the GS2MF technical development. Here each of the

key technology components that support GS2MF are discussed in detail. With analysis and justification behind each of them. Chapter four then pulls all these components together and discusses how the full test procedure operates. This includes an analysis of the results and comparison to traditional test methods. Once the test procedure is run and the data is collected, Chapter five seeks to address the issue of building a tyre model from this data. This chapter is not intended to be a tyre model parameterisation guide, as that is outside the scope of this thesis; however, it does prove that a representative MF-Tyre 6.1 tyre model can indeed be built using the GS2MF test data and describes how this can be done. Chapter six then draws the thesis to a close with conclusions and a discussion of potential future work.

2.0 Literature Review

This chapter provides a thorough review of existing literature on the specific area of tyre testing procedures as well as the related areas. The literature research begins with a high-level overview looking into tyres themselves. Including their components, structural make up and contact patch pressure before going onto the friction and sheer stress distribution. The core subject of the thesis is tyre testing procedures, so all relevant published material is analysed; however, designing a test procedure in isolation is not practicable. Instead research is also conducted into the tyre testing facilities that will be required to run such a test procedure. This is crucial to ensure that any new procedure is both able to run on the available test equipment and use it in the best possible way. Furthermore, the intention of the test procedure is to gather appropriate data for the parameterisation of tyre models. Therefore, research is also conducted into the various different types of tyre models as well as the optimisation techniques that are used to parameterise them.

2.1 Pure Tyre Behaviour

The structure of a tyre and the way it behaves under any given set of conditions is not trivial. Instead, tyres are extremely complex in their design, containing many components and highly confidential material formulations. Furthermore, the way a tyre works is equally as complex, with the constantly varying pressure distribution across the contact patch generating a variable amount of grip. This translates into sheer stresses that leads to a set of forces and moments being transferred into the wheel and ultimately the vehicle. Meanwhile, other performance attributes can be important, such as the modes at which the tyre vibrates causing unwanted noise and how the tread pattern disperses water at the required rate while also needing to look attractive. During tyre development, all these often-conflicting performance attributes must be considered before deciding on a final design.
(The Contact Patch – Introduction, 2017)

2.1.1 Tyre components

Tyres are highly complex structures built up of multiple components. The exact structure of a tyre, the material selection and particularly the details of the rubber compounds are all highly valuable intellectual property protected by the tyre manufacturers. The intellectual property is valuable due to tyre companies having to place significant investment into tyre design and development to stay competitive. If the exact details of a given tyre's compounds and structure became public, it could be copied by the competition and the tyre company that developed it would lose market share. However, the basic structure which is common to nearly all road car tyres is known. This is shown in Figure 2.1.1-A.

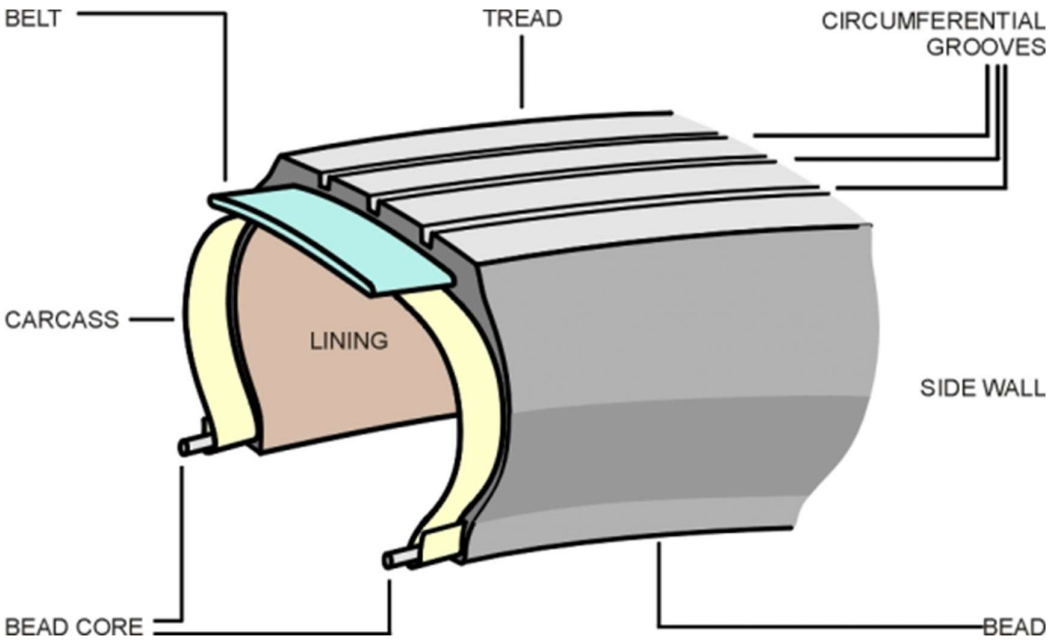

Figure 2.1.1-A. Component parts of a typical tyre. (The Contact Patch – Rubber Tyres, 2017)

The tread is the most well-known component of the tyre, it is a thick layer of rubber that is in direct contact with the road surface. With the exception of racing slicks, treads usually have a tread pattern, which is a repeating series of tread blocks and grooves that are designed to displace water from the contact patch. A tread with a low 'net to gross ratio', that is the ratio of tread block surface area to groove surface area, is likely to have good wet grip and aquaplaning performance; as there is a lot of space between the blocks for water and other material to be displaced. However, the smaller tread blocks are freer to move and flex, this reduces the stiffness of the tread and worsens the dry handling performance of the tyre (Gent and Walter, 2005, pp.2-15). On either side of the tread is the sidewall; this portion of the tyre is where the lettering and company advertising is placed. The sidewall also serves to protect the inner structure of the tyre from damage, such as scraping the tyre along a kerb. Further down from the sidewall is the bead which is the moulded rubber section where the tyre contacts the wheel rim. The shape of this bead is precisely specified in the ETRTO (European Tyre and Rim Technical Organisation) standards manual (ETRTO Standards Manual, 2017) or similar standards internationally such as the TRA (Tire and Rim Association) in north America (TRA, 2017). This standard ensures that any given tyre can be mounted to any appropriate wheel in a safe and consistent manner. Within the bead there is the bead core (also known as the bead bundle), this is an intertwined coil of strong high tensile steel wire. When mounting a tyre, this is forcibly stretched over the wheel such that it tightly contracts into the wheel rim thus securely seating the tyre to the wheel. Covering the entire inner surface of the tyre is the lining. This ensures an

air tight seal to maintain the air pressure within the tyre. The tyre's lining is fixed to the carcass (also known as the ply) which is a crucial structural member of the tyre. The plies are typically made of a strong flexible cord material, such as Nylon or Rayon (The Contact Patch – Rubber Tyres, 2017) and stretch laterally across the width of the tyre, wrapping around each of the bead cores. The plies are there to hold the whole tyre structure together and maintain its shape, they also help retain the internal forces generated by the high inflation pressure. The tyre's belt sits above the plies but only on the tread section of the tyre, not the sidewall. Like the bead core the belts are typically made from high tensile steel cord; however, the ones used in the belts are far thinner than those used in the bead. The purpose of the belts is to add additional reinforcement, structural integrity and puncture reliance to the tyre. These belts run circumferentially around the tyre, though are not quite parallel to the tyre's centre line; instead tyre manufacturers typically tune the angle of these to influence the tyre's performance.

The tyre structure described here is known as a radial tyre design (due to the plies running radially across the tyres) and are common amongst almost all road car tyres. Alternative constructions include so called cross-ply tyres. These tyres do not have steel belts and instead the plies run diagonally across the tyre in either direction typically crossing each other at a 90° angle, hence the name cross-ply. Without the steel belts, such a design usually results in a less rigid tyre that compromises the lateral grip performance. For this reason, cross-ply tyres are rarely used on modern road cars; however, they are still used in limited numbers on vintage cars.

2.1.2 Contact Patch Pressure Distribution

A tyre's forces and moments are generated by the contact patch, which is the area of the tyre that is in contact with the road surface. The size of this contact patch for a given tyre is dependent on the inflation pressure and the vertical load placed on the tyre. As the load is increased (at a given inflation pressure) the tyre deforms creating a larger contact patch. Likewise, if the load is held constant while the inflation pressure is reduced a similar deformation occurs. This is because it is the compressed air within the tyre that supports around 95% of the load (with the tyre sidewalls supporting the remaining 5%), therefore reducing the air pressure reduces the tyre's vertical stiffness and hence its ability to support the load also reduces. (The Contact Patch – Contact Patch, 2017)

The size of the contact patch is important to vehicle dynamics where it is often assumed that the larger the contact patch is the more grip there is available. While this can be true, in tyre engineering it is not just the size of the contact patch that is important but also the pressure distribution across the contact patch. At a given load, an underinflated tyre will place more load

on the edges of the contact patch, which will lead to uneven wear and an inefficient use of the tyre's available tread surfacing, reducing grip. Conversely an overinflated tyre increases the contact patch pressure close to the centre of the contact patch, again leading to uneven wear and poor grip. This means that there is a balance, where the tyre must be inflated to the correct pressure to support the load, while also evenly distributing the tyre pressure across the contact patch to make best use of the tyre's available tread surface. (Gent and Walter, 2005, pp.231-286)

When stationary, the longitudinal contact patch pressure distribution will be reasonably uniform; however, when rolling this can be more complex as the centre of pressure moves forward ahead of the centre of the contact patch, as shown in Figure 2.1.2-A.

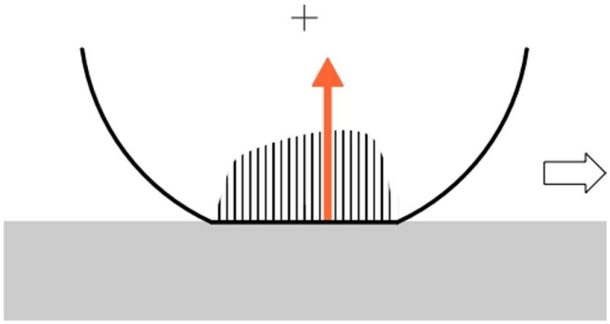

Figure 2.1.2-A. Longitudinal pressure distribution and centre of pressure. (The Contact Patch – Contact Patch, 2017)

The centre of pressure moved forward of the centreline of the contact patch due to each segment of the tread going through a cycle of loading and unloading at it passes through the contact patch. The tread material is not being perfectly elastic; instead, while the tread absorbs energy placed into it when pressure is applied at the front of the contact patch, not all this energy is recovered when the tread relaxes at the end of the contact patch. As a result, the contact pressure is higher during the loading (front) part of the contact patch and lower during the unloading (rear) part of the contact patch, shifting the centre of pressure forward. The differential in energy being largely transferred into heat, which warms the tyre as well as the road surface and surrounding air. (The-contact-patch.com, c2020-the-contact-patch, 2017)

2.1.3 Tyre Radii Definitions

Due to their flexible nature, there are several different radii that are relevant when defining a tyre. The relevant tyre radii are hence explained below.

Static Loaded Radius

The Static Loaded Radius (R_{l0}) is the distance from the wheel centre to the road surface while the tyre is loaded but not rotating. This is of importance to automotive engineers when calculating a vehicles static ride height and ground clearance. (The-contact-patch.com, c2020-the-contact-patch, 2017)

Static Unloaded Radius

The Static Unloaded Radius (R_o) is the distance from the wheel centre to the tread surface when the tyre is mounted to a wheel and inflated but not loaded or rotating. This is typically calculated via the Static Loaded Radius (R_{l0}) testing which is conducted under non-zero loads. Measuring the Static Loaded Radius and Static Unloaded Radius are not trivial as the vertical stiffness of a tyre is not constant. Instead a very low force can initially compress a tyre from its unloaded state; thereafter, as the load increases so does the stiffness. In an experimental setting, when the tyre is mounted to a test rig it is difficult to regulate the rig to a precise zero load; and a small inaccuracy in the rig's load application will compress the tyre and thus not measure the true Static Unloaded Radius. Instead the tyre is rolled to a series of non-zero vertical loads, which are easier for the rig to regulate, and then brought to a halt. While the tyre is held statically the distance between the wheel hub and the road surface is recorded giving the Static Loaded Radius (R_{l0}), the loaded results are then extrapolated to zero load. Unusually, this extrapolation technique gives a more accurate representation of the Static Unloaded Radius than attempting to measure it directly. (TNO Equation Manual, 2010)

Unloaded Tyre Radius

The Unloaded Radius ($R\Omega$) (also known as the 'Free Tyre Radius') is the distance from the wheel centre to the tread surface while the tyre is rotating. At low rotational speed, the Unloaded Radius is very close to the Static Unloaded Radius, with them being exactly equal at zero velocity. However, as velocity increases the tyre is subjected to centrifugal force which causes the tyre to swell and its radius to increase. Therefore, at high speed the Unloaded Radius is larger than the Static Unloaded Radius. In the MF-Tyre 6.1 tyre model, the Unloaded Radius definition is shown in Equation 2.1.3-A.

$$R\Omega = \mathrm{R0}\left(Qre0 + Qv1\left(\frac{\Omega \mathrm{R0}}{V0}\right)^2\right)$$

Equation 2.1.3-A. Unloaded Radius model used in MF-Tyre 6.1.
(TNO Equation Manual, 2010)

Where Qre0 and Qv1 are both model parameters, **Ω** is the wheels angular velocity, V0 is the nominal velocity (This is defined in Section 5.1.4 GS2MF Model Fitting on Base Calculations), R0 is the Static Unloaded Radius. (TNO Equation Manual, 2010)

Loaded Tyre Radius (rolling)

The Loaded Tyre Radius (RL) is the distance from the wheel centre to the road surface while the tyre is loaded and rotating. As the tyre is loaded it deflects and forms a flat contact patch at the road surface. This deflection (ρ) is equal to the Unloaded Radius (RΩ) minus the Loaded Radius (RL), where the Unloaded Radius is always larger than the Loaded Radius meaning the deflection can never be negative. The MF-Tyre 6.1 tyre model calculation of deflection is shown in Equation 2.1.3-B.

$$\rho = \max(\mathrm{R}\Omega - RL, 0)$$

Equation 2.1.3-B. Tyre deflection used in the MF-Tyre 6.1 tyre model. (TNO Equation Manual, 2010)

All the above radii can be thought of as special cases of the same radius; that being the distance between the wheel centre and the tread surface while under any combination of rolling or static and loaded or unloaded. Therefore, in the TYDEX standard the radius is defined simply as DSTWOWHC. (TNO Equation Manual, 2010. van Oosten, Unrau, Riedel and Bakker, 1999)

Effective Rolling Radius

The Effective Rolling Radius (Re) is the ratio of the forward velocity and the angular velocity of the wheel centre. It is therefore simple to calculate the Effective Rolling Radius when both values are known such as they are on a vehicle; where forward velocity is defined while the angular velocity can be measured. However, when running a computer simulation of a vehicle the angular velocity of the wheels and the Effective Rolling Radius are unknown. Therefore, in the MF-Tyre 6.1 tyre model Effective Rolling Radius is modelled using Equation 2.1.3-C.

$$Re = R\Omega - \frac{FZ0}{CZ}\left(D_{reff}\tan^{-1}\left(B_{reff}\frac{FZ}{FZ0}\right) + F_{reff}\frac{FZ}{FZ0}\right)$$

Equation 2.1.3-C. Tyre deflection used in the MF-Tyre 6.1 tyre model. (TNO Equation Manual, 2010)

Where D_{reff}, B_{reff} and F_{reff} are all model parameters. CZ is the vertical stiffness adapted for tyre inflation pressure. FZ is the vertical load, while FZ0 is the nominal vertical load. (The-contact-patch.com, c2020-the-contact-patch, 2017)

2.2 Tyre Testing Facilities

Before parameterising any empirical tyre model, a range of tests must be performed using a tyre test rig. The rig is used to measure the resulting force and moment components generated due to the distribution of pressure and stress in the contact patch. The load cases executed during the test are designed to map the conditions the tyre will see in service for various camber angles, slip angles and values of vertical force. It is also possible to drive or brake the tyre and measure the forces generated due to longitudinal slip. Complex simulations that aim to map a full range of behaviour involving combined driving or braking with cornering, can require an extensive programme of tyre tests to be performed. The rigs used for this are typically large and expensive pieces of equipment, as detailed below.

All the load case inputs (such as slip angle, slip ratio and load) as well as the output measurements (such as FX and FY) conform to the TYDEX standard and are detailed in the nomenclature.

2.2.1 Outdoor Testing

Outdoor tyre testing covers any objective tyre testing that is conducted outdoors rather than within an indoor laboratory. The most common form of outdoor testing involves various alternative designs of trailer rig. This is where articulating heads are mounted in trailers and used to gather handling data on public roads, racetracks and proving grounds. The articulating head is designed such that the test tyre roles along the ground surface while a regulated load, camber and slip angle is applied. At the same time, the instrumented head records the forces and moments generated by the tyre during the test. One such rig is the UMTRI (University of Michigan Transportation Research Institute) mobile rig photographed in Figure 2.2.1-A.

Figure 2.2.1-A. UMTRI Mobile rig photographed circa 1980. (original source unknown, photograph provided by M'gineering LLC, Akron OH, 2017)

The UMTRI Mobile rig was one of the first of its kind. It was developed at the University of Michigan, Ann Arbor, MI, and funded by the then Motor Vehicle Manufacturers Association (MVMA) which was later dissolved in 1999. The UMTRI rig was developed in multiple stages beginning in 1974 when the test station was mounted in the trailer. It was then capable of longitudinal testing only (with no slip angle). At the time, it was pulled by a conventional tractor and capable of measuring FX, FZ and MY. In 1980 the rig was upgraded; a long wheelbase tractor was built and a new test station was mounted within the tractors wheelbase. This added the ability to test the tyre at different slip angles with the help of a 4-compoonent spindle cell to record FY as well as FZ, MX and MY. In effect, this is two separate rigs; a free rolling rig mounted within the tractor that can measure lateral tyre performance, and a separate rig mounted to the trailer that can measure pure longitudinal performance. In 1990, the rig was upgraded again. This time a 6-compoonent spindle cell was designed and built in house at the university of Michigan to record FX, FY and FZ as well as MX, MY and MZ. This combined with a hydraulic disc brake enabled the testing of the tyre performance while under combined slip, where steering and braking are applied to the same tyre at the same time. The rig continued to be used in research applications until it was decommissioned after the year 2000 due to its lowering utilisation as newer facilities became available. (Winkler, C., (2017). Ervin and MacAdam, 1981)

Newer designs that build on the learning from the UMTRI Mobile rig include the FaReP mobile tyre test rig owned and operated by FKA (Forschungsgesellschaft Kraftfahrwesen mbH, Aachen) based in Aachen, Germany, shown in Figure 2.2.1-A. As well as the TNO TASS International Delft-Tyre Measurement Rig, Helmond, The Netherlands. Photographs of which are shown in Figure 2.2.1-C.

Figure 2.2.1-B. FKA mobile test rig. (FKA Tyres in Motion, 2013, pp.51)

Figure 2.2.1-C. TNO mobile test rig. (Tass International, 2017)

Both the FKA and TNO rigs build on the technology developed from the UMTRI Mobile rig. They are both under continual development and offer increased load capabilities and measurement accuracy over the UMTRI rig. Furthermore, both the FKA and TNO rigs are publicly available facilities that are often utilised by vehicle manufacturers, tyre companies and research organisations.

The key advantage of mobile outdoor rigs is that the tyre can be tested on any practical real road surface. The rigs can be relocated to test locations around the world and the tyre can be tested under the local conditions. For example; tyre testing can be conducted at winter test facilities on snow and ice surfaces, then the rig can be moved for summer testing on dry asphalt. These environmental effects can be captured in an MF-Tyre tyre model, amongst others, by using the tyre models in built scaling factors, (Braghin, Cheli and Sabbioni, 2007). This flexibility also increases the precision of the testing as the tyre can be tested under environmental conditions that are highly representative of real world use. Conversely however; testing outdoors typically reduces the accuracy of the results. As the local weather and uncontrollable environmental effects introduce additional causes for error in the tyre measurements. Furthermore, the use of a lorry adds significant constraints to the testing. For example; road cars are typically capable of travelling at very high speeds and hence it is important to test their tyres under similar high-speed conditions. However, lorries are only able to travel at much lower speeds, meaning high speed testing using such test apparatus is not possible. (IDIADA Tire Modeling, 2016)

An alternative approach to outdoor tyre testing is to instrument a vehicle and test the tyres while they are mounted to that vehicle. This is possible using wheel force transducers, which are wheels instrumented with load cells that can measure the forces and moments between the wheel rim and the hub. Such devices are available from Kistler, Winterthur, Switzerland who make the RoaDyn range of wheel force transducers. A photograph of the Kistler RoaDyn S635 sp is shown in Figure 2.2.1-D.

Figure 2.2.1-D. Kistler RoaDyn S635 sp, Wheel Force Transducer. (Kistler Wheel Force Transducers, 2016)

Using wheel force transducers, the tyres can be tested on the exact vehicle they are intended to be used with. Theoretically this means that the range of load cases achievable by the vehicle are automatically valid for the tyre; as the tyre and vehicle are intended to be used together. However, in practice the additional instrumentation added to the car causes its weight to increase significantly, this can mean make it challenging to test the tyre at the lower range of required vertical loads. An example of a fully instrumented vehicle, including all the ancillary instrumentation is shown in Figure 2.2.1-E.

Figure 2.2.1-E. Wheel Force Transducer equipped test vehicle operated by Jaguar Land Rover. (Smith, G. 2014)

Another advantage of wheel force transducers is that it offers the opportunity for subjective and objective assessment of the tyres to be conducted simultaneously. This can be useful for vehicle manufacturers who want to build links between the CAE simulations and the subjective test drivers.

In practice, instrumenting a vehicle with wheel force transducers is extremely challenging. A whole host of other instrumentation is required to obtain slip angles, slip ratios and camber angles, all is which require very careful installation to obtain a good level of accuracy. Once this data is obtained, the filtering and post processing of the data is also challenging, usually requiring the careful setup and application of a Kalman filter to reduce signal noise in the data channels (Best, 2010). Furthermore, additional post processing tools are required to obtain other necessary data channels, such as calculating slip ratio using GPS (Miller, Youngberg, Millie, Schweizer and Gerdes, 2001). Finally, once the resulting test data is processed it can still be difficult to use for tyre model parameterisation. Test data from rigs usually contains less signal noise and typically only one variable changes at a time, which makes it easier to identify and asses the tyre performance dependencies. Conversely, during on-vehicle testing the vertical loads, slip and camber conditions all change at the same time, which makes this process more difficult. (Conte, 2010. Braghin, Cheli and Sabbioni, 2011)

Even if done properly, the constraints of instrumenting a vehicle mean the accuracy of the setup will be lower than comparable trailer testing available from the FKA and TNO rigs, amongst

others. Furthermore, the on-vehicle approach is affected by all the uncontrollable environmental influences that affect trailer testing, such as changeable weather conditions.

2.2.2 Indoor Testing

Having failed to control the local weather conditions that cause problems with outdoor tyre testing, the need for an alternative solution remains. To this end, indoor test facilities were developed to generate more repeatable data by situating the test within environmentally controlled laboratories. The most common indoor test facilities are the various types of drum rig that can be found all around the world. These rigs are available in numerous different types; however, fundamentally they consist of a rotating steel drum (sometimes covered with a test surface) with the test tyre mounted to an articulating head that holds the tyre against the surface of the drum. The head can regulate the tyre's load, slip angle and other loading conditions while also measuring the forces and moments generated by the tyre. Photographs of old and new tyre drum rigs can be found in Figures 2.2.2-A and 2.2.2-B.

Figure 2.2.2-A. Dunlop tyre drum rig, circa 1940. (original source unknown, photograph provided by M'gineering LLC, Akron, OH, 2017)

Figure 2.2.2-B. Modern external drum tyre test rig. (MTS Measurement System, 2014)

The advantage of this setup is that the tyre can be tested across a range of load cases while under very consistent test conditions. This is due the rigs being able to accurately apply to requested load case, while the indoor nature of the testing means that the local temperature and moisture can be controlled. Due to this, many variations of drum rigs exist such as those used for force and moment testing, as well as others used for uniformity, rolling resistance, wear, durability, noise and cleat testing amongst others. However, drum rigs are less suitable for gathering handling data as they cause the tyre's contact patch to be curved rather than flat; this typically leads to inaccurate lateral force prediction. The need to correct for curvature effects form testing with drum rigs is recognised by the authors in (Pottinger, Marshall and Arnold, 1976) where the use of correction factors is considered when generating parameters for the Magic Formula tyre model.

A variation on the drum rig design is 'internal drum rig', such as the one found at KIT (Karlsruhe Institute of Technology) which is linked with the University of Karlsruhe, Karlsruhe, Germany, who test the tyre against the internal surface of a drum (Karlsruhe Testing Facilities, 2017). Here, a very large integral drum is driven by an electric motor with an articulating head next to the drum. The setup is such that the test tyre can be mounted to the articulated head and positioned against the inner surface of the drum. This setup is more complex and costly to operate than a conventional drum rig; however, the main advantage is that testing can be conducted on a wide variety of road surfaces. (Greßler, Gauterin, Hartmann and Wies, 2007)

shows results from successful experimentation using the internal drum rig covered with, a snow test surface. During these and similar tests, the tyre can be run on dry asphalt, then using the exact same apparatus the testing can repeated on snow and the results can be directly compared. Such flexibility is not available using any other type of tyre test equipment. Furthermore, the highly-controlled conditions available when using indoor rigs means that snow of the same properties can be generated repeatedly. As a result, tyre testing even on highly changeable surfaces can be repeated consistently. Testing is also not limited to dry asphalt and snow, instead different base surfaces are available, including steel, sand paper, asphalt and concrete, each of which can be made wet or covered with a controllable amount of snow or ice. Finally, cleats can also be added to gather data pertaining to the tyre's ride performance. Internal drum rigs such as this offer the widest possible set of controllable test conditions available; however, they are affected by the same fundamental issue that effects regular drum rigs, that being the curved contact patch. For this reason, they certainly have a place within a range of test apparatus but do not offer a complete solution for all testing. Photographs of the Karlsruhe internal drum rig can be found in Figure 2.2.2-C and 2.2.2-D. (Gnadler, Huinink, Frey, at al, 2005)

Figure 2.2.2-C. Karlsruhe internal drum rig, circa 1960. (original source unknown, photograph provided by M'gineering LLC, Akron OH, 2017)

Figure 2.2.2-D. Schematic combined with a photograph showing the layout and internal test surface (in this case covered with snow) of the Karlsruhe internal drum rig. (Greßler, Gauterin, Hartmann and Wies, 2007)

To address the issue of the curved contact patch, there was a need to test tyres on a flat surface. For this reason, the TIRF rig, operated by the Calspan Corporation, Buffalo, NY, was developed and brought into service in 1970 (Bird and Martin, 1973). The fundamental idea was to replace the single drum with two drums and a steel belt wrapped around them. This belt is supported between the two drums by an air or water bearing, creating a flat, level surface on which to test the tyre. The steel belt is covered with a test surface (typically sandpaper) to simulate a road surface. The test tyre is then mounted to an articulating head above the test surface which allows the tyre's load, slip angle, camber angle and rotational velocity to be controlled; in addition to the speed of the belt and inflation pressure of the tyre; meaning the test can be conducted under a wide range of load cases. The advantage of such a facility is that the tyre is tested on a flat surface, thus avoiding the issues with testing on a curved drum that causes the tyre to have a curved contact path which is not consistent with real world use. However, the disadvantage of the Calspan design is that the belt must transition between flat (between the drums) and curved (around the drums) conditions, which means the test surface is restricted to flexible materials such as sand paper. As such the rig design means testing cannot be conducted on asphalt or any similar paved surfaces that vehicles regularly drive on. This induces a new cause for error during testing. Furthermore, the flat surface rigs such as Calspan are far more expensive to

manufacture and maintain than the much simpler drum rigs, making them more expensive to operate. (Langer and Potts, 1980)

When using drum or flat-trac rigs there are always compromises; where drum rigs can offer asphalt testing but only on a curved surface and flat-trac rigs can offer a flat surface but not on asphalt. To address this, a completely new type of tyre test facility came out of beta testing in mid-2017 called Camber Ridge, Charlotte, NY. Camber Ridge offers a revolutionary solution to repeatable tyre testing on a flat asphalt surface. It does this with a large half-mile (800m) long oval test track paved with asphalt. There are rails on either side of this oval test track, onto which a self-propelled carriage is mounted called the 'Genesis Machine'. The Genesis Machine takes electrical power from the tracks and includes drive motors and control systems such that it can be propelled around the half-mile oval track. The test tyre is mounted to an articulating head contained within the Genesis Machine and rolls along the asphalt surface. The entire facility is contained within a large 3,437 square meter (37,000 square foot) building, which means the weather conditions can be controlled. A photograph showing the Camber Ridge track can be found in Figure 2.2.2-E and another showing the Genesis machine can be found in Figure 2.2.2-F.

Figure 2.2.2-E. One quarter of the track at the Camber Ridge facility Charlotte, NY. (Camber Ridge, 2017)

Figure 2.2.2-F. Camber Ridge Genesis Machine Charlotte, NY. (Camber Ridge, 2017)

This system offers numerous advantages over more traditional tyre test rigs. Outdoor trailer based rigs can test on flat asphalt but are subject to local weather conditions; this can reduce the efficiency of testing while having to work around the changing weather, it can also potentially ruin the crucial test repeatability. Drum and flat-trac rigs avoid changeable weather by testing indoors under controlled conditions. However, the curved surfaces of drum rigs mean that some tyre measurements (particularly lateral force) are inaccurate due to the tyre having an unrepresentative curved contact patch. Meanwhile, flat-trac rigs solve the issue of the curved contact patch but they can only use a flexible test surface, usually sand-paper, which is not perfectly representative of asphalt. The difference between the longitudinal force response of the same tyre tested in precisely the same way on sand paper compared to asphalt is shown in Figure 2.2.2-G.

Figure 2.2.2-G. Comparison of longitudinal force measurements from the sand paper surface of the Calspan rig (Y axis, labelled CFx) with exactly equivalent measurements (identical load case and test procedure) from the paved road surface used with the UMTRI rig (X Axis, labelled UFx). (M'gineering History of Tire Characterizing, 2016)

Figure 2.2.2-G shows results from running otherwise identical tests using specimens of the same tyre construction running on two different surfaces (sand paper and asphalt, where the surface is the only intended variable in the test). If the sand paper surface was equivalent to asphalt, then all data points on Figure 2.2.2-G would follow the straight diagonal line indicating that under any given condition the longitudinal force of a tyre while running on sand paper is the same when running on asphalt. Instead, the plot shows a significant difference between testing on the two surfaces and the complex hook shape is indicative of the highly complex nature of tyre friction across different surfaces. This demonstrates that a tyre running on sand paper does not perform the same as when it is running on asphalt. The route cause of this is not examined but is likely to be due to the very different surface roughness's of sand paper and asphault. With asphalt containing much larger surface undulations than sand paper. This phenomenon cannot

be captured by a simple change to the Mu (friction coefficient) of a road surface during vehicle simulation.

Camber Ridge handles this by testing the tyre on flat asphalt which is highly representative of the road surfaces commonly used around the world. Future plans for Camber Ridge also includes the ability to flood the track to test the tyre in wet and aquaplaning conditions. As well as 84m straight line rig that will provide both wet and dry testing capabilities on a variety of different pavements. The main drawback of Camber Ridge compared to more traditional approaches is that the increased cost and complexity of the facility make it more expensive to run and operate, of course these costs need to be handed over to the customer which make it a more expensive rig to use. However, these additional costs are somewhat offset by the fact that the lower friction of the asphalt surface (compared to sand-paper) means there is less friction induced heat during each test sweep. This means the tyre will not get as hot during each sweep and therefore will need less time to cool, hence reducing the overall test duration. This means that compared to flat-trac testing the test durations could reduce while the hourly cost will increase, potentially resulting in a similar overall cost. Unfortunately, due to the very recent opening of the Camber Ridge facility, timing and cost constraints means there was no opportunity to test there and include the analysis in this report.

2.2.3 Calspan Facility and NTRC MTS Flat-Trac LTRe facility

The Calspan TIRF rig (TIre Research Facility) was the first of its kind and brought online in 1970 as part C.A.L. (Cornell Aeronautical Laboratory, Buffalo, NY). At the time, C.A.L, was a research laboratory that formed part of the Curtiss-Wright Aeronautical Company (now known as the Curtiss-Wright Corporation, Charlotte, NC) but C.A.L was owned and manged by Cornell University, Ithaca, NY. In 1972, the laboratory changed hands again when it was transferred to the private sector. The new owners took the ‘CAL’ from Cornell Aeronautical Laboratory and added ‘SPAN’ as a nod towards the wing span of aircraft which are a key part of organisations research focus, to create the name Calspan; now known as the Calspan Corporation, Buffalo, NY. (Calspan History, 2010)

The original Calspan rig was the first high speed flat belt tyre testing facility in the world. It consists of two drums with a large belt rapped around them. One drum is used to drive the belt; while the other drum uses a proprietary control system which adjusts the angle of the drum relative to the ground such as to keep the belt from sliding off the drums when a lateral force is applied. Between the two drums there is an air bearing which is required to support the vertical load of the test tyre. Above this, the test tyre is mounted to a six ton articulating head which can apply load, slip angle, slip ratio and camber to the tyre; while also regulating inflation pressure.

A photograph taken in 1973 of the then new Calspan rig can be found in Figure 2.2.3-A. (Bird and Martin, 1973)

Figure 2.2.3-A. Calspan rig, Buffalo NY, photographed circa 1973. (original source unknown, photograph provided by M'gineering LLC, Akron OH, 2017)

Figure 2.2.3-A shows a 1973 photograph of the Calspan rig, where the complex system of hydraulic pipes used to drive the rig are visible in the background, while the articulating head can be seen painted yellow. The test tyre is shown lifted above the test surface. The belt wrapped around the two large drums and supported by the air bearing are shown in the bottom of the picture. (Bird and Martin, 1973)

Calspan's original drive system used an electric motor that was originally designed for use in World War Two submarines. This was connected via a drive shaft to a transfer box which split the drive between a gearbox which led to the drive drum and a hydraulic compressor. This compressor was used to generate hydraulic pressure which drove a hydraulic pump mounted to the back of the articulating head. With the articulating head constantly moving and flexible tubes not being strong or durable enough at the time, steel tubes used instead. These were connected by bearings to transfer the hydraulic pressure to the hydraulic pump (shown in the background of Figure 2.2.3-A). Here, it was used to generate a rotational torque able to push the

test tyre into positive of negative longitudinal slip. This drive system was still in use up until late 2015 when it was replaced with a modern electrical system. Now the Calspan rig uses an industrial motor mechanically connected to the drive wheel, while a separate state-of-the-art rare earth metal motor is mounted to the back of the articulating head (shown in Figure 2.2.3-A). The new system allows for up to 11,000Nm of torque to be applied to the rig while also drastically reducing the required maintenance and down time. However, the biggest advantage comes with the quality of the new systems controls, where a near instant torque response from the head motor allows for a very smooth regulation into and out of longitudinal slip.

Figure 2.2.3-B. Calspan rig, Buffalo, NY, photographed in 2016. (Photograph provided by Calspan Cooperation, Buffalo, NY 2017)

The Calspan rig is also subject to future improvements; with the rig's slip angle system scheduled to be updated in late 2018. This improvement is intended to overcome the reduced precision brought on by excessive wear to the 46-year-old gears used in the rig's steering system. The scheduled replacement of these along with the installation of newer, more modern motors and control systems are expected to significantly improve the accuracy and responsiveness of the rig's slip angle regulation.

Unfortunately for Calspan, in the late 1970's their rig development engineers were better than their patent process and thus in 1980 MTS (MTS Systems Corporation) Eden Prairie, MI, began building and marketing a succession of competing rigs based on the Calspan rig. When doing

this, MTS also copyrighted the commonly used brand name ‘flat-trac’. A photograph of the first MTS designed flat-trac rig, then known as the ‘Flat-Trac 1’, can be found in Figure 2.2.3-C.

Figure 2.2.3-C. MTS ‘Flat-Trac 1’, photographed in 1980. (original source unknown, photograph provided by M’gineering LLC, Akron OH, 2017)

The MTS design of flat-trac rigs use a different structure to the Calspan rig. The MTS design uses an A-frame with pivots at the bottom that are aligned with the test surface. A separate linear actuator is then used to move the A-Frame on these pivots which changed the camber of the test tyre. This effectively separates the camber adjustments from the articulating head, instead the entire A-frame cambers which simplifies the overall design. The slip angle adjustment is controlled by fixing the hub (where the tyre is mounted) to a shaft which passes vertically through the top of the A-Frame. This shaft can rotate, which regulates the slip angle as well as slide up and down such that the vertical load can be regulated. The two drums used in MTS rigs are also much smaller in diameter than those of the Calspan rig, which helps reduce the cost of manufacturing the machine. Finally, a water bearing is used to support the test tyre rather than an air bearing. (References: Pottinger, 2002. Jenniges, Zenk and Maki, 2003)

MTS currently offer five versions of the flat-trac rig (MTS Overview, 2005). They start with the Flat-Trac Classic which is the simplest and cheapest rig that MTS offer. It is only capable of free rolling manoeuvres and even then, can only reach slip angle angles of +/-15° and speeds of

up to 150km/h (MTS Flat-Trac Classic, 2005). These capabilities are increased with the Flat-Trac SS (Steady State), where the maximum slip angle is +/-30° and the maximum speed is 200km/h (MTS Flat-Trac SS, 2005). Both rigs are free rolling only, meaning they lack the ability to test the tyre in the longitudinal and combined conditions, for this a drive motor needs to be added to the articulating head. This capability is included in the Flat-Trac CT (Cornering and Traction), which can apply up to 2800Nm of torque in the braking or driving direction to the test tyre (MTS Flat-Trac CT, 2005). However, this 2800Nm of torque proved to be a limiting factor for a lot of customers which led to MTS offering the Flat-Trac CT+. The CT+ is a broadly similar design to the CT; however, it uses a larger drive motor to apply up to 6000Nm of torque to the tyre. This Flat-Trac CT+ model has proved to be very popular with many tyre companies purchasing them for private use along with both FKA (FKA Flat-Trac IV CT plus, 2016) and Smithers Rapra (Smithers Rapra, 2017) who each purchased Flat-Trac CT+ rigs which can be used publicly. Finally, the top of the range Flat-Trac rigs offered by MTS is the Flat-Trac LTR and LTRe (Light Truck and Racing enhanced). These are identical rigs apart from the drive motor, with the LTR having a motor able to delivery 5000Nm of torque (MTS Flat-Trac LTR, 2005), while the LTRe can deliver 10,000Nm (SoVaMotion, 2015). These are both highly capable rigs designed to test tyres used in everything from passenger cars, to the very high vertical loads of 30,000N needed for light aircrafts and trucks, to speeds of up to 320km/h relevant for race cars. An MTS LTRe rig was commissioned in 2012 and became operational in 2013, operated by the National Tire Research Centre (NTRC) at SoVaMotion in Alton, VA. This $11.2 million piece of equipment was partly funded by General Motors who contributed $5 million. However, the rig is publicly available to anyone, including research institutions as well as race teams, tyre companies and car companies. A rendered CAD drawing of the MTS Flat-Trac LTRe rig can be found in Figure 2.2.3-D. (Reference: GM Corporate Newsroom, 2012).

Figure 2.2.3-D. Rendered CAD drawing of the MTS Flat-Trac LTRe rig. (GM Corporate Newsroom, 2012).

Overall the Calspan rig and the MTS Flat-Trac LTRe rig are similar in their capabilities. Both offering very similar maximum loads and torque ranges, while also being able to provide highly accurate data. The six-ton head of the Calspan rig acts as a mass damper, effectively minimising any noise brought on by chatter or similar vibration in the tyre. Conversely the much lighter head of the MTS rig allows it to move faster, hence it has far higher maximum slip angle rates compared to Calspan. A comparison of the testing capabilities of Calspan and SoVaMotion is shown in Table 2.2.3-A.

Table 2.2.3-A. Summary of Calspan and SoVaMotion rig capabilities.
(Calspan 2016, SoVaMotion 2014)

Overall it is clear that there are advantaged and disadvantages of each rig. Therefore, through this project data was obtained from both the Calspan rig in Buffalo, NY (referred to as Calspan), and the MTS Flat-Trac LTRe rig operated by SoVaMotion in Alton, VA (referred to as SoVaMotion).

2.2.4 Summary of Tyre Testing Facilities

Overall there is no single tyre test facility currently available that can offer everything that is required for force and moment testing without any compromises, this is shown in table 2.2.4-A.

	Lorry	**Wheel Force Transducer**	**Drum**	**Camber Ridge**	**Flat Belt**
Flat Surface	Yes	Yes	No	Yes	Yes
Realistic Surface	Yes	Yes	Yes	Yes	No
Repeatable	No	No	Yes	Yes	Yes
Available	Yes	Yes	Yes	No	Yes

Table 2.2.4-A. Summary of advantages and limitations of various tyre test facilities.

The outdoor facilities can test the tyre on realistic surfaces, such as tarmac or asphalt. This is shown to be important in Figure 2.2.2-G where the tyre's performance is shown to differ when tested on sand paper. However, outdoor testing typically has poor repeatability due to uncontrollable variables such as the local weather conditions. Therefore, indoor testing on sand paper is more precise with a high level of consistency and repeatability, while outdoor testing is

more accurate due to the correct surface but less precise due to the variable test conditions. These compromises can be overcome using drum testing, which offer indoors test conditions on realistic paved surfaces. However, these introduce a new error due to the curved contact patch, which cannot be fully overcome. The only facility that attempts to overcome these inherent compromises is Camber Ridge, which attempts to deliver indoor repeatable testing on flat asphalt. However, while this appears to be an excellent facility and a great new fundamental design. Camber Ridge was not fully operational in time for the technical development phase of this project. Therefore, regrettably no data from Camber Ridge is included. Overall, based on this study it was decided that the Calspan rig, used in conjunction with the SoVaMotion rig, was the best available option.

2.3 Test Procedures

The Magic Formula (MF) is an empirical tyre model that is very widely used and has been proven to consistently provide an accurate representation of the tyre behaviour measured on tyre test rigs. However, to deliver this accuracy, the model requires the curve fitting of many parameters, such that it precisely represents the test data. A large parameter set requires a wide range of physical testing to be performed on a rig and the cost associated with the extended use of a tyre test facilities can become a limiting factor. As such, it is important to run a test procedure which controls the tyre rig in an efficient manner.

2.3.1 The Need for a Test Procedure

Tyre test procedures are not trivial as there are many conflicting aspects to consider. Tyres are temperature sensitive; therefore, to isolate the influence of any given variable, such as slip angle, a tyre should be held at a constant temperature during testing. This, however, is not practical. As when slip angle is increased from zero the tyre's contact patch transitions into slip, leading to frictional induced heat, which changes the tyre's temperature. Therefore, in practical terms, tyre temperature and slip angle are intrinsically linked. This must be considered during a test procedure to ensure the tyre is tested at an appropriate set of temperatures and slip angles. Furthermore, as the tyre slides across the test surface it will wear. This permanently changes the performance of the tyre itself affecting the repeatability of the testing. Also, the tyre needs to be tested across a wide range of conditions to parameterise a tyre model; maximising this range will increase the range of conditions the resulting tyre model will be valid within. Increasing the density of tests within this range will increase the fidelity and sensitivity of the resulting model. However, this all adds to the number of unique tests that need to run, which causes more wear to the test tyre and adversely effects its consistency. Therefore, a compromise must be found between running sufficient tests across a wide enough range of conditions without excessively wearing the tyre. This can be addressed by using multiple tyres of the same construction and

assuming manufacturing inconsistencies to be negligible. However, a further constraint is that tyre rigs are very expensive to use. Therefore, an excessively large test procedure, using multiple tyre specimens, can ultimately prohibit the number of different tyres contractions that can be tested within a given budget. This is hence also not trivial and the efficiency of a test procedure needs to be carefully considered.

Significant investment and consideration goes into the development of tyre testing equipment. However, once operational, far less consideration appears to be put into how best to use these facilities; it is hence suggested that this is a largely under researched subject. Furthermore, organisations that do develop test procedures, such as car companies and tyre manufacturers, are often unmotivated to publish their work. Instead, they stand to gain a competitive advantage by protecting their test procedures as intellectual property. Publishing the work will allow the competition of the publishers' company to use the technology and hence likely benefit from it. Meanwhile, very few customers will purchase cars or tyres based on the technical papers and patents published by the manufacturer. Hence publishing this sort of technology serves to benefit the competition while offering no discernible benefit in terms of increased sales for the author. For this reason, much of the research and development of tyre testing procedures remains unpublished, hence there is very little referenceable material on the subject. (Smith and Blundell, 2016)

2.3.2 Square Matrix

A common method of testing tyres to gather data for the parameterisation of MF-Tyre 6.1 tyre model involves covering a full range of tyre states and is often known as the 'Square Matrix' test method. This is an approach commonly used in the industry to test tyres over a range of input variables including load, camber angle, slip angle and slip ratio. It was described by Blundell (Blundell, 2000) although at the time the term Square Matrix was not in common use. The 'Square Matrix Free Rolling, Braking, Driving and Combined' testing procedures described below are published in the documentation accompanying MF-Tool (a tyre model fitting software package available from TASS International, Helmond, The Netherlands). (Delft-Tyre, 2017. TNO Measurement Requirements, 2010)

Square Matrix - Free Rolling

For free rolling, Square Matrix testing, typically a pair of sweeps is selected to gather low slip angle data at a 'low rate'; followed by high slip angle data at a higher rate. An example of these is shown:

Low Slip Angle Sweep (LAT): 0 → -2 → +15 → -15 → +2 → 0° at 4°/s
High Slip Angle Sweep (HAS): 0 → -5 → +28 → -28 → +5 → 0° at 12°/s

The low slip angle sweep allows better data to be collected on-centre (close to zero slip angle), while the high slip angle sweeps allows data to be collected out to larger slip conditions. These two datasets can then be used to parameterise the respective sections of an MF-Tyre 6.1 tyre model (LAT used for on-centre and HAS used for high slip angle regions). Additionally, a set of load cases are selected covering a range of constant loads, camber angles and inflation pressures. An example of these values for an arbitrary road vehicle tyre is shown in Table 2.3.2-A:

	Loads (N)	**Camber Angles (°)**	**Inflation Pressures (bar)**
1	3480	0	2.1
2	6960	-5	2.6
3	8700	5	3.2
4	10440		

Table 2.3.2-A. Summary of a typical set of loads, camber angles and inflation pressures used in the Square Matrix 'FreeRolling' LAT test procedure.

The low slip angle sweep and the high slip angle sweep are then conducted at every possible combination of load, camber and inflation pressure. This generates a free rolling Square Matrix data set totalling 72 (two sweep types × four loads × three camber angles × three inflation pressures = 72) individual sweeps. Due to the effect of excessive tyre wear, these 72 sweeps cannot all be conducted on the same tyre. Instead up to six tyre specimens are used; though the exact number depends on the tyre construction and selected load cases. Typically, a new tyre will be used for each sweep type and each inflation pressure. This means 12 'Low Slip Angle Sweeps' are conducted on the same tyre specimen, one sweep at every combination of load and camber angle whilst all at one inflation pressure. A new tyre will then be used for each of the remaining pressures (using three tyres). This is then repeated for the high slip angle sweeps, meaning six tyres are used in total.

Square Matrix – Braking, Driving and Combined (BrkDrv)

Square Matrix braking, driving and combined testing (BrkDrv) is conducted in a similar way to free rolling testing. In this case, one slip sweep is used and repeated under the same load cases used in free rolling. An example of such a 'BrkDrv' sweep is shown below:

BrkDrv Sweep 0 → -5 → +50→ -50 → +5 → 0 slip ratio at 20%/s

This sweep is then repeated at each of the same vertical loads, camber angles and inflation pressures as described in the free rolling testing. This generates a set of pure longitudinal data, where the tyre is tested under a variety of conditions all at zero slip angle. In order to test the combined (braking and driving whilst steering) performance of the tyre these tests are repeated at a range of four slip angles, as shown in Table 2.3.2-B.

	Loads (N)	**Camber Angles (°)**	**Inflation Pressures (bar)**	**Slip Angle (°)**
1	3480	0	2.1	-2
2	6960	-5	2.6	0
3	8700	5	3.2	2
4	10440			5

Table 2.3.2-B. Summary of a typical set of loads, camber angles and inflation pressures used in the Square Matrix 'BrkDrv' test procedure.

The 'BrkDrv' sweep needs to be run at every combination of load, camber and inflation pressure and slip angle. This generates a longitudinal and combined Square Matrix data set of 144 (one sweep type × four loads × three camber angles × three inflation pressures × four slip angles = 144 sweeps) individual sweeps taking around 4.2 hours to run (not including tyre change times). As with the free rolling testing not all tests can be conducted on the same tyre specimen, though up to 12 tyres may be needed, depending on the specific tyre being tested.

Square Matrix - Summary

The Square Matrix approach is simple and the resulting data sets are easy to analyse and process. The approach also gathers the necessary force and moment data to parameterise the Magic Formula tyre models.

Assuming the tyre begins each sweep at a consistently low temperature, then the start of any given sweep will always be cooler than the end. As frictional induced heat will cause the tyre temperature to rise during the sweep, which in term can cause the tyre performance to change. To address this the direction of these test sweeps could be inverted, such that the tyre sweeps to the left (negative slip angle direction) first and then to the right (positive direction). If the wider test procedure was the assembled with alternating 'left first' and 'right first' sweeps this would better balance the temperature effect on the test results. However, such a provision is not stated in the referenced sauce material of this test procedure. (Delft-Tyre, 2017. TNO Measurement Requirements, 2010)

Gathering a full Square Matrix dataset following this method takes approximately eight hours of rig time (not including tyre change or rig reconfiguration times). Furthermore, for vehicle dynamics applications it is very inefficient. Testing symmetrically across all sweeps means data is gathered under load cases unobtainable in a real car. Moreover, if an additional load case is required, such as testing at an additional load; every camber and inflation pressure sweep needs to be conducted at this extra load; whereas in practice only some of the sweeps may be required. Finally, the test procedure assumes all the load cases are equally important but in fact it may be beneficial to gather additional data in more important areas, such as close to zero slip where additional cornering stiffness data can be used to increase the accuracy of the model in this region.

2.3.3 TIME

First published in 1999 by Van Oosten et. al. (van Oosten, J. J. M., et al), the TIME project was a collaboration of 14 partners aiming to develop a common tyre measurement procedure in order to make data from various sources more comparable. This was a very extensive study including comparing data from six different tyres tested on 11 different tyre test rigs.
Overall the TIME project was split into five separate work packages. The first was to investigate the differences between testing the same tyres on multiple different test rigs. All of which are different types of tyre test rigs within indoor laboratories. The second part was a parameter sensitivity study to explain any differences in the test results observed in the first work package. Work package three involved testing the tyres on appropriate vehicles to understand the forces and load conditions exerted on them under realistic driving conditions. These load conditions were then used in work package four, which was to develop a new tyre testing procedure that tested the tyre under similar conditions to what it is expected to experience while used on an appropriate vehicle. Finally, work package five involved validating this new test procedure across all the different indoor test rigs used in work package one. (Oosten, Augustin, Gnadler and Unrau, 1998)

As part of the development work, the TIME project also identified ‘not-realistic’ tyre testing conditions in existing test procedures particularly in terms of tyre temperature and wear. To address this a ‘cruising’ type test was proposed where the tyre is rolling while subjected to load conditions in a similar fashion to a real vehicle. This new test procedure includes three key sections: a warm up, to heat the tyre into a temperature state closer to its standard operating conditions; a linear sequence, to gather cornering stiffness data at small slip and camber angles; and a non-linear section, to gather tyre force and moment data at larger slip conditions.

The particular load cases used in the TIME test procedure are based on the tyre's load rating which is a valid way of directly adapting the test procedure to suit the tyre being tested.
The main limitations of the TIME test procedure are that it was developed for earlier versions of the Magic Formula which were used for the procedures' validation. Hence it does not include any testing to capture the effect of changing inflation pressure which was introduced later in MF-Tyre 6.1. Additionally, the procedure is steady state only and does not include any attempt to capture the tyre transient response.

2.3.4 MICH2MF

The MICH2MF tyre testing procedure was developed by Buisson at Michelin, Clermont-Ferrand, France (Buisson, 2006). It is a 'cruise' type of test procedure which aims to advance on the TIME procedure to ensure the tyre's thermo-mechanical behaviour is consistent with real driving conditions. In this paper, the author points out that current mathematical models do not capture the effect of tyre temperature and that a tyre's performance is dependent on its history. With both cornering stiffness and grip characteristics being temperature dependant and the tyre temperature depending on its preceding load conditions; it is therefore important for a test procedure to be as close as possible to the load cases placed on a tyre by a real vehicle when driving. Based on this, the load cases used in the MICH2MF test procedure are calculated using both the size and load rating of the tyre being tested; as well as the average load conditions observed by driving vehicles on the Michelin Ladoux 'number three handling track'. This is an excellent approach and one which clearly builds on the previous test procedures.
The procedure also includes repeated testing at three different inflation pressures to enable pressure interpolation. However, the latter section of the test needs to be repeated at each pressure, which is inefficient.
The MICH2MF procedure build on the 'cruise' type of testing presented in the TIME procedure and develops the idea further by linking the load cases directly to the loads exerted on the tyre by a real vehicle. This is a sensible idea and means the tyre is tested in a scenario much closer to its intended running conditions. This idea of managing temperature is also sensible when it is not captured in the tyre model. However, MICH2MF is a symmetric test procedure, where the vehicles' lateral weight shift is considered to determine the vertical load of the testing but this load is applied symmetrically to both positive and negative slip angles. This means that the tyre is tested under load cases that are unobtainable in a real car, which is inefficient.

2.3.5 Summary of Test Procedures

Based on analysing the existing test procedures the following observations were made:

- Square Matrix testing is highly inefficient, using significantly more rig time and tyre specimens than are necessary. This is largely due to the procedure requiring the tyre to be tested in load cases that are unobtainable in a real car.
- The TIME and MICH2MF procedures demonstrate a 'cruise' type test procedure which is shown to be much more efficient than Square Matrix testing.
- The cruise type test procedure can also be more similar to the load cases exerted on a tyre when fitted to a vehicle, meaning the tyre is tested under more realistic conditions.
- The TIME and MICH2MF procedures are developed for the older MF-Tyre 5.2 tyre models and do not intrinsically including testing at multiple inflation pressures, which is relevant when fitting the newer MF-Tyre 6.1 tyre models. To gather inflation pressure sensitivity when running TIME, the entire test procedure needs to be repeated at each pressure, which loses efficiency. When running MICH2MF the later part of the test needs to be repeated, which again is inefficient.
- The TIME and MICH2MF procedures shows that test loads can be linked directly to the tyre's load rating. This ensures that a suitable set of vertical loads is used for each tyre construction.
- The MICH2MF procedure highlights that the tyre's performance is dependent on its test history meaning the temperature of the tyre needs to be managed throughout the test procedure. It attempts to achieve this by appropriately distributing the sweeps within the test based on the effect they are expected to have on the tyre's temperature and installing appropriate pauses after each sweep for the tyre to cool. However, no control system is used to ensure the tyre has actually cooled down as required.
- None of the test procedures include an integrated section of testing to gather data pertaining to the tyre's longitudinal or lateral relaxation length. Furthermore, no testing is included in either procedure to test the tyre's vertical stiffness and its sensitivity to forward velocity.
- In both the TIME and MICH2MF procedures, testing is symmetrical which means the tyre is being testing at load cases that are unobtainable in a car.

Overall the TIME and MICH2MF test procedures show that there are techniques available that can significantly improve on both the efficiency and data quality of Square Matrix approach to tyre testing. Analysis of these newer approaches also reveals that they themselves can be significantly improved upon in several ways. These include: closely relating the tyre test conditions to the load cases exerted on a tyre be a vehicle, improving the thermal regulation of a tyre during testing, incorporating ancillary testing such as relaxation length and inflation pressure sensitivity, and further improving the test efficiency. (Smith and Blundell, 2016)

2.4 Tyre Models

Its impractical to test a tyre at every conceivable load case it may be subjected to while on a vehicle. Instead a tyre is tested at a select few load cases and a model is used to predict the tyre performance between those test conditions. The tyre model can then be used as part of a full vehicle simulation and ultimately used within a vehicle development programme. There is no one tyre model that can simulate every characteristic of a tyre; the closest to this is finite element modelling but this requires far too much computational overhead to be practical as a vehicle simulation component. Instead, various empirical models are used for different applications such as ride or handling.

2.4.1 Tyre Model Overview

The appropriate method of modelling a tyre depends on the intended application and can range from large physical models using a finite element approach to represent the tyre structure and materials, to empirical models that represent the forces and moments measured in the tyre contact patch using a tyre test rig. The finite element approach requires detailed and confidential information regarding the tyre's material properties and construction; it is therefore best used internally by tyre manufacturers or for specialist research applications. (Guo, Bastien, Blundell and Wood, 2014)

Outside of tyre manufactures semi-empirical tyre models such as FTire (Gipser, 1999), CDTire (Gallrein, Baecker, Burger and Gizatullin, 2014) and RMOD-K (RMOD-K 7, 2016) are often used for ride analysis. These approaches are still very complex in their structure and resemble a hollow finite element method, where the tyre is represented by a discretised shell (FTire) or a flexible rim (CDTire and RMOD-K) along with a series of complex spring and damper assemblies. These models are semi-empirical models parameterised based on physical tyre tests along with measurable tyre geometry and construction information. Crucially this means they do not require the confidential tyre construction information needed to build finite element tyre models and therefore they can be used effectively outside of tyre manufacturers. However, a limitation of these models is that they are just barely real time capable. Where even with some of their functionality disabled to reduce computation overhead, a very powerful computer is required to run four of these tyre models simultaneously along with a vehicle model. This real-time capability is a pre-requisite for many vehicle dynamics tasks such as using a driving simulator which include a human-in-the-loop, where a human driver directly controls the vehicle model. Furthermore, while being suitable for ride simulations they are typically ineffective for handling simulation due to limitations in their friction models; however, ongoing developments into friction modelling techniques are likely to improve this.

Friction models often represent the tyre's contact patch as a brush, where the contact patch is discretised into bristles with the tip of each bristle contacts the road surface. One such model is the LuGre friction model which can be used to estimate pavement friction using data obtained from a locked wheel skid trailer (Rajapakshe, Gunaratne and Kaw, 2010). A complimentary method for thermal friction modelling is presented by Bo Persson, Forschungszentrum Jülich, Jülich, Germany, where surface roughness is measured and a master curve representing friction, sliding velocity and temperature is established. This master curve is then scaled based on the viscoelastic properties of the rubber (Lorenz, Persson, Fortunato, Giustiniano and Baldoni, 2013).

Despite these advances in technology, physically modelling friction and tyre behaviour will always be complex and challenging. Therefore, fully empirical models have proven to be the most widely used for simulating handling manoeuvres. Many researchers have developed handling models to support this; these include the Harty (Blundell and Harty, 2006), Fiala (Fiala, 1954) and TMEasy (Rill, 2013) models which use reasonably simple sets of equations to represent the tyre performance data generated via physical testing. The models offer significant advantages over spline fits or polynomial based models, where a single function may accurately represent a single tyre test case; however, there is no natural way to scale between load cases. An alternative approach to this is the Milliken non-dimensional tyre model (Kasprzak, Lewis and Milliken 2006) which builds on the work presented by Sharp and Bettella (Sharp and Bettella, 2003). The method works by normalising the test data such that various sweeps at different load conditions can be normalised into a single curve. This single curve can then easily be represented by any suitable equation and this combined with the normalisation factors can be used to represent the tyre's behaviour. These methods of normalisation can also be used in conjunction with the popular Magic Formula tyre model, although with the Magic Formula normalising is optional but not required like it is with the Radt/Milliken model.

Finally, another approaching to modelling tyre handling behaviour are the more complex thermo-mechanical models such as TaMeTirE (Durand-Gasselin, Dailliez, Mössner-Beigel, Knorr and Rauh, 2010). TaMeTirE is a temperature sensitive handling tyre model developed by Michelin, Clermont-Ferrand, France. It consists of three different models: a mechanical model of the tyre structure, a model of the rubber compound and a contact patch thermal model, all of which are assembled together to form TaMeTirE. The approach offers accurate, thermally sensitive tyre models that also include physical tyre attributes that can be tuned to estimate the effects of changing some aspects of the basic tyre construction. MuRiTyre which is developed by Wirth Research, Bicester, England, uses a similar approach; it is a multi-rib tyre model that contains various sub models for contact patch shape, friction and temperature amongst others

(Trevorrow and Gearing, 2015). However, MuRiTyre offers a few advantages over TaMeTirE. Firstly, the fidelity of MuRiTyre can easily be scaled depending on the required accuracy and available computational power. Secondly, TaMeTirE requires a specific set of data for the parameterisation, whereas MuRiTyre can be parameterised using almost any tyre data set; although the resulting model will only be accurate within the ranges of whatever data set is used. This is particularly useful in racing where formal tyre testing is often banned or not practical, in this case MuRiTyre models can often be parameterised using data directly from the instrumented race car.

2.4.2 Magic Formula

Over recent decades the most widely used tyre model is that developed by Pacejka and his associates. Originally referred to as the Magic Formula tyre model, this model is now commonly known as the MF-Tyre model and has been developed through many iterations, during which time its capability and the number of associated model parameters has been extended. The version of the Magic Formula model that forms the basis of the study presented here is the MF-Tyre 6.1 model, published in 2010 by Besselink et al (Besselink, Schmeitz and Pacejka, 2010). The wide-ranging capability of the model extends its usage from fundamental vehicle dynamics applications to more advanced studies such as research into anti-lock braking systems and traction control (Cadiou, Hadire and Chikhi, 2004). The main reason for MF-Tyre becoming so popular, is that it is technically mature and refined enough to offer accurate tyre modelling, while also being entirely open source, with all the models equations available in Pacejka's book (Pacejka, 2006) and journal papers. This means the capability of MF-Tyre is higher than most other open source tyre models whilst the licencing of the model itself is free. As a result, the model is widely integrated into a multitude of full vehicle simulation software, such as ADAMS (MSC Adams, 2017) and IPG CarMaker (IPG CarMaker, 2017), as well as tyre modelling fitting software such as MF-Tool (Delft-Tyre, 2017) and OptimumTire (OptimumTire, 2017).

The Magic Formula (MF-Tyre) model is an empirical tyre model developed for handling based vehicle dynamics modelling. It is designed to replicate force and moment tyre test data for pure lateral cornering, braking, driving and combined handling conditions. The Magic Formula model was first developed as a joint venture between Volvo, Gothenburg, Sweden, and Delft University of Technology, Delft, Netherlands (Bakker, Nyborg and Pacejka, 1987). At that time, the model was only valid for steady state pure cornering and braking. However, lateral and longitudinal forces as well as self-aligning torque were described accurately. In 1989 the Magic Formula model was updated to include combined cornering and braking, as well as plysteer,

conicity and rolling resistance (Bakker, Pacejka and Lidner, 1989). It was in this paper that the defining form of the Magic Formula as shown in Equation 2.4.2-A was first published.

$$Y(x) = D\sin(C\tan^{-1}(Bx - E(Bx - \tan^{-1}(Bx))))$$

$$Y(X) = y(x) + S_V$$
$$x = X + S_H$$

Equation 2.4.2-A, Magic Formula equation in its general form.
(Bakker, Pacejka and Lidner, 1989)

In this general form, Y(X) stands for either force or moment in the lateral or longitudinal direction and X represents the slip condition. The other parameters include:

B = stiffness factor
C = shape factor
D = peak factor
E = curvature factor
S_V = vertical shift
S_H = horizontal shift

In 1991 the tyre model was updated, (Pacejka and Sharp, 1991) then again in 1992 where Pacejka and Bakker (Pacejka and Bakker, 1992) published further updates to the Magic Formula model (now called "Version 3 of the Magic Formula"). Within this version lateral asymmetry was captured, as well as a more accurate representation of camber and accelerating forces. However, the transient response of the tyre was still not included; this was discussed in 1995 (Pacejka, 1995) and later published in 1997 (Pacejka and Besselink, 1997), by which time the model was now called "Delft Tyre 97". This version of the Magic Formula model employed concepts of pneumatic trail and residual torque to better model the self-aligning moment. It was also the first time that the relaxation length of the tyre was included in the model.
In 2010, a significant update to the Magic Formula was published (Besselink, Schmeitz and Pacejka, 2010). This expanded on the existing versions of the Magic Formula to include inflation pressure scaling such that the tyre model could be set by the end user to any inflation pressure within its tested range. Furthermore, improvements were made to the non-linear transient model and the ability to cope with high camber angles was included for motorcycle applications.

Throughout its development, the various versions of the Magic Formula tyre model have been widely used across the automotive industry as well as in academia for automotive handling applications.

2.4.3 Conclusion on Tyre Models

A very wide variety of different tyre models exist around the world which are used for all manner of different applications. In the automotive sector, a tyre model is only useful if it can be included in a full vehicle simulation. This constrains the useful tyre models to those that are compatible with the full vehicle simulation software used by car companies. Commonly used full vehicle simulation such as MSC ADAMS (MSC Adams, 2017), IPG CarMaker (IPG CarMaker, 2017), Simulia SimPack (Simulia SimPack, 2017) and VI-Grade (VI-Grade, 2017) who all support the TASS International, Delft-Tyre solver which enables the use of the Magic Formula tyre models, the most recent of which is MF-Tyre 6.1. This ease of compatibility, combined with the Magic Formulas ability to offer a good representation of the test data has led to it being the most widely used tyre model available, particularly for handling simulation. For this reason, MF-Tyre 6.1 is selected as the tyre model used throughout this project.

2.5 Tyre Model Parameterisation

Most organisations who use empirical models such as MF-Tyre 6.1, parameterise the models using their own proprietary software containing intellectual property which is rarely made public. Developing such software is possible since the Magic Formula is open source and can hence be coded into software such as MATLAB (MathWorks, Natick, MA). This allows organisations to have more control over exactly how the models are parametrised. This means they can focus on correlation of tyre models in key areas of importance, or batch processing the fitting process or developing advanced fitting techniques to improve the resulting models. This ultimately leads to a competitive advantage which the authors rarely publish; however, some papers are available that describe the fitting process.

2.4.1 Optimisation algorithms

Parameterising an MF-Tyre 6.1 tyre model from test data is not trivial. Instead an optimisation algorithm must be used due to the large number of coefficients present in the formulation and the fact that the tyre model is highly non-linear. There are various different optimisation algorithms that can be used to fit a Magic Formula tyre models with varying amounts of success. These include least-square minimisation, genetic algorithms and neural networks amongst many others. However, a persistent problem is that many of them require very accurate initial guesses of each coefficient. This may be possible if the user is modelling a tyre which is known to perform similarly to a tyre that they have already modelled. In such a scenario, the fitted coefficient from the first tyre model can be used as good initial guesses for the second tyre

model. However, if no such previous model exists then there is no clear way to generate the initial guesses. This leads to a problem, as initial guesses which are far from the ideal solution can cause the optimisation algorithm to diverge and become unstable, or converge on sub-optimal local solution.

Van Oosten (Van Oosten, 1993) published a paper detailing the optimisation method used within a bespoke software tool. Here it is stated that the software, written in Fortran, uses a subroutine 'E04FDF' to perform the optimisation, this is an unconstrained sum-square minimisation for nonlinear functions. The approach is commonly used in modelling, where the sum of the squares of the difference between the model and equivalent measured data point is minimised. Doing so, effectively reduced the error between the model and the test data, thus iteratively improving the fit. The approach is very robust; however, due to constraints in the software, only a limited number of data points can be used, 1,500 data points for pure slip fits and 2,000 combined fits. This is very constrictive when using larger data sets and can result in the data sampling rate having to be reduced to reduce the number of data points. It also effectively rules out the use of 'cruise' type test procedures such as TIME and MICH2MF which generate large amounts of data. More recently, this problem can be eased slightly by the availability of more powerful computing systems and newer Fortran compilers (Fortran version 5 was used in this case). However, the data point limitation cannot be overcome completely. Furthermore, the approach requires accurate starting values to converge quickly, if these are not valuable then the method remains robust but is slow to converge.

In 2004 a new method of determining the Magic Formula tyre model parameters was published that was based on the use of a genetic algorithms (Cabrera, Ortiz, Carabias and Simon, 2004). The approach builds on the approaches the Simplex search algorithm (Nelder and Mead, 1965) and the Neuro-Tyre optimisation process (Palkovics and El-Gindy, 1993). The result being a genetic technique that is simple to implement and converges quickly on a solution. Also discussed is that a randomly selected set of starting value can be used and the approach still converges on a reasonable solution. The findings of this study were further discussed in 2006, when the fitting method was named IMMa Optimisation Algorithm (IMA) (Ortiz, Cabrera, Guerra and Simon, 2006). Here, the benefits of the convergence rate, ease of implementation and lack of a need for accurate starting values are again demonstrated. In this case with a more robust sensitivity assessment of the starting values.

A broader assessment of six different parameterisation approaches was presented in 2014 (Alagappan, Narasimha Rao and Krishna Kumar, 2014). Here the authors point out that while the IMA approach is robust and able to use randomly selected starting values, it requires the

optimisation to be bounded. This means some prior knowledge of the search area is still required before a fit can be initiated. Also demonstrated, is that most algorithms that work well in certain situations perform poorly in other situations; finally concluding that the three most robust approaches are: trust region reflective (Coleman and Li, 1996), differential evolution (Storn and Price, 1997) and bounded cuckoo search (Yang and Deb, 2009).

2.5.2 Tyre Model Toolkits

Most Magic Formula tyre model parameterisation tools are developed internally within companies and not made public. However, despite this, off-the-shelf Magic Formula parameterisation software is available, such as MF-Tool (Delft-Tyre, 2017) and OptimumTire (OptimumTire, 2017) amongst others. MF-Tool is developed by TASS International, Helmond, The Netherlands, which is an organisation linked with the Delft University of Technology, Delft, Netherlands which is where Professor Hans B. Pacejka developed the first formulation of the Magic Formula tyre model (Bakker, Nyborg and Pacejka, 1987). MF-Tool offers a straight forward Magic Formula parametrisation solution; however, it is more suited to the Square Matrix or similar test procedures as it does not support the constantly varying load cases generated by more complex test procedures. OptimumTire, developed by OptimumG, Denver, Colorado, can parameterise Magic Formula models using constantly varying load cases and is hence the selected software.

The parameterisation method used within MF-Tool is based on tools with the MATLAB optimisation toolbox (MATLAB Optimization Toolbox, 2017). While the optimisation algorithm used in OptimumTire is stated only as a ‘genetic algorithm’, with no further information given. It is understood that neither organisation want to share their fitting methods for fear of losing their competitive advantage. This mirrors a common occurrence across the tyre testing and modelling landscape where organisations are often secretive and rarely publish technical material due to intellectual property concerns.

2.6 Literature Review Summary

The presented literature review covers a wide range of tyre related areas; ranging from tyres themselves, through to test rigs and procedures to run on these rigs, onto tyre models and then optimisation approaches to parameterise these tyre models. In compiling all the published material together, it became apparent that tyre test procedures are a heavily under researched area. This is evident by the distinct lack of published material on the subject.

2.6.1 Literature Review Analysis

There is a large and rich pool of material covering tyres themselves. This includes several books, hundreds of papers and other material that covers all the various aspects of tyre’s themselves. Such as their construction, inner workings, materials and different performance

attributes, a selection of which are referenced here. Tyre testing facilities and equipment is again a well-documented area. While there are relatively few peer-reviewed journal papers there are numerous technical reports, patents and benchmark studies that cover various aspects of test rig design and operation.

When researching into existing tyre test procedures it was found that there is very minimal published material available. There are some documents covering the Square Matrix test procedure and its variations; however, these are all variations of the same basic idea and generally do not present anything fundamentally new. The TIME project does present a new method of a 'cruise' type of test procedure and demonstrates some advantages of it. This is reinforced by the MICH2MF paper which builds on the ideas presented in TIME. Aside from these, no other relevant test procedure publications were discovered. It is hypothesised that additional test procedures exist; however, these are developed by companies and retained as confidential intellectual property rather than being published. This suggests that further published research into test procedure design will be of value to the wider tyre engineering and testing community.

Like tyres themselves, the area of tyre models is also very well documented, with hundreds of tyre models developed and published around the world being used for various specific applications. Of this, a handful of models are more commonly used and discussed here, with the Magic Formula being the most widely used and is highly relevant for this thesis. There are dozens of papers specifically on the Magic Formula itself as well as on its parameterisation; a selection of which are referenced. Furthermore, there is wealth of available material on optimisation and curve fitting in general, with a good selection of material specifically on fitting tyre models.

Overall it is identified that the area of tyre testing procedures is an under researched and under published area with minimal published information available. Furthermore, this area is important to anyone using the very common Magic Formula tyre model, as well as organisations testing tyres for performance benchmarking or other applications. Furthermore, the analysis of the Square Matrix test procedure revealed many flaws which could be addressed. While dissemination of the TIME and MICH2MF procedures revealed that each of them present excellent and innovative approaches to tyre testing; however, they each have shortfalls and there is plentiful scope for further improvement.

2.6.2 Literature Research Influence on Present Research

It became clear from the literature research that there is significant scope to improve on the existing tyre test procedures. Also apparent, is that various versions of the Magic Formula tyre model are by far the most widely used for handling simulation across the world and the latest version of the model (at time of writing) is MF-Tyre 6.1. Therefore, an improved tyre testing procedure will be developed to provide data for the parameterisation of MF-Tyre 6.1 tyre models. The majority of the testing will be carried out using the Calspan rig with additional testing conducted at SoVaMotion. These are two of the leading facilities in the world able to provide high quality data to support the test procedure development. Once testing is complete, the tyre model will be fitted to the data using OptimumTire developed by OptimumG, Denver CO. OptimumTire is an advanced fitting tool that supports the latest version of the tyre model and (unlike MF-Tool) is also able to facilitate the fitting of the model to large datasets.

The development of the new test procedure will be a complex process and must consider numerous, often conflicting, objectives (such as balancing the need for a large data set to maximise the fidelity and valid range of the model with the need to minimise rig time and cost as much as possible). Therefore, the development of the test procedure shall be broken down into separate technology components. This allows each isolated technology to be developed and then later integrated into a complete test procedure.

Upon successful completion, the final test procedure shall be named after its creator, the tyre model it provides data for and in recognition of the test procedure from which it is inspired. To that end the new test procedure shall be known as: GS2MF, Gregory Smith (to) 2 Magic Formula, in a naming format consistent with MICH2MF.

3.0 GS2MF Technology Components

The GS2MF test procedure is in fact three separate tests conducted on two specimens of the same tyre construction. The first test is ‘GS2MF FreeRolling’, where the tyre is mounted to the test rig such that it can freely rotate about its Y axis, thus ensuring a free rolling state with zero slip ratio. This procedure is primarily used to test the cornering performance of the tyre as well the lateral relaxation length and rolling radius. The second test ‘GS2MF BrkDrv’, requires the test rig to be able to control the slip ratio of the tyre. This procedure is used to test the tyre’s braking and driving performance while under pure longitudinal conditions as well as combined longitudinal with steering conditions. The third test, ‘GS2MF StaticLong’, is a simple static test procedure designed to gather data pertaining to the tyre’s longitudinal stiffness, this can then be used to calculate the tyre’s longitudinal relaxation length.

The primary reason for separating the tests is that some facilities require the rig to be reconfigured to support these test modes. The data presented here was obtained from the Calspan and SoVaMotion rigs. At the Calspan facility, the ‘GS2MF FreeRolling’ tests are run with the rig 'un-coupled' meaning the tyre is not connected to the drive motor and is free to rotate around its Y axis, this ensures a pure free rolling test condition. The ‘GS2MF BrkDrv’ and ‘GS2MF StaticLong’ tests are run with the rig in its 'coupled' configuration, meaning the tyre is mechanically linked to the drive motor allowing its longitudinal slip ratio to be controlled.

All the data presented is from various specimens of a particular 255/55R20 110W high performance SUV All-Season road car tyre, mounted to an 8.5J lab wheel. The exact tyre used shall remain confidential to anonymise the presented data.

3.1 GS2MF Fundamental Overview

GS2MF is a flat-trac tyre testing procedure used to generate suitable data for the parameterisation of MF-Tyre 6.1 tyre models to be used in the full vehicle simulation of road cars. Inspired by MICH2MF and TIME2, it is designed to overcome some of the limitations of more traditional Square Matrix style test procedures.

GS2MF moves away from the Square Matrix approach of conducting a test sweep at every possible combination of input conditions and replaces this with a 'cruise' type test procedure as used in MICH2MF and TIME2. A cruise type test procedure places the tyre under load cases similar to those it would experience when driven on a physical vehicle. Whereby, the tyre is run on a flat-trac rig from the start to the end of the test through a series of load cases in between. Using such a test method, GS2MF aims to better link the tyre testing to load cases the tyre will be subjected to when used on a vehicle. GS2MF also aims to significantly reduce the overall rig

time required to gather all necessary data which will reduce the financial cost of the testing. While reducing costs, GS2MF also aims to improve on the data quality by reducing hysteresis as well as better managing the tyre temperature variations during testing.

GS2MF consist of two separate test procedures, these are: 'FreeRolling' and 'BrkDrv'. Each of these test procedures consist of multiple sections designed to gather different types of data relevant to fitting MF-Tyre 6.1 tyre models. These test sections along with key components of the GS2MF test procedure are detailed in the forthcoming chapters.

3.2 Rig Limitations and Constraints.

When developing a test procedure, it is important to consider the limitations of the rig that will be used to run the test. GS2MF is designed to be run on flat-trac rigs and hence needs to work within the limitations of these rigs. The primary rig used in the development of GS2MF is the Calspan rig, though GS2MF has also been run successfully on the SoVaMotion rig. Both rigs offer some of the highest possible capabilities available worldwide, nonetheless there are still limiting factors that need to be considered.

3.2.1 Rig Configuration - Coupling

To parameterise MF-Tyre 6.1 tyre models it is important to obtain data that isolates the tyre's pure cornering behaviour. To acquire this data testing must be conducted with the tyre operating in a true free rolling test condition (where the tyre is free to rotate about its Y axis ensuring a constant slip ratio of zero). If the slip ratio is not zero, a proportion of the tyre's capacity is being used to generate longitudinal force, meaning the tyre is under a combined test condition where less lateral force will be generated at any given slip angle.

To ensure a true free rolling condition is achieved the operators at Calspan physically remove a drive shaft connecting the wheel and tyre assembly to the drive motor; thus ensuring the tyre is completely free to rotate about its Y axis. SoVaMotion use a very different design of flat-trac rig where removal of such physical connections is not possible. Instead a control system commands the drive motor to apply torque as necessary to compensate for the drive motors own internal inertia. The advantage of such a system is that free rolling and brake drive testing can be conducted without ever having to reconfigure the rig, leading to both less down time between tests as well as more flexibility in test designs. The main disadvantage is in the quality of the test data. Most notably the level of noise in the overturning moment (MXW) channel is far higher when the drive motor is connected. The Calspan rig can use a similar system to run free rolling testing while coupled but the additional noise in the overturning moment channel is very significant. This is shown in Figure 3.2.1-A.

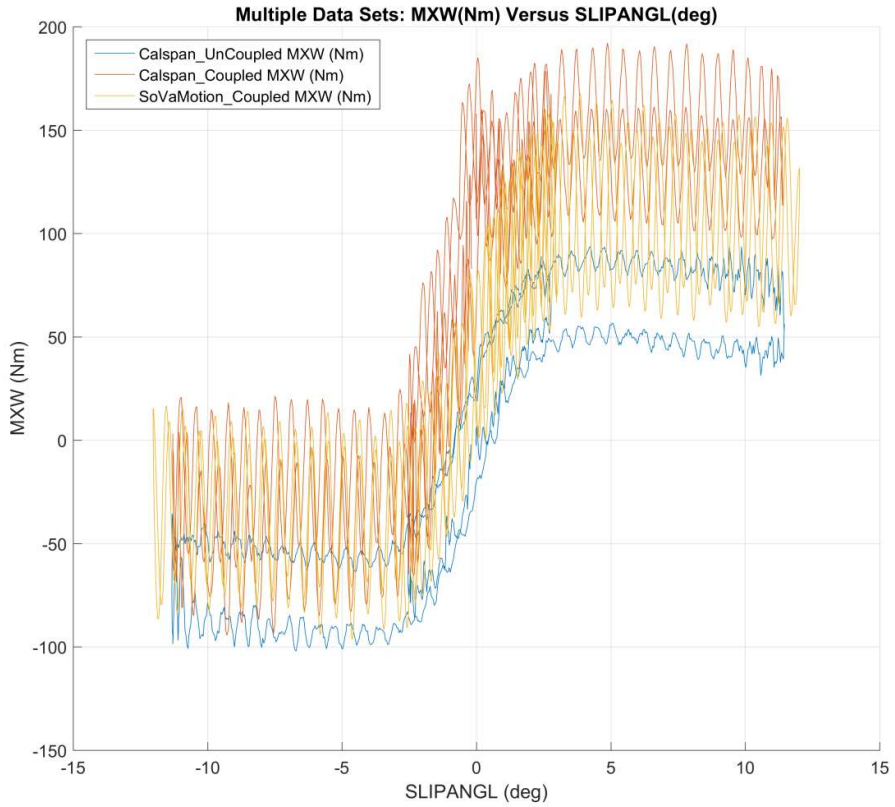

Figure 3.2.1-A. Data Comparison of Calspan Un-Coupled, Calspan Coupled and SoVaMotion Coupled, for Overturning Moment, MXW (Nm) versus Slip Angle, SLIPANGL (°).

Figure 3.2.1-A shows a comparison of un-coupled test data from Calspan with coupled data from Calspan as well as coupled data from SoVaMotion. The plot shows the significant increase in noise that comes from either rig when the drive system is physically coupled to the wheel and tyre assembly. This noise is caused by very slight misbalancing or misalignment in the test rigs. Un-coupling the drive motor reduced the effect of any such misalignment. Most notably, the hysteresis in the overturning moment is only visible in the un-coupled Calspan data. This hysteresis is completely lost within the noise of either data set obtained via coupled testing. For this reason, it was decided that whenever possible 'GS2MF FreeRolling' should be run with the rig's drive system un-coupled. This dictated the need for GS2MF to consist of two separate test procedures ('FreeRolling' and 'BrkDrv'), however such an approach also means GS2MF can be run on either type of rig without any alterations.

If either rig can improve their testing systems and reduce the overturning moment noise when coupled; then there could be an opportunity to update GS2MF to take advantage of not having to reconfigure the rig. This could involve redistributing the testing across the two GS2MF test procedure ('FreeRolling' and 'BrkDrv') such as to better balance the tyre wear between them;

or if the test tyre's durability allows, the two procedures could be combined into one, thus only requiring one tyre specimen to run.

3.2.2 Rig Performance Limitations

Both the Calspan facility and the SoVaMotion flat-trac rig are designed to test a very large range of tyres, including those from: aircraft, large trucks, all sizes of road cars and race cars amongst others. To achieve this, they are extremely powerful and able to apply test loads and torques that are far in access of what is required for typical road car tyre testing. For this reason, most of the requirements of GS2MF are well within the limits if the rig's force and moment operating capabilities. However, the design of these rigs to withstand such large forces necessitates a very strong and unavoidably heavy construction. This weight results in them not being able to change from load case to load case as quickly as would be ideal. This is particularly evident in the Calspan facility where the articulating head weighs around six tons. With such a heavy mass, its slip angle control system is only able to move the head at a maximum of 12°/s. This proved to be the only significant constraint in the rig's capability and was especially relevant when designing the variable rate steering sweep as detailed in forthcoming chapters.

3.3 Vertical Load Linked to Tyre Load Rating

When designing a flat-trac test procedure, it is important to consider what the test data and resulting tyre model will be used for. From looking at how the tyre model is going to be used it is possible to decide upon the required range of conditions that the model must be valid across. This information can then be used to determine the required range of test conditions that need to be included in the data that is used to populate the resulting tyre model. Using such an approach; the range of slip angles, slip ratios and camber angles can be decided upon based on the slip conditions observed during relevant manoeuvres with a physical or simulated vehicle. In a similar way, the required range of forward velocities in most cases can be set based on the common usage of the vehicle. This will be valid for most road cars but may need to be reconsidered when testing tyres for super high-performance road cars or race cars. The same is true for inflation pressures, which on road cars typically fall within a reasonably consistent range. However, the vertical load does not only depend on the required manoeuvre and use case but also the vehicle itself. A heavy vehicle, such as an SUV, will put more load into each tyre than a lightweight sport car, even when doing similar manoeuvres. Therefore, tyres intended to be used with these different vehicles can be tested under the same slip angles, slip ratios, camber angles, forward velocities and inflation pressures, but not under the same vertical loads. For this reason, the vertical loads used during GS2MF need to be defined as factors of a nominal load and this nominal load need to be dependent on the vehicles weight.

Unfortunately, using the vehicles weight directly as an input to the test procedure causes practical problems. Firstly, the vehicle weight is often not known at the point of testing the tyres. This is because within a vehicle OEM's product development process, tyre testing and building MF-Tyre 6.1 tyre models is often carried out early on, well before final vehicle weights have been established. Secondly, the vehicle weight is not an absolute value and is not constant. Instead the vehicles weight changes depending on several factors, such as: the specification of the individual vehicle, the number of passengers, luggage and fuel in the vehicle amongst others. A more robust approach is to consider that GS2MF is a procedure to test the tyre, not the tyre and vehicle together. Therefore, instead of the GS2MF nominal load being dependant on the vehicles weight directly, it is instead dependent on the tyre's load rating. The assumption being that the tyre (and resulting tyre model) of given load rating are suitably matched to the vehicle. This is a reasonable assumption as vehicle manufactures are well placed to do this.

With the tyre's load rating being an absolute value the GS2MF nominal load is defined as 65% of the tyre's ETRTO load rating (ETRTO Standards Manual, 2017). The numerous actual test loads are then defined as factors of this nominal load. The range of these test loads are detailed in Table 3.3-A where a tyre with an ETRTO load rating of 110 is used as an example.

Table 3.3-A shows the range of load factors for the 'GS2MF FreeRolling' and 'GS2MF BrkDrv' test procedure. The example shown is for a tyre with a load rating of 110. This equates to a load rating of 1,060kg according to the ETRTO standard, or 10,388N (1060kg × 9.81m/s^2 = 10,388N); 65% of this load rating gives a nominal load of 6,752N (65% of 10388 = 6,752N). The tested loads within GS2MF are then defined as factors of this 6,752N nominal load. 'GS2MF FreeRolling' tests the tyre between 0.4 and 2.0 times the nominal load, which in the example shown equates to a tested range of: 2,701 to 13,504N. For 'GS2MF BrkDrv' the range is 0.25 to 2.25, which in this example equates to a tested range of 1688 to 15,192N.

	Load Factor	**Example Test Loads, (N)** Tyre Load Rating: 110 Nominal Load: 6,752
'FreeRolling' Minimum Load	0.4	2,701
'FreeRolling' Maximum Load	2.0	13,504
'BrkDrv' Minimum Load	0.25	1,688
'BrkDrv' Maximum Load	2.25	15,192

Table 3.3-A. Summary of the load factors used in GS2MF and example test loads for a tyre of load rating 110.

Tyres are designed to operate above their load rating for short periods of time, such as in emergency manoeuvres. The load rating is the maximum 'every day' load the tyre will be subjected to. It is therefore necessary to test a tyre at 15,192N when it is only rated at 10,388N as shown in the example. This is because while a vehicle may place up to 10,388N onto the tyre during normal driving conditions, this load could increase substantially during an extreme manoeuvre such as a double lane change. The resulting tyre model built from this data will be used to investigate how the vehicle behaves during such manoeuvres so gathering data in this range of loads is important.

3.4 Warmup

A tyre's performance can change significantly depending on its temperature. Race tyres for example need to have extremely high levels of peak performance. To deliver this tyre, manufacturers maximise peak performance in various ways but this usually compromises the tyre's operating window. This means race car tyres must be hot and maintained within a very small temperature range to work effectively. Conversely, road car manufacturers want their tyres to be as thermally insensitive as possible. This makes their cars more consistent and predictable to drive in all weather conditions making them safer for everyday drivers; however, this comes at the compromise of outright performance. Therefore, an attribute balance must occur between the tyre's thermal consistency and ultimate performance. Car companies cannot compromise all the tyre performance to gain near perfect thermal consistency as this will unfavourably compromise the dynamics of the vehicle. Inevitably this leads to road car tyres being thermally sensitive, even if not as sensitive as race car tyres. When testing road car tyres on a flat-trac rig, it is therefore important to take the tyre temperature into account. As any tests conducted when the tyre is cold will not be representative of the tyre's warm performance. For this reason, it is important to warmup the tyre at the start of the test procedure before normal testing can commence. (Phelps 1976)

To investigate the required warmup procedure a test was conducted to establish exactly how warm the tyre needed to be. Ideally this would be close to the tyre's operating temperature when being used on a car but this 'running temperature' is impossible to define. Road cars are bought and used all over the world in radically different climates and driven in very different ways, therefore the running temperature could be as low as -30°C for cars used in the arctic circle but up to over 100°C for cars used on track days. A range this wide is not useful and hence a different approach was needed. To facilitate this, a block of five Graph Sweeps were created (as described in section 3.9 on Graph Sweeps). These sweeps consisted of testing the tyre at nominal load, which is based on the tyre's ETRTO load rating, at 0, -3 and +3° of camber; after which an additional two sweeps were conducted at zero camber but 3000N above and 3000N below the nominal load. These load conditions are well within the usual operating condition of the tyre and hence the temperatures achieved during these sweeps will be close to what the tyre will experience when under similar conditions on a car. To observe how the tyre temperature responds to these sweeps this block of Graph Sweeps were repeated eight times to ensure the tyre temperature was fully stabilised. The results of this test are shown in Figure 3.4-A.

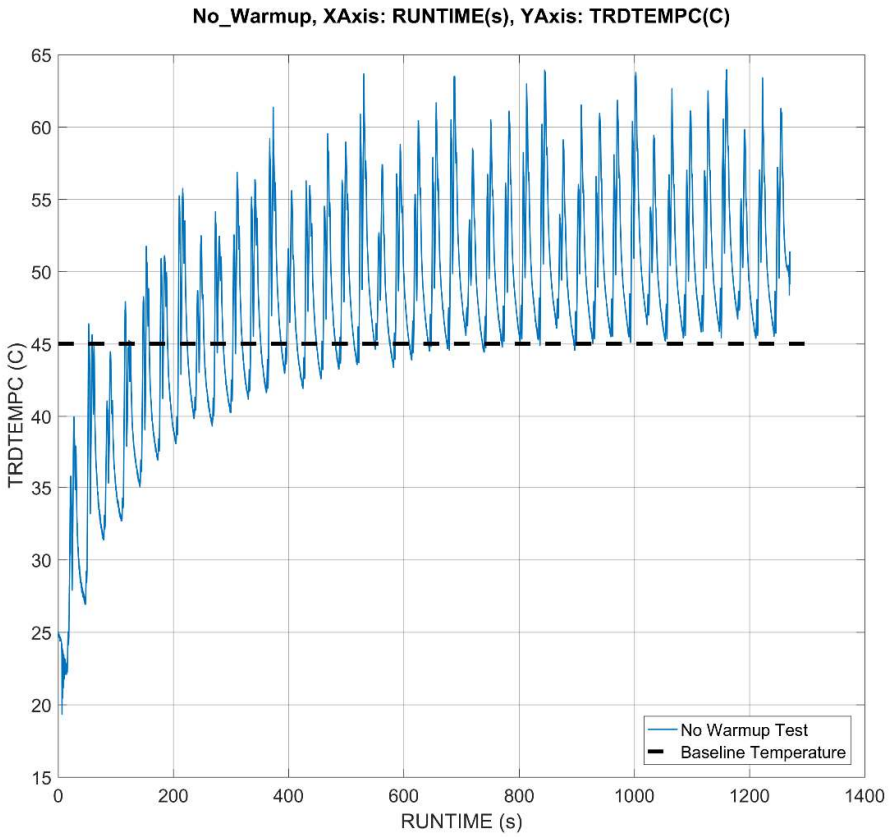

Figure 3.4-A. Tyre tread temperature, TRDTEMPC (°C) versus Runtime, RUNTIME (s). Repeated Graph Sweeps without a warmup, also showing the 45°C baseline temperature.

Figure 3.4-A shows that the tyre temperature started at around 20°C (room temperature) and then increased until around 600s into the test. After this point the temperature stabilised into a constant pattern. The pattern involved the tyre heating to between 58 and 64°C during each sweep before cooling down to around 45°C between each sweep. It is this 45°C baseline temperature which is critical for the test procedure as this is an estimate of the running temperature of a tyre on a vehicle. This is highly variable as the actual running temperature is dependant on local weather conditions; however, 45°C was selected as reasonable value for common driving conditions. The peak temperature during each sweep is dependent on the load case during the sweep itself, with high energy sweeps heating the tyre more than low energy ones. These variations in peak temperature are valid and can be implicitly captured in the MF-Tyre 6.1 tyre model so long as each sweep starts from the same temperature (Buisson, 2006). It is therefore necessary to ensure a warmup procedure can heat the tyre such that the baseline temperature is 45°C.

To develop the necessary warmup procedure a study was conducted using the same warmup used within MICH2MF (Buisson, 2006). This warmup consisted of a block of several sweeps repeated three times. However, it was observed during pre-testing that the tyre temperature did not continue to increase during the third block of sweeps. It is therefore suggested that this third block of heating is not required. To investigate this, further tests were conducted using just the first block of sweeps and then the first two block of sweeps from MICH2MF. The results are shown in Figure 3.4-B.

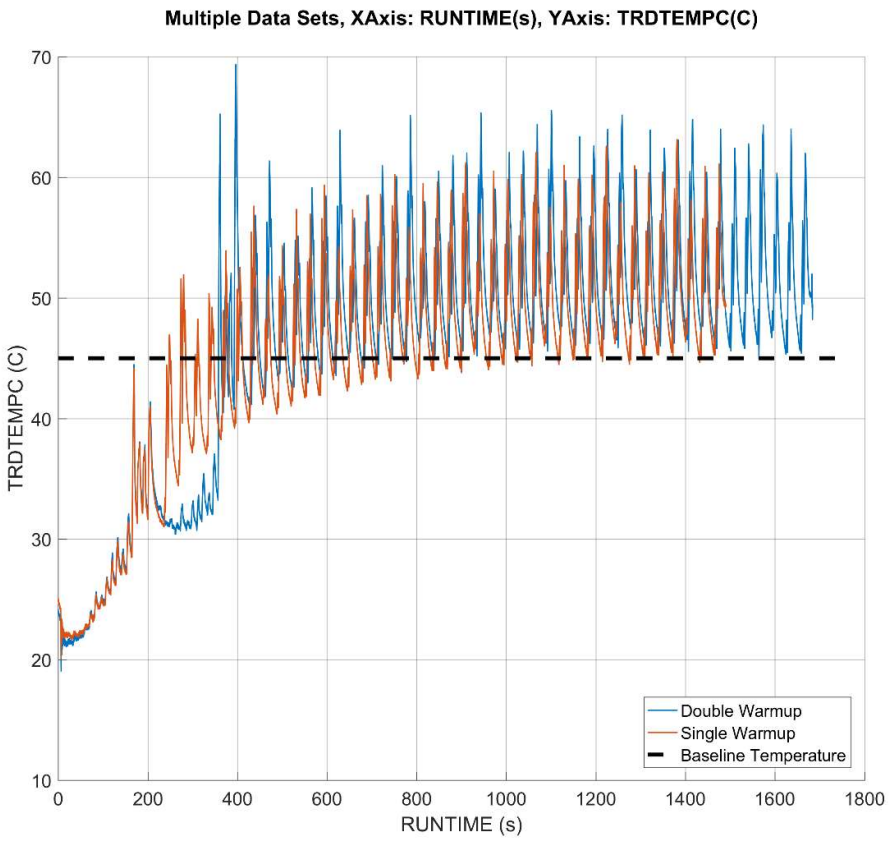

Figure 3.4-B. Warmup profiles when using a single and double block of warmup sweeps, also shows the baseline temperature.

Figure 3.4-B shows that at the end of the single block of warmup sweeps (235s into the test) the tyre had only reached 31°C, after which the tyre temperature continues to increase towards the 45°C baseline temperature. This concludes that one block of heating was not sufficient to heat the tyre. However, after the double block of warmup sweeps which ended after 430s the tyre was at 42°C, which is very close to the 45°C target baseline temperature. To confirm that this is a suitable amount of heating for the tyre's performance to become consistent, three identical sweeps were extracted from the repeated Graph Sweep data and compared to each other. The sweeps selected for comparison were the 1st sweep immediately after the warmup ended, where the tyre is coolest. Also selected were the 6th and 11th sweeps, each of which are an identical load case to the first sweep but conducted later in the test where the baseline temperature had reached the steady 45°C baseline. A plot showing the comparison between these sweeps can be found in Figure 3.4-C, (sweep1, Sweep6, Sweep11 etc. are the 1st, 6th and 11th sweeps as detailed above).

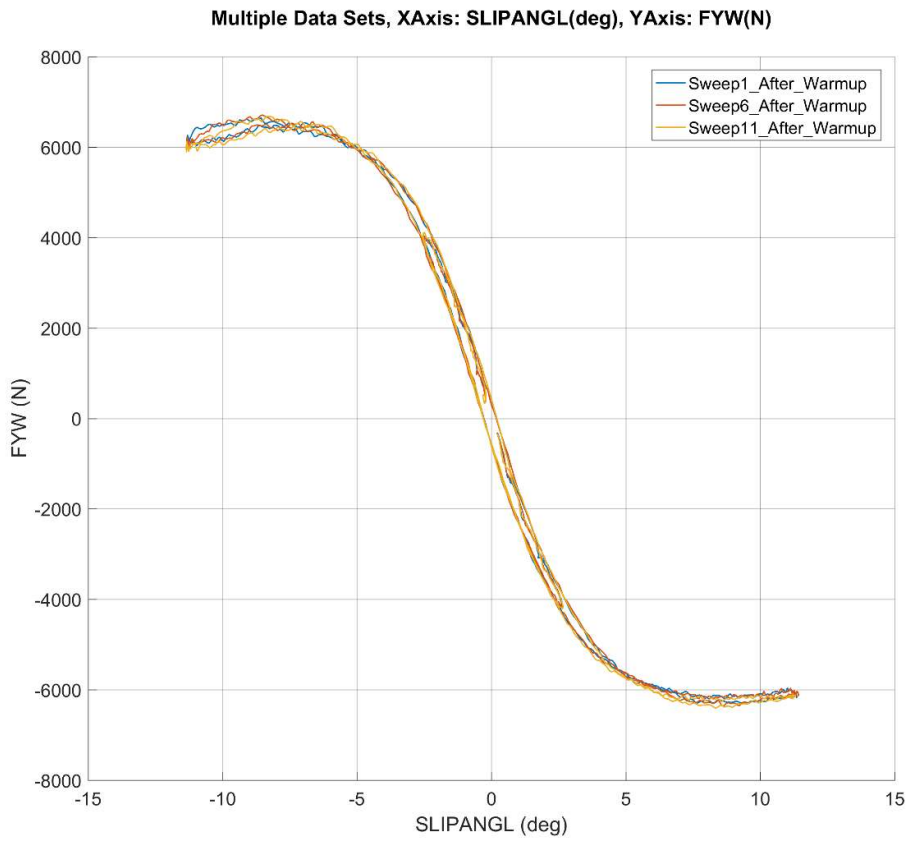

Figure 3.4-C. Comparison between sweeps immediately after the warmup with sweep further along the test procedure.

Figure 3.4-C shows that there was no noticeable change to the tyre's performance between the first sweep immediately after the warmup and similar sweeps from further along the test procedure where the tyre is thoroughly heated. This confirms that the double block warmup procedure is sufficient to heat the tyre to a point at which it performs consistently. This was selected as the warmup procedure and used at the start of both the 'GS2MF FreeRolling' and 'GS2MF BrkDrv' test procedures.

3.5 Thermal Logic

Once the warmup procedure has sufficiently heated the tyre, it is important to regulate this temperature as accurately as possible. If each test sweep is conducted very quickly one after another the frictional induced heat generated during these sweeps will not have time to disperse. Instead, the tyre temperature will rapidly increase to well beyond the temperature range it will typically experience when being used on a vehicle. As result the tyre will overheat and its measured performance characteristics will not be representative of its typical on-vehicle performance.

To prevent the tyre from overheating, thermal pauses are placed between each sweep. During these thermal pauses, the tyre runs at zero slip such that no friction induced heat is generated. This means any residual heat in the tyre can disperse into the air/water bearing as well as the surrounding air. Traditionally the duration of these thermal pauses is pre-determined and programmed into the test procedure prior to running the test. The issue here was that the required duration of each thermal pause depends on the tyre temperature during the preceding sweep. This temperature is primarily induced by sliding friction which is dependent on the amount of grip the tyre can generate during the sweep. Therefore, to accurately predict the thermal pause duration, one must already know the tyre's grip characteristics before conducting the test. However, the purpose of the test is to measure the tyre's grip characteristics. This means multiple iterations of the test procedure must be run on any new tyre to determine the appropriate duration of the thermal pauses. This is very costly and extremely inefficient.

To overcome this, a thermal logic control system was developed in conjunction with the Calspan Corporation who operate the Calspan rig in Buffalo, NY. When using the thermal logic system, the duration of the thermal pauses are not pre-defined, instead only their presence after each sweep is stated in the test procedure along with the target baseline temperature. When running the test, the rig's control system recognises a thermal pause and activates the thermal logic system. In doing so the rig maintains the thermal pause whilst monitoring the tyre temperature. It will continue to prolong the thermal pause until the tyre temperature reaches the target baseline temperature, once it does it will automatically trigger the next test sweep. This is shown in Figure 3.5-A.

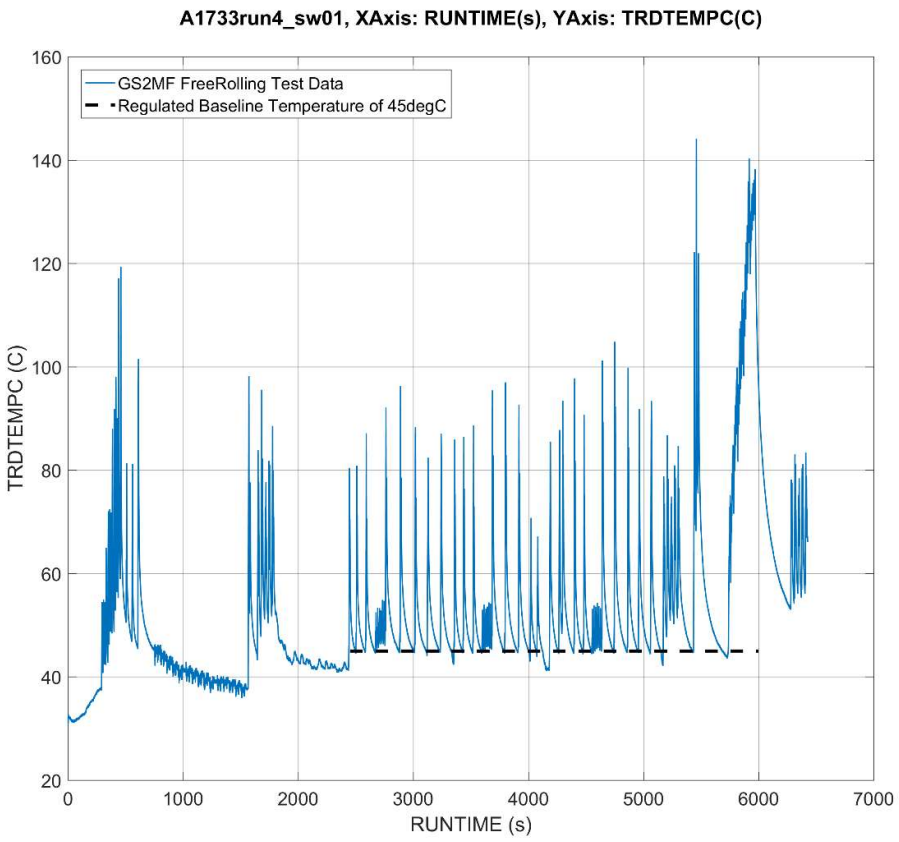

Figure 3.5-A. Tyre temperature during a full test and the thermal logic regulated baseline temperature which is active between 2,450 and 6,000s.

Figure 3.5-A shows the thermal logic system used to ensure each sweep starts at 45°C. In this case the data shows a flash temperature of over 140°C, this in not unusual as the data is obtained from laser temperature sensors that only capture the temperature of the outer most surface of the tire. The laser does not propagate into the rubber meaning the temperature is recorded from a material of close to zero mass (just the absolutely surface of the rubber) meaning it can change temperature extremely quickly.

This thermal logic system eliminates the need for running multiple test iterations to estimate the required thermal pauses. It also absolutely ensures that the tyre temperature is controlled and each sweep starts at exactly the required baseline temperature. Furthermore, the system allows for changes to the test procedure to be implemented at lower cost as changes can be made quickly without having to reiterate each time. Ideally, the system would operate by using a weighted assessment of various tyre temperatures, such as the central, inner and outer tread surfaces, the inner liner temperature, sidewall temperature as well as the actual internal bulk temperature. However, such a system is not yet available and instead only the tyre's central tyre

surface temperature (TRDTEMPC) is used. Despite this, the current system works effectively and overall the use of it leads to a significant increase in both test efficiency and robustness.

3.6 Variable Rate Sweep

3.6.1 Variable Rate Sweep Introduction

Traditional tyre force and moment testing is conducted on flat-trac rigs in the form of sweeps. This is where a tyre is tested at a load case where the vertical load, camber angle and inflation pressure are all set and held constant. The tyre is then maintained in a 'FreeRolling' state, where no braking or driving torque is applied as it is swept through a range of slip angles. Alternatively, a 'BrkDrv' (Driving and Braking) sweep is conducted where the tyre's slip angle is held constant and torque is applied to the tyre to sweep it through a range of slip ratios. The purpose of such sweeps is to measure the tyre's longitudinal and lateral force performance over a range of slip conditions. These sweeps are then repeated over a range of load cases (different vertical loads, camber angles and inflation pressure combinations) to build up a dataset of how the tyre behaves under many different conditions. The data can then be used to build tyre models that are able to reproduce the tyre's handling response within this range of test conditions.

When conducting sweeps, it is important to consider the slip rate; that is the rate of change of slip as applied by the rig. For free rolling sweeps, the slip rate is the rate at which slip angle is changed, for 'BrkDrv' testing the slip rate is the rate at which the slip ratio is changed. In either case the slip rate can have a significant effect on the tyre's behaviour. An example of two free rolling sweeps at different slip angle rates is shown in Figure 3.6.1-A.

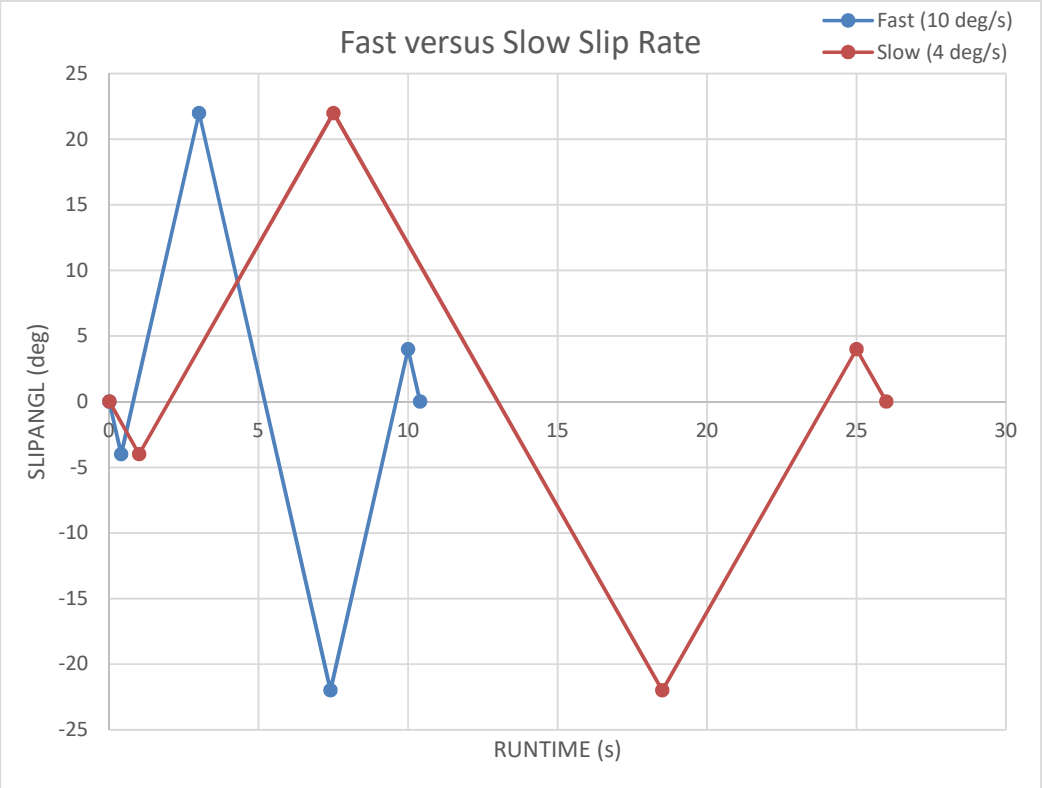

Figure 3.6.1-A. 'FreeRolling' sweeps at 10 and 4°/s.

Figure 3.6.1-A shows the slip angle sweep shape for two 'FreeRolling' sweeps conducted at 10 and 4°/s. During these sweeps, the tyre will be placed under identical load cases; however, the rate at which the tyre moves through these load cases is different. It is this rate of change through a test sweep that can induce two different types of hysteresis into the test data, these are mechanical hysteresis and thermal hysteresis.

Mechanical Hysteresis

Mechanical hysteresis occurs at low slip conditions where the tyre crosses through zero slip at a high slip rate. Tyres do not react instantly when their load case is changed. Instead, if a tyre is running in a steady state condition and a step change is applied to the tyre's inputs (such as a sudden change in the slip position), then there is a delay while the tyre reacts to the change. After this delay the tyre will reach a new steady state condition generating different forces and moments than before. This delay could be described as a time, or phase lag; however, doing so means the magnitude of the delay is dependent on the tyre's forward velocity. To simplify this, the delay is instead described as a distance known as the relaxation length.

This hysteresis is most evident when looking at the forces generated close to zero slip, where there can be very significant differences (in the order of thousands of Newtons) between forces

generated at zero slip when the tyre is transitioning from negative to positive slip, compared to when the tyre is transitioning from positive to negative slip. This is demonstrated in Figure 3.6.1-B which shows the lateral force (FYW) versus slip angle (SLIPANGL) plot for a tyre tested at an extremely high slip angle rate of 30°/s, the data is coloured by run time (RUNTIME).

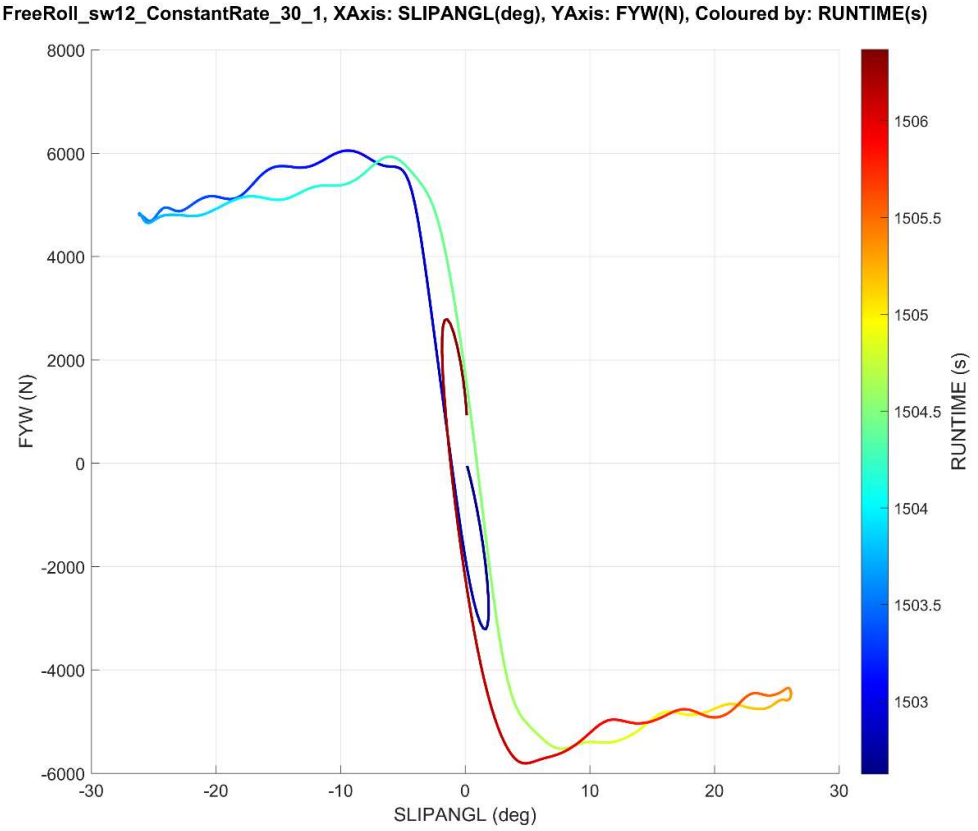

Figure 3.6.1-B. Lateral force versus slip angle coloured by runtime for a constant rate free rolling sweep conducted at 30°/s.

Figure 3.6.1-B shows the tyre started the sweep at zero slip angle while generating close to zero lateral force (dark blue), meaning there was minimal ply steer and conicity effects. The tyre then went to around +2° of slip angle before sweeping out to -28°. Upon returning the tyre transitions from negative to positive slip angles, crossing zero at around 1,504.5s (green) while generating +1,730N of lateral force. It then slips out to +28° of slip angle before returning to cross zero again, this time from positive to negative, at around 1,506s (red) generating close to -2,220N of lateral force. The calculation of mechanical hysteresis is simply the maximum force generated at zero slip minus the minimum force generated at zero slip. In this case, testing the tyre under these highly transient conditions caused a 3,950N (+1,730 -- 2,220 = 3,950N) on-centre mechanical hysteresis loop.

Mechanical hysteresis of this magnitude makes it difficult to extract an accurate cornering stiffness as it is highly dependent on the slip angle direction of travel; similarly, it is difficult to extract other key tyre performance metrics such as the Residual Self Aligning Torque (RSAT) and Residual Cornering Force (RCF). In post processing, this problem can be improved upon by filtering the data. However, depending on the filtering used this can often induce other untoward effects, therefore it is far more robust to minimise the hysteresis as much as possible and acquire the best possible data from the physical testing. Doing so maximises the quality of the original data and minimises the need for filtering as far as possible. Furthermore, it is difficult to fit a representative MF-Tyre 6.1 tyre model to this data using the existing commercially available fitting tools, MF-Tool (Delft-Tyre, 2017) and OptimumTire (OptimumTire, 2017). Both tools require steady state (low hysteresis) data for the initial part of the fitting process. Once this is complete, the transient components of the tyre model are fitted afterwards. Ideally mechanical hysteresis would be eliminated completely but this is impossible as doing so would require changing the slip at a rate of zero, meaning the slip will not be changed at all.

Thermal Hysteresis

Thermal hysteresis is brought on by the tyre changing temperature during testing and its performance changing as a result. While testing a tyre on a flat-trac rig, some heat is generated by the mechanical stretching and relaxing of the tyre's sidewall as it rotates. However, the majority of the heat within a tyre is generated by sliding friction. This frictional induced heat is generated whilst the tyre is loaded and the contact patch is sliding under high slip conditions. Spending more time under these high slip conditions results in more heat being generated in the tyre. When testing road car tyres a common type of thermal hysteresis is where the tyre starts a sweep close to its optimal temperature, the additional friction induced heat then causes the tyre's temperature to increase beyond its optimal temperature. As a result, the tyre's ability to generate grip at a given slip condition reduces. This typically leads to hysteresis loops appearing in the data. A sketch showing this type of thermal hysteresis is shown in Figure 3.6.1-C.

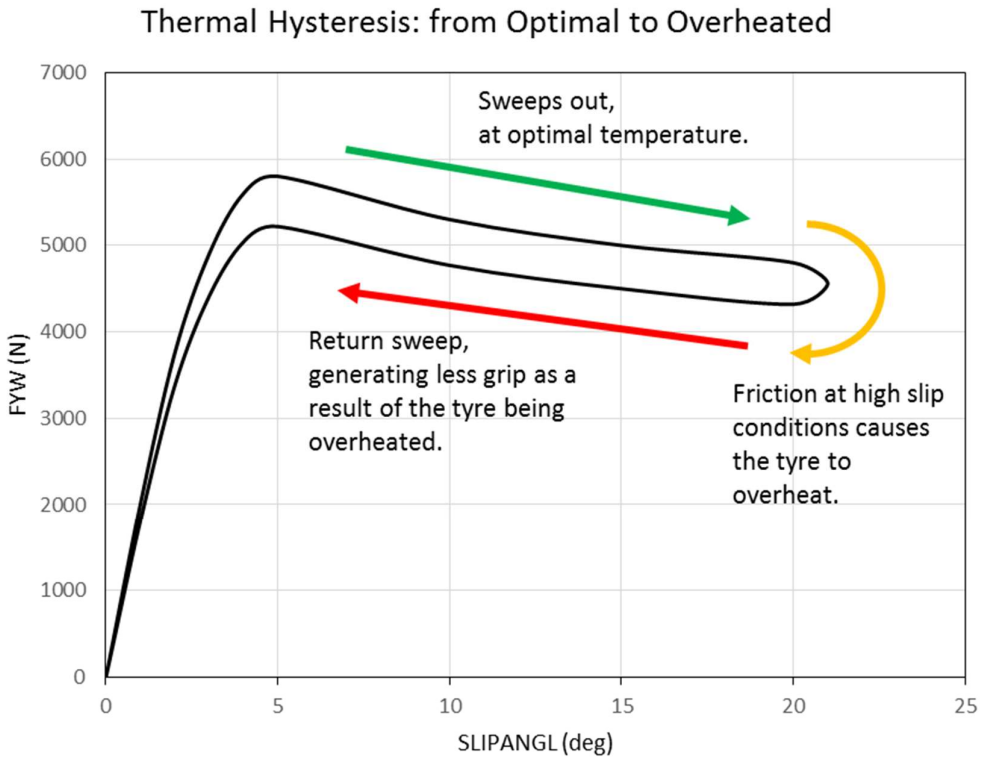

Figure 3.6.1-C. Sketch showing the typical shape of a thermal hysteresis loop when the tyre begins the sweep close to its optimal temperature and overheats as a result of the test.

The hysteresis loop shown in Figure 3.6.1-C is typical when testing a tyre that has been sufficiently warmed prior to conducting the test and then overheated during the test. As the tyre has already been warmed close to its optimal temperature it generates more grip during the 'out sweep' (from low to high slip). Once at a high slip condition sliding friction causes the tyre to overheat and grip to reduce as a result. Then during the 'return sweep' (from high back to low slip) the tyre is overheated and generates less grip than it did during the out sweep, hence a hysteresis loop is observed. However, the thermal hysteresis behaviour of a tyre is not always the same. Figure 3.6.1-D shows how thermal hysteresis can loop in the opposite direction when the sweep begins with the tyre at a different thermal condition.

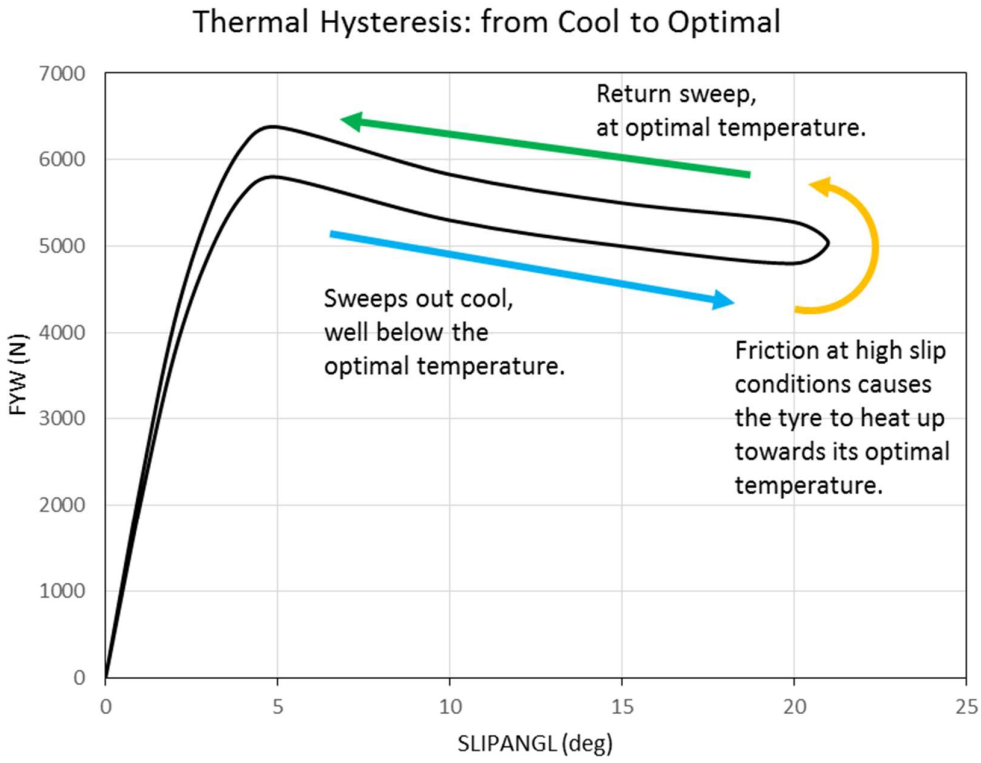

Figure 3.6.1-D. Sketch showing the typical shape of a thermal hysteresis loop when the tyre begins the sweep at a cool temperature and warms towards its optimal temperature as a result of the testing.

In Figure 3.6.1-D the tyre is not sufficiently warmed prior to beginning the test. In this case due to the tyre being below its optimal temperature it generates less grip during the 'out sweep'. Once at a high slip condition the sliding friction generates additional heat in the tyre, causing its temperature to rise towards its optimal operating condition. As a result, during the 'return sweep' the tyre is closer to its optimal temperature and hence generates more grip than it did during the 'out sweep'. This type of thermal hysteresis behaviour is more common when testing race car tyres which are designed to operate at very high temperatures and do not operate well at low temperatures.

Another alternative form of thermal hysteresis is when a tyre begins a sweep slightly below its optimal temperature. As such, during the out sweep the tyre generates slightly less than its optimal force. Friction at high slip then causes the tyre to become slightly overheated, meaning its operating at slightly above its optimal temperature. As a result, during both the out and return sweeps the tyre generates slightly less than its optimal force output. During this form of hysteresis, the tyre's thermal hysteresis loops are very small or even non-existent, and the tyre

behaviour is more homogeneous; however, it also means that no data is obtained with the tyre operating at its optimal thermal state.

Another alternative occurrence is that a given tyre could simply be very thermally insensitive. When designing tyres for road vehicles, tyre companies will often do what they can to make a tyre as thermally insensitive as possible. Doing so means the tyre will behave very consistently in all weather conditions which can increase safety, as the driver will not be surprised by a change in the tyre's grip. When testing such tyres very little thermal hysteresis will be observed.

Due to the highly complex nature of thermal hysteresis it cannot be captured in a tyre model without the inclusion of a sophisticated thermal model, which is not present in MF-Tyre 6.1. Therefore, since the behaviour cannot be explicitly captured in the tyre model it should instead be minimised as much as possible.

As shown, there are many different forms of thermal hysteresis making it difficult to robustly measure its effect in a consistent manner. Instead, the thermal hysteresis can be quantified indirectly by measuring the tyre's temperature variation during each sweep. This has the added benefit of removing any variability due to different tyre's having different thermal sensitivities. Furthermore, during the test schedule presented here, the lowest temperature during each sweep it regulated at 45°C by means of thermal pauses using the rig's control system (See Section 3.5 on Thermal Logic). With the low temperature regulated, thermal hysteresis is directly related to the peak temperature observed during each sweep. This can easily be measured and is used as a robust method to quantify the cause of thermal hysteresis, if not the thermal hysteresis directly.

The peak temperature is heavily influenced by the vertical load and sliding velocity. However, the constraint is that the vertical loads and velocities required during the testing are determined based on the vehicle that the tyre is intended to be used with. Naturally, it is important to test the tyre under similar load cases to those it will be subjected to when in use on a vehicle. If the tyre is to be used on a heavy vehicle but testing is only conducted at low loads, then the resulting MF-Tyre 6.1 tyre model must be extrapolated to higher loads. This will drastically reduce the model's accuracy and stability. Likewise, testing a race car tyre only at low forward velocities will not result in useful data. Therefore reducing thermal hysteresis by lowering the tested loads and velocities is rarely a viable option, as data is required at these high slip high load conditions. Instead, thermal hysteresis can be minimised by reducing the amount of time a tyre spends at the high slip load cases, where frictional induced heat is generated. This reduces the amount of time available for heat to build up in the tyre. To achieve this, the slip rate can be increased to sweep the tyre out and back from a high slip condition as quickly as possible. However, using

higher slip rates induced mechanical hysteresis, (discussed in the mechanical hysteresis section) so the testing is compromised either way.

An additional problem linked to the thermal hysteresis is the significant cool down time that needs to be allotted after any given sweep to ensure the tyre returns to a consistent baseline temperature. It is essential that these thermal pauses are completed before the next sweep is triggered to ensure temperature does not creep up during the test procedure. The duration of these thermal pauses can be far longer than the actual test sweeps, hence they contribute significantly to the overall test duration and cost. However, failure to allow sufficient time for the tyre to cool will result in heat building up through the test procedure, meaning different sweeps would be conducted under different test conditions, effectively invalidating the test.

Furthermore, significant tyre wear often occurs during the same load cases (tyre loaded while at a high slip condition), that induce temperature and thermal hysteresis. This is because both the tyre wear and heat are generated by the high sliding power present during these load cases. This tyre wear can also affect the tyre's performance and hence is another reason to minimise the time spent in these high-energy load cases. A method of quantifying the effect of tyre wear is discussed in Section 3.9 on Graph Sweeps.

Inherent Compromise

The conflicting advantages and disadvantages of flat-trac testing using a high versus low slip rate mean the overall quality of the resulting test data is compromised either way, this is summarised in Table 3.6.1-A.

	Low Slip Rate	**High Slip Rate**
Mechanical Hysteresis	+ Better	- Worse
Thermal Hysteresis	- Worse	+ Better
Cornering Stiffness Accuracy	+ Better	- Worse
RSAT and RCF Accuracy	+ Better	- Worse
Tyre Wear	- Worse	+ Better
Test Duration	- Worse	+ Better

Table 3.6.1-A. Summary of advantages and disadvantages of using a low versus a high slip rate.

Using a low slip rate results in the test sweep being conducted very slowly and the overall sweep takes longer. This slow rate of change means the tyre's sidewall does not deform significantly and the relaxation length is always very low, minimising mechanical hysteresis. However, the low slip rate also means the tyre spends more time at high slip conditions which

causes both increased wear on the tyre as well inducing heat. This additional heat leads to both increased thermal hysteresis and longer cool down times required to allow the heat to disperse. Conversely if a high slip rate is used then the tyre's sidewall is deformed as it passes zero slip which causes significant mechanical hysteresis; this makes MF-Tyre 6.1 fitting more difficult, as well as making cornering stiffness, RSAT and RCF measurements less accurate. However, the high slip rate means less time is spent at high slip conditions and less heat is generated; this reduces thermal hysteresis and tyre wear as well as reducing the required length of cool down times between each sweep, shortening the overall test duration.

Variable Rate

To address the inherent compromises that exist when using either a 'low or high rate' of slip a novel variable rate 'shark tooth' sweep was developed. The variable rate sweep uses a 'low rate' of slip at low slip angles and changes to a 'high rate' of slip at higher slip angles. This aims to achieve a sweep with all the advantages of both the low and high constant rate sweeps, while minimising the disadvantages. A comparison between a constant and variable rate sweep is shown in Figure 3.6.1-E.

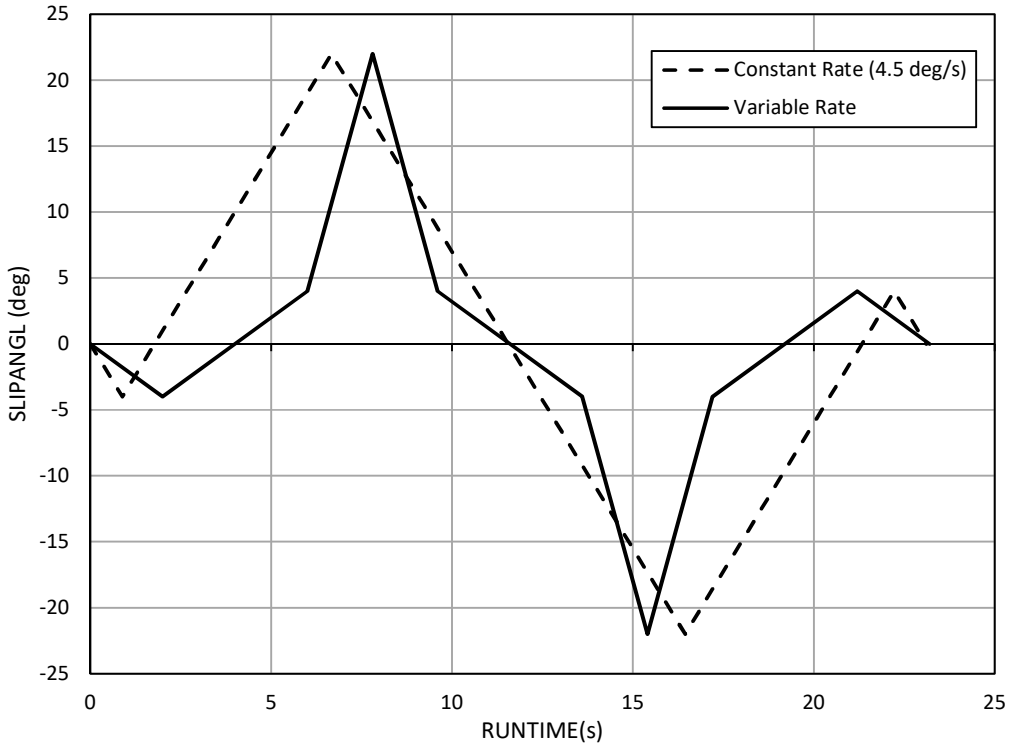

Figure 3.6.1-E. Comparison between a constant rate sweep and variable rate sweep.

Figure 3.6.1-E shows a 4.5°/s constant rate sweep and how it compares to a variable rate sweep. In this example, the two sweeps are designed to reach the same maximum slip angles (+/-22°) in the same amount of time (23s). However, the area under the variable rate sweep is visibly lower than that of the constant rate sweep. This means the tyre spends less time at high slip conditions, resulting in less wear and less temperature build up during the variable rate test.

There are three main variables that define how a variable rate sweep is different from a constant rate sweep, these are detailed in Table 3.6.1-B.

Name	Description	Example Value (Used in Figure 3.6.1-E)
'Low Rate'	Rate of change of slip used during low slip conditions.	2°/s
'High Rate'	Rate of change of slip used during high slip conditions.	10°/s
'Threshold'	Magnitude of slip that defines the transition between the 'low rate' and 'high rate' conditions.	4°

Table 3.6.1-B. The three variables of a variable rate sweep.

Each of these three variables can be tuned to better suit the given application with the objective being to minimise the inherent compromises that come with using either low or high constant slip rate sweeps. To that end a thorough test schedule was set up and run using the SoVaMotion rig. Full details of the test schedule, results and analysis can be found in the forthcoming chapters.

3.6.2 Free Rolling Variable Rate Sweep

A thorough investigation was carried out to find the optimal setup of variable rate sweeps for both GS2MF Free Rolling and 'BrkDrv' applications. For free rolling applications, the test tyre is free to rotate about its X-axis on the flat-trac rig, meaning slip ratio is always close to zero; during these tests, the investigation focuses around changing the slip angle. For 'BrkDrv' application the rig's drive motor is connected to the test tyre and slip angle is held at zero; during these tests, the investigation focuses around changing the slip ratio.

Sweep Naming Convention

A specific naming convention was devised to name and reference each test throughout the variable rate sweep investigation. The naming convention includes important information relating to the setup of each sweep and is detailed in Table 3.6.2-A with examples below.

Order	Definition	Example
1	Rig Configuration	'FreeRolling', BrkDrv
2	Sweep Number	sw14, sw15, sw16
3	Sweep Type	Constant Rate, Variable Rate
4	Slip Rate (Constant Rate sweeps only)	'FreeRolling' (Slip Angle): 10 (10°/s), 12 (12°/s) 'BrkDrv' (Slip Ratio): 20 (20%/s), 30 (30%/s)
5	'Low Rate' (Variable Rate sweeps only)	'FreeRolling' (Slip Angle): LR4 (4°/s), LR6 (6°/s) 'BrkDrv' (Slip Ratio): LR20 (20%/s), LR30 (30%/s)
6	'High Rate' (Variable Rate sweeps only)	'FreeRolling' (Slip Angle): HR18 (18°/s), HR20 (20°/s) 'BrkDrv' (Slip Ratio): HR40 (20%/s), HR50 (30%/s)
7	'Threshold' (Variable Rate sweeps only)	'FreeRolling' (Slip Angle): TH4 (4°), TH6 (6°) 'BrkDrv' (Slip Ratio): TH8 (8%), TH10 (10%)
8	Repeated Number	1 (first sweep), 2 (second run of identical sweep)

Table 3.6.2-A. Structure and definitions of the sweep data naming convention used for the variable rate investigation.

Three examples of sweep names are:

1) FreeRoll_sw6_ConstantRate_12_1

   Meaning: The rig is configured for 'FreeRolling' (FreeRoll), this is sweep number 6 in the test sequence (_sw6), this is a constant rate sweep (_ConstantRate), the slip rate is 12°/s (_12), this is the first running of this particular sweep (_1).

2) FreeRoll_sw25_VariableRate_LR4_HR12_TH4_4

   Meaning: The rig is configured for 'FreeRolling' (FreeRoll), this is sweep number 25 in the test sequence (_sw25), this is a variable rate sweep (_VeriableRate), the 'low rate' is 4°/s (_LR4), the 'high rate' is 12°/s (_HR12), the 'threshold' is 4° (_TH4), this is the 4^{th} time this sweep has been run (_4).

3) BrkDrv_sw22_VariableRate_LR10_HR30_TH16_1

   Meaning: The rig is configured for braking and driving (BrkDrv), this is sweep number 22 in the test sequence (_sw22), this is a variable rate sweep (_VeriableRate), the 'low rate' is 4%/s (_LR4), the 'high rate' is 30%/s (_HR30), the 'threshold' is 16% (_TH16), this is the first time this sweep has been run (_1).

Free Rolling, Test Schedule

When carrying out tests on a flat-trac rig it is important to design a suitable test schedule. This is because tyres are highly sensitive to their history; with wear and other factors causing irreparable changes to the tyre's performance (Buisson, 2006). The test schedule used to evaluate the free rolling variable rate sweep is detailed in Table 3.6.2-B.

Sequence	**Test**
1	Warmup
2	FreeRoll_sw1_VariableRate_LR4_HR12_TH4_1
3	FreeRoll_sw2_ConstantRate_4_1
4	FreeRoll_sw3_ConstantRate_6_1
5	FreeRoll_sw4_ConstantRate_8_1
6	FreeRoll_sw5_ConstantRate_10_1
7	FreeRoll_sw6_ConstantRate_12_1
8	FreeRoll_sw7_ConstantRate_14_1
9	FreeRoll_sw8_ConstantRate_16_1
10	FreeRoll_sw9_ConstantRate_18_1
11	FreeRoll_sw10_ConstantRate_20_1
12	FreeRoll_sw11_ConstantRate_25_1
13	FreeRoll_sw12_ConstantRate_30_1
14	FreeRoll_sw13_VariableRate_LR4_HR12_TH2_1
15	FreeRoll_sw14_VariableRate_LR4_HR12_TH4_2
16	FreeRoll_sw15_VariableRate_LR4_HR12_TH6_1
17	FreeRoll_sw16_VariableRate_LR4_HR12_TH8_1
18	FreeRoll_sw17_VariableRate_LR4_HR12_TH10_1
19	FreeRoll_sw18_VariableRate_LR2_HR12_TH4_1
20	FreeRoll_sw19_VariableRate_LR4_HR12_TH4_3
21	FreeRoll_sw20_VariableRate_LR6_HR12_TH4_1
22	FreeRoll_sw21_VariableRate_LR8_HR12_TH4_1
23	FreeRoll_sw22_VariableRate_LR4_HR6_TH4_1
24	FreeRoll_sw23_VariableRate_LR4_HR8_TH4_1
25	FreeRoll_sw24_VariableRate_LR4_HR10_TH4_1
26	FreeRoll_sw25_VariableRate_LR4_HR12_TH4_4

27	FreeRoll_sw26_VariableRate_LR4_HR14_TH4_1
28	FreeRoll_sw27_VariableRate_LR4_HR16_TH4_1
29	FreeRoll_sw28_VariableRate_LR4_HR18_TH4_1
30	FreeRoll_sw29_VariableRate_LR4_HR20_TH4_1
31	FreeRoll_sw30_VariableRate_LR4_HR25_TH4_1
32	FreeRoll_sw31_VariableRate_LR4_HR30_TH4_1
33	FreeRoll_sw32_VariableRate_LR4_HR12_TH4_5

Table 3.6.2-B. Variable Rate Investigation, Free Rolling Test Schedule.

The test schedule starts with a tyre warmup procedure, full details of this procedure can be found in Section 3.4 on Warmup. After the warmup, constant rate sweeps are conducted at various different rates to establish a baseline. Following the constant rate sweeps, a series of different variable rate sweeps are conducted where the 'low rate', 'high rate' and 'threshold' are all changed independently so their influences could be fully investigated. There is one Graph Sweep that is repeated five times throughout the test. This allows data from these repeats to be compared to one another to quantify any change to the tyre's performance during the testing.

Free Rolling, Test Validation

A series of identical Graph Sweeps were repeated five times through the test sequence, these included the first and last sweeps. An analysis of these sweeps allows conclusions to be drawn as to how the performance of the tyre itself has changed as a result of the testing. The results from this analysis are shown in Figure 3.6.2-A.

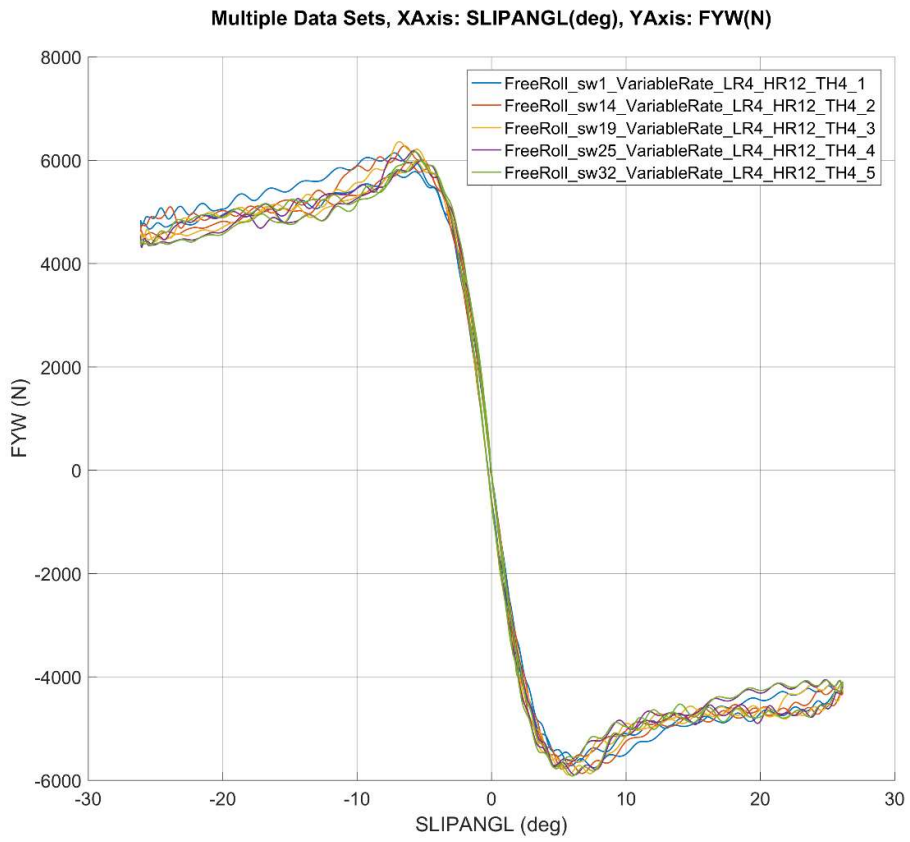

Figure 3.6.2-A. Lateral force versus slip angle for the five identical sweeps tested repeatedly throughout the test procedure.

Figure 3.6.2-A shows a comparison of the sweeps that are repeated throughout the free rolling testing. Typically, as a tyre wears the drop off after the peak will become more severe and the cornering stiffness will increase due to the reduced height of the tread blocks leading to less tread shuffle. None of this was evident in Figure 3.6.2-A as the results show very little variation in the tyre's performance. This means test results from the start to the end of the test sequence are comparable to one another. Further information on this principal can be found in Section 3.9 on Graph Sweeps.

Free Rolling, Constant Rate Sweep Analysis

Figure 3.6.2-B shows the mechanical hysteresis that is present when crossing zero slip at constant steering rates of 4 to 30°/s. The high steering rate sweep at 30°/s shows a hysteresis loop of around 4,100N (+1,900 - -2,200 = 4,100N) at zero slip angle, this reduces to only 700N (+100 - -600 = 700N) when the slowest 4°/s slip rate was used. This 83% reduction in mechanical hysteresis demonstrates the importance of using a low slip rate when crossing zero slip.

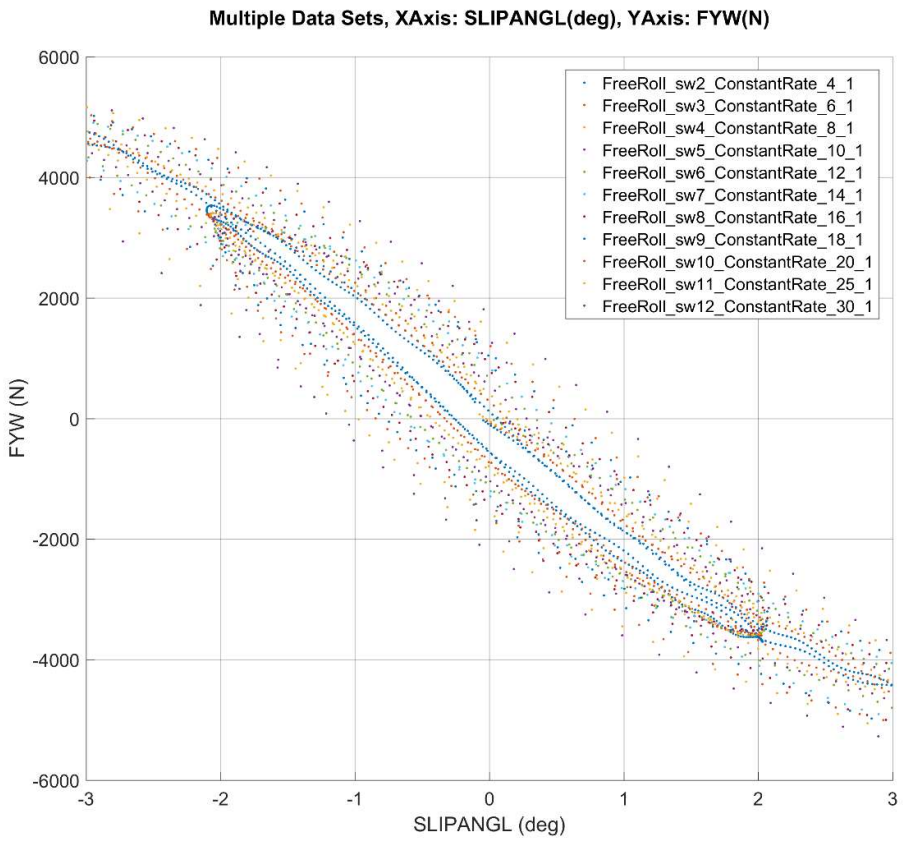

Figure 3.6.2-B. Comparison of constant rate sweeps close to zero slip angle.

Figure 3.6.2-B also shows how using a lower slip rate effectively increases the data sampling rate. The maximum available sampling rate is limited by the instrumentation being used on the flat-trac rig; therefore, the sampling rate per unit of time cannot be increased. However, when using a lower slip rate, the sampling rate per unit of slip angle effectively increases. This means more sample points are available when calculating cornering stiffness, RSAT and RCF, making these calculations more accurate.

Figure 3.6.2-C shows a comparison of the temperature profiles of each constant rate sweep. Here it can be seen that the tyre reaches its highest temperature of 106.5°C during the slowest sweep, this is due to the tyre spending more time at high slip angles where the friction induced heat is generated. Conversely, the tyre only reaches 82.5°C during the fastest sweep. This means using a faster sweep reduces test duration in two ways: firstly, the sweep itself is conducted faster; secondly the tyre reaches a lower peak temperature and hence takes less time to cool back down to a 45°C baseline temperature. This is shown by the reducing pause times between each sweep in Figure 3.6.2-C.

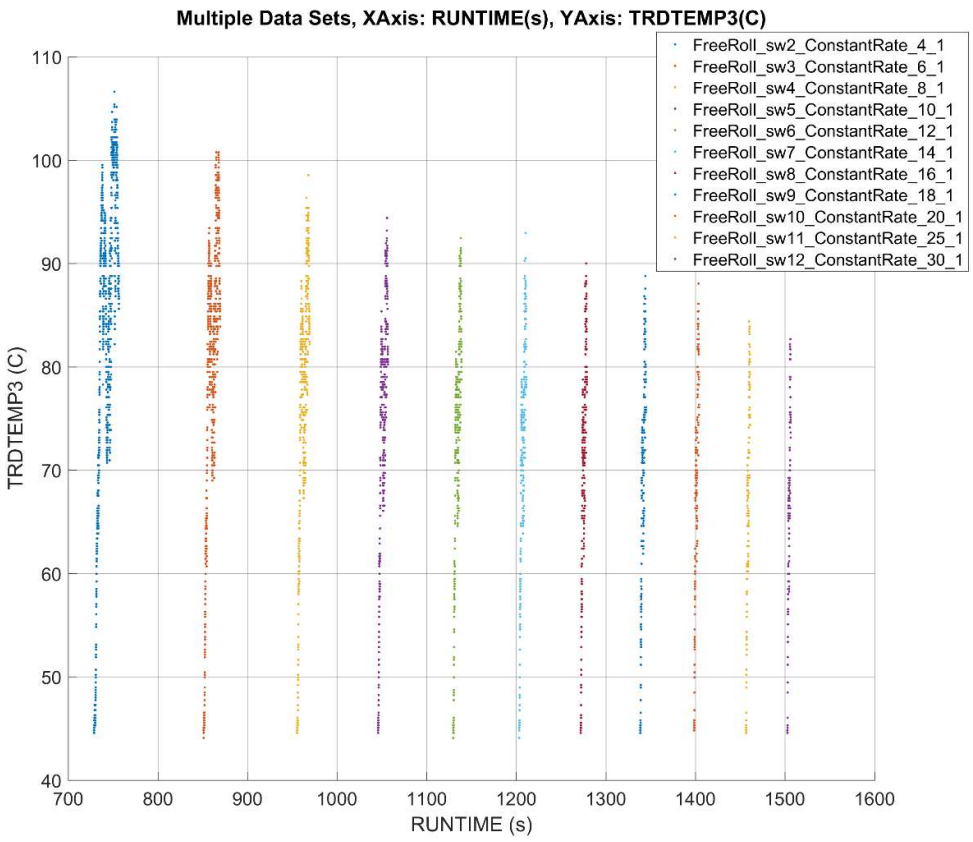

Figure 3.6.2-C. Tyre outer surface temperature versus runtime for the free rolling constant rate sweeps.

Figure 3.6.2-C also demonstrates that the duration of the cool down times (gaps between each sweep) are significantly longer than the duration of the sweeps themselves. The total duration of this block of testing shown in Figure 3.6.2-C is 815.7s (from the end of sweep FreeRoll_sw1 to end of FreeRoll_sw12); of that the total duration of all the sweeps is 115.9s and the total duration of all the thermal pauses is 699.8s. This means that over this block of testing 85.8% of the rig time is spent waiting for the tyre to cool down, while only 14.2% of the time is used running sweeps to gather useful force and moment data. The duration of these thermal pauses mainly depends on the peak temperature the tyre reaches during the preceding sweep. A hotter tyre takes longer to cool than a less hot tyre. Therefore, to meet the objective of reducing overall rig time and costs, focus should be placed on designing tests that reducing the peak temperature of the tyre, thus reducing the required cool down time. This will likely have a more positive impact on test efficiency than focusing on reducing the duration of the sweeps themselves (as test sweeps equate to just 14.2% of the overall rig time while the thermal pauses make up the remaining 85.8%). More details of exactly how the rig executes the thermal pauses can be found in Section 3.5 on Thermal Logic.

Further analysis as to the cause of this heat and the effect on tyre wear was carried out by observing the tyre's sliding energy, the calculations for these can be found in the nomenclature. Figure 3.6.2-D shown the accumulative sliding energy for each of the constant rate sweeps.

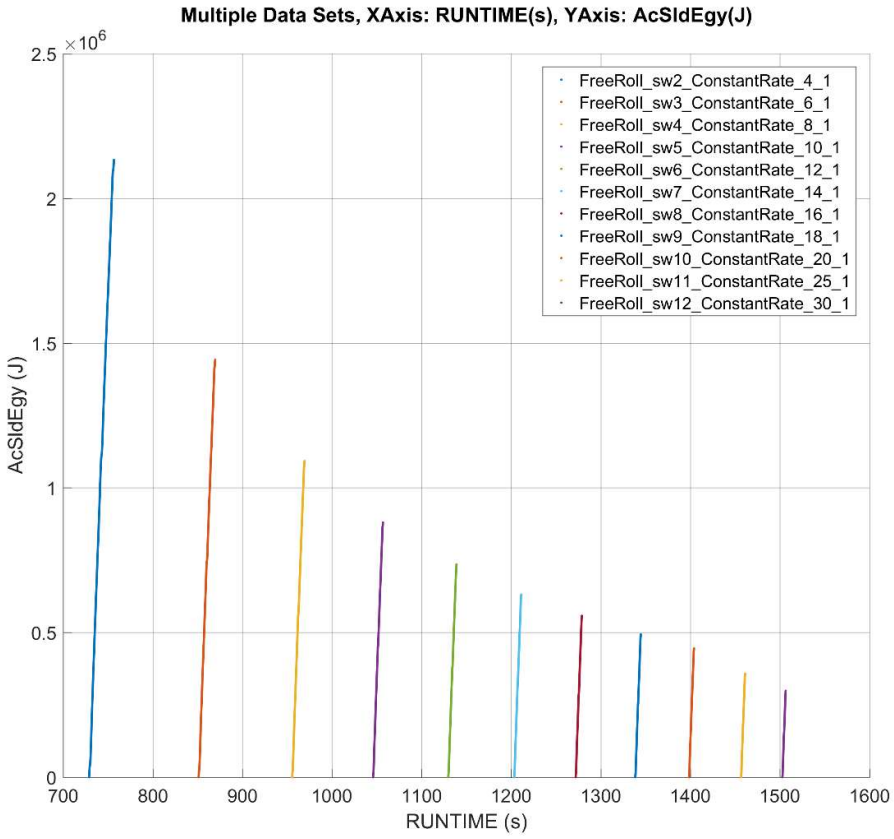

Figure 3.6.2-D. Accumulative sliding energy (AcSldEny) versus runtime for each of the 'FreeRolling' constant rate sweeps.

Figure 3.6.2-D shows the accumulative sliding energy of each of the constant rate sweeps, such that the peak of each sweep shows the total sliding energy for that sweep. This is calculated by first using trigonometry to calculate the total force vector (FXY) using the longitudinal and lateral forces (FX and FY). The velocity vector (VXY) can be calculated similarly using the measured forward velocity (VX) and the slip angle (SA) which is the angle between the tyre's direction of travel and the forward velocity. The product of these channels (FXY and VXY) gives the sliding power of the tyre during the sweep. The sweeps shown are all conducted under the same load and peak slip angles so the sliding power through each sweep is very similar, however the duration of the sweeps are very different. Therefore, an accumulative integration of the power with respect to time (using the 'cumtrapz' function within MATLAB 2016a (MathWorks MATLAB, 2017)) gives the accumulative sliding energy (or frictional energy), the

final value of which is the total amount of sliding energy during the sweep. Details of these calculations can be found in the Sliding Power and Energy Section of the nomenclature. This total sliding energy is directly proportional to the tyre wear incurred during the sweep. The exact relationship between the two is highly dependent on the particular tyre and the road surface conditions amongst other factors.

Tread depth (the measure of tyre wear) cannot be measured directly while the tyre is in motion. Instead the rig's radius measurement is used to impart the change in tread depth. This radius measurement is accurate to within 0.1mm and shows a general reduction in tyre radius of around 1.4mm over the entire 32 sweep test procedure. This means each of the 32 sweeps is recorded at one of the 14 (1.4mm / 0.1mm = 14) possible measurements within the 1.4mm range. With this level of accuracy, it is impossible to resolve each of the 32 sweeps uniquely and it is therefore impossible to record the change in radius before and after each sweep. For this reason, a conclusive relationship between tread wear and sliding energy cannot be obtained using the available equipment. However, the general trend across the test demonstrated that the magnitude of tyre wear is directly related to the measurable quantity of sliding energy. Therefore, sliding energy can still be used as an indicator of the amount of wear caused to a tyre as a result of running any given sweep. It just cannot be correlated precisely to a change in tread depth. Using such an approach Figure 3.6.2-E shows that during the slowest constant rate sweep the total sliding energy was 2,133kJ, whereas during the fastest constant rate sweep the total energy was just 299kJ, a reduction of 86%. While the exact effect this has on tyre wear cannot be quantified, it is realistic to assume that such a large change in sliding energy will have a significant (if not precisely known) effect on tyre wear.

The total sliding energy can also be related directly to the peak temperature during each sweep as shown in Figure 3.6.2-E.

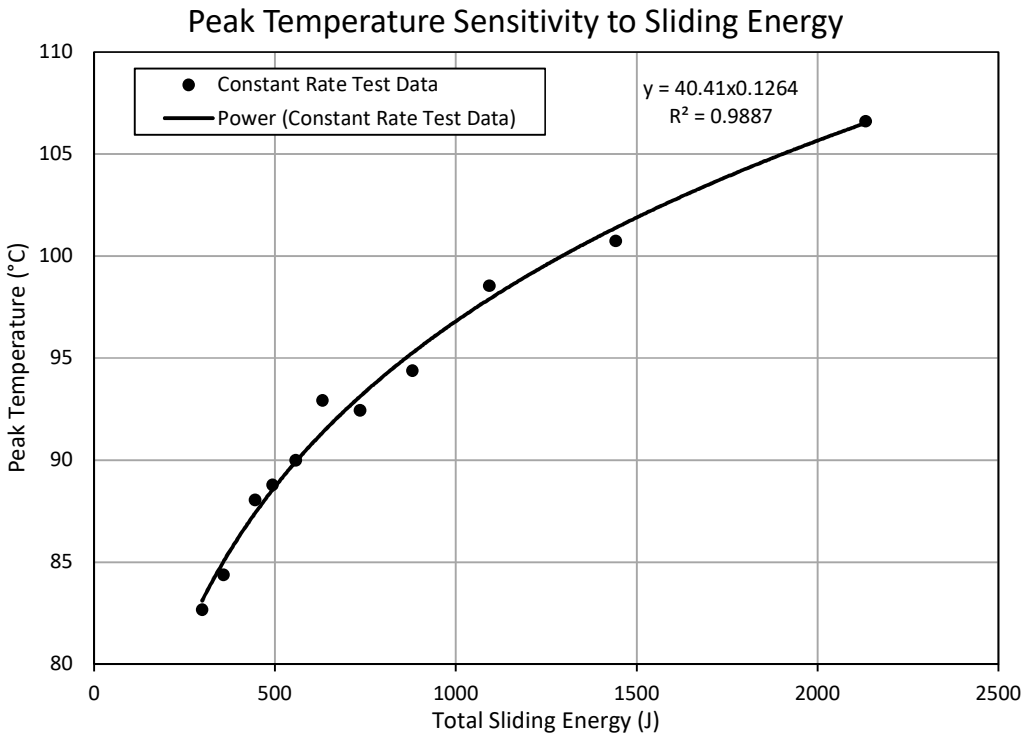

Figure 3.6.2-E. Correlation between peak temperatures during each sweep compared to the total sliding energy.

Figure 3.6.2-E shows that there is a very strong correlation between peak temperature and sliding energy. This is expected and demonstrates that the sliding energy causes frictional induced heat which is the primary source of heat in the tyre during this sort of testing.

This concludes that minimising the time spent testing at load cases that induce high sliding power will reduce the sliding energy. In doing so, both the tyre's wear and peak temperature are reduced. Reducing tyre wear results in a more consistent performance from the tyre during the test procedure; while reducing the peak temperature mean less cool down time is required after each sweep, resulting in increased test efficiency.

Free Rolling, Variable Rate – 'High Rate' Analysis

The 'high rate' is the slip angle rate used at slip angles beyond the 'threshold'. A range of different 'high rates' were tested to fully evaluate their effect on tyre performance. The range of 'high rates' goes from 6 up to 30°/s, during this block of testing the 'low rate' is held at 4°/s and the 'threshold' is held at 4°. The sliding power can then be calculated as the product of force and velocity vectors (FXY and VXY). Finally, integrating the sliding power with respect to time gives the sliding energy. Full details of these calculations can be found in the nomenclature.

Figure 3.6.2-F shows that increasing the higher slip rates ('high rate') have no discernible effect on lateral force performance close to zero slip angle and a small effect on performance further from zero. This is expected as the 'high rate' is only used at slip angles greater than the 'threshold'. At slip angles beyond the 'threshold' the results show that the faster 'high rates' also have little effect on lateral force, only reducing the 'effective' frequency of the vibration in this region. The actual frequency of the tyres vibration remains the same; however, when using a lower slip rate the vibration is observed over a longer time period, this appears as a higher frequency vibration when plotted against slip angle position. Conversely using a faster rate means the vibration is observed over a shorter time period, when plotted against slip angle this appears as a lower 'effective' frequency of vibration.

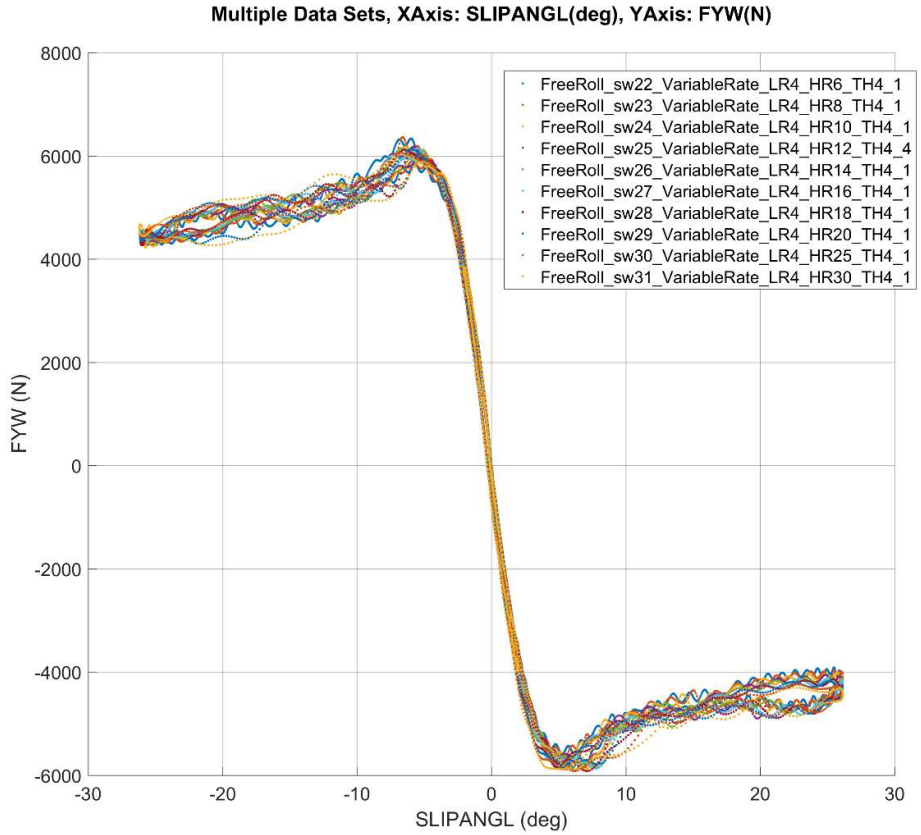

Figure 3.6.2-F. Lateral force versus slip angle for free rolling variable rate sweeps set to different 'high rates'.

The lack of any lateral force variation between the different high slip rates is supported by (Rill, 2006) where Rill demonstrates that relaxation length reduces with slip angle. In the paper, a different tyre and test setup is used. However, a tyre tested at similar loads is shown to have a relaxation length of 0.6m at zero slip angle, which reduces by 75% to just 0.15m once it reaches 4° of slip angle, which is selected here as the 'threshold', this is shown in Figure 3.6.2-G.

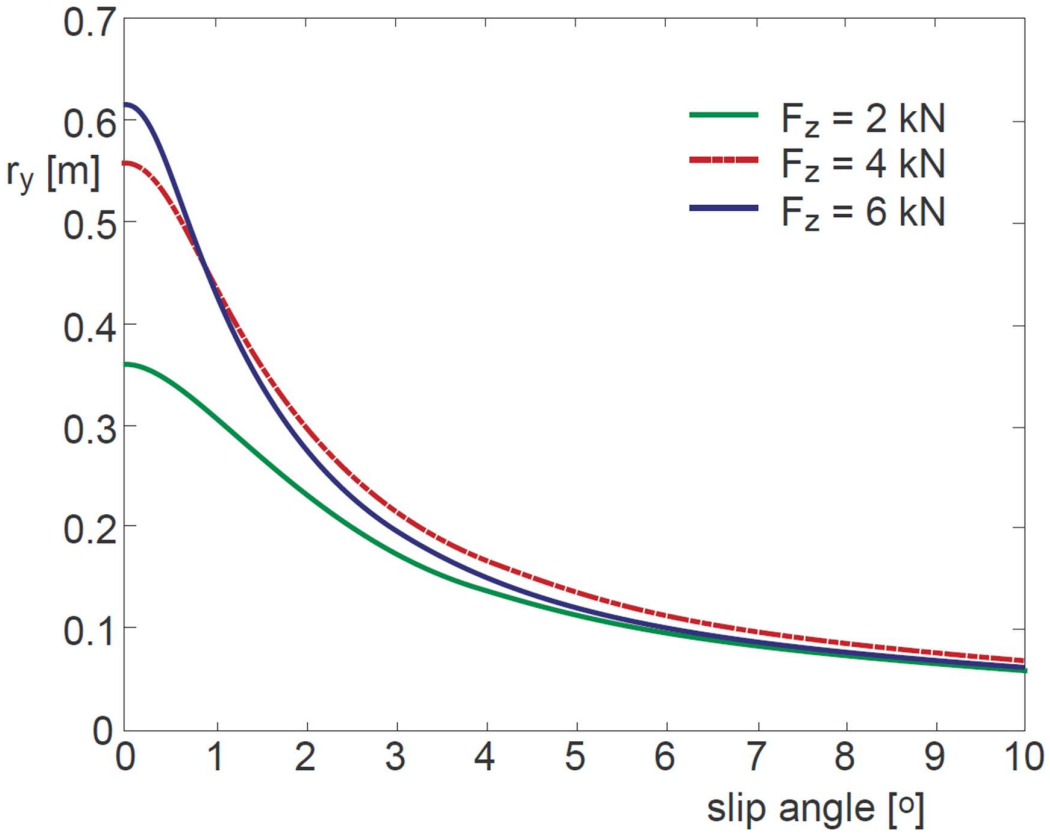

Figure 3.6.2-G. Relaxation length versus slip angle for a tyre at three different vertical loads. (Rill, 2006)

It is realistic to assume that the SUV tyre used here will behave similarly. This reduction in relaxation length explains why there is little to no mechanical hysteresis beyond the 4° 'threshold'. Hence, any practical 'high rate' could be used so long as it is only implemented at slip angles beyond this 'threshold', as the tyre will react very quickly due to the relaxation length being very short. As a result, the 'high rate' has little to no effect on mechanical hysteresis, instead it will only influence temperature which in turn could affect thermal hysteresis.

Whilst the 'high rate' has little effect on lateral force, Figure 3.6.2-H shows the very significant effect the 'high rate' has on tyre temperature; where the peak temperatures during each sweep have a direct and very linear correlation to the 'high rate' used during the sweep. During the sweep with a 'high rate' of 6°/s the tyre's peak temperature reaches 114.4°C, whereas during the 30°/s 'high rate' sweep the tyre only reaches 77.8°C; a 32% reduction. This change in temperature explains some of the minor variations seen in the lateral forces at high slip conditions. However, road car all-season SUV tyres such as the ones used in this test are engineered by tyre manufacturers to be as thermally in-sensitive as possible. This is a safety

feature to ensure that when they are fitted to a customer's vehicle the tyres always perform in a similar and predictable way, whatever the weather. This explains why only minimal variation is overserved at high slip conditions despite the tyre temperature being quite different.

From a testing efficiency perspective, lower temperatures have a significant effect on overall test duration and cost. Following the highest temperature sweep the tyre took 88s to cool down to a steady 45°C baseline temperature, whereas the lowest temperature sweeps only required 32s to cool. This equates to a 64% reduction in test duration, which reduces overall testing costs significantly. This is shown in Figure 3.6.2-H.

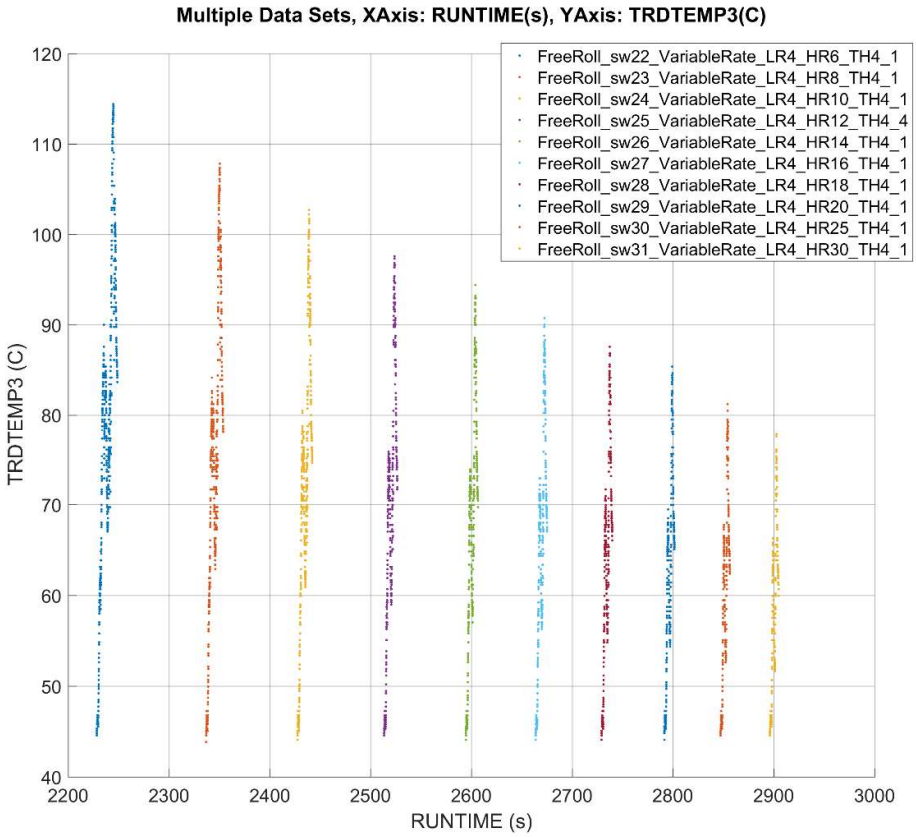

Figure 3.6.2-H. Tyre tread surface temperature versus time for free rolling variable rate sweeps using different 'high rates'.

Overall the results show that despite the significant difference in temperature, there is little difference in the tyre's lateral force performance when using the fastest possible 'high rate'. The testing also showed that tyre temperature and cool down times reduce significantly when a fastest 'high rate' is used. Therefore, in the interest of maximising test efficiency the fastest 'high rate' the test rig will allow appears to be the optimal solution. It is conceivable that even faster 'high rates' would provide better data; however faster rates are not currently possible due

to the wear and potential damage this can cause to the test rig. If faster rates were possible it is expected that they will result in little change to the tyre's force outputs while further reducing peak temperatures.

Free Rolling, Variable Rate – 'Low Rate' Analysis

The 'low rate' is the slip angle rate used when slip angle is below the 'threshold'. A range of 'low rates' from 2 to 8°/s were tested to evaluate their effect on the overall tyre performance. Throughout this block of tests, the 'high rate' was held at 12°/s and the 'threshold' was held at 4°. Figure 3.6.2-I suggests that the 'low rate' has a significant effect on the mechanical hysteresis close to zero slip angle. This reflects the same conclusions drawn from the analysis of the constant rate sweeps.

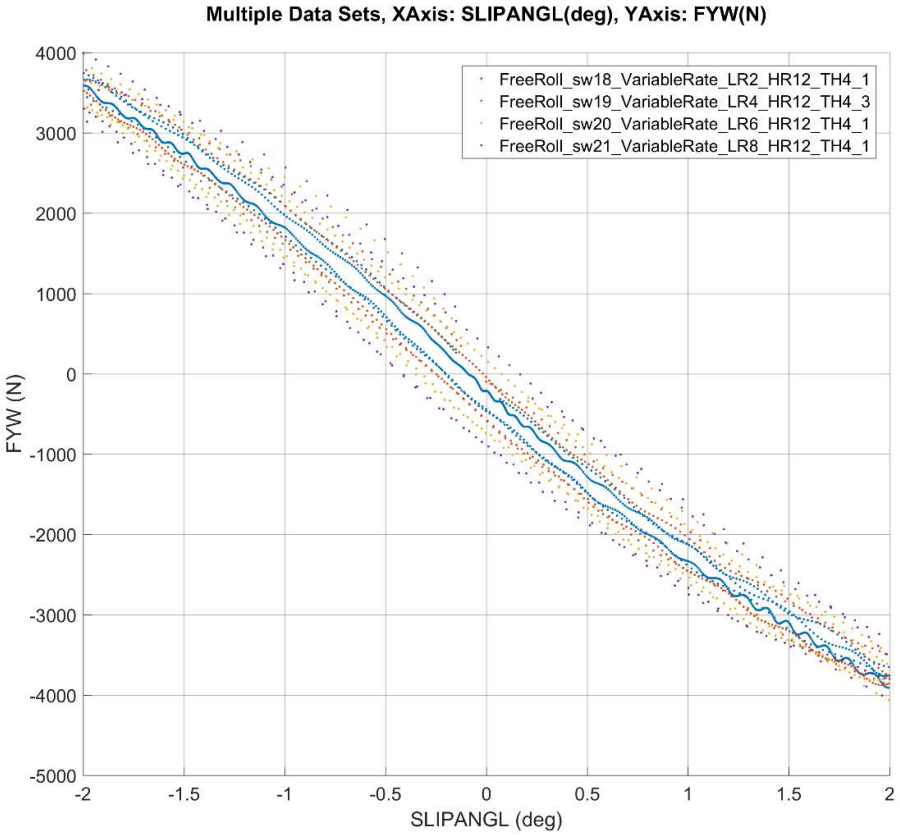

Figure 3.6.2-I. Lateral force versus slip angle close to zero for free rolling variable rate sweeps each set to a different 'low rate' ranging from 2 to 8°/s.

Figure 3.6.2-I shows that during the highest 'low rate' sweep 'Sweep 21' (with a 'low rate' of 8°/s) the mechanical hysteresis loop is around 1,300N (+400 - -900 = 1300N), whereas during the lowest 'high rate' sweep 'Sweep 18' (with a 'low rate' of 2°/s) the mechanical hysteresis loop is reduced to around 300N (-200 - -500 = 300N). This means using a 'low rate' of 2°/s

rather than 8°/s reduces mechanical hysteresis by 84%. This makes the calculation of cornering stiffness, RSAT and RCF much easier and more accurate. Furthermore, reducing the slip and rate in this region effectively increases the sampling rate, meaning there is higher resolution data available to make these calculations.

Further analysis revealed that the 'low rate' had no discernible effect on lateral force away from zero slip angle where all sweeps performed similarly, this is expected as the 'low rate' is only used at slip angles within the 'threshold', which in this case is set to 4°. The 'low rate' also had little effect on overall temperature. Peak temperatures during the sweeps ranging from 91.2 to 101.4°C, meaning the cool down times after each sweep are also similar.

Based on this data and analysis, a 'low rate' of 2°/s gives the best overall result. With a very small increase in rig time resulting in significantly better data, with much lower hysteresis and more data points available to calculate cornering stiffness, RSAT and RCF. The temperature profile using a 'low rate' of 2°/s is largely unaffected and comparable to faster rates, this also has minimal effect on tyre wear as the 'low rate' is only used at low slip angles were sliding power and hence tyre wear is minimal.

Free Rolling, Variable Rate – 'Threshold' Analysis

The 'threshold' is the slip angle at which the test switches between the 'low rate' and 'high rate'. Figure 3.6.2-J shows a comparison of variable rate sweeps using different 'thresholds' ranging from 2 to 10°. During each of the sweeps within this block of testing the 'low rate' was held at 4°/s and the 'high rate' was held at 12°/s. The results in Figure 3.6.2-J show very little difference between the sweeps.

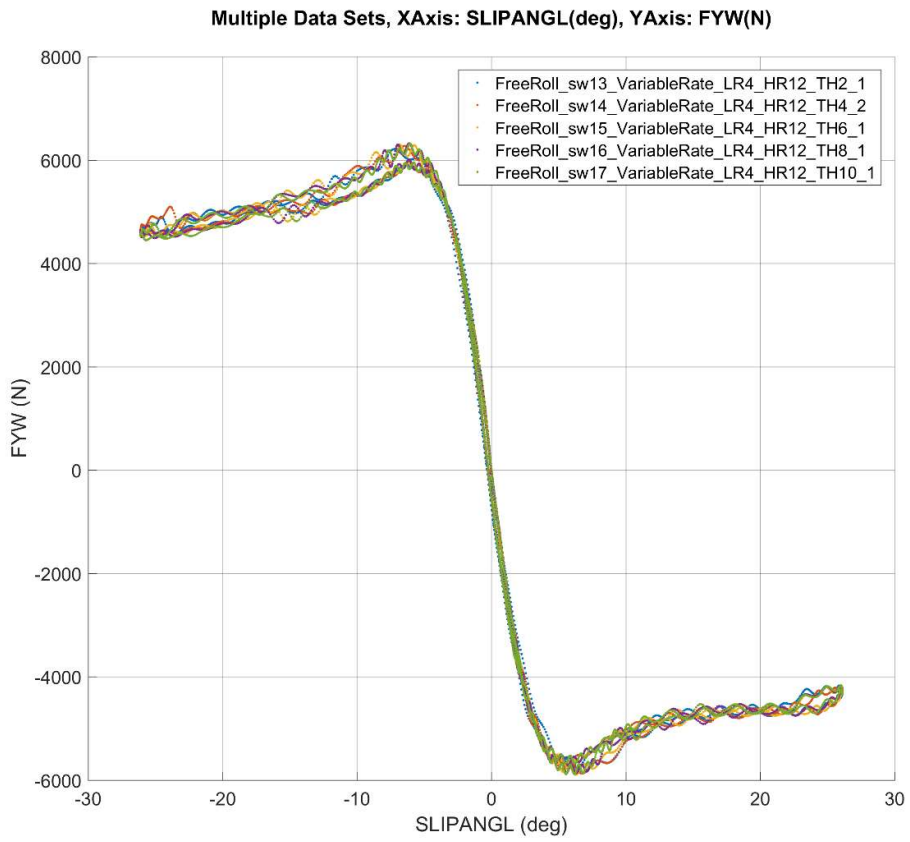

Figure 3.6.2-J. Lateral force versus slip angle comparing different 'thresholds' used in free rolling variable rate sweeps.

The lateral force performance of the tyre shown in Figure 3.6.2-J is very similar during these sweeps. The test tyre is asymmetric and consistently generates more absolute lateral force in the negative slip angle range (steering left, peaking at just over 6000N) compared to the positive slip angle range (steering right, peaking at just under 6000N). All tests were configured with the tyre mounted to the rig such that it is representative of the right-side tyres of a vehicle. In this configuration, when steering to the left, a vehicle's weight shifts to the right, meaning the right-side tyres are under higher load and hence responsible for generating most of the cornering force. Asymmetric tyre designs takes advantage of this and the tyre is designed to be more optimal when steering left. In this load case (steering left with asymmetric tyres) the left-side tyres are sub-optimal, but since they are under less vertical load they have less influence and the net result is an overall benefit to vehicle performance.

The temperature profiles of these sweeps shown in Figure 3.6.2-J are also very similar, with the lowest peak temperature being 92.9°C and the highest being 94.9°C, a variance of just 2.1%. As a result, the required thermal pause times and overall duration are also similar.

The overall results show that the 'threshold' has little effect on either the forces or the temperatures. However, the cornering stiffness is of particular importance for tyre models used in vehicle dynamics. Therefore, it makes sense to gather high quality, low hysteresis data in this region. The research presented by Rill (Rill, 2006) and discussed previously the 'high rate', shows that relaxation length reduces with slip angle in a non-linear fashion and that by 4° the relaxation length has reduced by 75%, shown in Figure 3.6.2-G. Based on this a 'threshold' of around 4° was selected. This gives a large, 8° range of data where the tyre is testing at the lowest slip rate, which as demonstrated in the previous sections, gives the best data to obtain accurate measurements of cornering stiffness, RSAT and RCF.

BrkDrv, Test Schedule

As with the 'FreeRolling' variable rate sweep investigation, a complete schedule of testing was carried out to investigate how the variable rate sweep performs during 'BrkDrv' (Braking and Driving) testing. A new tyre specimen was used for each test. This time the slip angle was held at 0° throughout the test procedure and torque was applied to the test tyre by means of a drive motor which can control the tyre through a range of slip ratios. The full test procedure can be found in Table 3.6.2-C.

Sequence	**Test**
1	Warmup
2	BrkDrv_sw1_VariableRate_LR10_HR30_TH10_1
3	BrkDrv_sw2_ConstantRate_10_1
4	BrkDrv_sw3_ConstantRate_20_1
5	BrkDrv_sw4_ConstantRate_30_1
6	BrkDrv_sw5_ConstantRate_40_1
7	BrkDrv_sw6_VariableRate_LR10_HR30_TH10_2
8	BrkDrv_sw7_VariableRate_LR20_HR30_TH10_1
9	BrkDrv_sw8_VariableRate_LR30_HR30_TH10_1
10	BrkDrv_sw9_VariableRate_LR40_HR30_TH10_1
11	BrkDrv_sw10_VariableRate_LR10_HR20_TH10_1
12	BrkDrv_sw11_VariableRate_LR10_HR30_TH10_3
13	BrkDrv_sw12_VariableRate_LR10_HR40_TH10_1
14	BrkDrv_sw13_VariableRate_LR10_HR50_TH10_1
15	BrkDrv_sw14_VariableRate_LR10_HR60_TH10_1
16	BrkDrv_sw15_VariableRate_LR10_HR30_TH2_1

17	BrkDrv_sw16_VariableRate_LR10_HR30_TH4_1
18	BrkDrv_sw17_VariableRate_LR10_HR30_TH6_1
19	BrkDrv_sw18_VariableRate_LR10_HR30_TH8_1
20	BrkDrv_sw19_VariableRate_LR10_HR30_TH10_4
21	BrkDrv_sw20_VariableRate_LR10_HR30_TH12_1
22	BrkDrv_sw21_VariableRate_LR10_HR30_TH14_1
23	BrkDrv_sw22_VariableRate_LR10_HR30_TH16_1
24	BrkDrv_sw23_VariableRate_LR10_HR30_TH18_1
25	BrkDrv_sw24_VariableRate_LR10_HR30_TH10_5

Table 3.6.2-C. Variable Rate Investigation, 'BrkDrv' Test Schedule.

An identical warmup procedure was used at the beginning of both the 'FreeRolling' and 'BrkDrv' tests, more details of this can be found in Section 3.4 on Warmup.

After the warmup, constant rate sweeps were conducted at four different slip ratio rates to establish a performance baseline. Following this, a series of different variable rate sweeps were conducted where the 'low rate', 'high rate' and 'threshold' are all changed independently so their influences could be fully investigated. There is one 'BrkDrv', 'Graph Sweep' that is repeated five times throughout the test. Analysis of the tyre performance during this repeated sweep allows conclusions to be drawn as to how the tyre itself changed as a result of the testing. 'BrkDrv' testing at positive longitudinal slip requires torque to be applied via the rig's drive motor. This means more energy is being added to the system which can often lead to the tyre reaching greater temperatures and wearing faster compared to 'FreeRolling' testing. For this reason, additional focus was placed on analysing the temperature profiles and comparing the wear level using the five repeated sweeps.

BrkDrv, Test Validation

Five identical Graph Sweeps were run repeatedly throughout the test procedure. Figure 3.6.2-K shows the longitudinal force versus longitudinal slip comparison between these identical sweeps included in the 'BrkDrv' test procedure. It therefore shows how the performance of the tyre itself changes as a result of the testing.

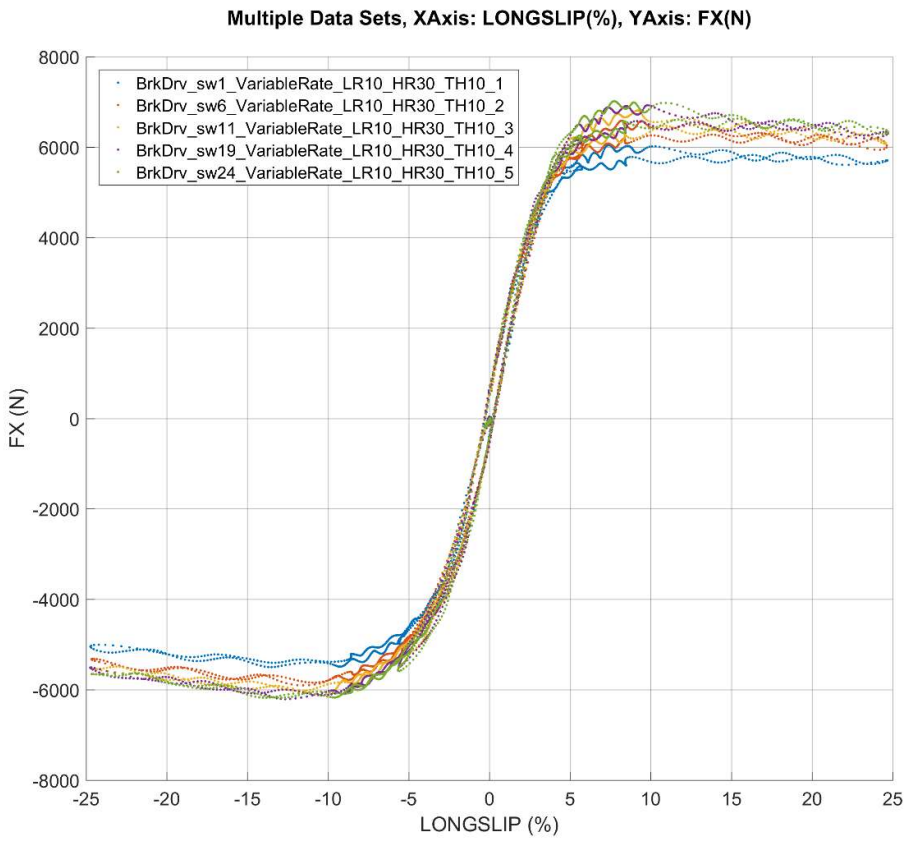

Figure 3.6.2-K. Longitudinal force versus slip ratio for the five identical sweeps tested repeatedly throughout the test procedure.

The data in Figure 3.6.2-K shows that the tyre behaved similarly throughout the test; however, the first sweep (BrkDrv_sw1) appears to be an outlier; generating around 400N less longitudinal force at high slip conditions compared to the other four sweeps. The reason for this is not clear, as both temperature and wear during this sweep are similar to the other sweeps. Also, the data shows the rig applied the load case correctly and there are no other anomalies in the data to explain it. It is proposed that the difference could be due to the 'breaking in' of the tyre. This is where the performance of a new tyre can change as release agents and other contaminants are removed during testing or physical driving, also the internal structure of the tyre may need to be 'broken in' before the performance becomes more homogeneous. This however, cannot be proven with the available data; also time, budget and logistic restrictions mean there is no opportunity to re-run the testing. The outlier only occurs at the very start of the procedure; thereafter the tyre remains consistent and performs as expected for the vast majority of the test. This is shown by the data from the other four sweeps (BrkDrv_sw6, 11, 19, 24) being very similar to one another, while only the first sweep (BrkDrv_sw1) performs differently. For this reason, it can be concluded that this test is still valid and the data can be relied upon.

BrkDrv, Constant Rate Sweep Analysis

During the first section of the 'BrkDrv' test procedure, four different constant rate sweeps were carried out to observe the effect of changing slip ratio rate. Tests were conducted at constant slip rates of 10, 20, 30 and 40%/s. Figure 3.6.2-L shows the results of these tests at slip ratios close to zero, where the mechanical hysteresis can be observed.

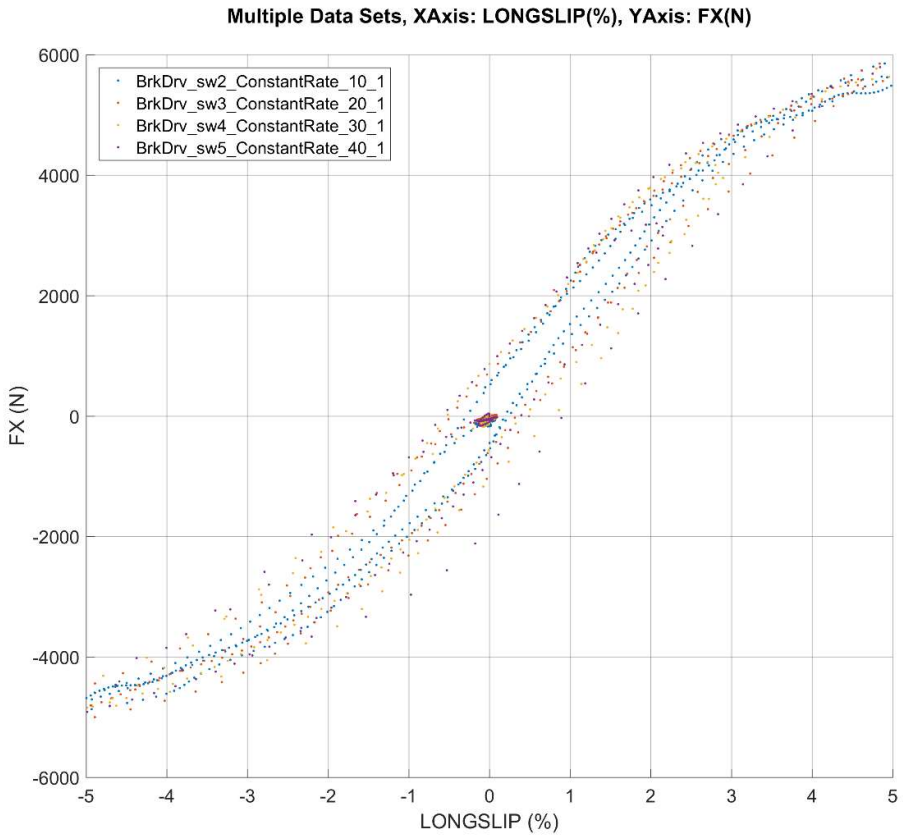

Figure 3.6.2-L. Longitudinal Force FX (N) versus slip ratio LONGSLIP (-) for 'BrkDrv' constant rate sweeps at different slip rates, zoomed into slip stiffness section.

The results shown in Figure 3.6.2-L correlate with the tyre's lateral free rolling behaviour where the slower rate reduces mechanical hysteresis close to zero slip. In this case the slowest slip ratio rate of 10 %/s (BrkDrv_sw2) induced around 1,050N (+500 - -550 = 1050N) of hysteresis while the 40 %/s sweep (BrkDrv_sw5) induced around 2,700N (+900 - -1800 = 2700N) of hysteresis. This means using the slower slip rate reduces hysteresis by around 61%.

Figure 3.6.2-M shows the same longitudinal force versus slip ratio data as presented in Figure 3.6.3-L, however, Figure 3.6.2-M shows the data over the complete range of testing; for clarity, only two sweeps are shown at 10 and 40%/s.

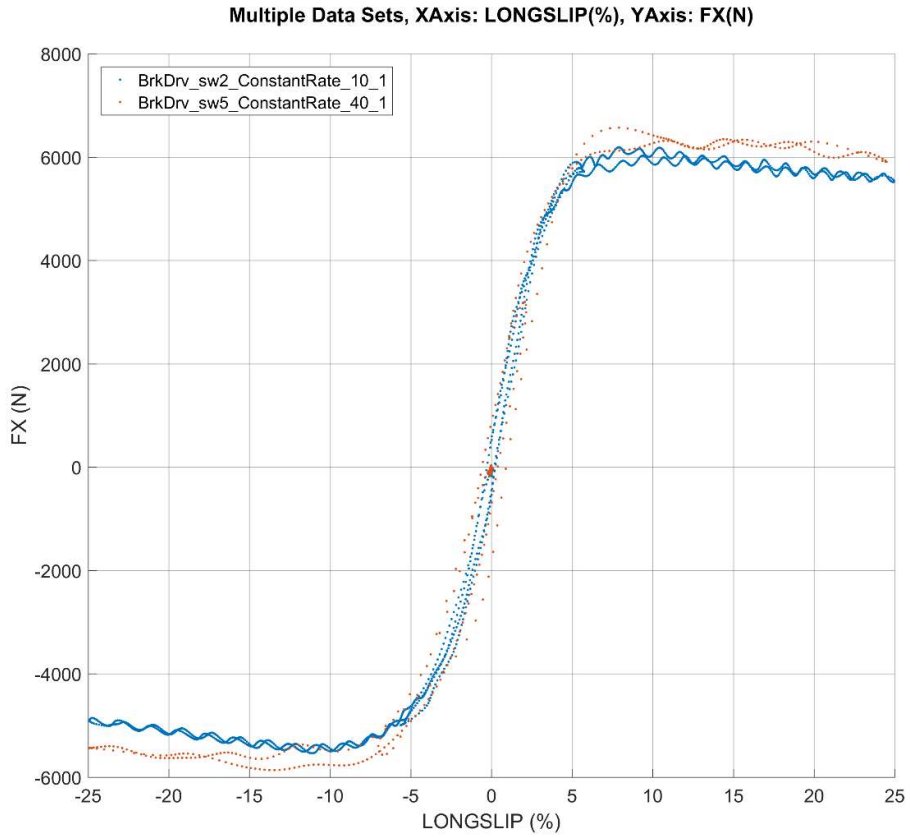

Figure 3.6.2-M. Longitudinal Force FX (N) versus slip ratio LONGSLIP (-) for 'BrkDrv' constant rate sweeps at different slip rates.

Figure 3.6.2-M shows the effect the different slip rate had on tyre performance when at high slip conditions. Here it can be observed that the slow rate of 10%/s caused the tyre to generate significantly less grip at high slip ratios compared to the sweep conducted at 40%/s. This is due to the extended amount of time the tyre spends at high slip condition during the slow rate sweep causing it to heat up to 92.0°C and remain at high temperatures for a few seconds, while during the 40%/s the tyre only reached 74.4°C. The thermal profiles of the sweeps can be found in Figure 3.6.2-N. The overheating during the slow rate sweep caused the tyre to operate outside of its optimal temperature range, this is demonstrated by the loss of grip that occurs in the high slip region of the 10 %/s test. Figure 3.6.2-N also shows that after the 10%/s sweep where the tyre reached 92.0°C it took 16.2s to cool back down to the 45°C baseline temperature before the next sweep could be triggered. This long cool down time indicates that this was not a flash temperature on the tires surface, which would cool down very quickly and have minimal effect

on tyre performance, but instead the heat had propagated deeper into the rubber taking longer to cool and having a greater effect on performance. During the 40%/s sweep the tyre only reached 74.4°C and took just 8.8s to cool. This means that the overall duration of the faster sweep was 45.7% shorter than the slower sweep.

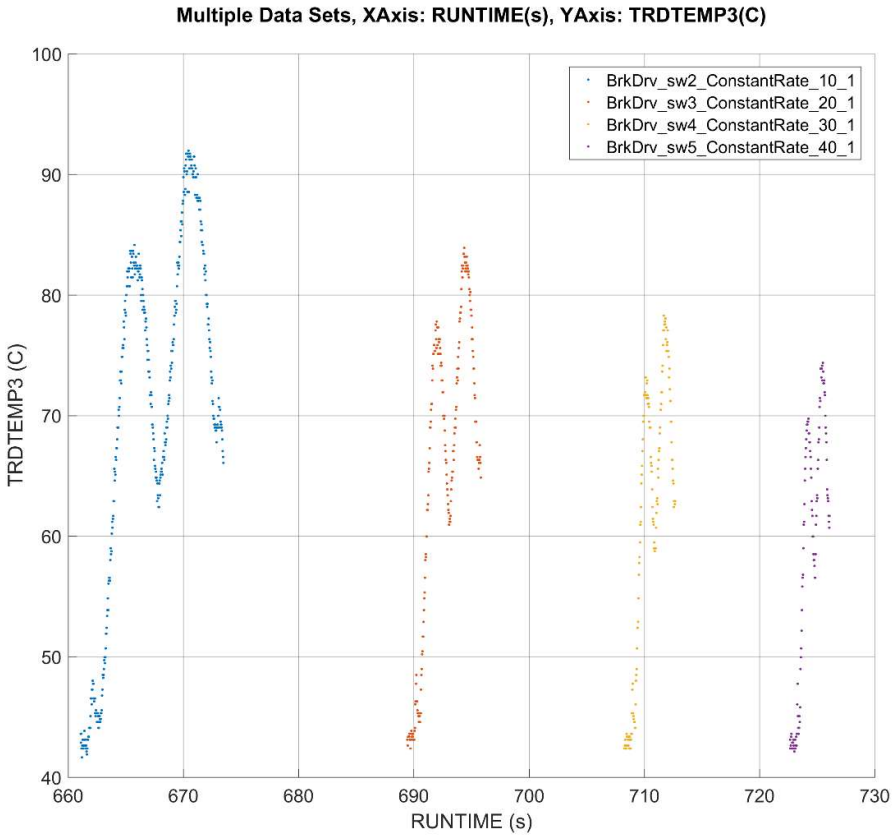

Figure 3.6.2-N. 'TRDTEMP3' (tyre outer surface central tread temperature) versus runtime for the 'BrkDrv' constant rate sweeps.

Overall these 'BrkDrv' constant rate sweeps demonstrate the same inherent compromise that was shown to exist in the constant rate free rolling sweeps. That being the slow sweep generates low levels of mechanical hysteresis but temperatures are higher causing both a loss of grip at high slip conditions and longer cool times. The 'high rate' sweep addressed these issues keeping temperature and cool down times lower, however it generated more mechanical hysteresis. It can therefore be concluded that either option compromises the data in some way.

BrkDrv, Variable Rate – 'High Rate' Analysis

Five different variable rate sweeps were conducted at different 'high rates' to investigate the effect on tyre performance. 'High rates' of 20, 30, 40, 50 and 60%/s were tested. The rig could apply slip ratios at even higher rates; however, initial pre-tests showed that this caused the tyre

to slip on the rim and invalidated the result. Therefore, a maximum slip ratio change rate of 60%/s was decided upon. This is valid for this particular tyre, wheel, vertical load and inflation pressure combination. However, rim slippage could occur at different longitudinal slip conditions when testing different wheels and tyres. Therefore, this maximum change rate of 60%/s is only valid for this particular test setup and should be reconsidered when testing alternative wheel and tyre combinations or drastically different load cases, (such as very low inflation pressure where the tyre is more likely to slip on the wheel rim). Testing alternative conditions was considered out of scope for this project; furthermore, the results from testing at the five selected 'high rates' reveal very little observable difference in the tyre performance. This is shown in in Figure 3.6.2-O.

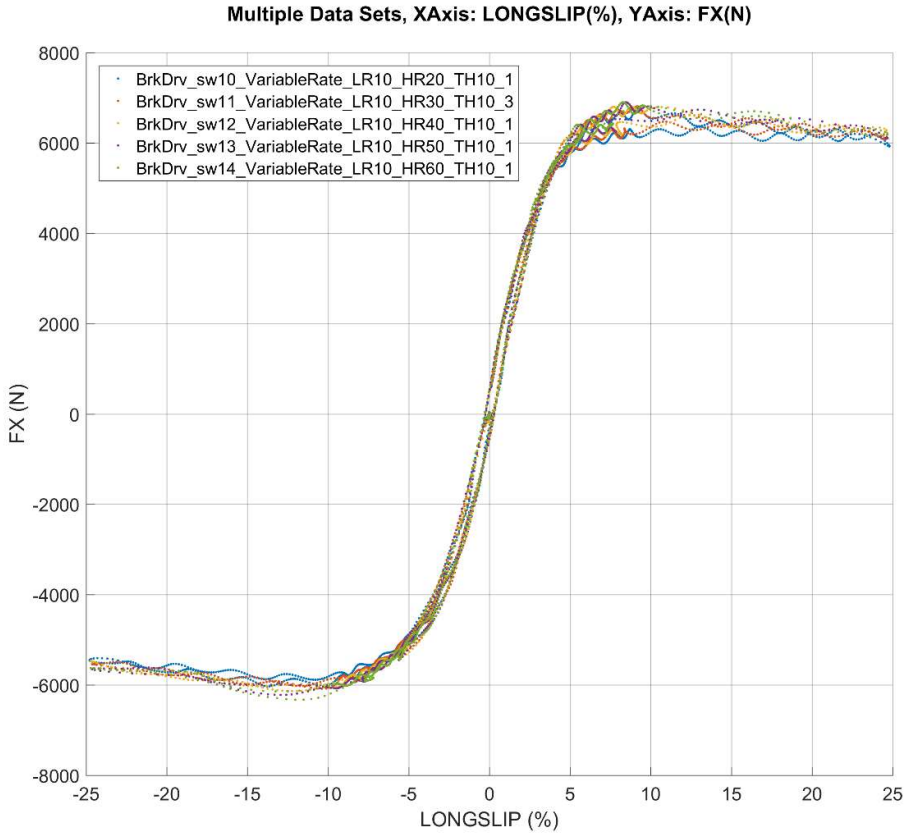

Figure 3.6.2-O. Longitudinal force versus longitudinal slip for 'BrkDrv' variable rate sweeps set to different 'high rates'.

Figure 3.6.2-O shows the resulting longitudinal slip sweeps where is can be observed that the data is asymmetric, with peak FX at positive longitudinal slip being greater than 6000N while the peak at negative slip is close to 6000N. This is common during longitudinal slip testing where the data cannot be assumed to be symmetrical. If the braking and tractive performance of a tyre was consistently similar then the testing could be halved by only testing one side of the

slip curve (either positive or negative longitudinal slip); however, this not being the case necessitates testing across the complete longitudinal slip range.

The force profiles of the five sweeps showed very little sensitivity to the longitudinal slip 'high rate'. However, the thermal profiles of the five sweeps shown in Figure 3.6.2-P do show some differences. The thermal profiles show that there are significant differences in temperature when using different 'high rates' in a variable rate sweep. During the testing with a 'high rate' of 20%/s (BrkDrv_sw10) the tyre peaked at 82.4°C and took 11.1s to cool down, the sweep with a 'high rate' of 60%/s (BrkDrv_sw14) peaked at 73.1°C and took 9.2s to cool down.

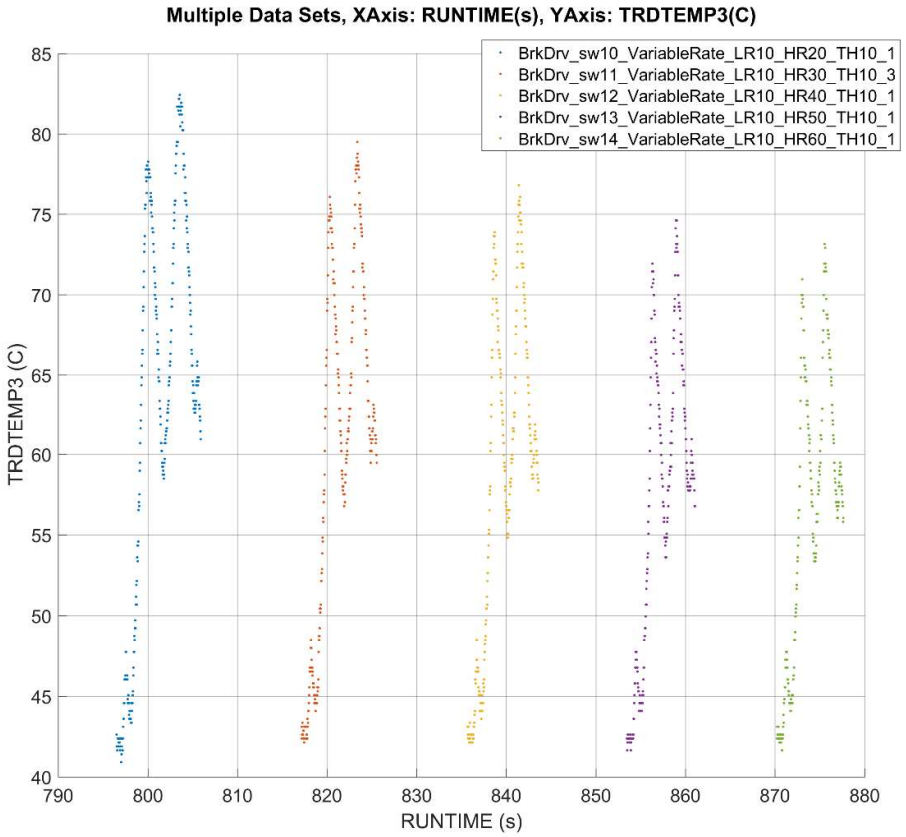

Figure 3.6.2-P. Tyre tread surface temperature versus time for 'BrkDrv' variable rate sweeps using different 'high rates'.

This section of the testing shows that using the faster 'high rate' sweep had no negative effect on the longitudinal force data but lead to a 17.1% reduction in the required cool down times hence increasing efficiency. The maximum slip rate is determined by when the tyre slips on the rim which in this case occurred at rates above 60%/s.

BrkDrv, Variable Rate – 'Low Rate' Analysis

Four test sweeps were conducted to investigate the effect of changing the 'low rate' during the variable rate sweep. These tests were conducted using 'low rates' of 10, 20 30 and 40%/s. While conducting these tests, where the tyre's contact patch transitions between non-sliding, through partial sliding and into full high slip testing, the amount of grip the tyre generates becomes highly variable. Furthermore, the tyre's transition between 'grip' and 'slip' is not naturally a smooth one; hence a very powerful motor with a very fast responding control system is required to regulate this transition as smoothly as possible, avoiding unwanted noise in the test data. This effect is worsened by commanding a very slow transition through these slip states. Pre-testing on this combination of test rig, tyre and load case revealed that 10%/s was the slowest slip ratio rate that could be accurately and precisely controlled by the rig. Therefore, the low limit was set at 10%/s.

The longitudinal force results from this testing are shown in Figure 3.6.2-Q and demonstrate a similar trend seen in previous sweeps where hysteresis is minimised when using a slow slip rate. In this case the slowest rate sweep of 10%/s (BrkDrv_sw6) resulted in around 1100N (+600 - -500 = 1100N) of hysteresis at zero slip ratio, while the fastest slip rate of 40%/s (BrkDrv_sw9) resulted in around 2,800N (+900 - -1900 = 2800N) of hysteresis.

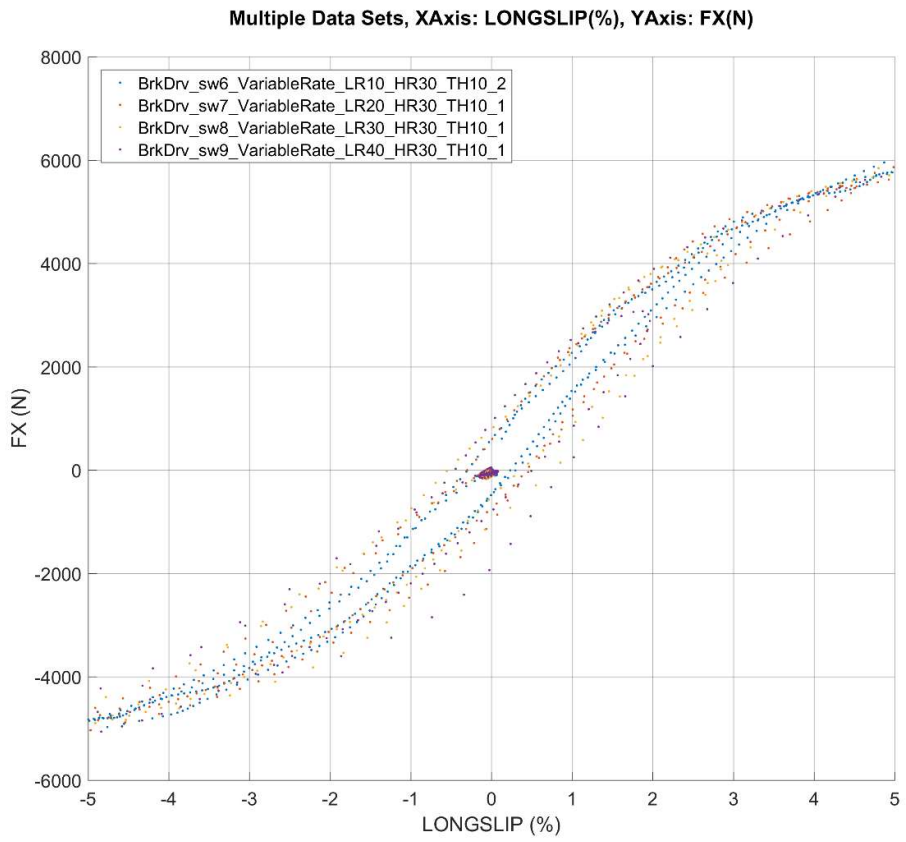

Figure 3.6.2-Q. Longitudinal force versus slip ratio close to zero for 'BrkDrv' variable rate sweeps each set to a different 'low rate'.

Thermal analysis of these sweeps reveal that each sweep peaked at almost the same temperature of 78°C. The data shows that the 'low rate' has no discernible effect on temperature or test efficiency, however the lowest 'low rate' of 10%/s causing a significant 60.7% reduction in mechanical hysteresis compared to the highest 'low rate' of 40%/s. It can therefore be concluded that the optimal 'low rate' to use is 10%/s and is therefore included in GS2MF.

BrkDrv, Variable Rate – 'Threshold' Analysis

A series of tests were conducted to investigate the effect of changing the 'threshold' at which the variable rate sweeps switched between the 'high and low rates'. The effect on longitudinal force is shown in Figure 3.6.2-R.

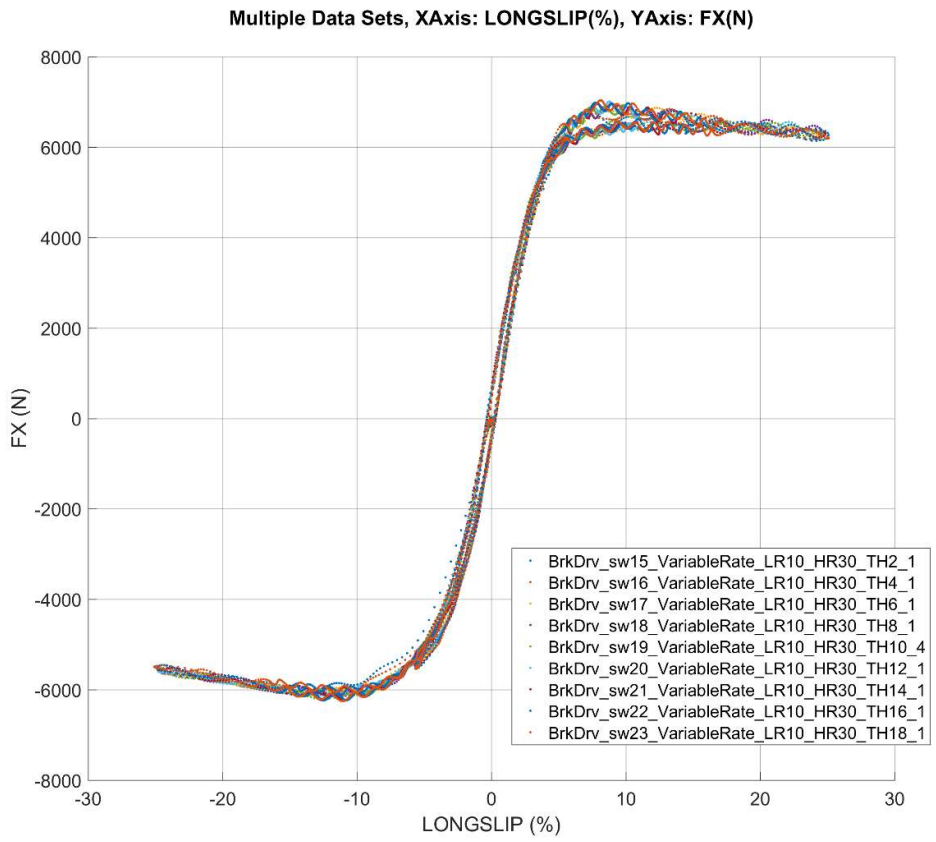

Figure 3.6.2-R. Longitudinal force versus slip ratio comparing different 'thresholds' used in 'BrkDrv' variable rate sweeps.

The force profiles in Figure 3.6.2-R show very little difference between the sweeps. Likewise, a thermal analysis of the sweeps reveals that there is only a small difference of around 7.8°C between the coolest sweep ('threshold' of 2% peaking at 77.1°C) and the warmest sweep ('threshold' of 18% peaking at 84.9°C). Overall, the data shows that the tyre has very little sensitivity to the 'threshold' between the 'low and high rates' of the variable rate sweep. In this case, further analysis was conducted looking at the duration of the sweeps themselves, the results of this are shown in Figure 3.6.2-S. Here, it can be seen that the low 'threshold' of 2% results in a sweep duration of a little over 6s, whereas the highest 'threshold' of 18% results in a sweep that is just over 10s long. This is due to the lower 'threshold' meaning the tyre spends more time at the faster rate, reducing overall duration.

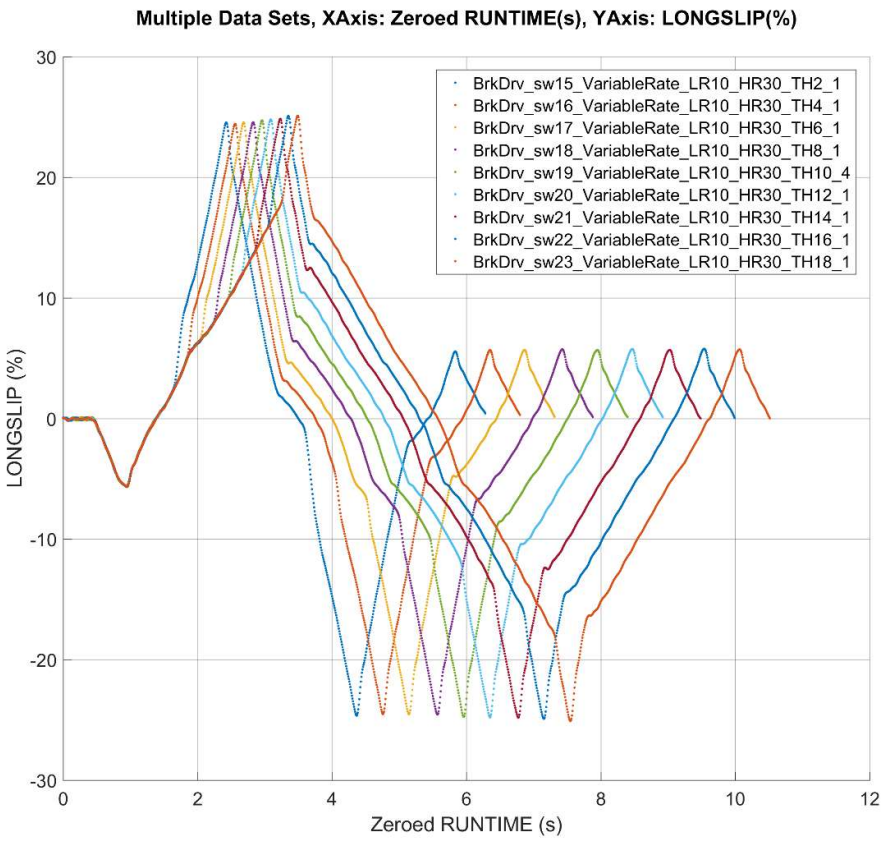

Figure 3.6.2-S. Longitudinal slip versus zeroed runtime (all sweeps starting from 0s) for 'BrkDrv' sweeps at different 'thresholds'.

Overall, all the sweeps generated very similar data. The lowest 'threshold' of 2% resulted in equally good quality longitudinal force data compared to the others, while generating slightly less heat, as well as having the shortest overall duration. An even lower 'threshold' would reduce test duration very slightly. However, doing so would result in less data being available to extract accurate values for crucial tyre performance metrics such as slip stiffness. A 'BrkDrv' variable rate sweep 'threshold' of 2% is therefore the optimal choice and is selected for use in the 'GS2MF BrkDrv' test procedure.

Variable Rate Sweep Summary ('FreeRolling' and 'BrkDrv')

Having fully tested the influence of each parameter required in the setup of variable rate sweeps applied to both 'FreeRolling' and 'BrkDrv' testing, it is possible to draw conclusions as to the optimal setup of the sweeps. For 'FreeRolling' testing the optimal setup is shown in Table 3.6.2-D.

'FreeRolling'	**Optimal Value**
'High Rate'	30°/s
'Low Rate'	2°/s
'Threshold'	4°

Table 3.6.2-D. Optimal variable rate sweep setup for 'FreeRolling' testing.

The 'high rate' was determined to be the highest rate the test rig could apply. It's therefore possible that this is not in fact the ideal 'high rate' to be used in the testing. However, testing was conducted at both Calspan and using the SoVaMotion rig which offers some of the fastest maximum slip angle rates currently available. As such, it is both not possible and not valuable to continue this testing to determine if faster 'high rates' offer any discernible advantage. Even if there was a theoretical advantage, this could not be realised in practice due to the lack of available of rigs with ultra-high slip rate capability. The selected 'low rate' is the lowest rate used during the investigation. The 2°/s 'low rate' provides on-centre data with very low mechanical hysteresis and no notable thermal problems. Lowering this further will increase the overall test duration as well as tyre wear without any discernible improvements to the already non-problematic data. A total of nine different slip angle 'thresholds' were tested with the results showing very little difference between them. The 'threshold' of 4° was selected based on the reduction of relaxation length at this slip angle balanced with the requirement to reduce overall test duration.

BrkDrv	**Optimal Value**
'High Rate'	60%/s
'Low Rate'	10%/s
'Threshold'	2%

Table 3.6.2-E. Optimal variable rate sweep setup for 'BrkDrv' testing.

Table 3.6.2-E shows a summary of the optimal variable rate sweep for 'BrkDrv' testing. The 'high rate' of 60%/s was determined based on any faster 'high rates' causing the tyre to slip on the rim. This value is therefore specific to this particular combination of tyre, wheel, vertical load and inflation pressure, all of which contribute to wheel slippage. A different load case combination or a tyre with a tighter bead seat could result in faster 'high rates' being used, alternatively an adhesive could be used to strengthen the bond between the wheel and the tyre. If a faster 'high rate' could be used it is expected to have little to no effect on the longitudinal force data but could further reduce peak temperatures and hence reduce the required cool down times. A 'low rate' of 10%/s was selected based on the accuracy of the longitudinal slip control

system. The testing was conducted at the SoVaMotion rig which offers slip control that is similar or better than almost anywhere else available. Yet even here slip rates lower than 10%/s could not be used reliably without compromising the smoothness of the slip regulation. A slip ratio 'threshold' of 2% was selected as this offered the lowest overall sweep duration while in no way adversely affecting the data. Lower 'thresholds' could be used but 2% allows for a suitably wide range of data from which to extract accurate slip stiffness values.

'FreeRolling', Variable Rate versus Constant Rate

Further analysis was carried out to compare and understand the benefits of the optimised variable rate sweep, compared to the more commonly used constant rate sweep. Figure 3.6.2-T shows a lateral force comparison between the optimised variable rate sweep and the fastest and slowest constant rate sweeps.

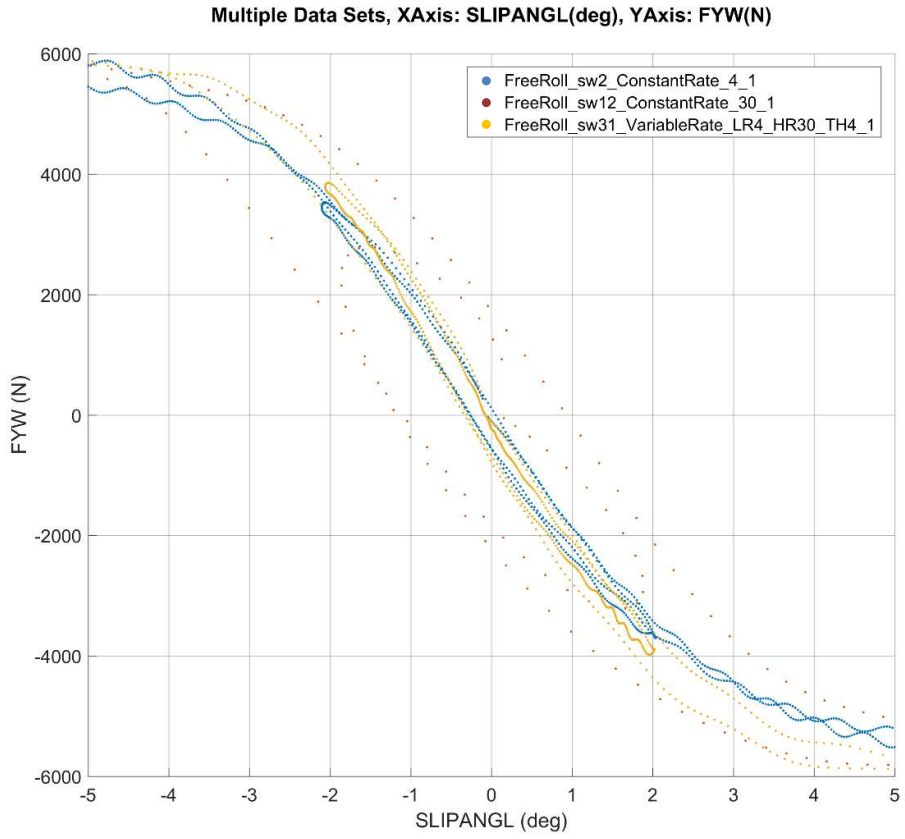

Figure 3.6.2-T. Lateral force versus slip angle for the fastest and slowest free rolling constant rate sweeps, along with the variable rate sweep at a reduced slip angle range of -5 to +5°.

Figure 3.6.2-T shows that close to zero slip angle, the fastest constant rate sweep caused the tyre to generate a large mechanical hysteresis loop of 4,100N (+1900 - -2200 = 4100N) at zero slip angle, this reduces significantly during the slowest constant rate sweep to just 700N (+100 - -

600 = 700N). This reduced hysteresis is matched by the variable rate sweep during which the tyre generates almost exactly 700N of mechanical hysteresis. This is expected as both sweeps are operating at the same slip rate during this region. Figure 3.6.2-U shows the same sweeps as Figure 3.6.2-T; however, the data is shown over the full tested range of slip angles.

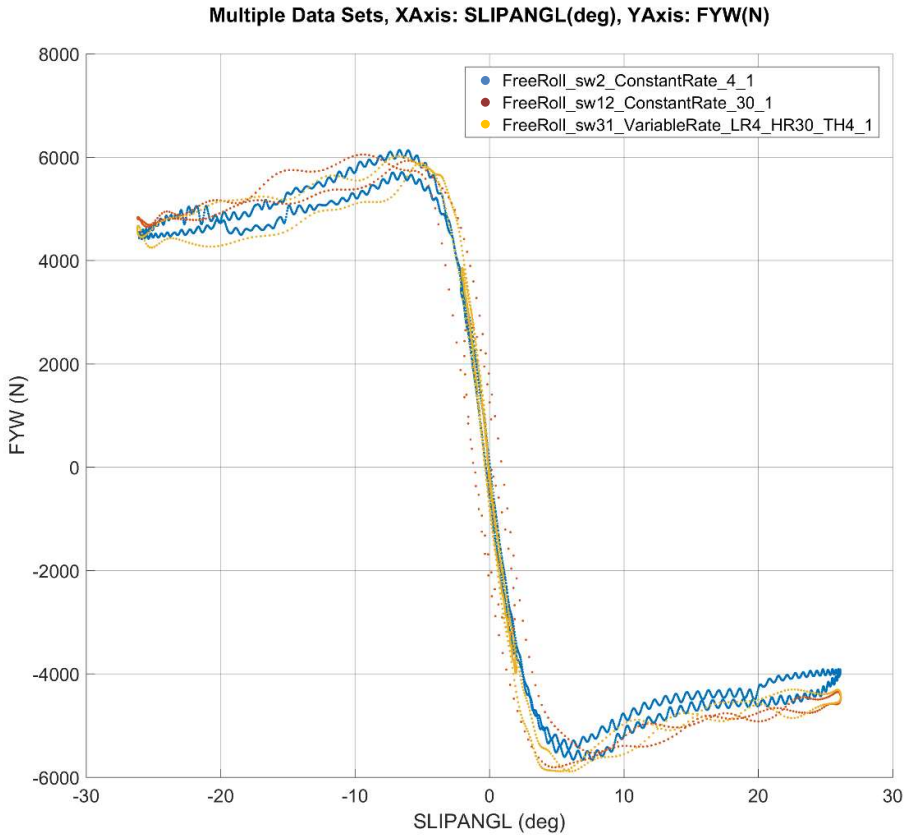

Figure 3.6.2-U. Lateral force versus slip angle for the fastest and slowest free rolling constant rate sweeps, along with the variable rate sweep.

Figure 3.6.2-U shows that at high slip conditions the variable rate sweep is comparable to the fastest constant rate sweep. While the slowest constant rate sweep generates around 500N less lateral force at high slip conditions, this is particularly evident on the positive slip angle side. This grip reduction during the slow constant rate sweep is due to the tyre overheating, as shown in the temperature profiles in Figure 3.6.2-V.

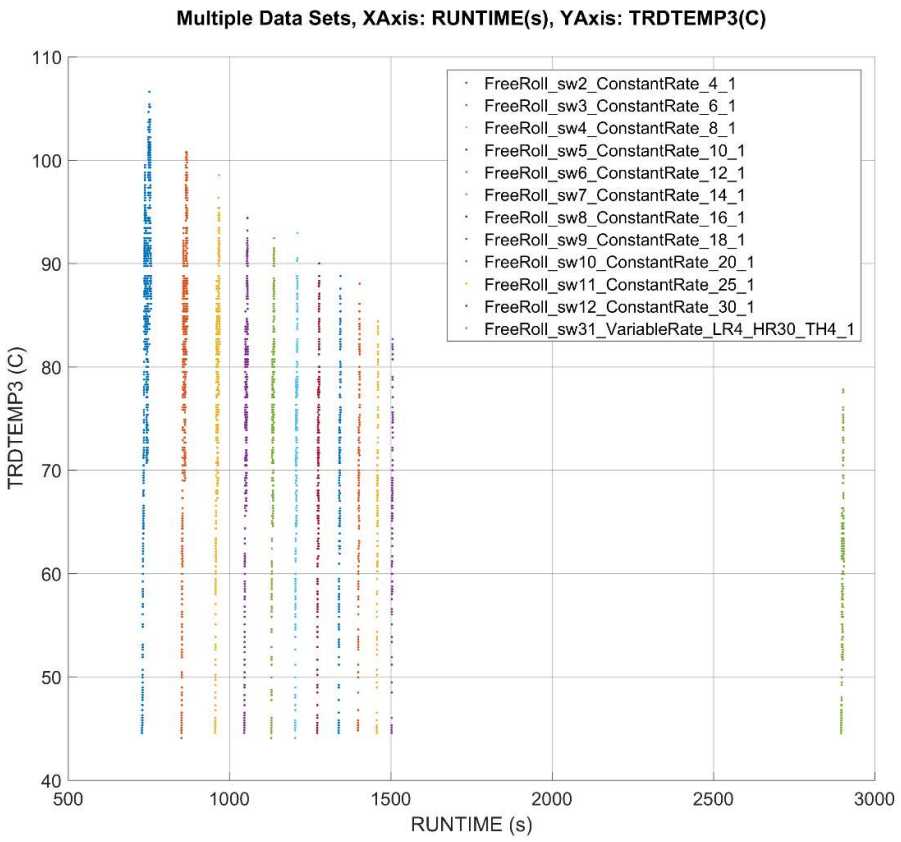

Figure 3.6.2-V. Tyre temperature versus time for all free rolling constant rate sweeps compared to the optimised variable rate sweep.

Figure 3.6.2-V shows that during the low constant rate sweep the tyre temperature peaked at 106.6 °C, causing the reduced grip at high slip conditions observed in Figure 3.6.2-U. This overheating and the resulting drop in tyre performance is not evident in the fastest constant rate sweep where the tyre temperature peaked at 82.5°C, or during the variable rate sweep where the tyre peaked at just 77.8°C. This is well within the tyre's optimal operating conditions. These peak temperatures also affect the required cool down times before the tyre reaches a steady 45°C baseline temperature. Following the constant low slip rate sweep the tyre took 94.3s to cool; however, after the constant high slip rate sweep the tyre took 38.2s to cool. However, after the variable rate sweep the tyre took just 33.7s to cool which is a significant reduction compared to either of the constant rate sweeps. The overall performance of the variable rate sweep compared to the constant rate sweeps is summarised in Table 3.6.2-F.

'FreeRolling'	Low Slip Rate	High Slip Rate	Variable Rate
Mechanical Hysteresis	+ Better	- Worse	+ Equal to 'low rate'
Thermal Hysteresis	- Worse	+ Better	+ Equal to 'high rate'
Cornering Stiffness Accuracy	+ Better	- Worse	+ Equal to 'low rate'
RSAT and RCF Accuracy	+ Better	- Worse	+ Equal to 'low rate'
Tyre Wear	- Worse	+ Better	+ Equal to 'high rate'
Test Duration	- Worse	+ Better	+ Equal to 'high rate'

Table 3.6.2-F. Summary of the performance advantages of the variable rate sweep for free rolling applications.

The variable rate sweep equalled the low mechanical hysteresis observed during the constant low slip rate sweep, which is 83% (4,100N to 700N) lower than the fastest constant rate sweep. Meanwhile, the variable rate sweeps peak temperature of 77.8°C is 5.7% (82.5°C to 77.8°C) lower than the constant high slip rate sweep and 27% (106.6°C to 77.8°C) lower than the constant low slip rate sweep. This means that both thermal hysteresis and the required cool down times are better than any of the constant rate sweeps. The variable rate sweep uses a low slip rate over a wide enough range to extract accurate values of cornering stiffness, RSAT and RCF equalling the performance of the constant low slip rate sweep. Finally, the reduced time spent at high slip conditions means the total sliding energy during the variable rate sweep is low, meaning tyre wear will be low. This demonstrates that the variable rate sweep was successful in maximising overall data quality and avoiding the inherent compromise that comes with using constant rate sweeps, at the same time minimising test duration and wear.

'BrkDrv', Variable Rate versus Constant Rate

A detailed analysis was carried out to assess the benefits of the now optimised 'BrkDrv' variable rate sweep over the constant rate sweeps. As previously discussed, the tyre demonstrated some unexpected behaviour during the start of the 'BrkDrv' test sequence. During these first few sweeps the tyre generated less peak grip than expected, which is likely due to the new tyre not being fully 'broken in'. Problems and unexpected tyre behaviours such as these, are reasonably common when testing tyres. Therefore, five identical Graph Sweeps were included in the test procedure to allow any changes in the tyre's performance to be assed, as shown in Figure 3.6.2-K which can be found within Section 3.6.2 on BrkDrv, Test Validation.

The issues arising due to the inconsistencies of the tyre performance can be seen in Figure 3.6.2-W. This figure shows the first five sweeps of the test sequence, this includes 'BrkDrv_sw1' which is the first of the Graph Sweeps, along with 'BrkDrv_sw2-5' which are the constant rate

sweeps; also shown is ‘BrkDrv_sw14’ which is the closest sweep to the optimal variable rate setup. ‘BrkDrv_sw14’ has a slightly different ‘threshold’ to the optimal setup, however this was shown in Section 3.6.2 on BrkDrv, Variable Rate – threshold Analysis, to have a small influence on runtime and crucially no discernible influence on tyre performance.

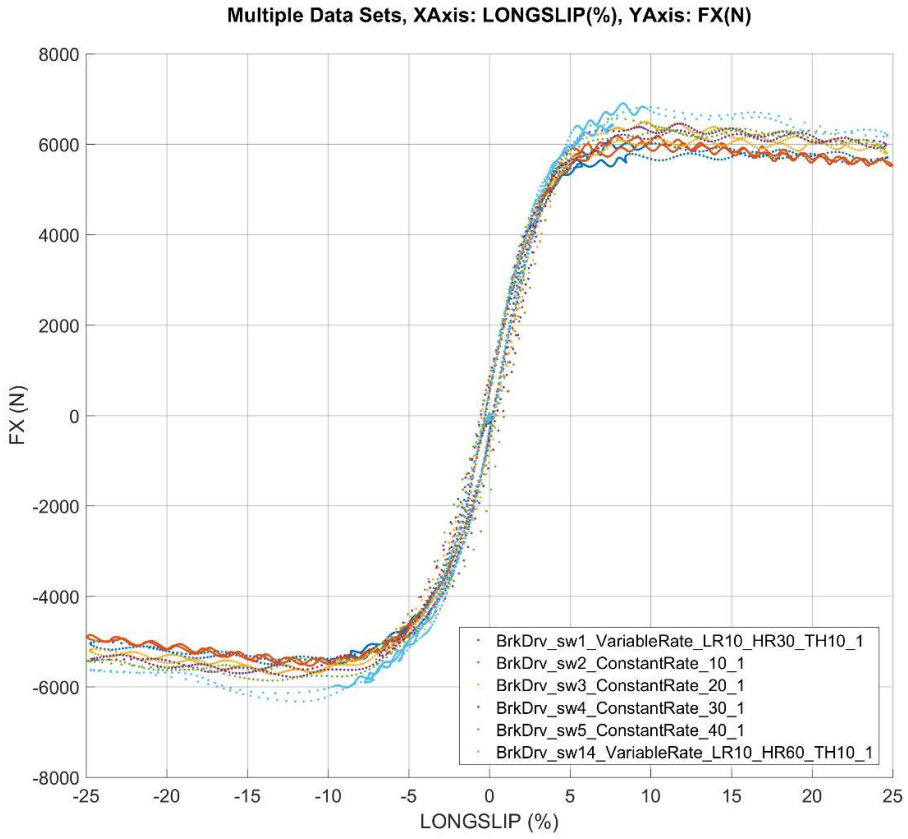

Figure 3.6.2-W. Longitudinal force versus slip ratio for the ‘BrkDrv’ constant rate sweeps, along with the optimal variable rate sweep and Graph Sweep.

Looking closely at Figure 3.6.2-W it can be observed (particularly at the positive high slip region of the plot), that the peak grip of the tyre changes significantly; from 5,650N (BrkDrv_sw1) to 6,450N (BrkDrv_sw5) at +10% slip, an increase of 14.2% across these five sweeps. Usually changes like this will correlate to a change in the setup of the sweep, such as the slip rate. However, in this case the sweep setups do not change in such a consistent manner, the temperature trends are also not consistent and the increase in peak force correlates precisely to the order at which the sweeps were conducted, shown in Figure 3.6.2-W. Each proceeding sweep generates more grip than the last, demonstrating that the tyre itself is changing due to the testing. This behaviour is consistent with the tyre being broken in; and this is further reinforced by the fact that the tyre’s performance changes over the first few sweeps and then stops

changing further into the test sequence. After this, the tyre's high slip performance becomes very consistent. This can be seen in Figure 3.6.2-R which can be found in Section 3.6.2 on BrkDrv, Variable Rate – threshold Analysis.

To address this issue and prove that the variable rate sweep is comparable to constant rate sweeps an indirect comparison was completed using the repeated Graph Sweeps as an intermediary, this process is described below:

1. The first Graph Sweep conducted at the very start of the test (BrkDrv_sw1) was compared to the constant rate sweeps (BrkDrv_sw2-5) which were conducted immediately after this first Graph Sweep; this plot can be found in Figure 3.6.2-W. The plot shows that the first Graph Sweep, which was conducted before the tyre performance had stabilised, matches the high slip performance of the constant rate tests, which were also conducted before the tyre performance had stabilised.
   Summary: The constant rate sweeps correlates to the first Graph Sweep.

2. The change in the tyre's performance throughout the test can be assessed by comparing the five identical Graph Sweeps repeated through the testing. This plot can be found in Figure 3.6.2-K (See Section 3.6.2 on BrkDrv, Test Validation). The plot shows that the tyre's longitudinal force during the first sweep is lower than the following sweeps. As discussed, this is due to the tyre performance stabilising during the first few sweeps.
   Summary: The repeated Graph Sweeps show the tyre's performance changes.

3. The variable rate sweep (BrkDrv_sw14) was then compared against the two Graph Sweeps closest to it in the test sequence, (BrkDrv_sw11 and 19). These sweeps were conducted after the tyre performance had stabilised. This comparison showed that the longitudinal grip performance of the tyre was very similar across these sweeps. A plot showing this can be found in Figure 3.6.2-X.
   Summary: The optimal variable rate sweep correlates to Graph Sweeps from later in the test sequence.

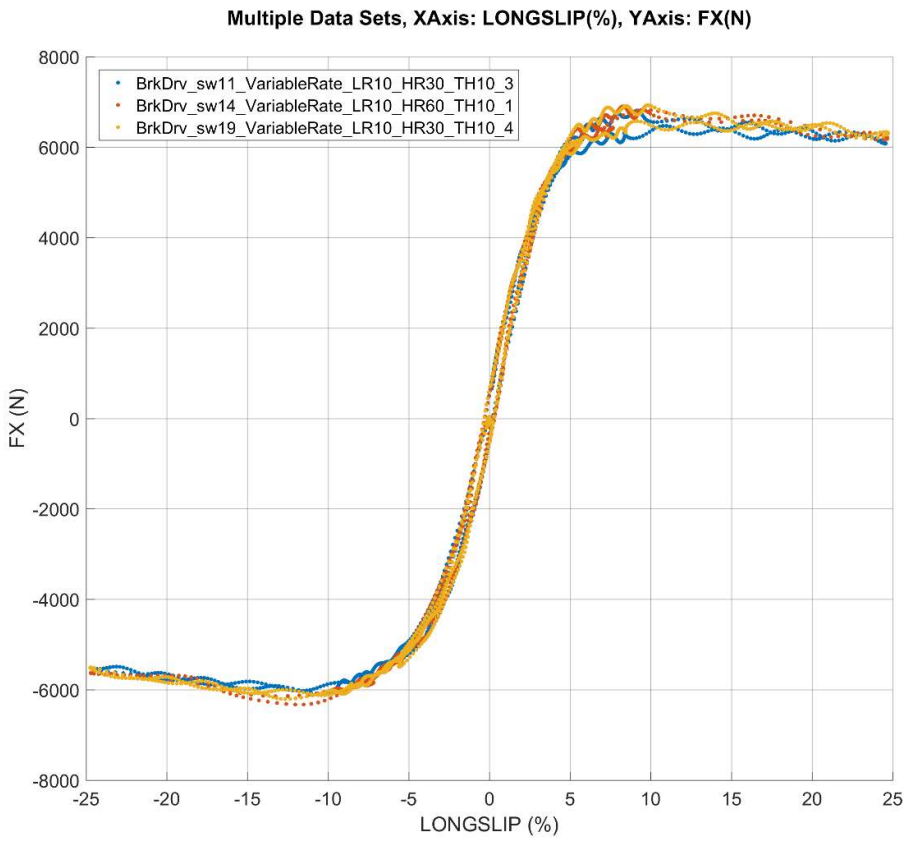

Figure 3.6.2-X. Comparison of the optimised variable rate sweep compared to the nearest two Graph Sweeps within the test sequence.

Through this indirect comparison, it can be inferred that the optimised variable rate sweep correlates to the constant rate sweeps. The constant rate sweeps correlate to the first Graph Sweep. The five Graph Sweeps demonstrate the change to the tyre itself. Finally, the optimised variable rate sweep correlates to the Graph Sweeps from after the tyre performance has stabilised. This means that the observed difference between the constant and variable rate sweeps is due to the tyre itself changing and not because of the test sweep. It is also shown that the optimised variable rate sweep does not in any way reduce the quality of the data compared to the traditional constant rate sweeps. Furthermore, the issue with the tyre itself changing only affects the high slip performance. Therefore, a direct comparison of the constant versus variable rate sweeps can be made in terms of the on-centre performance. This is shown in Figure 3.6.2-Y.

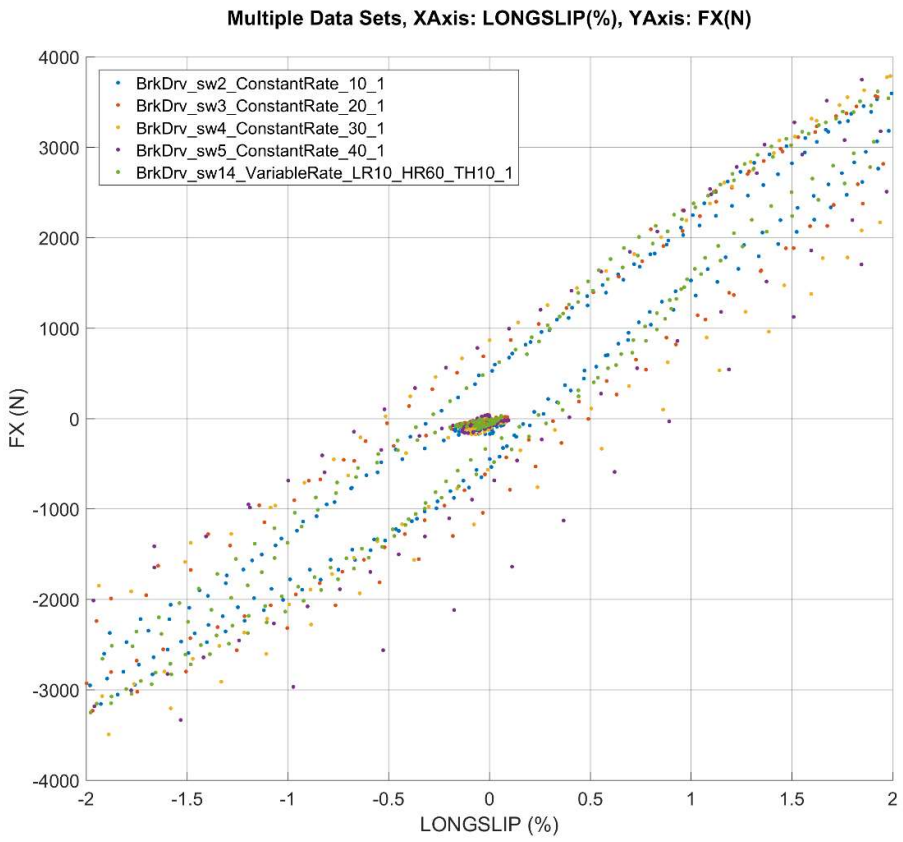

Figure 3.6.2-Y. Longitudinal force versus slip ratio close to zero for the 'BrkDrv' variable rate sweep compared to the constant rate sweeps.

Figure 3.6.2-Y shows that the fastest constant rate sweep conducted at 40%/s (BrkDrv_sw5) induced around 2,700N (+900 --1800 = 2,700N) of hysteresis, whilst the slowest constant rate sweep conducted at 10 %/s (BrkDrv_sw2) induced around 1,050N (+500 --550 = 1,050N). The variable rate sweep (BrkDrv_sw14) generated almost identical hysteresis to the best of the constant rate sweeps, meaning it matched the best possible performance in this region. This is expected as the 'low rate' section of the variable rate sweep is conducted at the same slip rate as the slowest of the constant rate sweeps, that being 10%/s.

Figure 3.6.2-Z shows the thermal profiles of the constant rate sweeps compared to the variable rate sweep.

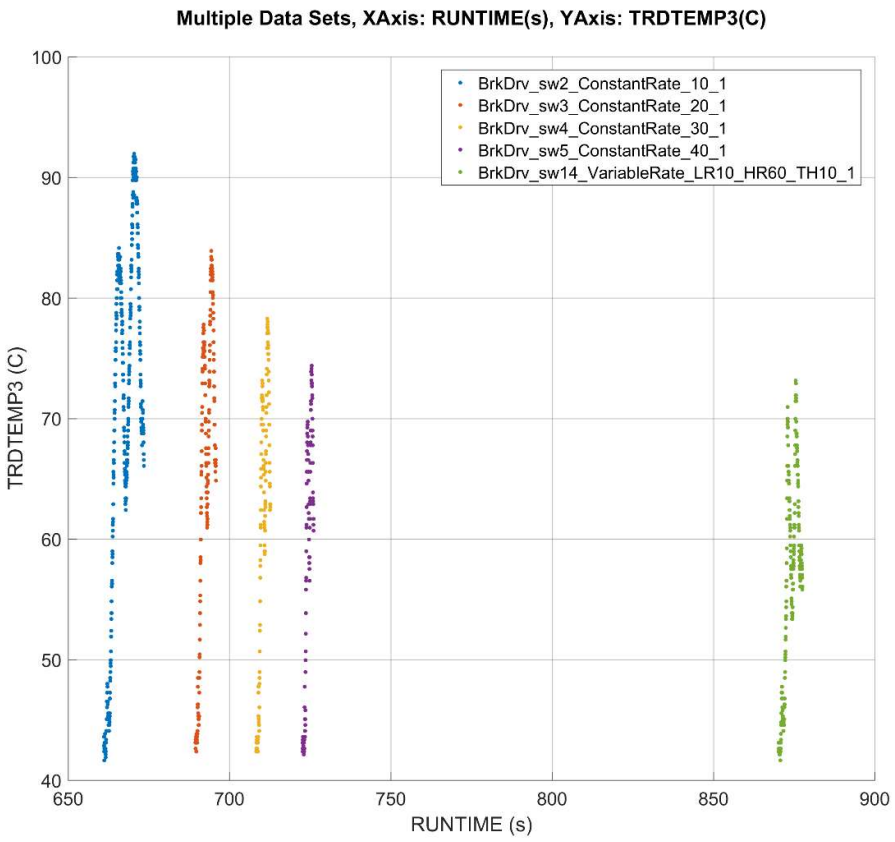

Figure 3.6.2-Z. Tyre temperature versus time for all 'BrkDrv' constant rate sweeps compared the optimised variable rate sweep.

Figure 3.6.2-Z shows that during the hottest constant rate sweep, conducted at 10%/s the tyre reached 92.0°C, while during the coolest sweep the tyre only reached 74.4°C. This low peak temperature is matched by the variable rate sweep where the tyre reached 73.1°C. This means that the thermal hysteresis during the variable rate sweep will be equal to the best of the constant rate sweeps. The required cool down time are also improved in the variable rate sweep. With the 10%/s constant rate sweep taking 16.2s to cool and the 40%/s constant rate sweep taking 8.8s, while the variable rate sweep matched this also taking 8.8s to cool. The overall performance of the variable rate sweep compared to the constant rate sweeps is summarised in Table 3.6.2-G.

BrkDrv	Low Slip Rate	High Slip Rate	Variable Rate
Mechanical Hysteresis	+ Better	- Worse	+ Equal to 'low rate'
Thermal Hysteresis	- Worse	+ Better	+ Equal to 'high rate'
Slip Stiffness Accuracy	+ Better	- Worse	+ Equal to 'low rate'
Tyre Wear	- Worse	+ Better	+ Equal to 'high rate'
Test Duration	- Worse	+ Better	+ Equal to 'high rate'

Table 3.6.2-G. Summary of the performance advantages of the variable rate sweep compared to low and high constant slip rate sweeps, for 'BrkDrv' applications.

Overall, the 'BrkDrv' variable rate sweep matched the mechanical hysteresis of the best constant rate sweep; that being 1,050N generated during the slowest 10%/s sweep. The peak temperature during the variable rate sweep was 73.1°C, a slight improvement on the best constant rate sweep during which the tyre reached 74.4°C. This means that the thermal hysteresis and cool down times of the variable rate sweep are also equal to the best constant rate sweep. The variable rate sweep uses a slow rate of 10 %/s close to zero slip meaning slip stiffness measurements can be made as accurately as they can during the low constant rate sweep. Finally, a 'high rate' is used at high slip conditions to minimise the amount of time spent in this region, minimising tyre wear down to similar levels to the constant 'high rate' sweep.

Variable Rate Conclusion

Overall, the investigation into the new variable rate sweep proved to be successful. The data consistently showed that for both 'FreeRolling' and 'BrkDrv' applications the variable rate sweep can provide significant and measurable improvements over a more traditional constant rate sweep. A summary of the benefits of the variable rate sweep for 'FreeRolling' testing can be found in Table 3.6.2-H.

‘FreeRolling’	Constant ‘Low Rate’ (4°/s)	Constant ‘High Rate’ (30°/s)	Optimal Variable Rate	Variable rate % difference compared to the best performing constant rate.
Mechanical Hysteresis, N	700	4100	300	57.1
Peak Temperature, °C (Thermal Hysteresis)	106.5	82.5	77.8	5.7
Total Duration, s (Sweep + Cool Down)	122.27	41.94	42.55	-1.5

Table 3.6.2-H. ‘FreeRolling’ summary table, variable rate sweep compared to constant rate sweep.

Table 3.6.2-H shows a summary of the key measurable benefits of using a variable rate sweep compared to a constant rate sweep for free rolling tests. The table shows that the variable rate sweep significantly improved on the mechanical hysteresis generated by even the best performing constant rate sweep (a 57.1% improvement over the constant low rate sweep). The lowest temperature during a sweep is regulated at 45°C by the thermal pause system (See section 3.5 on Thermal Logic) hence the peak temperature during the sweep directly relates to the thermal hysteresis. Peak temperature is also far easier to measure robustly as opposed to measuring thermal hysteresis directly. Figure 3.6.2-Z shows that the tyre’s peak temperature was lower during the variable rate sweep compared to the best of the constant rate sweeps (77.8°C compared to 82.5°C, a 5.7% improvement). This reduction in peak temperature will lead to a reduction in thermal hysteresis. Also shown is the fact that the best performing constant rate sweep for mechanical hysteresis is not the best for thermal hysteresis. This demonstrates that when using a constant rate sweep, a compromise exists where either the mechanical or thermal hysteresis can be minimised, but not both at the same time. Whereas the variable rate sweep successfully minimised both forms of hysteresis in the same sweep. Finally, the total duration of the variable rate sweep, that being the duration of the test sweep itself plus the duration of the required cool down afterwards, was a negligible 0.6s longer than the fastest constant rate sweep. Overall this demonstrates that the variable rate sweep avoided the inherent compromise between mechanical and thermal hysteresis by successfully minimising both. This improvement in data quality came at a negligible cost in overall runtime of 0.6s. Table 3.6.2-I shows similar benefits when using the variable rate sweep for ‘BrkDrv’ testing applications.

'BrkDrv'	Constant 'Low Rate' (10 %/s)	Constant 'High Rate' (40 %/s)	Optimal Variable Rate	Variable rate % difference compared to the best performing constant rate.
Mechanical Hysteresis, N	1050	2700	1050	0.0
Peak Temperature, °C (Thermal Hysteresis)	92	74.4	73.1	1.7
Total Duration, s (Sweep + Cool Down)	28.6	12.23	12.72	-4.0

Table 3.6.2-I. 'BrkDrv' summary table, variable rate sweep compared to constant rate sweep.

Table 3.6.2-I shows the benefits of using a variable rate sweep for 'BrkDrv' applications. In this case, the mechanical hysteresis generated during the variable rate sweep is exactly equal to that of the best performing constant rate sweep. This is due to both sweeps using the same slip rate at low slip conditions. Meanwhile, during the variable rate sweep the tyre's peak temperature is slightly lower than during the best performing constant rate sweep, an improvement of 1.7% (from 74.4°C to 73.1°C). This low peak temperature leads to equally low thermal hysteresis. The total duration (sweep duration plus cool down duration) of the 'BrkDrv' variable rate sweep is 0.5s shorter than the best performing constant rate sweep. Overall, as with the 'FreeRolling' application, the 'BrkDrv' variable rate sweep is shown to avoid the compromise between mechanical and thermal hysteresis that is present when using constant rate sweeps and this is achieved without any cost to the test efficiency.

The exact magnitude of these improvements are specific to the test setup used during this investigation. If a different tyre or rig are used, then the precise magnitude of the improvements will likely be different. As different tyres have different thermal properties. However, the basic trends will be similar. Based on this along with the clear improvements in data quality demonstrated by using the variable rate sweep. This new sweep shape was widely implemented into both the 'FreeRolling' and 'BrkDrv' GS2MF test procedures.

3.7 Asymmetric Loading

When a vehicle is driven along a road, the vertical load over each tyre changes depending on the manoeuvre and driving conditions. To investigate this, a vehicle dynamics analysis was conducted using vehicle simulation software (IPG CarMaker) to look at the weight transfer of a vehicle and link this to the tyre's slip angles. The slip angles, load and cambers within the 'GS2MF FreeRolling' test procedure were then determined to replicate this vehicle behaviour.

This was done to ensure the tyre is testing under similar conditions to that it will be subjected to when mounted to an appropriate vehicle. (IPG CarMaker, 2017).

The convention used in GS2MF is that a vehicle right side tyres are tested, tyre models built from this data can later be mirrored to reflect the left side tyres. This is valid even in asymmetric tyres, where a right-side tyre steering left behaves the same as a left side tyre steering right, assuming all other aspects are equal. When considering a vehicle's right-side tyre, the load increases from the static load when steering to the left and decreases when steering to the right; this is due to the weight transfer across the axle of the vehicle during cornering. As slip angle increases this weight transfer continues until either the front or rear tyres break traction, at which point the vehicle enters understeer or oversteer. After this point, the tyres are saturated and unable to provide any additional grip, hence slip angle can continue to increase but no further weight transfer can occur. This weight transfer and saturation is not considered during traditional Square Matrix testing, where a vertical load is defined for each sweep. Then testing is conducted through a complete range of both positive and negative slip angles at this constant load. This means the tyre is tested under load cases it will never experience on a vehicle under normal driving conditions. Gathering tyre data under these conditions is not useful and adds to the cost of the testing as well as contributing to the wear on the test tyre. Therefore, a new test sweep was developed to take this load transfer into account and change the tested vertical load based on the tyre's slip angle.

The vehicle dynamics simulation (carried out using IPG CarMaker) was used to investigate the magnitude of the lateral weight transfer across a vehicle. This was achieved by applying a very slow steering rate to the vehicle on a flat surface at constant forward velocity; as the slip angle slowly increased the weight transfer could be observed. Repeating this testing using a range of different vehicles and tyres as well as cambered road surfaces showed that the magnitude of this weight transfer is not constant. Since it is impractical to simulate every possible combination of influences, a 30% safety factor was applied to the maximum and minimum weight transfer observed in the testing to widen the range of tested loads. This was intended to increase robustness and cover unknown load conditions of future vehicles that do not currently exist. (IPG CarMaker, 2017)

The result of this investigation was three sweeps (high, medium and low average load) that cover the required range of weight transfer conditions. All test loads in GS2MF are dependent on a nominal load calculated using the ETRTO (European Tyre and Rim Technical Organisation) load rating of the tyre being tested, which equates to 6,752N in this case. Therefore, within each of the three sweeps, the load conditions of the tyre when steering to the

left (negative slip angle) and to the right (positive slip angle) are defined as factors of the nominal load. These load factors for each sweep along with the actual test loads for an example tyre with an ETRO load rating of 110 are shown in Table 3.7-A.

Nominal Load = 6752N **(example tyre with ETRTO load rating of 110)**	**Load factor, negative slip angle.** **(Steering Left)**	**Test Load, N. negative slip angle.** **(Load factor × nominal load)**	**Load factor, positive slip angle.** **(Steering Right)**	**Test Load, N. positive slip angle.** **(Load factor × nominal load))**
High Load Sweep	1.8	12154	0.6	4051
Medium Load Sweep	1.6	10803	0.4	2701
Low Load Sweep	1.4	9453	0.2	1350

Table 3.7-A. Vertical load factors used with the asymmetric sweep, also shows are examples of actual loads based on an example tyre with a load rating of 110.

Also noted from the vehicle dynamics simulation, was that understeer or oversteer typically occurred when the tyre reached around 5° of slip angle. This was considered as the point as which saturation occurs, after which no more load transfer can take place while slip angle continues to increase. This is shown in Figure 3.7-A.

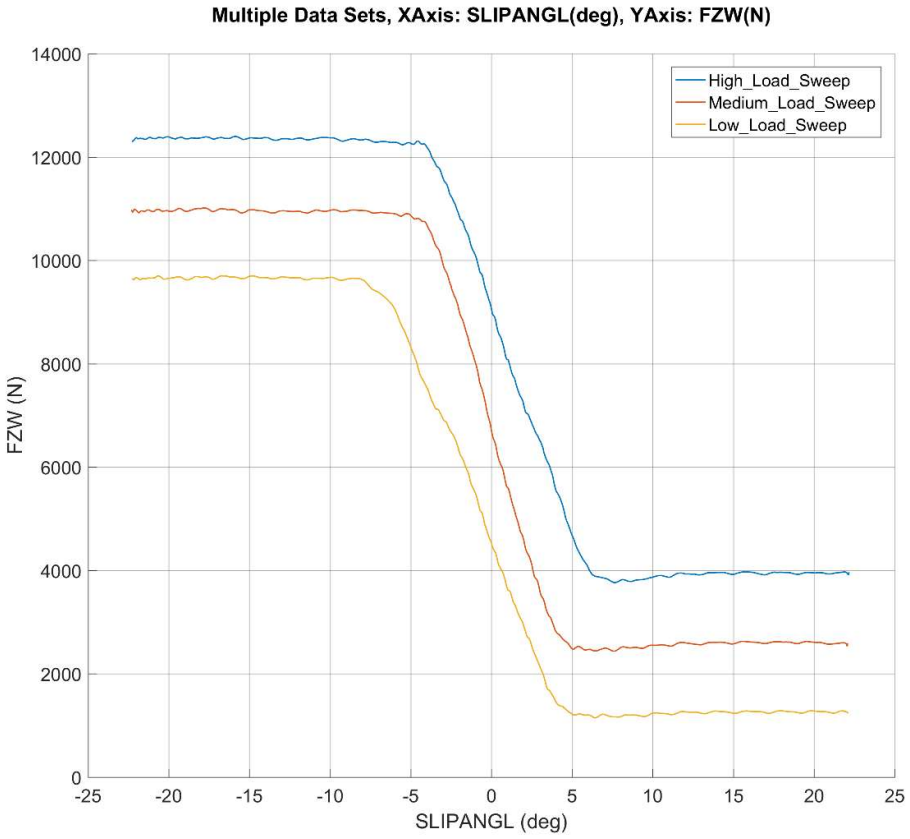

Figure 3.7-A. Vertical load, FZW (N) versus slip angle, SLIPANGL (°) for the three asymmetric load sweeps covering the typical range of vehicle lateral weight shift conditions.

The load cases shown in Figure 3.7-A, as well as the saturation slip angle of 5°, are suitable for the range of different saloon, SUV and road based sports cars used in the vehicle dynamics simulations. However, while the fundamental trends which are driven by the lateral weight shift of a vehicle while cornering will always remain true. The exact values used may need to be reassessed if GS2MF is to be used for very different applications, such as race cars. To maximise the robustness of GS2MF, one single sweep is included where the vertical load changes with slip angle in the opposite direction. This is included to gather some limited data to cover highly unusual vehicle dynamic events, such as a roll over or driving on a road with high adverse camber. The data form this sweep also helps to maximise the stable range of the resulting MF-Tyre 6.1 tyre model built from the data.

During the vehicle dynamics simulation, results were also obtained to determine how the tyre's camber angle changed because of the increasing slip angle. Under steady state driving conditions on a flat surface, a tyre's camber angle is directly related to the vertical load, this is based on the vehicles kinematics and suspension geometry. However, the magnitude of this

sensitivity varies significantly across different vehicles and suspension types. Therefore, in the interests of test robustness, GS2MF included some sweeps where camber is dependent on slip angle to increase the data density in the most common regions; but significant testing is also conducted at a range of camber and slip angles independently of one another. This is shown in Figure 3.7-B.

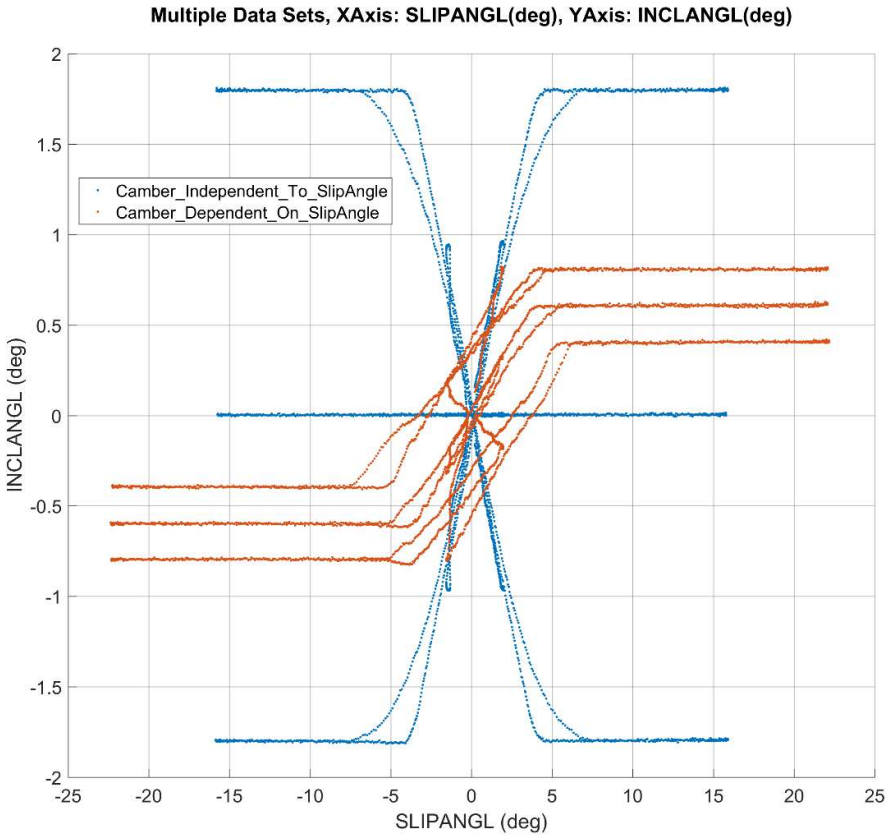

Table 3.7-B. Two examples where camber is dependent on slip angle and where camber is independent of slip angle.

The variable rate slip angle sweep can be used in conjunction with the asymmetric load sweeps. During the asymmetric load sweeps, the vertical load and camber angle changes with slip angle; during the variable rate sweep the slip angle rate of change is dependent on slip position. Applying both to the same sweep means slip rate, camber and load are all dependant on the slip angle and the benefits of both sweeps can be applied at the same time. This is used extensively through GS2MF.

Asymmetric loading was also considered for use in the 'GS2MF BrkDrv' test procedure, where vertical load would be linked with slip ratio rather than slip angle. However asymmetric loading relies on only testing right side tyres and mirroring them for use on the left side. The assumption

being that negative slip angle on a right-side tyre is equivalent to positive slip angle on a left-side tyre. While valid for a tyre's lateral behaviour this is not valid longitudinally; as a tyre's positive and negative longitudinal slip equate to accelerating and braking which are typically asymmetric.

3.8 Vertical Load Sweeps

When considering a test procedure, it is important to consider the amount of wear each sweep causes to the tyre and attempt to minimise this as much as possible. This is contradictory to the requirement of delivering an MF-Tyre 6.1 tyre model that is valid across the widest possible range of load cases. To do this, the test data used to build the model must also cover the widest possible range of load cases, including testing at high slip and high load conditions which cause the most wear to the tyre. To balance these conflicting requirements a new and novel way of testing at extreme conditions is presented. The vertical load sweep allows data to be gathered under extreme high slip angle, high load conditions while minimising tyre wear. This is achieved by changing the fundamental nature of the test sweep.

During a regular sweep used in Square Matrix testing, the tyre is set to the test load, this is then held constant while the slip angle is swept through a range of conditions, after which the load is reduced. This sweep shape can be useful as it allows data to be gathered at every slip angle position leading up to and returning from the peak slip angle, all at the specified vertical load. However, problems occur when there is a need to test the tyre at extreme load cases, where both the vertical load and peak slip angle are very high. Carrying out a traditional sweep to these extreme conditions will cause significant wear to the tyre, irreparably effecting its future performance. Furthermore, while there is a need to gather data at these extreme conditions, there is no need to gather data transitioning to and returning from these extreme conditions. As this transition goes through normal load cases that are already captured throughout the test procedure.

To address this the vertical load sweep steers the tyre to a high slip angle while at very low load; meaning very low sliding energy, hence very low heat generation and low wear. Then once at the high slip angle condition the vertical load is ramped from low to high and back again as quickly as possible. This gathers data at high slip conditions very quickly, minimising wear on the tyre. This sweep's shape is shown in Figure 3.8-A.

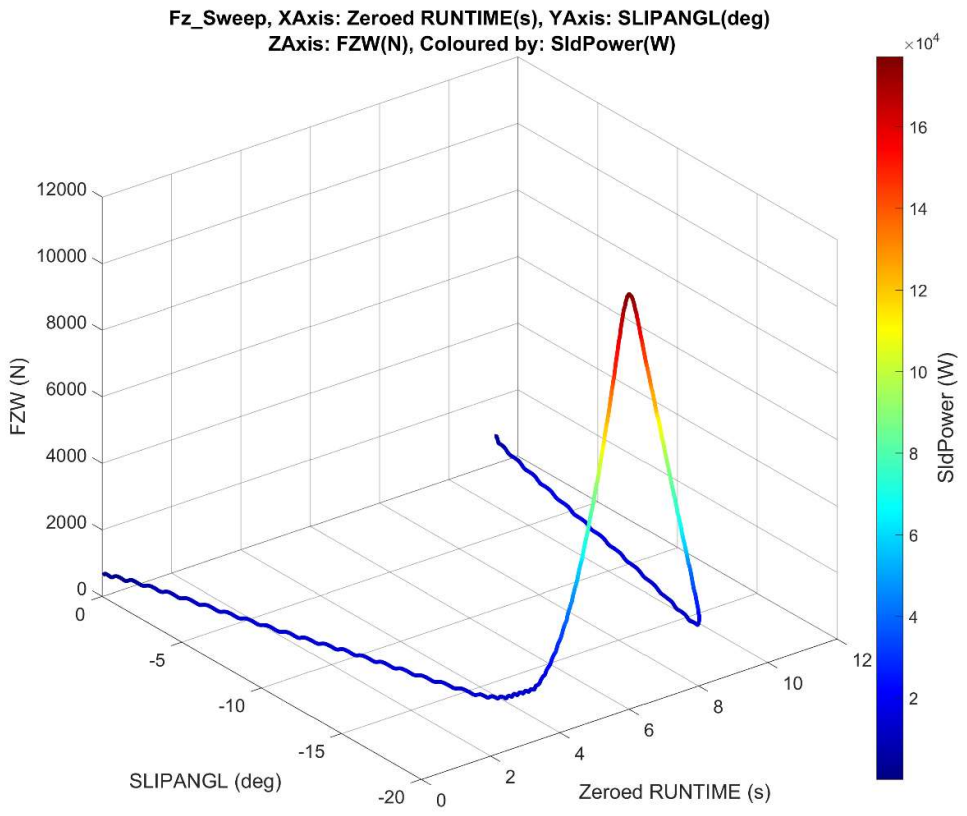

Figure 3.8-A. Vertical load sweep shape, coloured by sliding power (W).

Figure 3.8-A shows that the vertical load sweep spends a minimal amount of time at high sliding power regions, reducing the temperature and overall wear on the tyre while still gathering data in this high slip region.

A regular sweep (where the tyre was held at a constant load while slip angle was changed) was also conducted as a comparison to the vertical load sweep. The regular sweep and vertical load sweep were conducted under comparable conditions, where both reached the same peak of -18° of slip angle at a load of 11,500N. During the regular sweep, the tyre reached a peak temperature of 96.3°C and the total sliding energy was calculated to be 1,126kJ; while during the vertical load sweep the tyre only reached 87.1°C and the total sliding energy was 496kJ. This means that the sliding energy was 56% lower during the vertical load sweep compared to the regular sweep, drastically reducing wear. However, the vertical load sweep generates no data at lower slip angles while at the high load, meaning it cannot completely replace the regular sweeps which do gather useful data in this region. The vertical load sweep can however, be used to gather data in extreme load cases that cannot be reached during a regular sweep without severely damaging the tyre. A demonstration of this is shown in Figure 3.8-B.

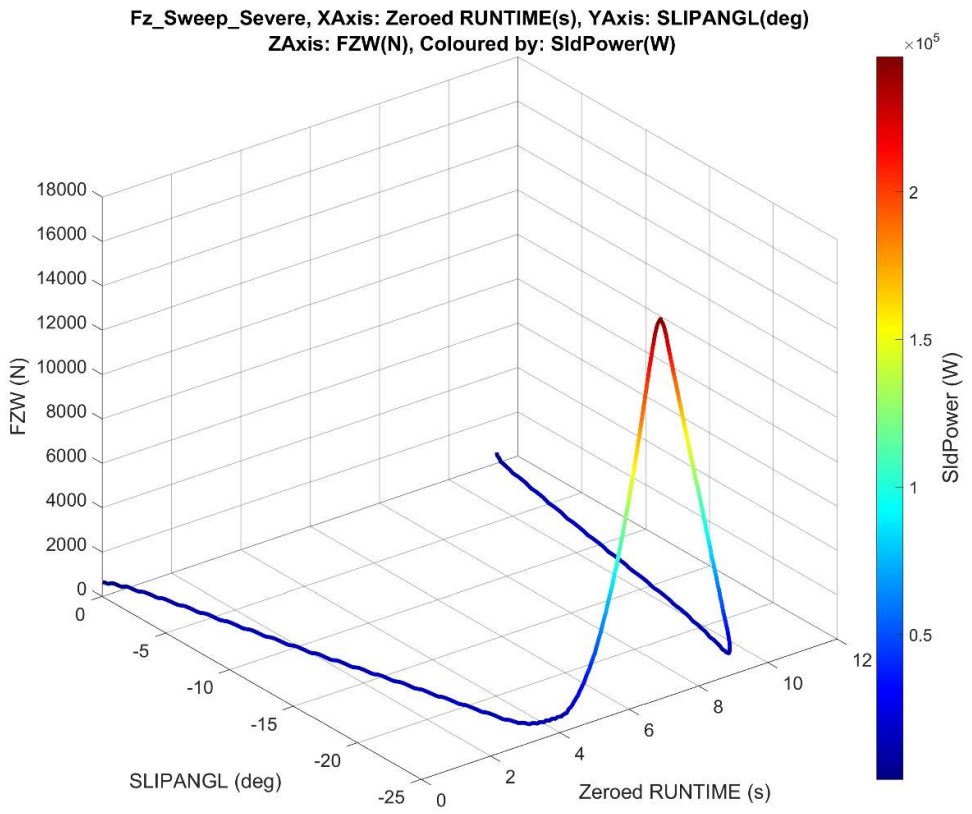

Figure 3.8-B. Vertical load sweep used to gather data in extreme load case.

Figure 3.8-B shows a vertical load sweep that reached an extremely high slip angle of -25° while also under a high peak load of 17,000N. Achieving this load condition using a regular sweep would cause enormous wear to the tyre, permanently changing its performance. However, the total sliding energy during this vertical load sweep was just 633kJ, which is 43.8% less than the regular sweep that only reached -18° of slip angle at a load of 11,500N. This demonstrated how the vertical load sweep can be used to gather data in extreme load cases without subjecting the tyre to excessive sliding energy leading to high levels of heat and wear.

Overall the vertical load sweep offers a viable addition to regular sweeps as a method of measuring tyre performance while under extreme load cases. An equivalent regular sweep causes more wear to the tyre but also gathers additional potentially useful data from the transition to and from the extreme load case. Where the vertical load sweep only gathers useful data at the extreme load case it does so whilst causing significantly less wear to the tyre. The real advantage of the vertical load sweep is it allows some minimal data points to be obtained at load conditions that could not practically be reached using regular sweeps, due to excessive

wear. With this data, the resulting MF-Tyre 6.1 tyre model will be valid across a wider range of load cases. Therefore, GS2MF incorporates both sweep types within the test procedure.

3.9 Graph Sweeps

When testing tyres, there are often unforeseen problems with the testing or expected behaviour observed in the tyre's performance. Furthermore, the tyre itself can change as a result of the testing. To highlight and quantify these occurrences Graph Sweeps are incorporated into the 'GS2MF FreeRolling' and 'BrkDrv' test procedures. These Graph Sweeps involve repeating the exact same sweeps twice during the testing procedure, allowing the data from these identical sweeps to be compared to one another.

In GS2MF, blocks of five Graph Sweeps are used within the free rolling and 'BrkDrv' test procedures. For free rolling, the first sweep is at zero camber and 6,000N of load, sweeps two and three are the same but at 9,000 and 3,000N of load respectively, then sweeps four and five are at 6,000N of load but at -3 and +3° of camber angle. For 'BrkDrv' the vertical loads are the same as those used in the free rolling Graph Sweeps; however, instead of changing camber angle for the last two sweeps inflation pressure is changed instead to 2.1 and 3.3bar respectively for sweeps 4 and 5. These sets of Graph Sweeps are identical for every running of the test procedure on every tyre. This means they can always be directly compared to one another. Figure 3.9-A shows a comparison between Graph Sweeps 1 and 2 of a successful running of the 'GS2MF FreeRolling' test procedure.

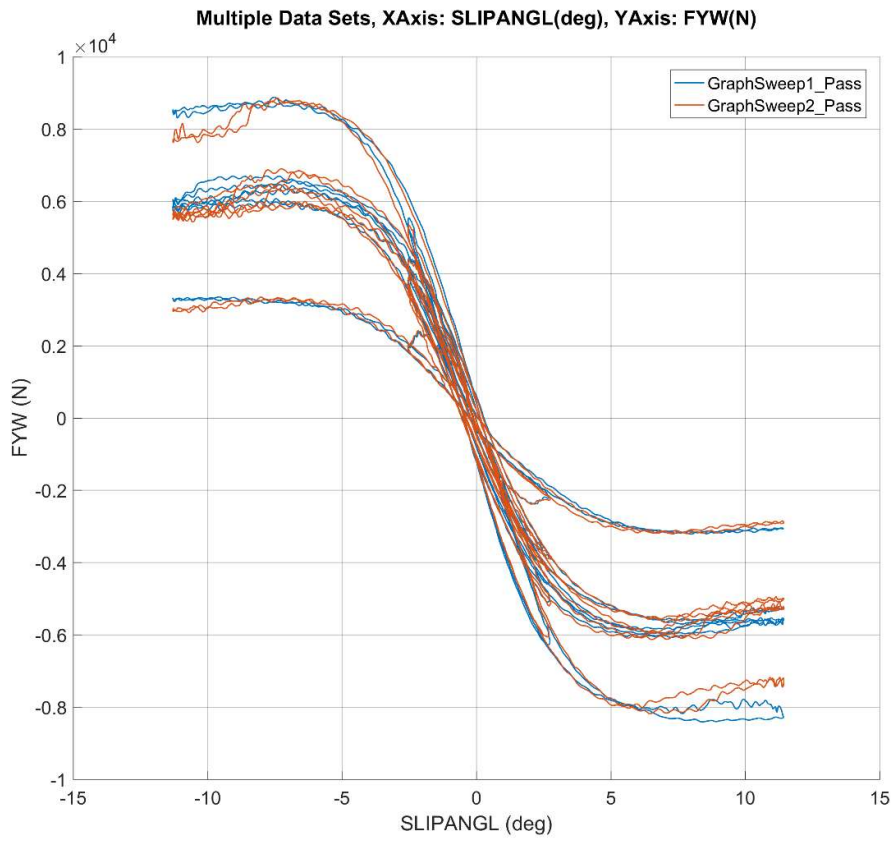

Figure 3.9-A. Graph sweeps 1 and 2, shows little change in the tyre's lateral force performance.

Comparing the lateral force results from Figure 3.9-A shows that there little change in the tyre's lateral force performance from the beginning to the end of the test procedure. There is a small difference at high load, high slip angle conditions which is due to the tyre chattering. Chatter is where the lack of any compliance or damping in the rig can cause the tyre to vibrate. The tire's natural frequency changes as it wears which means the load cases at which chatter occurs also change with wear. In this case chatter occurred at the given high load, high slip angle load case only once the tyre was worn. During rig testing nothing can be done to avoid chatter if it occurs, other than testing at a different load case. In this situation this was not practical as the varying tyre performance at a given load case is being investigated. However, the chatter only effects one region of one dataset so has minimal effect overall. Furthermore, chatter rarely occurs on a physical vehicle as the effect is cancelled out by dampers and bushes in the suspension system. The rest of the data in Figure 3.9-A sh
ows that overall the tyre did not significantly change as a result of the testing. This is further verified by Figure 3.9-A which shows the change in radius of the tyre at the start and end of the testing.

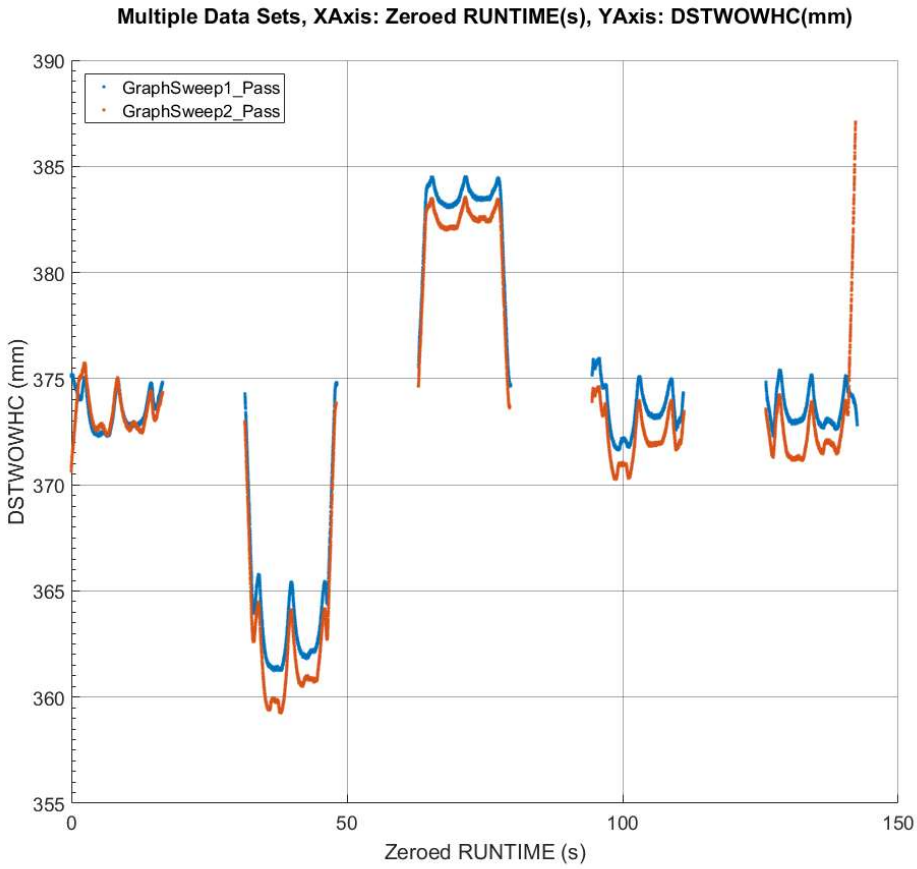

Figure 3.9-B. Graph sweeps 1 and 2 show little change in the tyre's radius.

Figure 3.9-B shows that during this test the 'DSTWOWHC' or distance between the wheel centre and road surface (Loaded Radius) changed by an average of around 1mm during the same sweeps conducted at the start and end of the testing. This shows that as a result of the testing the tyre wore by just 1mm, which is well within the acceptable longevity of a road car tyre. Demonstrating that the testing did not excessively damage the tyre and that the data gathered between these two Graph Sweeps can be used for the parameterisation of MF-Tyre 6.1 tyre model.

Figure 3.9-C shows the tyre's lateral force performance after a mistake was made while setting up the test rig. In this case the tyre's load rating was incorrectly entered into the rig's control system, causing the tyre to be tested under a set of vertical loads that were far higher than it should have been subjected to. As a result, the tyre was excessively worn and its performance changed significantly, meaning the results from this test were not useful for parameterising an MF-Tyre 6.1 tyre model.

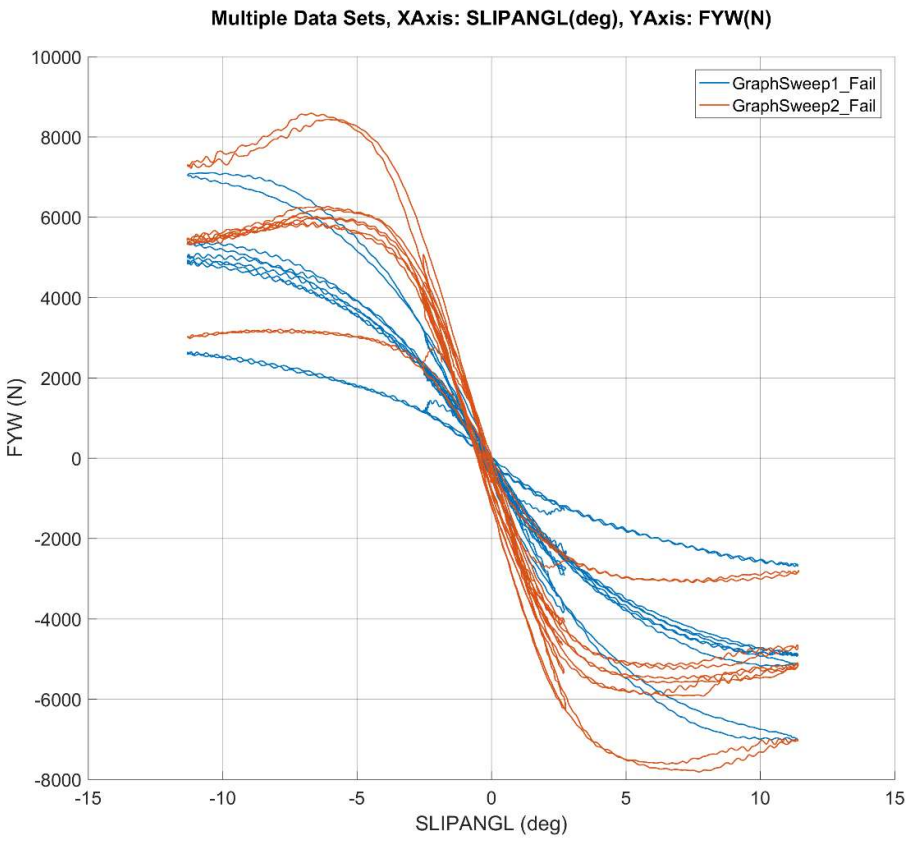

Figure 3.9-C. Graph sweeps 1 and 2 showing significant change in tyre performance.

Figure 3.9-C shows that the Graph Sweeps highlight the fact that the tyre's lateral force performance changed significantly during the testing (due to highly significant wear), in this case because of a mistake being made while setting up the test that led to the tyre being run at much to higher vertical loads. Since the Graph Sweeps highlighted this error it was easy for the test operators to recognise that the test needed to be repeated using a new tyre specimen. Without the Graph Sweeps it would be difficult to recognise this change in the tyre's performance, as all other sweeps during the test procedure are conducted under different load cases, making a direct comparison of the data impossible.

Figure 3.9-D shows another way in which the Graph Sweeps can be useful, in this case for comparing the difference in tyre performance between very different tyre constructions.

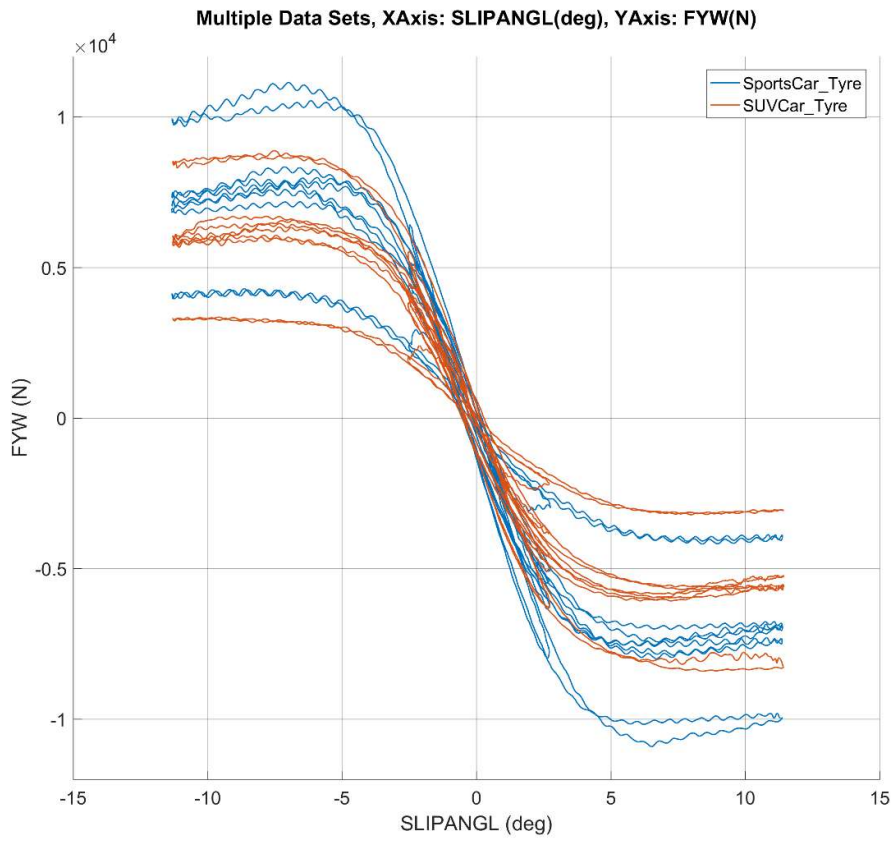

Figure 3.9-D. Lateral force performance comparison between an SUV and a sports car tyre.

Figure 3.9-D shows a comparison between Graph Sweep 1 extracted from running GS2MF on two completely different tyres. Since the Graph Sweep load cases are identical regardless of the tyre being tested this data provides a direct comparison between the two tyres. This can be useful for quickly assessing the differences in performance between tyres at data level, without having to parameterise tyre models.

3.10 Rolling Radius

The MF-Tyre 6.1 tyre model not only captures the force and moment behaviour of the tyre but also models other tyre attributes, such as the vertical stiffness. To parameterise this component of the tyre model data needed to be gathered of the tyre's vertical force versus displacement (radius) at various load conditions. This simple test involved the tyre running straight ahead at zero slip angle while the vertical load was stepped to seven discreet loads; these range from 0.1 to 2.2 times the nominal load. This set of seven loads is then repeated at three different forward velocities, these are 16.6, 38.8 and 5.5m/s (60, 140 and 20kph respectively). These were decided upon to provide data over the range of forward velocity typical for on road driving, if GS2MF was to be adapted for a different application, such as testing race car tyres, then these velocities

will need to be reconsidered. Finally, the block of testing at seven loads and three velocities is then repeated at three inflation pressures. Figure 3.10-A shows a portion of this test procedure for one inflation pressure.

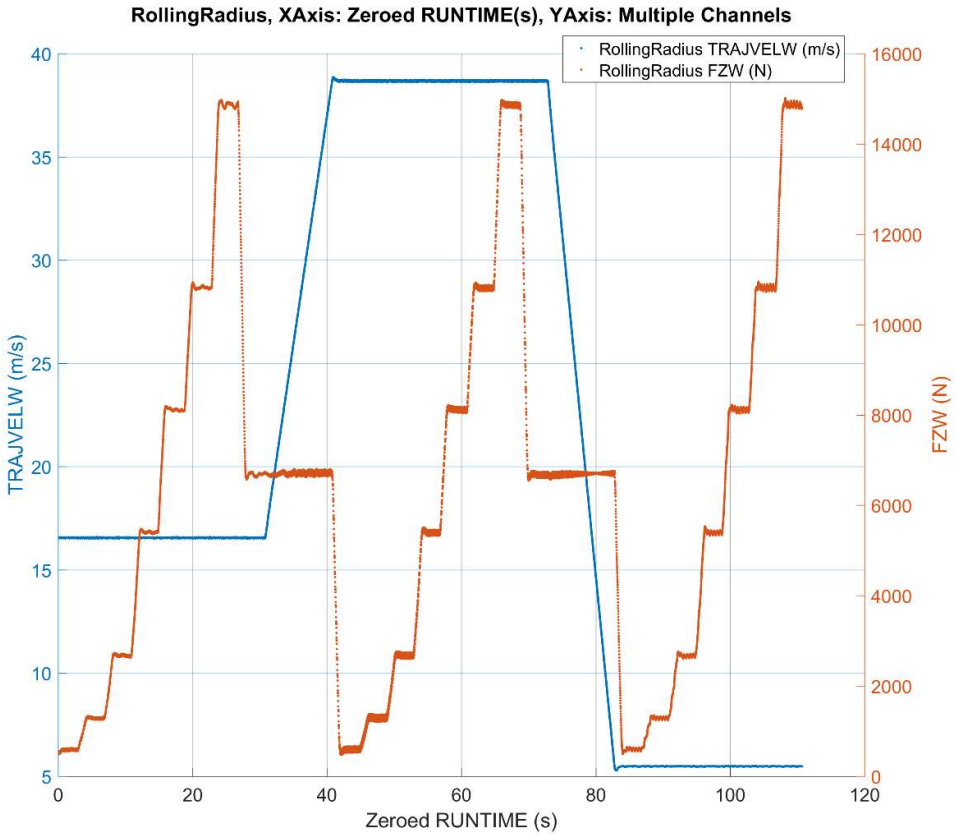

Figure 3.10-A. Rolling radius test procedure for one inflation pressure.

Using this data plots of vertical load versus Loaded Radius can be generated as shown in Figure 3.10-B.

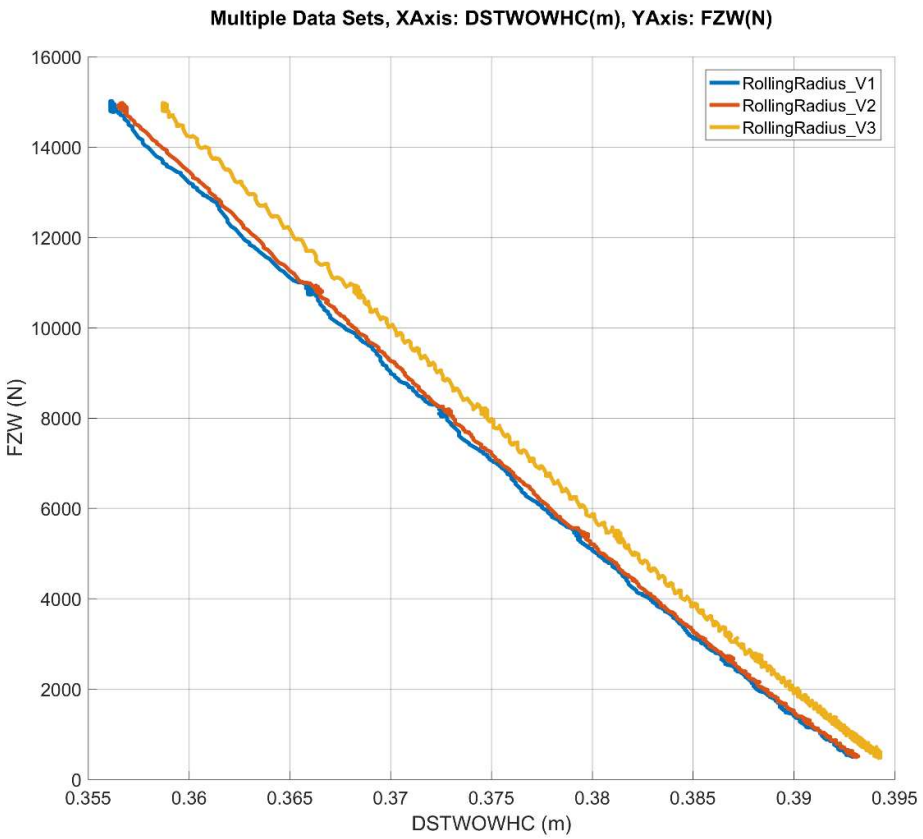

Figure 3.10-B. Rolling radius data showing vertical load versus Loaded Radius, the gradient of which is the tyre's vertical stiffness under the given conditions. RollingRadius_V1, _V2 and _V3 correspond to forward velocities of 5.5, 16.6 and 38.8m/s respectively.

Figure 3.10-B shows a plot of vertical load versus the distance between the wheel centre and the road surface, which is the Loaded Radius. The data shown is at one inflation pressure and three forward velocities; RollingRadius_V1, _V2 and _V3 correspond to 5.5, 16.6 and 38.8m/s respectively. The gradient of each of these lines represents the vertical stiffness at that given condition, which is modelled within the MF-Tyre 6.1 tyre model. More details of this can be found in the GS2MF Fitting chapter 5.0.

3.11 On-Centre Behaviour

Previous chapters discuss methods of capturing tyre performance data at very high slip angles. This is important as the resulting tyre model built from this data can be used by vehicle manufacturers to ensure their cars perform safely in emergency situations. However, most every day on-road driving is conducted at very low slip angles, within a few degrees of zero. Therefore, on-centre tyre performances such as cornering stiffness, residual self-aligning torque (RSAT) and residual cornering force (RCF) are all particularly important to vehicle

manufacturers. Furthermore, they are all highly sensitive to temperature and wear. So, while these values could be extracted from data during regular sweeps, this would result in less accurate measurements of these particularly important values, as the normal force and moment sweeps always cause the tyre to heat up significantly during the sweep. For this reason, specific testing is included in the 'GS2MF FreeRolling' test procedure to gather accurate data in this especially important on-centre region.

The on-centre test sequence is carried out as follows. First the tyre is steered to 1° of slip angle and held in this position. Since the slip angle is low, very little heat is generated while the tyre is held at just 1°. Furthermore, by holding the tyre at this slip angle multiple tests can be conducted very quickly, whereas steering between 0 and 1° for each test would add significantly to the overall test duration. While held at 1° slip angle, the vertical load is changed to five discreet loads, ranging from 0.7 to 2.0 times the nominal load. Once this is complete, the tyre is held at 0° slip angle and the five loads are repeated; they are then repeated again at -1° of slip angle. Finally, this whole block of testing is repeated at three inflation pressures. The block of testing for one inflation pressure is shown in Figure 3.11-A. During this test the rig targets 1, 0 and -1° of slip angle, however, as shown the actual slip angles are around 0.05° off of the target slip angle. These rig control limitations do not cause a problem as the actual slip angles are used in the calculations rather than target slip angles.

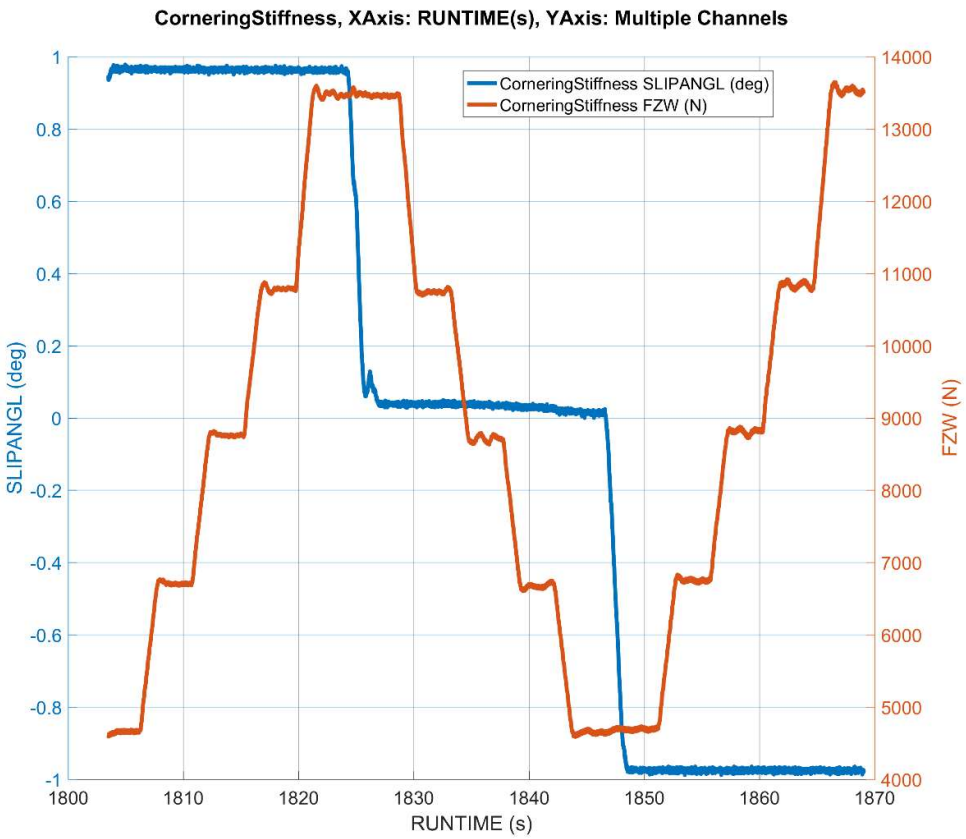

Figure 3.11-A. 'GS2MF FreeRolling' On-Centre test sequence.

The data obtained from this testing can be used to quantify cornering stiffness, RSAT and SCF. Figure 3.11-B shows a plot of lateral force versus slip angle where cornering stiffness can be calculated.

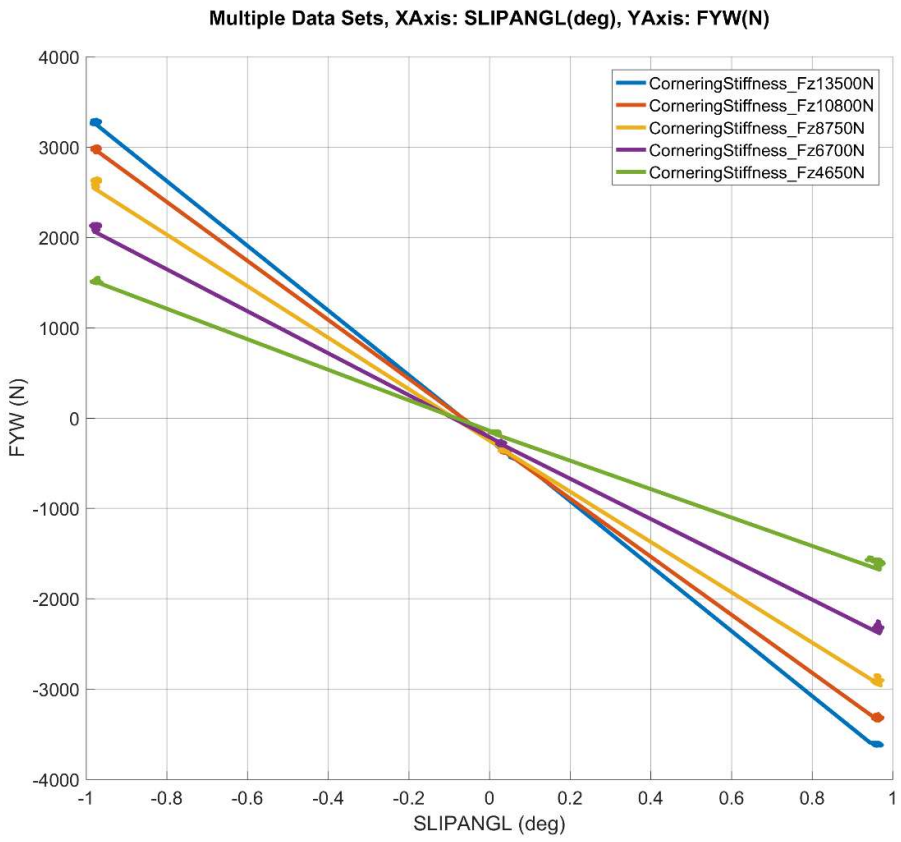

Figure 3.11-B. Lateral force versus slip angle for the on-centre data coloured by vertical load.

Figure 3.11-B shows that the data itself is 'clumped' at -1, 0 and 1° of slip angle and at each of the five vertical loads. These clumps are averaged and used to fit five straight lines each representing one of the five vertical loads. This clumping is due to the nature of the test procedure, where the tyre is held at the given slip angle while the load is stepped between the five conditions, as shown in Figure 3.11-A. Using the data presented in Figure 3.11-B cornering stiffness can be calculated as the gradient of each of the coloured lines. Taking the middle load of 8,750N as an example. The tyre generated 2,600N of lateral force at -1° of slip angle and -2,900N of lateral force at 1° slip angle; this equates to a cornering stiffness of 2,750N/°. Figure 3.11-C shows a similar plot, this time showing self-aligning torque (MZ) rather than lateral force (FY).

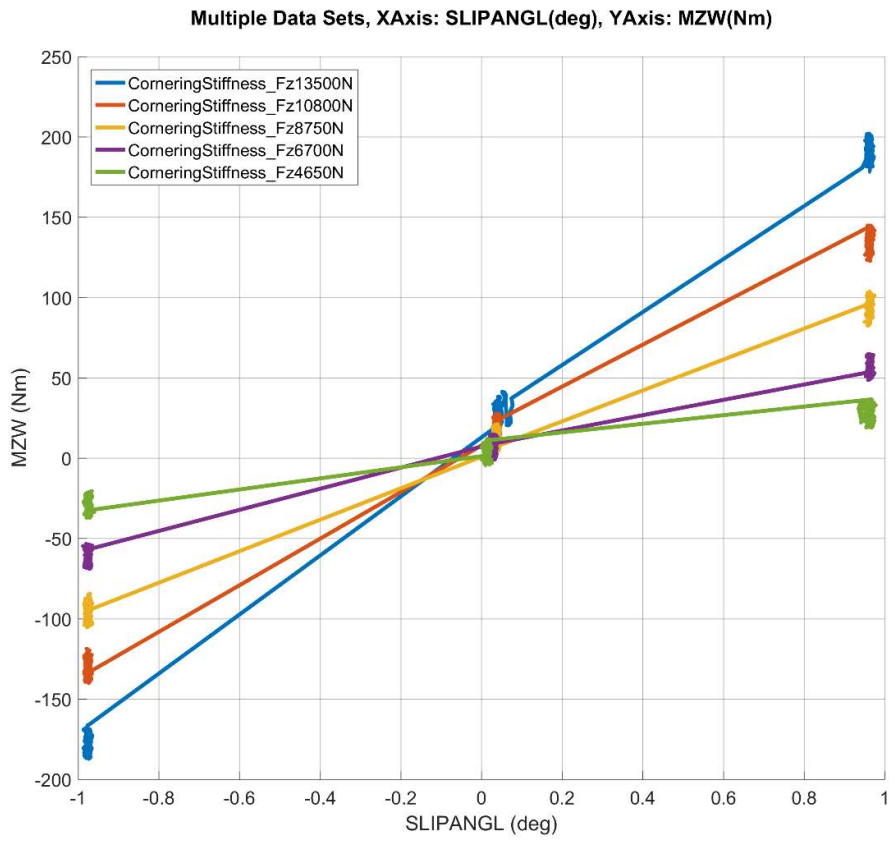

Figure 3.11-C. Self-aligning torque versus slip angle for the on-centre data coloured by vertical load.

Using Figures 3.11-B and 3.11-C together the values for RSAT and RCF can be deduced. To do this, five straight lines are fitted to the data, one for each load, that pass through the three slip angles. These five lines are also shown in Figures 3.11-B and 3.11-C coloured the same as the data points.

RSAT is the self-aligning torque generated at the slip angle position at which zero lateral force is generated. Taking the middle load data of 8,750N as an example. In Figure 3.11-B it can be observed that the data representing the 8,750N load case (CorneringStiffness_FZ8750N, coloured yellow) generated zero lateral force at -0.09° of slip angle. Figure 3.11-C shows that at -0.09° slip angle the tyre generated -8Nm of self-aligning torque, so in this case the RSAT is -8Nm. Similarly, RCF is the lateral force generated at the slip angle position at which zero self-aligning torque is generated. Again, taking the middle load data of 8,750N as an example, using Figure 3.11-C we can observe that zero self-aligning torque at 8,750N of vertical load occurs at -0.01° slip angle, Figure 3.11-B shows that at this slip angle the tyre generated -222N of lateral force. This means the RCF for this load case is -222N.

This demonstrates that this on-centre sequence of testing provides highly data that can be used to calculate important tyre performance metrics such as cornering stiffness, RSAT and RCF. While these values are not typically used directly in the parametrisation of MF-Tyre 6.1 tyre models the data from this section is used in the pure FY fitting as detailed in Section 5.2.1 on Fy Pure. Furthermore, the values calculated form this data can be used in several other ways; for example, checking the accuracy of resulting tyre models or benchmarking and comparing the performance properties of different tyre constructions.

3.12 Relaxation Length

Previous sections have all discussed methods of acquiring and processing steady state force and moment data. However, tyres on a vehicle are rarely in a steady state condition and they do not react instantaneously to a change. Instead, anytime a tyre's load case is changed there is a delay before the tyre responds with a change to its force and moment performance. For example, hypothetically, if a tyre's slip angle was changed instantaneously there would not be an instantaneous change to the tyre's lateral force. Instead, the sidewalls of the tyre would stretch and deform, the contact patch will start to rotate and change shape, grip will build up and after a time there will a change to the tyre's lateral force. Considering this response as a time delay will cause it to be dependent on the tyre's forward velocity, so instead it is calculated as a distance travelled and referred to as the relaxation length.

Several pre-existing methods exist to determine the relaxation length of a tyre. The first such method detailed in (Wei and Dorfi, 2014) is a sinusoidal test; where the tyre is rolling at a constant load case, while slip angle is changed following a sinusoidal input which leads to a sinusoidal lateral force output. The phase lag between the slip angle and lateral force can then be related to the relaxation length. This is a common and generally acceptable method. However, in practice due to limitations in the rig's control systems neither the slip angle input nor lateral force output are perfectly sinusoidal. This can cause difficulties and subsequent inaccuracies when post processing the data. Wei and Dorfi (Wei and Dorfi, 2014) also presents a pendulum test which involves mounting the tyre such that it can rotate in the vertical and lateral directions, while rolling at a constant velocity. A lateral displacement is then applied to the tyre while the natural frequency and damping of the resulting motion can be related to the relaxation length. However, such apparatus was not available and hence this method was not investigated. A third indirect method of acquiring the relaxation length, also detailed in Wei and Dorfi (Wei and Dorfi, 2014) is to calculate relaxation length as the ratio of cornering stiffness to lateral stiffness. Where cornering stiffness can be extracted from regular force and moment testing while lateral stiffness can be measured by loading a non-rolling tyre while applying a lateral displacement; the gradient of the resulting lateral force versus lateral displacement plot is

the lateral stiffness. This method is effective, but it requires the flat-trac rig to be stopped and reconfigured which adds to the test duration and reduces efficiency. However, an adaption of this method is used in GS2MF to measure longitudinal relaxation length as the ratio of slip stiffness to longitudinal stiffness, where this method proved to be the most efficient. Finally, (Wei and Dorfi, 2014) Wei and Dorfi also detailed a fourth method for measuring relaxation length, referred to as a Step-Steer test. Conceptually this test involves applying an instantaneous change in slip angle to a rolling tyre, the subsequent build up in lateral force then allows the relaxation length to be measured directly. However, an instantaneous change in slip angle is impossible for a physical rig. Therefore, an adaption to this test involves rolling the tyre at zero slip angle, bring it to a halt, then applying a steer angle (slip angle at zero velocity) to the non-rolling tyre, before rolling the tyre again while holding the slip angle. This adapted version of the Step-Steer test still allows relaxation length to be measured directly from the resulting data. It also requires no special rig configuration and can hence be integrated directly into the 'GS2MF FreeRolling' test procedure. Such an approach gathers suitable data for the parametrisation of the lateral relaxation length component of the MF-Tyre 6.1 tyre model and it does so without the need for an extra test, which reduces testing costs.

3.12.1 Lateral Relaxation Length

The Step-Steer method used within GS2MF involves rolling the tyre forward at a slow 1m/s; the tyre is then brought to a stop before being statically steered to -2° of slip angle, after which the tyre is accelerated back to 1m/s. As the tyre is accelerated the lateral force build up can be observed and measured. By relating this lateral force build up to the distance travelled the relaxation length can be measured directly. After 10s (long enough to gather sufficient data points to calculate and average lateral force) the tyre is steered back to 0° of slip angle and the test is then repeated in the other steering direction to +2°. This allows the positive and negative slip angle response of the tyre to be averaged in case the tyre performs asymmetrically. This pair of tests is repeated at five loads ranging from 0.75 to 2.0 times the tyre's nominal load, then this block of testing is repeated at three inflation pressures. Figure 3.12.1-A shows the test sequence of a pair of Step-Steer tests at one load and one inflation pressure.

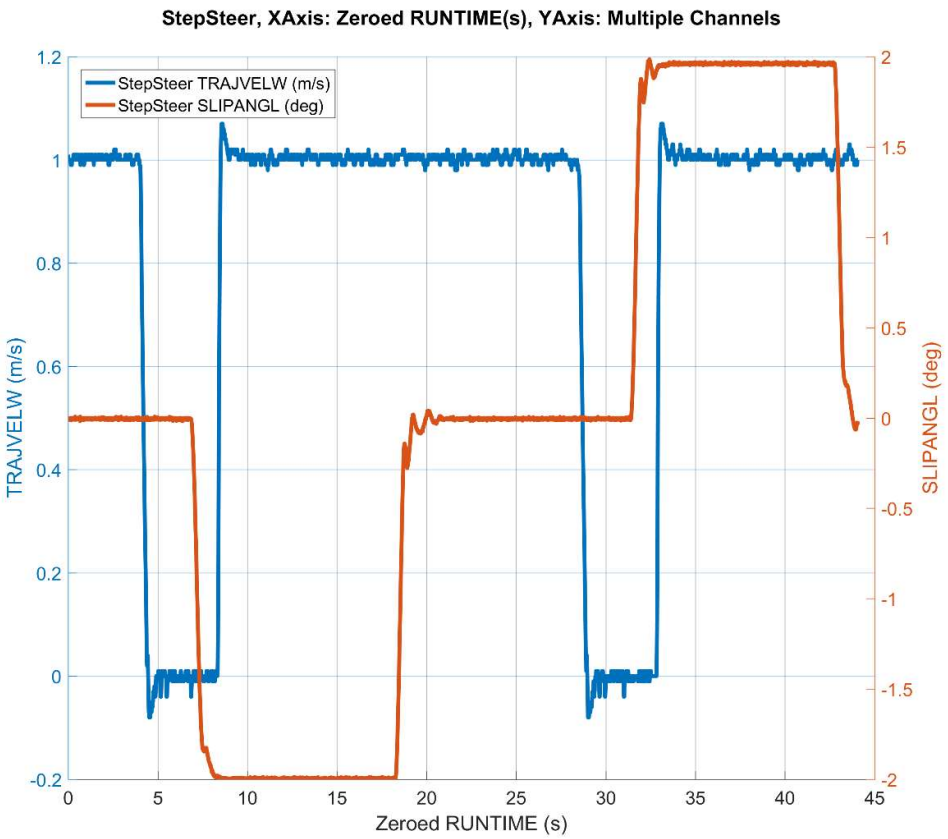

Figure 3.12.1-A. Step-steer test sequence for a pair of tests to negative and positive slip angles, at a constant load and inflation pressure.

Figure 3.12.1-A shows both the forward velocity (TRAJVELW) and the slip angle (SLIPANGL) channels for the Step-Steer section of the 'GS2MF FreeRolling' test procedure. The relaxation length can be measured directly from the build-up in lateral force that occurs after the tyre begins to accelerate back to 1m/s from 0m/s while held at a constant slip angle, this is shown in Figure 3.12.1-B.

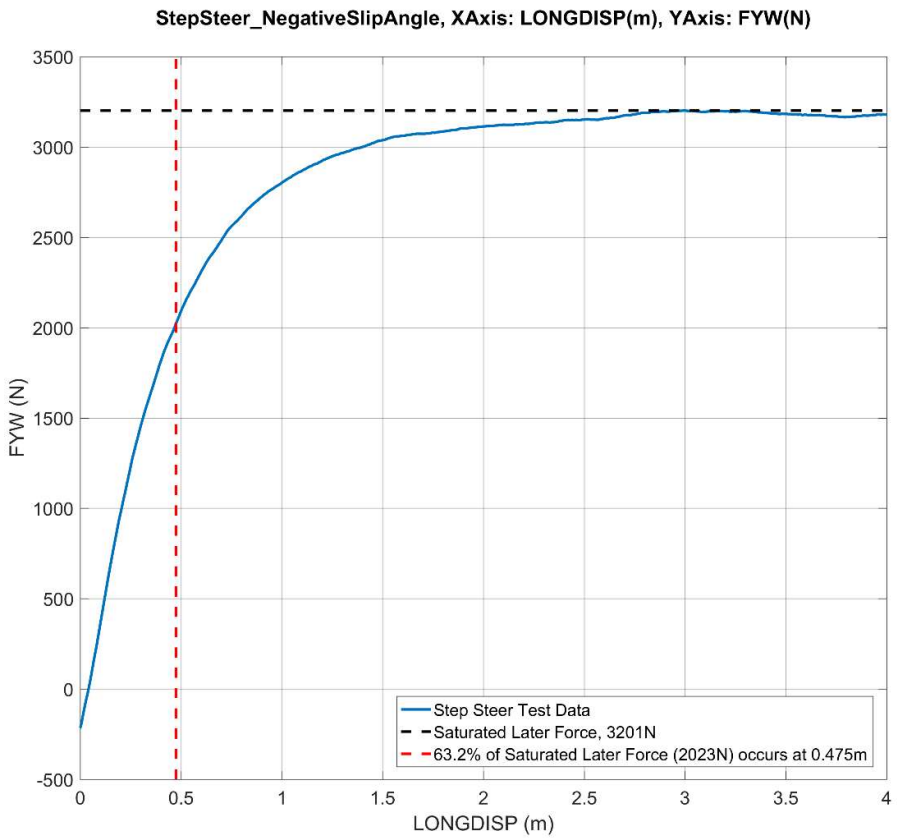

Figure 3.12.1-B. Lateral force build up over longitudinal distance travelled (Fz is 5100N); also shown is the peak lateral force of 3,201N and the longitudinal displacement at which the lateral force reaches 63.2% of the peak, that being 2,023N which is reached at 0.475m.

Figure 3.12.1-B shows the build-up in lateral force when the tyre accelerated while held at a constant slip angle. The lateral force (FYW) is plotted against longitudinal displacement (LONGDISP) which is calculated using the measured runtime and forward velocity channels. To interpret the relaxation length, we must first determine the saturated lateral force, this is the maximum lateral force generated by the tyre under this load case, which is 3,201N shown by the black dashed line in Figure 3.12.1-B. The relaxation mechanism in a tyre is assumed to be a first order system, in this case used to model the response of lateral force to slip angle. The relaxation length is a physical interpretation of the time constant which characterises the rise or fall rate of a first order system. As such the relaxation response conforms to Equation 3.12.1-A:

$$1 - \frac{1}{e} \approx 63.2\%$$

Equation 3.12.1-A. Time constant equation for an increasing single order system. (Laptak, 2006)

In practical terms, this means the relaxation length is the distance covered until the tyre reaches 63.2% of its saturated lateral force. In this case 63.2% of the saturated lateral force is 2,023N (63.2% of 3,201 = 2,023N), which occurs after the tyre has travelled 0.475m, as shown by the dashed red line in Figure 3.12.1-B. However, in this case the tyre did not generate zero lateral force at zero longitudinal displacement, instead zero lateral force occurred at 0.05m. This small correction is required due to zero displacement being at an arbitrary point marked by the test rig when the change in forward velocity is triggered, it hence does not consider the delay in the rig's response between triggering the forward acceleration and it occurring. The response error can be accounted for by simply subtracting it from the distance covered to reach 63.2% of the saturated lateral force. This means that the tyre's relaxation length is 0.425m (0.475 – 0.05 = 0.425m) in this case.

Using such a method repeated over a range of vertical loads and inflation pressures means a suitable data set pertaining to the tyre relaxation length and its sensitivity to load and pressure can be established. This data is then used to parametrise the relaxation length model included in the MF-Tyre 6.1 tyre model.

3.12.2 Longitudinal Relaxation Length

The Step-Steer test used to measure lateral relaxation length cannot be applied to longitudinal relaxation length. This is because the test would require a near instant application of slip ratio; this can be achieved using the flat-trac rig's powerful electric drive motor however it causes the test tyre to slip on this rim, invalidating the test. Instead the stiffness ratio method is used, where the longitudinal relaxation length is defined as the ratio of slip stiffness to longitudinal stiffness. Slip stiffness can be extracted from the 'GS2MF BrkDrv' force and moment test procedure; however, the static longitudinal stiffness must be measured using a special set of static longitudinal testing which forms 'GS2MF StaticLong'.

During the static longitudinal testing, the tyre is rolled forward at a constant load case and then brought to a halt, the flat-tracs' road belt is then moved while the tyre is held still; effectively dragging the tyre longitudinally across the road surface, only it is the road surface rather than the tyre that moves. As the road surface moves, the tyre's longitudinal force builds up until saturating. The tyre's longitudinal stiffness can then be calculated by determining the rate at which this longitudinal force builds in relation to the longitudinal displacement. This is shown in Figure 3.12.2-A.

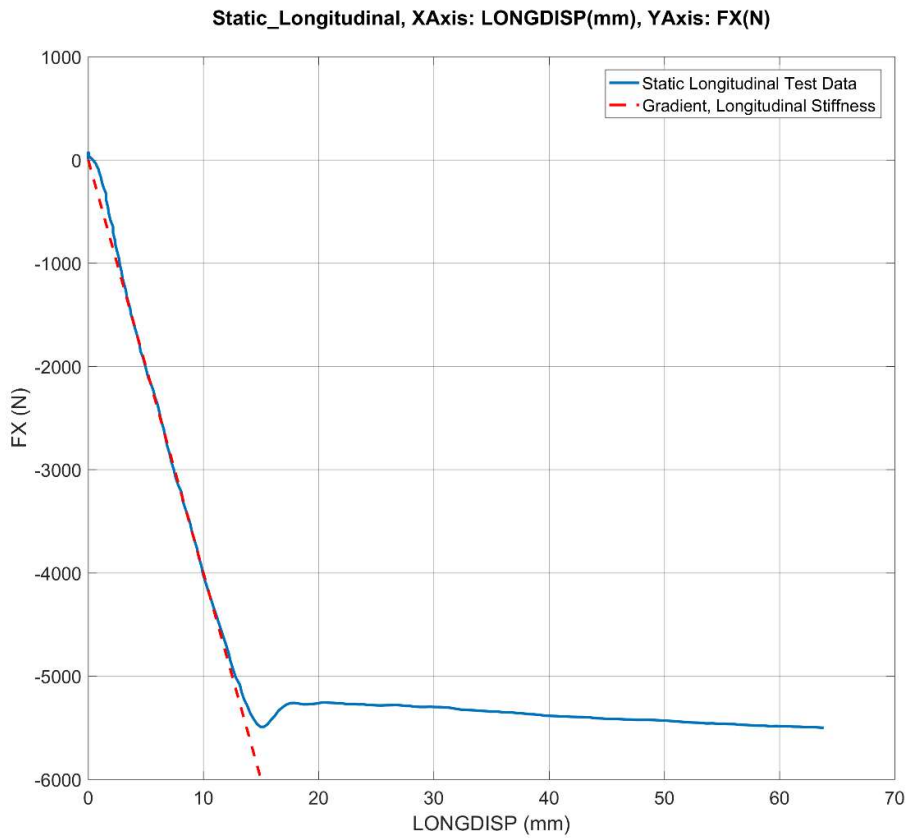

Figure 3.12.2-A. Results from an example static longitudinal test at 5,400N of vertical load, also shown is the linear fit to determine the longitudinal stiffness.

Figure 3.12.2-A shows the longitudinal force versus longitudinal displacement results from a single static longitudinal test. Also shown is how a straight line can be fitted to the linear section of the data, the gradient of this line is the static longitudinal stiffness. This test is then repeated at six discreet loads ranging from 0.4 to 1.4 times the tyre's nominal load. Ideally additional testing would be carried out at higher loads, up to around 2.0 times the nominal load; however, doing so resulted in tearing the sand paper surface used on the test rig which both invalidated the test and required time to fix. Therefore, a maximum load of 1.4 times the nominal load is used. These six tests are then repeated at three inflation pressures. Since only one value is extracted from each test there is a large degree of error that can occur from calculating the longitudinal stiffness. For this reason, the whole set of testing is repeated four times allowing the results to be averaged.

When fitting the MF-Tyre 6.1 tyre model, the 'FX Pure' part of the tyre model is used to estimate slip stiffness values at each of the load cases used in the static longitudinal testing. The longitudinal relaxation length is then calculated as the ratio of slip stiffness (from the FX Pure

model) to the longitudinal stiffness (shown in Figure 3.12.2-A). A longitudinal relaxation length model is then fitted to these calculated relaxation length values.

3.13 'GS2MF BrkDrv' Components

Where practical the 'GS2MF BrkDrv' test procedure uses some of the technology and sweep shapes also used in the 'GS2MF FreeRolling' procedure. 'GS2MF BrkDrv' features the same warmup procedure as that of 'GS2MF FreeRolling'. Also, the thermal logic system used in 'GS2MF FreeRolling' to automatically trigger the next test sweep after the tyre cools to 45°C is used and carried over. The thermal logic is setup the same way to ensure that the tyre is regulated at the same temperature between the two test procedure, this is crucial to ensure that data from the two tests is compatible with each other. 'GS2MF BrkDrv' also features Graph Sweeps, like those used in 'FreeRolling', at the start and end of the test that can be used to assess how the tyre's performance changes as results of the testing. The variable rate sweep used in 'GS2MF FreeRolling' is carried over into the 'GS2MF BrkDrv' procedure, only it is the slip ratio that changes at a non-constant rate rather than slip angle.

Some technologies, such as the asymmetric loading, do not carry over into the 'GS2MF BrkDrv'. This is because the asymmetric loading relies upon the assumption that a right-side tyre steering to the left is equivalent to a left-side tyre steering to the right, which is valid even in asymmetric tyres. However, this assumption does not hold true in the longitudinal direction where a front tyre under braking is not equivalent to a rear tyre under acceleration. This is because tyres often have very different acceleration and braking performance. For this reason, asymmetric loading is not present in the 'GS2MF BrkDrv' procedure.

3.14 GS2MF Technology Components Summary

Chapter 3.0 summarised the various methodologies that were developed within GS2MF. These include linking the test loads to the tyre's load rating, thus ensuring that each tyre is tested at an appropriate load case. The process to warmup the tyre was discussed, as well as the thermal logic system used to maintain the tyre at a constant baseline temperature throughout the testing. These are both crucial to ensure the tyre performs consistently. The novel variable rate sweep was introduced and discussed in detail, covering how it was developed to reduce both thermal and mechanical hysteresis, which leads to a reduction in tyre temperature and associated reduction in the required cool down times. As a result, this leads to a significant reduction in the overall test duration and associated costs. Other new methodologies were introduced such as: asymmetric loading, where a vehicles lateral weight shift while cornering is considered and used to define the test loads based on slip angle; and the vertical load sweeps used to gather data at high slip conditions while minimising wear. This inclusion of Graph Sweeps was discussed as a method to determine if the test tyre has changed as a result of the testing. Finally, test methods

for Rolling Radius, On-Centre Behaviour and Relaxation Length were introduced. In Chapter 4.0 these various methodologies are used together to form practical test procedures that generate data which can be used to parameterise MF-Tyre 6.1 tyre models.

4.0 GS2MF Full Procedure

GS2MF consists of three distinct test procedures: the 'GS2MF FreeRolling', 'GS2MF BrkDrv' and 'GS2MF StaticLong' each of which can be considered as composites procedures made of made up of various components (as detailed in previous chapters). All three test procedures can be run on most flat-trac rigs though some reconfiguration may be required, such as un-coupling the rig's drive motor to ensure a pure free rolling test condition. This section details the overall structure of each test procedure and how the various components are assembled together to form efficient test sequences. The data obtained from running these tests can be used for the parametrisation of the MF-Tyre 6.1 tyre model. These tyre models can then be used within road car companies as part of the vehicle development process.

The majority of testing is conducted at high slip and high load conditions that are rarely seen on a road car, while only minimal testing is conducted at lower, more commonly occurring load cases. This is because the importance of the data is not based on the amount of time a vehicle is expected to spend at any given range of conditions. Instead it is critically important for auto makers to have tyre models that are valid across a wide range of load cases to simulate extreme driving situations, such as accident avoidance. These manoeuvres are very unusual and a typical vehicle will spend very little time driving in such situations. However, when they do occur, it is critical that the vehicle performs safely. Hence the need for significant amounts of tyre testing in high slip and other extreme conditions.

4.1 'GS2MF FreeRolling' Overview

The 'GS2MF FreeRolling' test procedure is designed to capture all the force and moment data required to populate the lateral force and overturning moment sections of the MF-Tyre 6.1 tyre model. This includes full sensitivity to vertical load, camber angle, and inflation pressure. Furthermore, the 'GS2MF FreeRolling' test procedure also gathers data used to parametrise the lateral relaxation and vertical stiffness components of the MF-Tyre 6.1 tyre model. Finally, Graph Sweeps are included to determine if the test procedure itself has caused excessive wear to the tyre. An overview of all the component technologies that build up the 'GS2MF FreeRolling' test procedure is shown in Table 4.1-A.

Section Number	Section Name	Description
1	Warmup	Heats up and breaks in the new tyre.
2	Step Steer	Lateral Step-Steer tests to establish the relaxation length.
3	Heating Sweep	A single sweep to heat up the tyre after the low energy Step-Steer testing.
4	Graph Sweep 1	New tyre comparison test, compared to Graph Sweep 2.
5	On-Centre and Rolling Radius	On-Centre testing of Cornering Stiffness, RSAT (Residual Self-Aligning Torque) and RCF (Residual Cornering Force) along with the Rolling Radius.
6	FandM_1	Force and moment testing at the first inflation pressure, regulated at 2.1bar (example pressure).
7	FandM_2	Force and moment testing at the second inflation pressure, regulated at 2.6bar (example pressure).
8	FandM_3	Force and moment testing at the third inflation pressure, regulated at 3.3bar (example pressure).
9	Graph Sweep 2	Worn tyre comparison test, compared to Graph Sweep 1.

Table 4.1-A. Brief summary for 'GS2MF FreeRolling' component sections.

Table 4.1-A shows a brief summary of the component sections that make up the 'GS2MF FreeRolling' test procedure. These components are visually shown in Figure 4.1-A and then detailed in the coming sections.

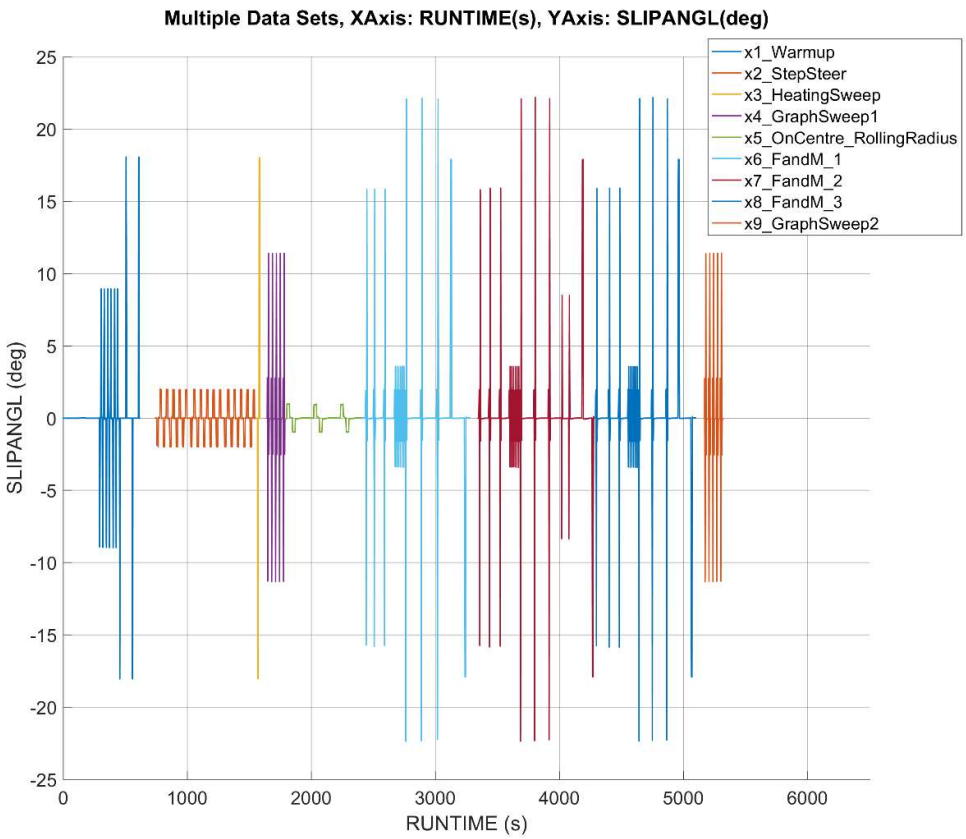

Figure 4.1-A. Overview of the 'GS2MF FreeRolling' test procedure divided into sections.

Figure 4.1-A shows the full 'GS2MF FreeRolling' test procedure built up from its various sections. The details of each of these sections is discussed below.

4.1.1 Warmup

The GS2MF warmup procedure is designed to warm the tyre from room temperature to 45°C, as detailed in the warmup section (See Section 3.4 on Warmup) and shown in Figure 4.1.1-A.

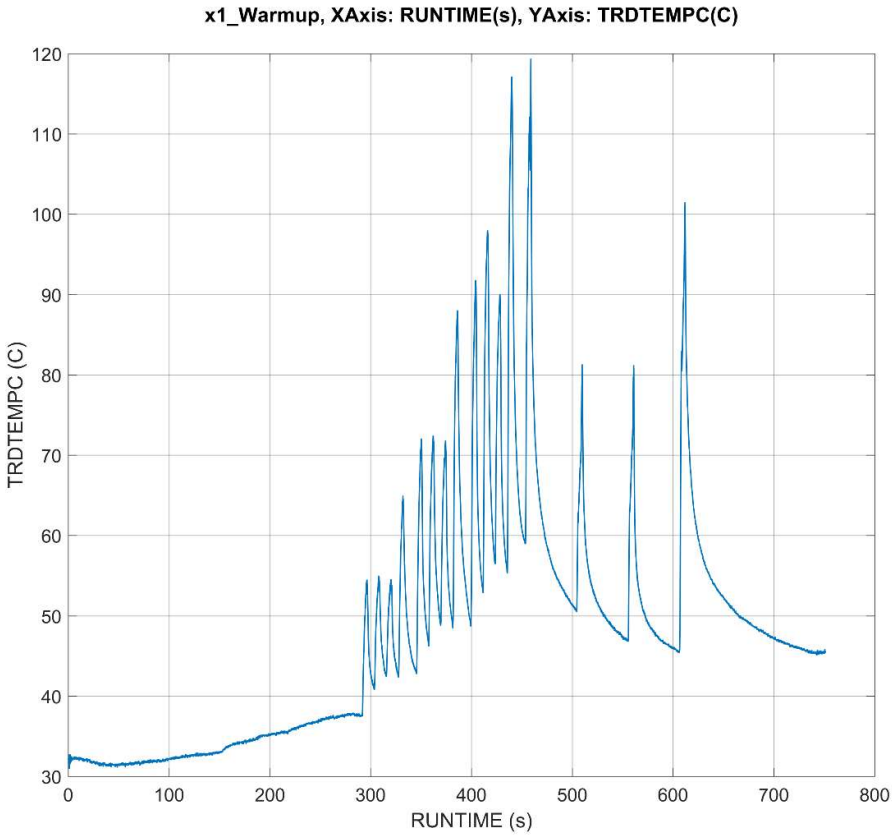

Figure 4.1.1-A. The result from running the warmup section of the 'GS2MF FreeRolling' test procedure.

Figure 4.1.1-A shows the results from running the warmup section of the 'GS2MF FreeRolling' test procedure. The warmup successfully warmed the tyre from room temperature to the required 45°C baseline temperature. This ensures the tyre is appropriately conditioned and warmed to a typical temperature observed during on-vehicle use. This is detailed in section 3.4 on Warmup.

4.1.2 Step-Steer, (Lateral Relaxation Length)

After the warmup is complete the Step-Steer testing is begun (See Section 3.12 on Relaxation Length). This portion of the testing is conducted early in the procedure as it is a very low sliding energy test, just 1,474kJ over the entire 800s Step-Steer sequence. This means the tyre will be subjected to very minimal wear as a result of this testing, hence the tyre's performance will not be altered for the forthcoming test sections. Furthermore, this allows the crucial Step-Steer testing to be conducted on the tyre while in its optimal condition, that being warm but not worn. This results in high quality, accurate data being used to calculate the tyre's lateral relaxation length. The Step-Steer test routine is shown in Figure 4.1.2-A.

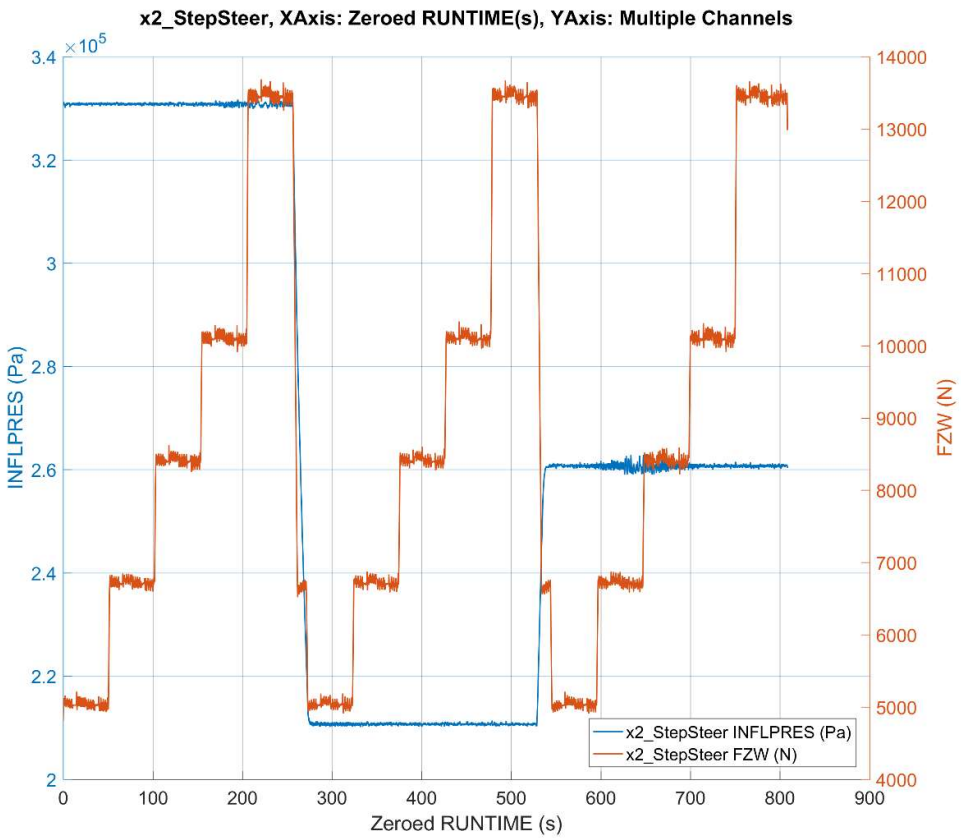

Figure 4.1.2-A. Results from running the Step-Steer section of the 'GS2MF FreeRolling' test procedure.

Figure 4.1.2-A shows the load cases used in the Step-Steer section of the 'GS2MF FreeRolling' test procedure. During each plateau in the vertical load two Step-Steer tests are conducted, one at a positive and one at a negative slip angle. This allows any asymmetry in the tyre's performance to be averaged, as the MF-Tyre 6.1 tyre model does not support the asymmetric modelling of relaxation length. This limitation in the model is of little significance as the results show that the left and right relaxation lengths were consistently similar. Therefore, averaging them and using this data to parameterise the model caused it to accurately capture the tyre's behaviour, this is detailed in section 5.2.9 on transients.

4.1.3 Heating Sweep

The heating sweep is a single sweep added to reheat the tyre after the Step-Steer test sequence. The tyre typically cools during the low sliding energy of the Step-Steer tests, this results in the tyre temperature falling being below the 45°C baseline temperature. This is shown in Figure 4.1.3-A.

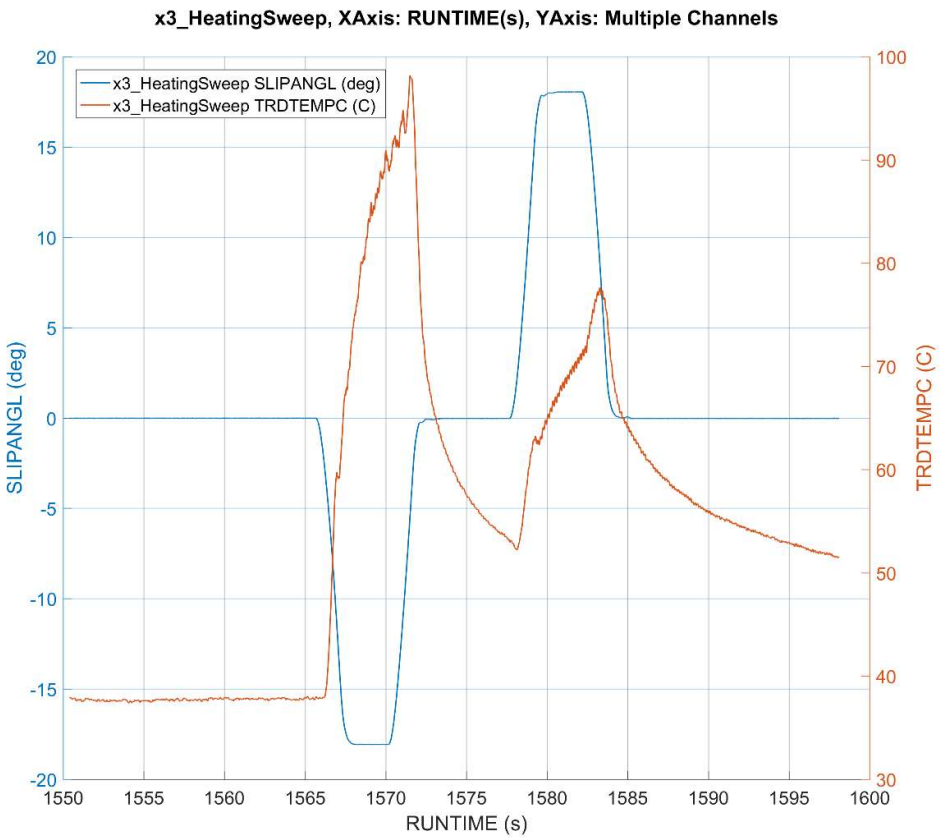

Figure 4.1.3-A. Results from running the heating sweep section of the 'GS2MF FreeRolling' test procedure.

Figure 4.1.3-A shows the tyre's temperature during the heating sweep. Here it can be seen that the tyre temperature after the preceding Step-Steer test was 38°C, well below the 45°C baseline temperature. By the end of the heating sweep, where the tyre returns to zero slip angle, the tyre temperature has risen to 65°C. After this the thermal pause system (detailed in section 3.5 on Thermal Pause) holds the tyre at zero slip angle until the tyre cools to the 45°C baseline temperature before automatically triggering the next sweep, this maintains the thermal consistency of the tyre.

4.1.4 Graph Sweep 1

Graph Sweep 1 is run to establish a tyre performance benchmark while the tyre is in its optimal condition, that being fully up to temperature and at this point still only lightly worn. Data collected here is then compared to the identical Graph Sweep 2 which is run at the end of the test procedure. Doing so highlights any changes to the test tyre itself, which will manifest as inaccuracies in the resulting tyre model built using the test data. (See Section 3.9 on Graph Sweeps)

4.1.5 On-Centre and Rolling Radius

The On-Centre testing, used to establish values for cornering stiffness, RSAT (Residual Self-Aligning Torque) and RCF (Residual Cornering Force) are integrated amongst the Rolling Radius tests, which are used to establish the tyre's vertical stiffness (See Section 3.10 on Rolling Radius and Section 3.11 on On-Centre Behaviour). The amalgamation of these tests together reduces the total number of times the tyre's inflation pressure needs to be changed. As this process takes around 20s for each pressure change the integration of these tests saved three changes, totalling around 60s of test duration. Figure 4.1.5-A shows the On-Centre and Rolling Radius tests conducted at one of the three inflation pressures, this test sequence is then repeated at the other two inflation pressures.

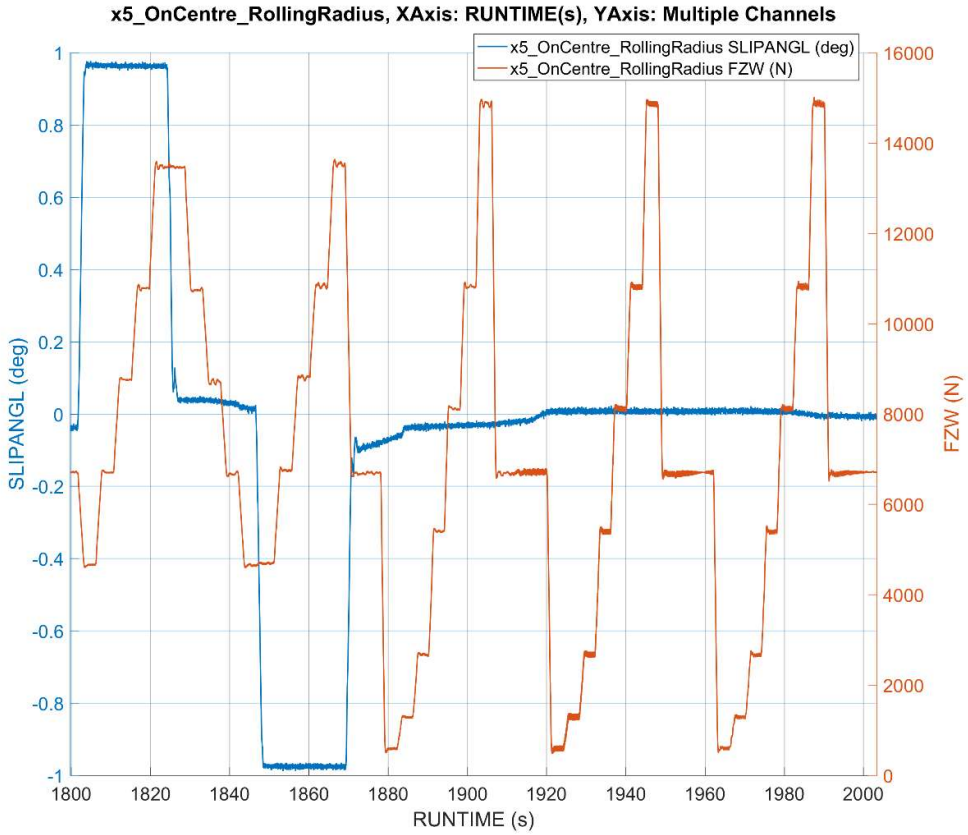

Figure 4.1.5-A. The result from running the first third (one inflation pressure) of the On-Centre and Rolling Radius sweep section of the 'GS2MF FreeRolling' test procedure.

Figure 4.1.5-A shows the On-Centre testing up to 1,875s, after which the Rolling Radius test is conducted. All of which is run at the same inflation pressure. After this, the same test is repeated at the remaining two inflation pressures. After post-processing this data cornering stiffness, RSAT and RCF can be extracted from the On-Centre data (See Section 3.11 on On-Centre Behaviour), this can be used to benchmark key tyre performance metrics against other tyres.

This is often useful for vehicle manufacturers to quickly assess different tyres from multiple manufacturers. Meanwhile, the Rolling Radius data extracted from the second section of the test, can be used to parameterise the vertical stiffness components of the MF-Tyre 6.1 tyre model.

4.1.6 FandM_1 (Force and Moment part 1, Inflation Pressure 2.1bar)

After the Step-Steer, Graph Sweep 1, On-Centre and Rolling Radius sections are complete, the 'GS2MF FreeRolling' test procedure moves onto the force and moment testing. This is the core of 'GS2MF FreeRolling' and is responsible for gathering data pertaining to the tyre's free rolling force and moment performance. The breakdown of the force and moment section is complex and features a series of 14 sweeps at various loads, slip angles and camber angles. These are detailed in Figure 4.1.6-A.

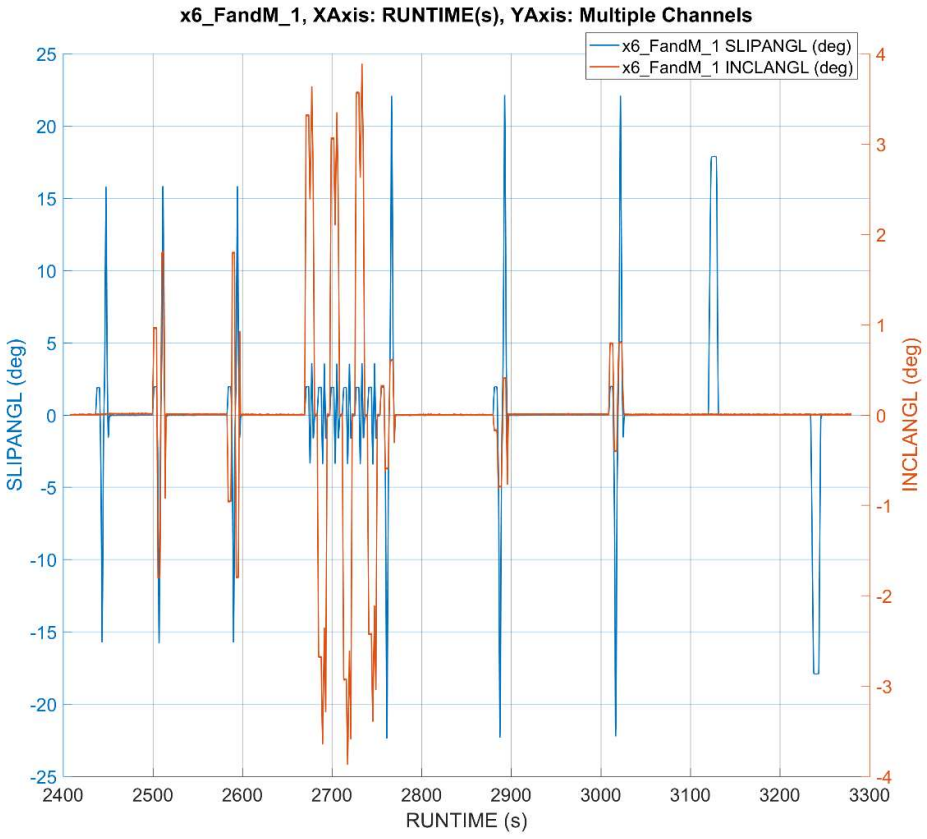

Figure 4.1.6-A. Results from running the first force and moment section of the 'GS2MF FreeRolling' test procedure.

Figure 4.1.6-A shows how the slip and camber angles changes through the first section of the force and moment testing, all run at a single inflation pressure. Asymmetric loading (See Section 3.7 on Asymmetric Loading) is used during all the sweeps in this section, to link the

tested load to the slip angle in such a way as to mimic the lateral load transfer of a vehicle during cornering. The first sweep is a steering sweep at zero camber to a medium peak slip angle of 16°, which is representative of reasonably severe vehicle dynamics manoeuvres. Then there is a steering sweep with medium camber of 1.8° acting in the same direction as the slip angle, this is followed by a sweep with adverse camber acting in the opposite direction to the slip angle. This allows the pure steering (zero camber) effect, as well as both polarities of camber effect to be captured in the resulting tyre model, which is critical for simulating everyday driving conditions. After this, there is a series of close to centre sweep at low peak slip angles of 4° but with a high camber angle of 3°; these obtain further data pertaining to the tyre's camber sensitivity. Following this, there are three sweeps where small amounts of camber angle, (around 0.8°) act in the same direction as the slip angle, but this time to higher peak slip angles of 22°. This represents a more severe vehicle dynamics manoeuvre. Finally, there are two vertical load sweeps (See section 3.8 on Vertical Load Sweeps) that test the tyre to high loads of 12,000N while also at high slip angles of 18°, designed to capture data under very high load conditions, representative of a vehicle at GVW (gross vehicle weight). Altogether, this section builds up a rich data set over a wide and varied range of load cases. This allows the tyre's lateral force and overturning moment to be modelled and made sensitive to slip angle, camber angle and vertical load. Therefore, the resulting tyre model will be suitable for simulating a wide range of vehicle dynamics manoeuvres.

4.1.7 FandM_2 (Force and Moment part 2, Inflation Pressure 2.6bar)

The second force and moment section is a repeat of the first, however it is conducted at the second inflation pressure of 2.6bar. This combined with the third force and moment section enables the resulting tyre model to be sensitive to inflation pressure. Which facilitates the user to tune the tyre's inflation pressure and observe a change in simulated vehicle level performance. This section continues to employ asymmetric loading as used in the first force and moment section; where the vertical load is adjusted based on the direction and magnitude of the peak slip angle, such as to simulate the loading placed on the tyre when used on a road vehicle. This is where a right-side tyre steering to the left will experience a load greater than the static load, as the vehicles weight will shift to the right; conversely, when steering to the right the right-side tyre will experience a load lower than the static load, as the vehicles weight shifts to the left. This data can then be mirrored to represent the left side tyre. However, this second force and moment section features two sweeps where the vertical load is tested at an adverse direction with respect to slip angle. This is to ensure that the resulting tyre model built from the data is valid across the widest possible range of load conditions. This is shown in Figure 4.1.7-A.

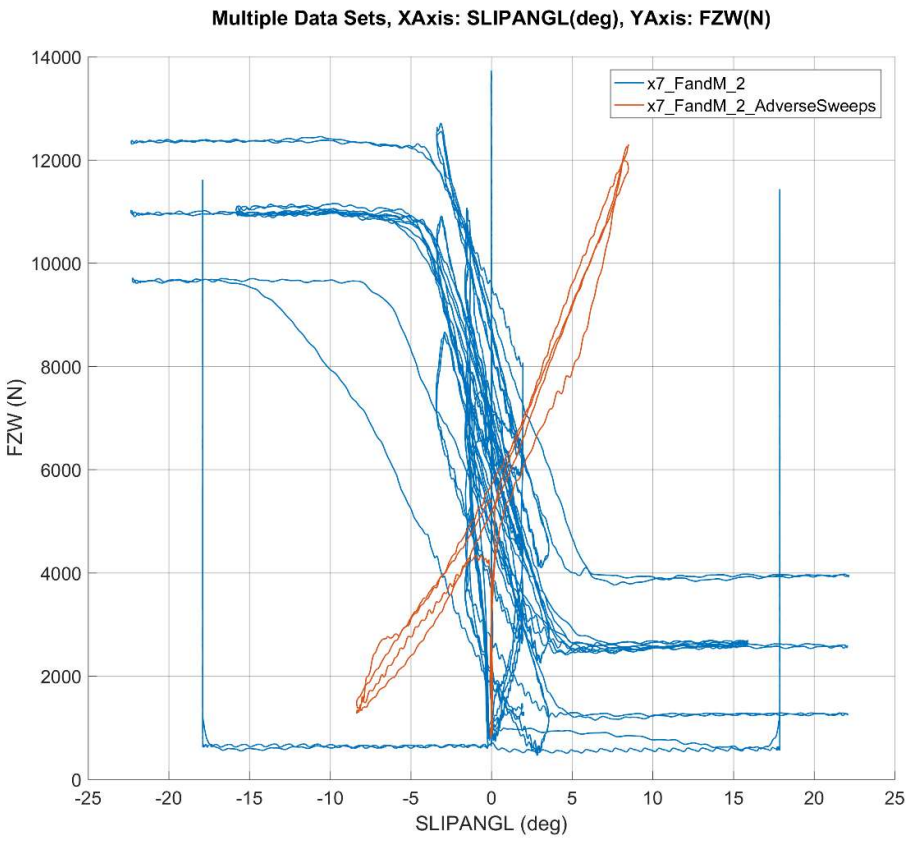

Figure 4.1.7-A. Results from running the second force and moment section of the 'GS2MF FreeRolling' test procedure.

Figure 4.1.7-A shows that the adverse sweeps act in the opposite direction to most sweeps in this portion of the test procedure. This data is to ensure that the resulting MF-Tyre 6.1 tyre model built from this data is at least mathematically stable in highly unusual load cases even if the correlation will likely be poor. This means that the resulting tyre model is less likely to cause a vehicle simulation system to crash, even when simulating extreme load cases. At such conditions, the simulation will be less accurate than when close to zero slip; however, this is unavoidable without using a more advanced tyre model that is able to take into account the significant change in tyre temperature (and associated change in performance) that occurs at such extreme slip conditions. Such tyre models are beyond the scope of this project, which focus on the more commonly used MF-Tyre 6.1 tyre model.

4.1.8 FandM_3 (Force and Moment part 3, Inflation Pressure 3.3bar)

The third repeat of the force and moment section of the 'GS2MF FreeRolling' test procedure is identical to the first; however, this time it is conducted at the third inflation pressure of 3.3bar. Gathering a full set of force and moment data at all three inflation pressures means the resulting

tyre model can accurately and robustly capture the tyre's inflation pressure sensitivity. This facilitates the user to tune inflation pressure during vehicle dynamics simulations.

4.1.9 Graph Sweep 2

Graph Sweep 2 is the final test to be run on the tyre at the end of the 'GS2MF FreeRolling' test procedure. This test marks the end of the test procedure, after which the tyre will be discarded having collected all necessary data from it. The results from Graph Sweep 2 can be directly compared to Graph Sweep 1, which was conducted towards the beginning of the test when the tyre was in its optimal condition. A comparison between the two shows how the performance of the tyre has not significantly changed as a result of the testing. This is shown in Figure 4.1.9-A.

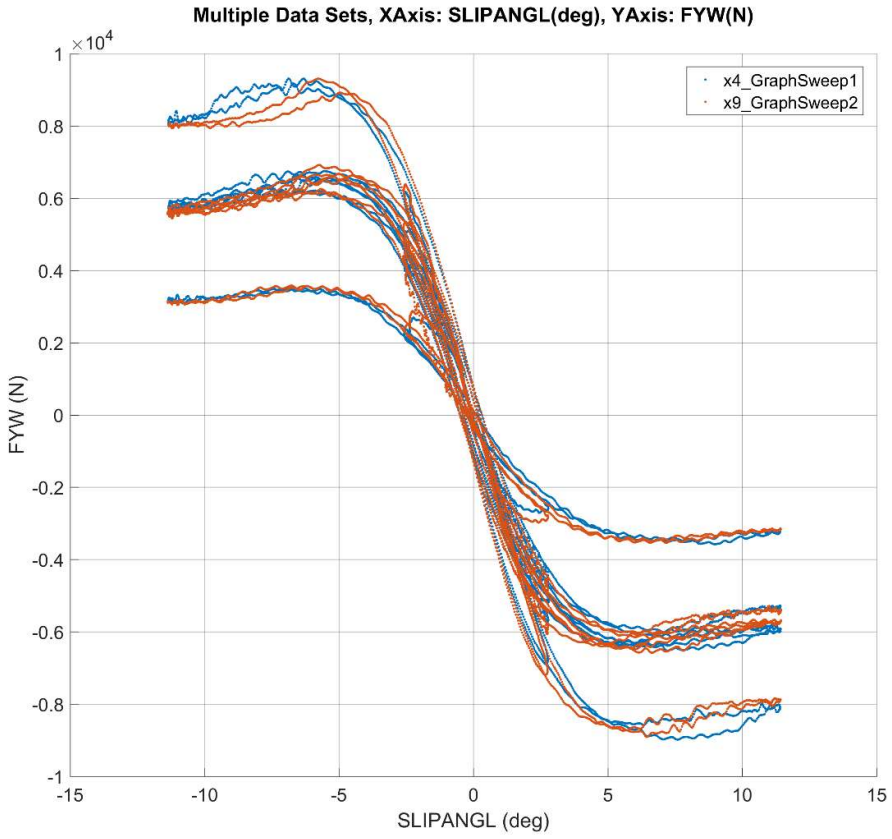

Figure 4.1.9-A. Results from running the Graph Sweep 1 and 2 sections of the 'GS2MF FreeRolling' test procedure.

Figure 4.1.9-A shows that in this case the Graph Sweeps match very well. Indicating that the tyre's performance has not significantly changed as a result of the testing.

4.2 'GS2MF BrkDrv' Overview

The 'GS2MF BrkDrv' test procedure is designed to gather all the necessary data required to populate the pure longitudinal and combined sections of the MF-Tyre 6.1 tyre model. As with 'GS2MF FreeRolling', the 'GS2MF BrkDrv' test procedure is built up of separate sections, with each section designed to gather a different type of data. This is summarised in Table 4.2-A.

Section Number	Section Name	Description
1	Warmup	Heats up and breaks in the new tyre.
2	Graph Sweep 1	New tyre comparison test, compared to Graph Sweep 2.
3	Pure Long A - Zero Camber	Pure longitudinal testing at zero camber to establish the tyre's load sensitivity.
4	Pure Long B - Low Camber	Addition to pure longitudinal testing to establish camber sensitivity at low camber angles (+/-3°).
5	Combined A - High Slip Angle	Combined testing at high slip angles (+/-9°) while at low camber angles (+/-3°).
6	Pure Long C - High Camber	Addition to pure longitudinal testing to establish camber sensitivity at high camber angles (+/-5°).
7	Combined B - High Slip Angle	Combined testing at high slip angles (+/-9°) while at high camber angles (+/-5°).
8	Combined C - Mid. Slip Angle	Combined testing at medium slip angles (+/-6°) while at zero camber angle.
9	Combined D - Very Low Slip Angle	Combined testing at close to On-Centre, with very low slip angles (+/-1°) while at zero camber angle.
10	Inflation Pressure A	Testing to establish the combined and longitudinal regulated inflation pressure sensitivity.
11	Extreme A	Testing at extreme high load and high slip angle conditions.
12	Graph Sweep 2	Worn tyre comparison test, compared to Graph Sweep 1.

Table 4.2-A. Brief summary for 'GS2MF BrkDrv' component sections.

Table 4.2-A shows an overview and brief description of the components that make up the 'GS2MF BrkDrv' test procedure. These components are visualised in Figure 4.2-A.

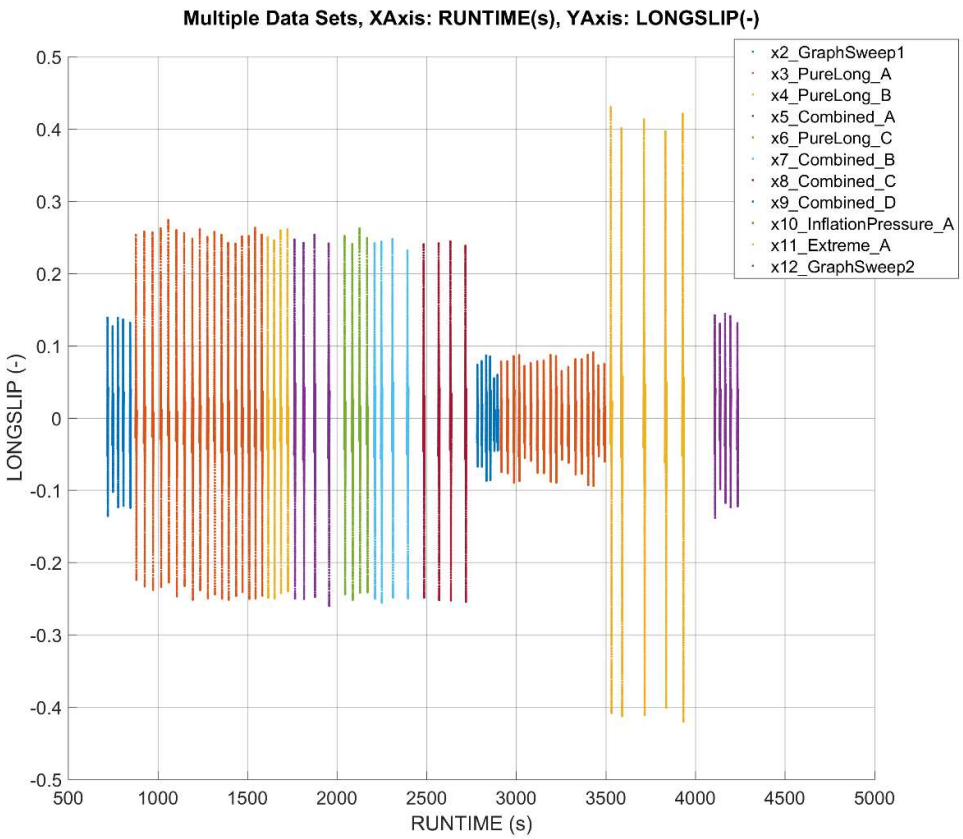

Figure 4.2-A. Overview of the 'GS2MF BrkDrv' test procedure divided into sections. The initial warmup and the cool down data between each sweep has been removed.

Figure 4.2-A shows the 'GS2MF BrkDrv' test procedure assembled from its separate sections and coloured accordingly. Each of these sections are described in the corresponding section below.

4.2.1 Warmup

The warmup test procedure is used to heat and condition the new tyre before force and moment testing commences, this is identical to that used in the 'GS2MF FreeRolling' procedure. Using the same warmup procedure ensures synergy between the two test procedures and ensures the forthcoming tests are conducted under similar conditions. This means the results from the two test procedures are comparable and can later be used to parameterise one tyre model. The warmup is not shown in Figure 4.2-A as it is identical to that shown in Figure 4.1.1-A (See Section 4.1.1 on 'GS2MF FreeRolling' Warmup) and further detailed in the warmup development section (See section 3.4 on Warmup).

4.2.2 Graph Sweep 1

Graph Sweep 1 is the first of two Graph Sweep sections used to assess the change in the tyre's performance as a result of the testing. Data obtained from this section will later be compared the identical sweeps of Graph Sweep 2. By doing so, any difference in tyre behaviour between the two tests can be attributed to a change to the tyre itself caused as a result of the testing. This information can hence be used to determine if the tyre was excessively worn or otherwise damaged during the test procedure (See Section 3.9 on Graph Sweeps). If excessive wear or damage is present then the test may need to be modified and repeated using a new tyre specimen.

4.2.3 Pure Long A - Zero Camber (SA +/-0°, Camber 0°)

The 'Pure Longitudinal Part A' section includes 18 variable rate sweeps (See Section 3.6 on Variable Rate Sweeps), testing the tyre at six loads ranging from 0.5 to 2.0 times the nominal load and three inflation pressures to gather data over a wide range of test conditions. All the testing in this section is to a peak slip ratio range of +/- 25%. This results in a full and complete sub-set of data that can be used to determine the tyre's pure longitudinal grip behaviour and its sensitivity to load and inflation pressure. The data from this section is shown in Figure 4.2.3-A.

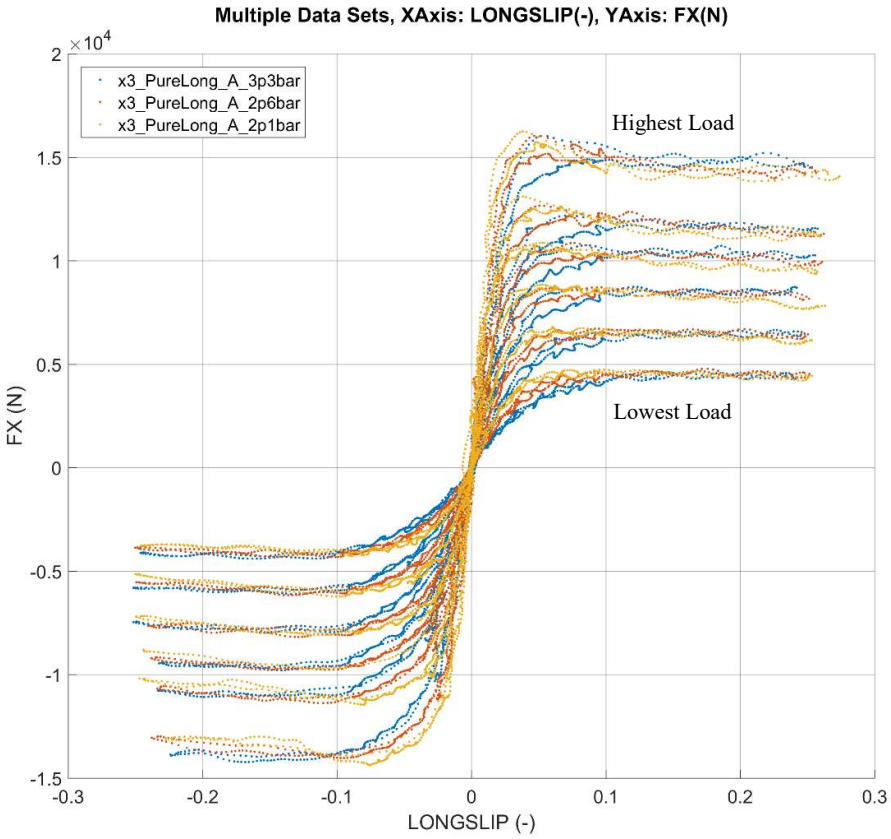

Figure 4.2.3-A. Longitudinal force versus slip ratio for the GS2MF BrkDrv, Pure Long A data section.

Figure 4.2.3-A shows the tyre's pure longitudinal performance as well as its sensitivity to load and inflation pressure. The plot is coloured by inflation pressure, while the different vertical load sweeps are also visible, the lower vertical load sweeps generating a maximum of around +/-4000N of longitudinal force while the highest load sweeps generate around +/-15,000N of force. Within each load set, the pressure sensitivity can also be observed. The lowest inflation pressure (coloured yellow) consistently shows a higher slip stiffness compared to the highest inflation pressure (coloured blue). This is consistent with what would be expected from this type of testing. While a higher inflation pressure stiffens the tyre's structure, it also reduces the size of the contact patch. This smaller contact patch makes the tyre easier to rotate in lateral testing, reducing cornering stiffness and easier to move longitudinally, reducing slip stiffness.

4.2.4 Pure Long B - Low Camber (SA +/-0°, Camber +/-3°)

The 'Pure Longitudinal Part B' section contains only four sweeps. The sweeps are similar to those used in 'Pure Longitudinal Part A' however, this time camber is applied. The vertical load of the sweeps are 0.75 and 1.25 times the nominal load with -3 and +3° of camber applied at

each load, making four sweeps in total. This gathers data pertaining to the pure longitudinal camber sensitivity, which is typically minimal but some tyres show a reduction in longitudinal force even when a low camber is applied. Inflation pressure is maintained at the middle pressure (2.6bar) throughout. Figure 4.2.4-A shows the results from this section of testing.

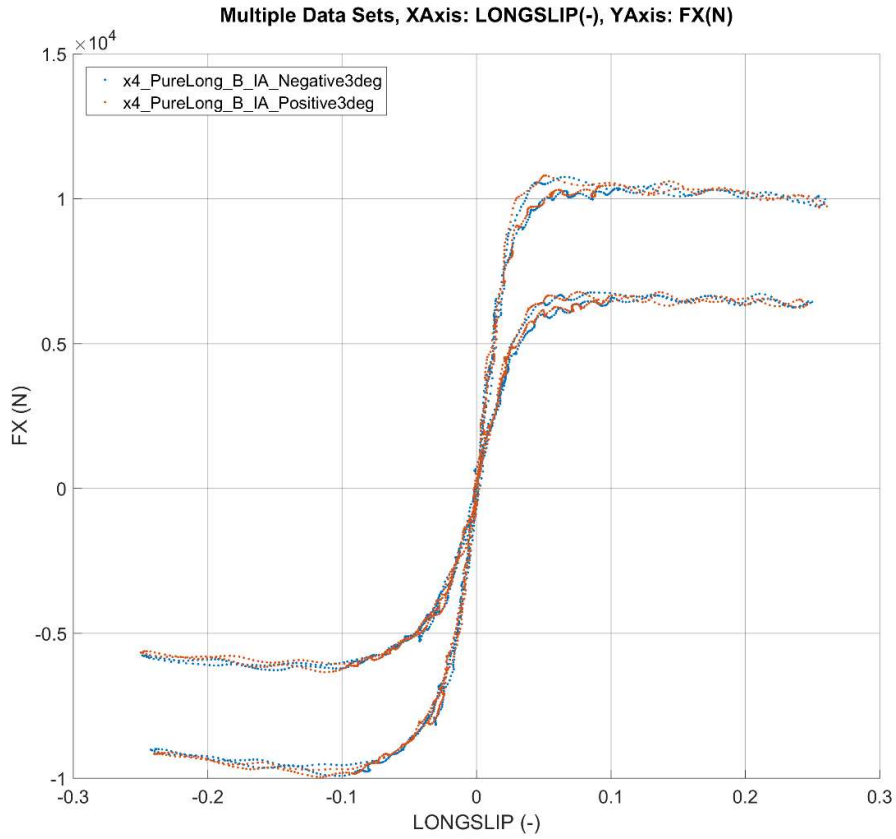

Figure 4.2.4-A. Longitudinal force versus slip ratio for the GS2MF BrkDrv, Pure Long B data section.

Figure 4.2.4-A shows that in this case, the positive and negative camber had a virtually identical effect on the tyre's longitudinal performance. This test tyre is a symmetrical design; therefore, this result is expected. However, when testing asymmetric tyres, it could be possible to observe a difference in the way positive and negative camber angles effects the tyre's longitudinal performance. In either case, the presence of any camber angle typically reduces the tyre's longitudinal performance. This can be captured in the 'FX Pure and Combined' part of the model parametrisation by using the 'Pure Longitudinal Part A' results which are run at zero camber, in conjunction with the 'Pure Longitudinal Part B' results presented here which include camber. This is detailed in section 5.2.3 on FX Pure and Combined.

4.2.5 Combined A - High Slip Angle (SA +/-9°, Camber +/-3°)

The fifth section of the 'GS2MF BrkDrv' test procedure is 'Combined Part A' where the tyre is tested in combined longitudinal and lateral load cases. The sweeps in this section are similar to those of previous sections, longitudinal slip ratio sweeps to a maximum of +/-25%; in this case all at a constant inflation pressure. However, this time the tyre is set to a given slip angle and held there whilst the longitudinal sweep is conducted, thus testing the tyre in a combined situation where both slip angle and slip ratio are applied simultaneously. This data is crucial, as this combined state is the most common use case for a road vehicle, where steering and either acceleration or braking inputs are applied at the same time.

Slip angles of 8.5° and -8.5° were tested at two different vertical loads and with zero, 3 and -3° of camber, creating 12 sweeps in total. These are designed to represent a vehicle under a high slip combined condition such as sever handling or an avoidance manoeuvre. However, the principal of asymmetric loading (See Section 3.7 on Asymmetric Loading) was applied here, such that testing is assumed to be conducted on right side tyres; meaning, positive slip angles were only tested at the low load and negative slip angles were only tested at the high load. This is representative of the lateral weight shift of a vehicle during cornering. Applying asymmetric loading in this way removed the need for testing six out of the 12 possible loading conditions. Furthermore, at this stage no testing was conducted where the camber angle acts in an adverse direction to the slip angle. This is an unusual load case that only occurs during highly extreme manoeuvres and is covered in other sections of the test procedure (see section 4.1.7 on Force and Moment part 2). Here, the right-side tyre is only tested at negative camber angles, that is the top of the tyre tilting inwards towards the centre line of the car. These adverse camber tests are not needed, since they are covered within the 'FreeRolling' procedure, resulted in a further two load cases being removed. This means, of the original 12 possible load case combination only four were necessary. Removing these significantly reduced the overall test duration and increased efficiency. Table 4.2.5-A details the 12 possible load cases and specifies which were included or removed.

Sweep No.	Slip Angle	Load	Camber	Included
1	+8.5°	low	0	Yes
2	+8.5°	low	Positive	No. Adverse camber.
3	+8.5°	low	Negative	Yes
4	+8.5°	High	0	No. Asymmetric Loading
5	+8.5°	High	Positive	No. Asymmetric Loading
6	+8.5°	High	Negative	No. Asymmetric Loading
7	-8.5°	low	0	No. Asymmetric Loading
8	-8.5°	low	Positive	No. Asymmetric Loading
9	-8.5°	low	Negative	No. Asymmetric Loading
10	-8.5°	High	0	Yes
11	-8.5°	High	Positive	No. Adverse camber.
12	-8.5°	High	Negative	Yes

Table 4.2.5-A. Load cases that were included in the test procedure or deemed to be unnecessary and removed.

The results of the combined testing are very different from the pure longitudinal testing. This is visualised in Figure 4.2.5-A which compares a combined sweep from this section with an otherwise identical pure longitudinal sweep from the ‘Pure Longitudinal Part A’ section.

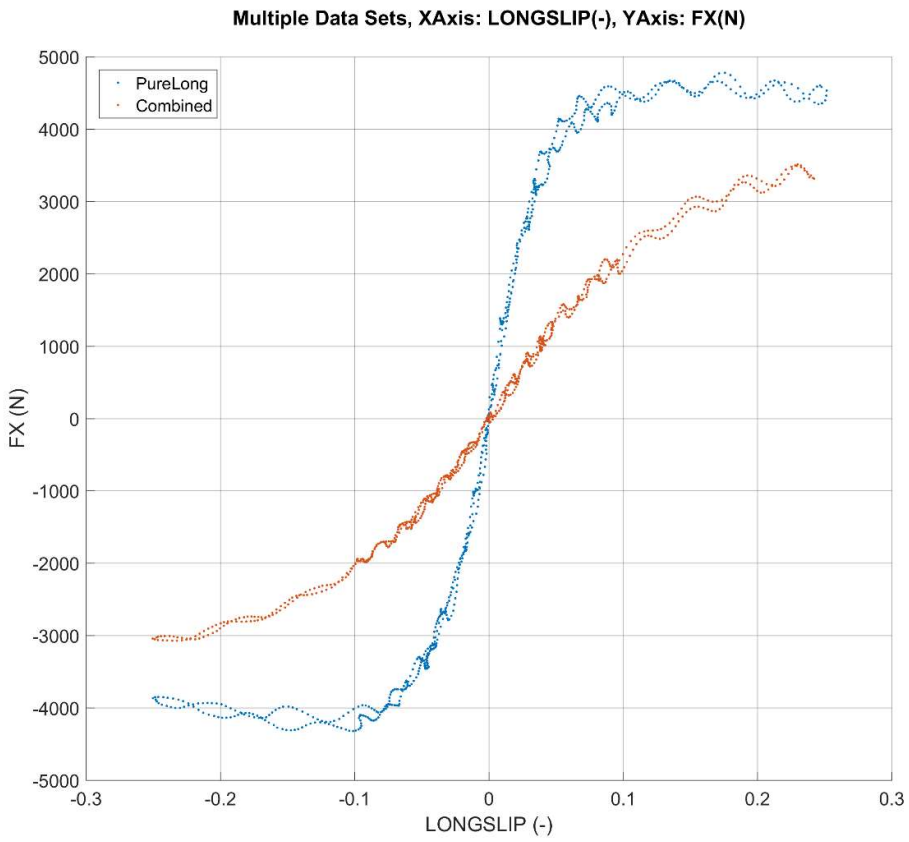

Figure 4.2.5-A. Comparison between two otherwise identical longitudinal sweeps; one is a pure longitudinal sweep conducted at zero slip angle and the other is a combined sweep conducted at 8.5° of slip angle.

Figure 4.2.5-A shows that the combined sweep generated far less longitudinal force across the entire slip ratio range compared to the pure longitudinal sweep. This is because the slip angle is causing the tyre to generate a lateral force, so there is less capacity remaining in the tyre for it to generate longitudinal force. This is shown by these same two sweeps plotted as a friction ellipse in Figure 4.2.5-B.

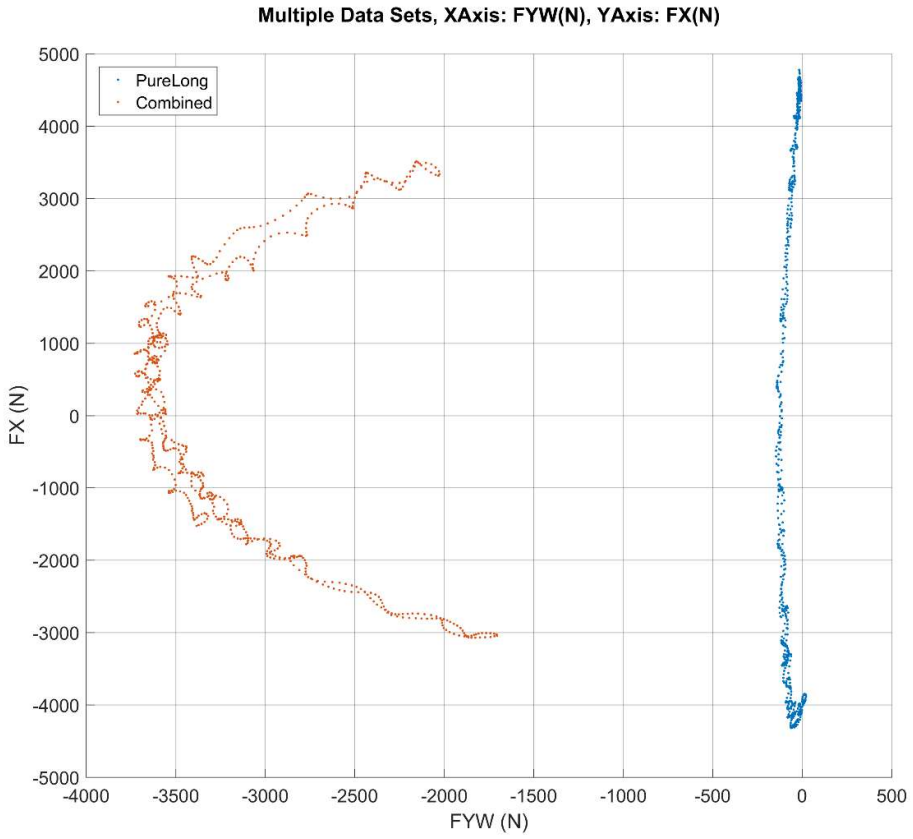

Figure 4.2.5-B. Friction ellipse of two otherwise identical longitudinal sweeps; one is a pure longitudinal sweep conducted at zero slip angle and the other is a combined sweep conducted at 8.5° of slip angle.

Figure 4.2.5-B shows that the combined sweep generated a maximum of around 3,500N of longitudinal force, while the pure long sweep generated 4,800N. However, while the combined sweep was generating the 3,500N of longitudinal force it was also generating 2,000N of lateral force in the negative (left) direction. At this point the vector sum of the forces for the combined test is 4,031N (longitudinal and lateral), while the vector sum of the pure longitudinal force remains at 4,800N (pure longitudinal). This means that the tyre generates a lower total force during combined testing compared to pure longitudinal testing; where the tyre is shown to be more efficient when generating force in just one direction. This reduction in combined forces varies between tyres and its hence important to test the tyre under these conditions. The complex nature of the combined load case can be captured in the MF-Tyre 6.1 tyre model which is later built from this data. This means the resulting tyre model will be valid for this combined load case which is very common for road vehicles, that being steering while at the same time accelerating or braking.

The increased efficiency in pure directional load cases is why drivers are taught to brake before a corner, steadily drive through it and then accelerate out of the corner. This approach means the tyre is under pure braking, then transitions into pure lateral steering, before transitioning again into pure acceleration. Throughout this process the tyre is always at its more efficient loading condition where it can generate the highest possible total amount of grip. Conversely braking into a corner means the tyre must generate longitudinal braking force while also generating lateral steering force, this places the tyre into a loading condition where it is less effective.

4.2.6 Pure Long C - High Camber (SA +/-0°, Camber +/-5°)

The 'Pure Longitudinal Part C' component of the 'GS2MF BrkDrv' test procedure is an exact repeat of 'Pure Longitudinal Part B'; that being pure longitudinal testing with positive and negative camber and two vertical loads. However, while Part B tested the tyre at +/-3° of camber, Part C tests the tyre at +/-5° of camber. This high camber angle is to measure the expected reduction in the tyre's longitudinal performance while a high camber is applied. A comparison of these two tests is shown in Figure 4.2.6-A.

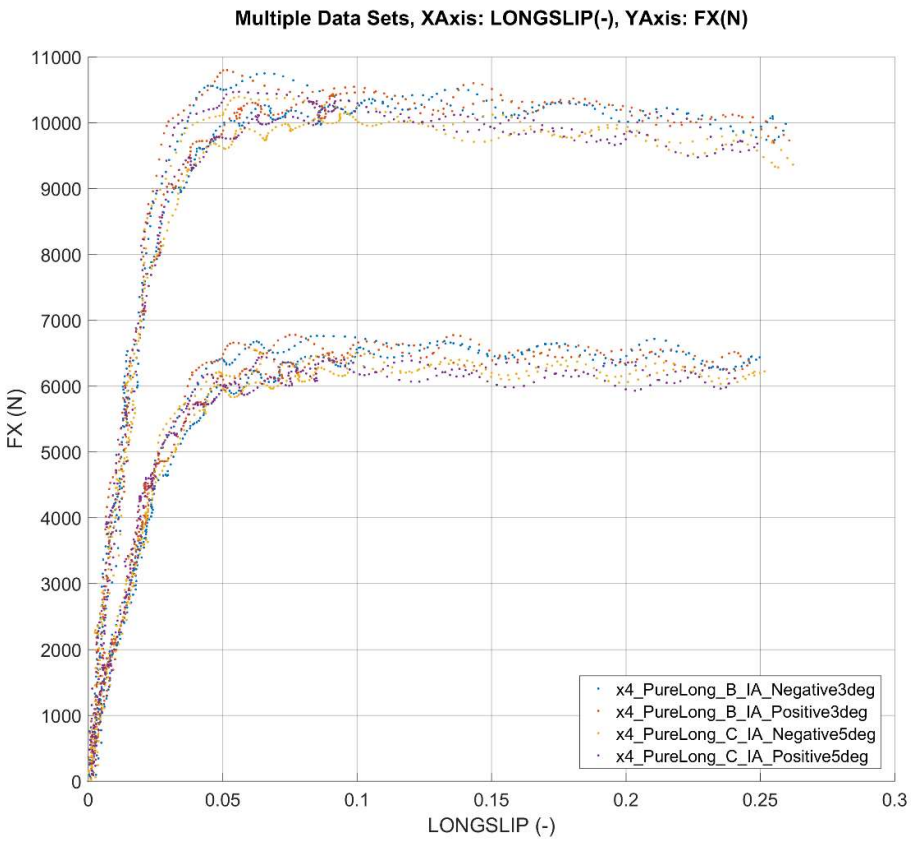

Figure 4.2.6-A. A comparison of pure longitudinal camber sensitivity at +/-3° and +/-5° of camber.

Figure 4.2.6-A shows that during both the high and low vertical load tests, the peak longitudinal force is slightly higher at 3 and -3° of camber (red and blue respectively). Whilst the same sweeps run at 5 and -5° camber (purple and yellow respectively) generate slightly less longitudinal force throughout the sweeps. This demonstrates the expected result that camber typically has an adverse effect on longitudinal force. However, the magnitude of this effect changes between tyres and using this data the camber effect can be captured in the resulting MF-Tyre 6.1 tyre model. This is crucial, as the same +/-5° of camber that has a negative effect on the longitudinal performance, has positive effect on the lateral performance. Therefore, measuring and modelling this relationship allows a vehicle dynamics analysis to be carried out to find the best balance between attributes and determine the optimal overall setup for the vehicle.

4.2.7 Combined B - High Slip Angle (SA +/-9°, Camber +/-5°)

The ‘Combined Part B’ test is a repeat of ‘Combined Part A’ but this time run at different camber angles. Where ‘Combined Part A’ tests the tyre’s camber sensitivity during combined testing at +/-3° camber with camber acting favourably with slip angle to simulate everyday driving. ‘Combined Part B’ repeats this testing at +/-5° of camber; however, this time the camber acts against the slip angle, simulating extreme manoeuvres where the vehicle approaches a rollover. These combined tests with camber applied are used to determine the complex nature of how camber can have a negative effect on longitudinal force and lateral force. This is shown in Figure 4.2.7-A.

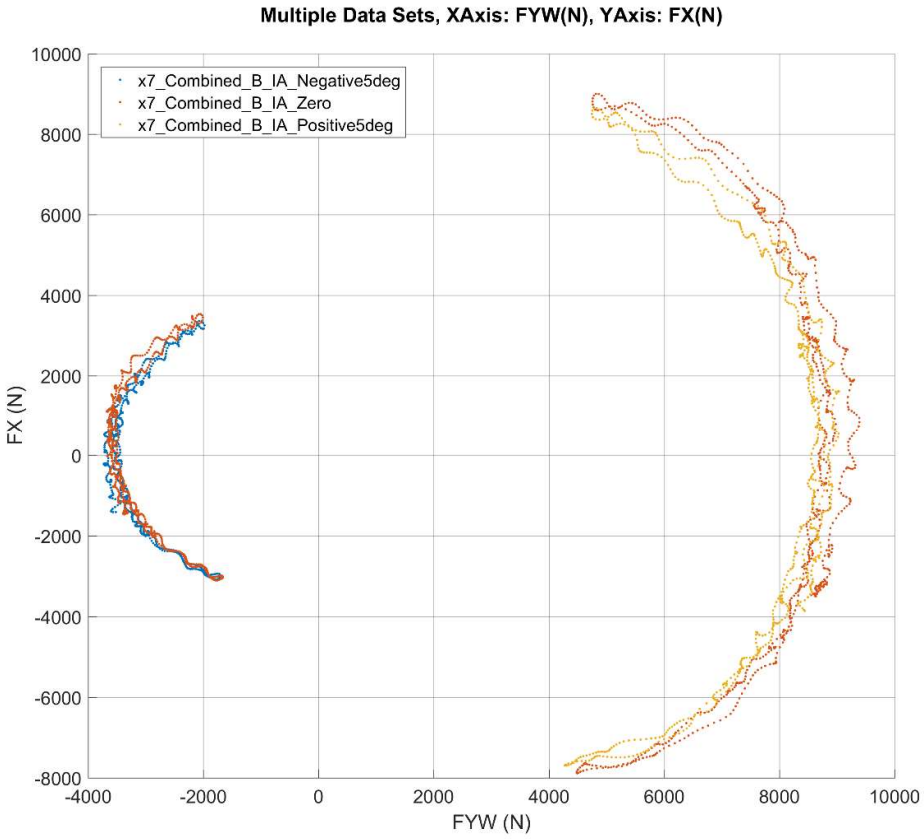

Figure 4.2.7-A. Friction ellipse of the tyre under combined testing with and without camber.

The large inverted ‘C’ shape on the right of Figure 4.2.7-A is from longitudinal sweeps while the tyre is steering left (negative slip angle) hence under a high load, the smaller ‘C’ shape on the left is from the tyre steering right (positive slip angle), while under a low load. While steering to the left (large inverted ‘C’), the tyre generated more force in all directions while at 0° of camber angle (red) compared to the sweep at 5° of camber (yellow), this shows that as expected, the 5° of camber acting against the slip angle had a negative effect on the tyre’s

overall grip. This is less evident when steering to the right under lower load where the camber had little to no affect.

This test tyre is a robust SUV tyre designed to perform similarly in all conditions, which explains the relatively small change in lateral force as a result of the applied camber. However, this will not hold true for high performance sports car of similar tyres which are far more sensitive to camber. Due to this inconsistency between difference tyres it is important to capture this data and use it in the model parametrisation.

4.2.8 Combined C - Mid Slip Angle (SA +/-6°, Camber 0°)

The 'Combined Part C' component of 'GS2MF BrkDrv' is very similar to previous combined sections. This time featuring four longitudinal sweeps at 6 and -6° of slip angle at zero camber and four mid-range vertical loads. This is a very common range of load cases used during vehicle dynamics simulations. It is therefore particularly important that the resulting tyre model built from this data is representative over this range of load cases. This section compliments the previous combined tests and gathers additional data at the medium load cases.

4.2.9 Combined D – Very Low Slip Angle (SA +/-1°, Camber 0°)

The 'Combined Part D' section differs from previous components in that it focuses on the close to centre, every day driving region of the tyre's performance. Since the clear majority of road car driving is conducted within this range of load conditions, it is important to gather additional data to ensure the resulting tyre model built form this data is representative and valid within this range. Here, six longitudinal sweeps are conducted at just +/-1° of slip angle, while at zero camber over a range of three vertical loads. Furthermore, the peak slip ratio of each sweep is reduced from 25% to just 10%. This is designed to better represent the common every day driving of a vehicle used on a public road.

4.2.10 Inflation Pressure A – Low Slip Angle, Three Inflation Pressures (SA +/-3°, Camber 0°)

The section 'Inflation Pressure Part A' is similar to 'Combined Part D' in that it gathers additional data at low combined slip conditions, which are very common in regular road vehicle use. In this case the slip ratio range is +/-10% at slip angle of -3 and 3° over a range of three loads. At each of the three loads, longitudinal sweeps are conducted at both -3 and 3° of slip angle, totalling six sweeps. These six sweeps are then repeated at three inflation pressures making 18 sweeps overall. With this data, a good understanding of the longitudinal and combined inflation pressure sensitivity can be established. This inflation pressure sensitivity is shown in Figure 4.2.10-A.

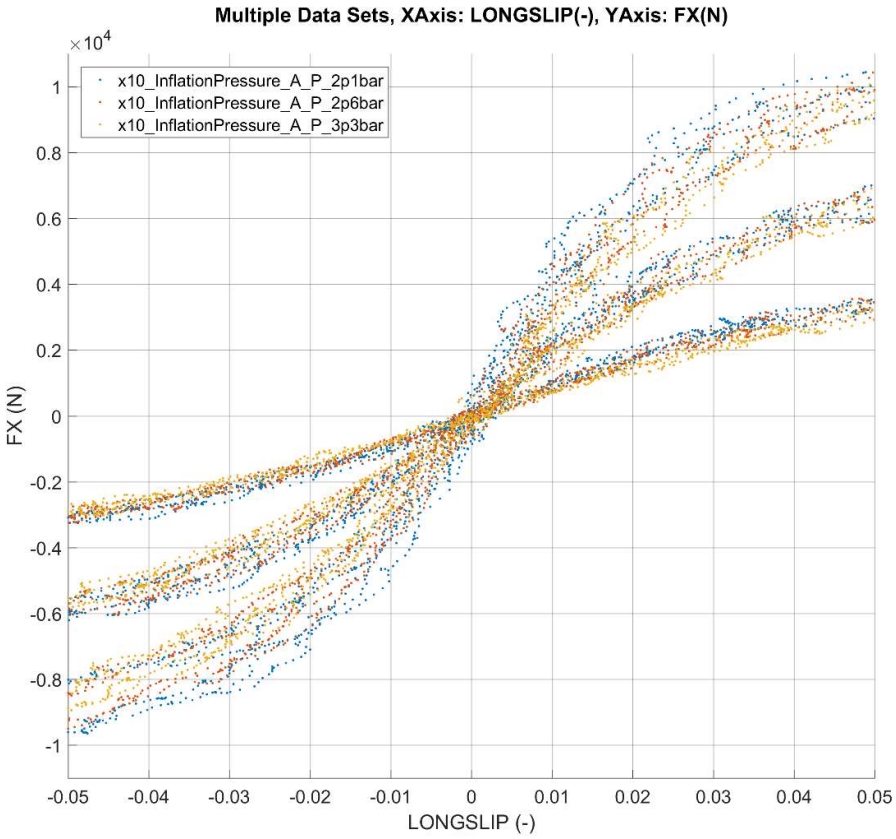

Figure 4.2.10-A. Close to centre pressure sensitivity of combined longitudinal testing.

Figure 4.2.10-A shows that slip stiffness (gradient of the linear centre section) is highest when the tyre is at its lowest inflation pressure (blue) and the slip stiffness is lower when the inflation pressure is increased (yellow). This is consistent with what would be expected, while also being consistent with the tyre's free rolling performance. The MF-Tyre 6.1 tyre model includes the capability of scaling the resulting tyre model to any inflation pressure within the tested range. Therefore, it is important to acquire this data and use it in the model parameterisation such that vehicle dynamics engineers using the tyre model can adjust the inflation pressure to suit the requirements of the vehicle.

4.2.11 Extreme A – High Slip Angle, High Load. (SA +/-18°, Camber 0°)

The penultimate section of the 'GS2MF BrkDrv' test procedure is 'Extreme Part A'. In this section, longitudinal sweeps are first conducted at the nominal load while the tyre is held at high slip angles of -12° and then +12°. After this, two additional sweeps are conducted, first with the tyre loaded to just 0.25 times the nominal load while at a very large +18° of slip angle, then the tyre is loaded to 2.0 times the nominal load and tested at -18° of slip angle. This data makes sure the resulting tyre model is valid across the widest possible range of load conditions. These load

cases are representative of extreme manoeuvres that are rarely seen in a typical road vehicle; however, they are highly important as the vehicles performance during these conditions can be an important factor in preventing road traffic accidents. For this reason, road car manufacturers design the cars to perform well in such extreme conditions. This is facilitated by the resulting tyre model being valid in this range. The extreme load case test is located at the end of the force and moment section of 'GS2MF BrkDrv' such that any excessive wear to the tyre (brought on by the extreme test conditions) has no effect on any other force and moment testing. Furthermore, the 'Graph Sweep 2' test section which follows the 'Extreme A' section is included to allow any excessive wear to be assessed.

4.2.12 Graph Sweep 2

Graph Sweep 2 is an exact repeat of Graph Sweep 1, which is conducted at the beginning of the test procedure, after the warmup (See Section 3.9 on Graph Sweeps). Graph Sweep 1 is a series of five sweeps conducted while the tyre is in its ideal condition, of being warmed up to its optimal temperature but not yet significantly worn. Graph Sweep 2 is a repeat of Graph Sweep 1 but it is conducted at the very end of the test procedure after the tyre has been well used. By comparing the results of Graph Sweep 1 and 2, conclusions can be drawn as the change in the performance of the tyre itself and the validity of the test. If the comparison shows a highly significant change to the tyre performance it may be necessary to modify the procedure and repeat the test using a new tyre specimen. The comparison between the two dataset its done visually, as there is no standardised reliable process for quantifying the difference. Such a process would be valuable; however, its development would be highly complex and would require multiple different datasets from a wide range of sources, it is hence outside the scope of this project. The visual comparison is shown in Figure 4.2.12-A.

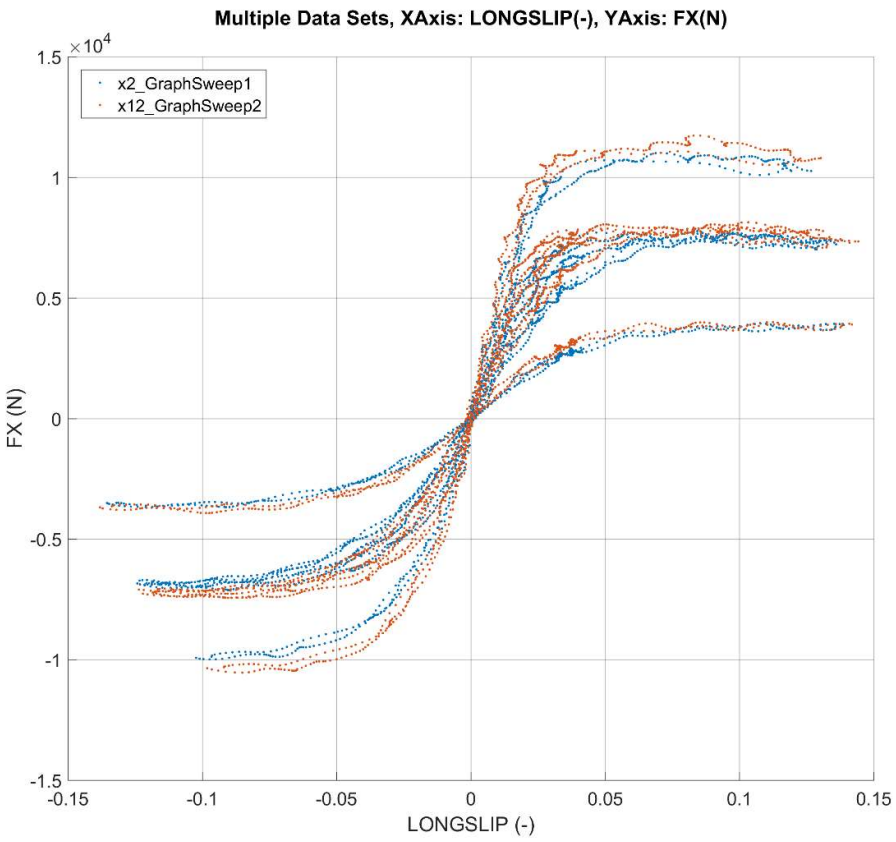

Figure 4.2.12-A. Comparison of Graph Sweeps 1 and 2 for the GS2MF'BrkDrv' test procedure.

Figure 4.2.12-A shows that the longitudinal performance of the tyre itself has changed slightly during the testing. With Graph Sweep 1 generating marginally less grip than Graph Sweep 2. Also during Graph Sweep 2 the slip stiffness of the tyre is slightly higher compared to Graph Sweep 1. The difference between the two is slight, however to determine the cause of this difference both the temperature and tyre wear were investigated. Figure 4.2.12-B shows a temperature comparison between the middle (third of five) sweep from Graph Sweep 1 and 2.

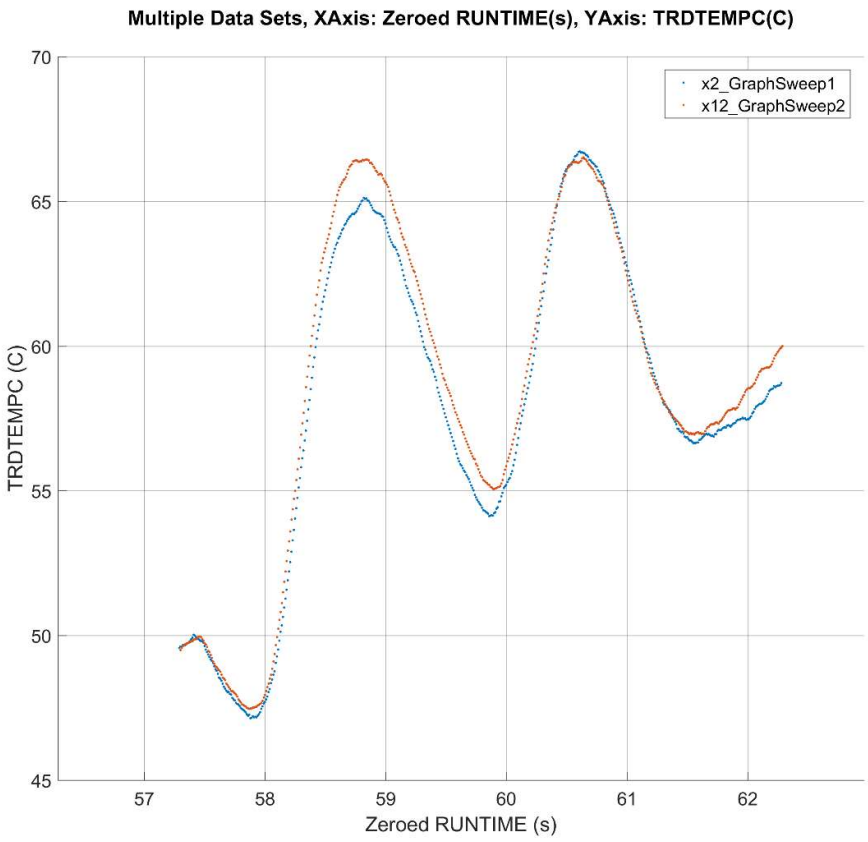

Figure 4.2.12-B. Temperature profile of the middle of the five sweeps that make up Graph Sweeps 1 and 2.

Figure 4.2.12-B shows that the temperature of the tyre during Graph Sweep 1 and 2 are very similar, with a maximum of 1.5°C difference between them. This rules out any thermal variation being the cause of the slight differences in the tyre performance. Figure 4.2.12-C is a similar plot of the same sweeps, this time showing the distance between the test surface and the wheel centre which is indicative of the tyre wear.

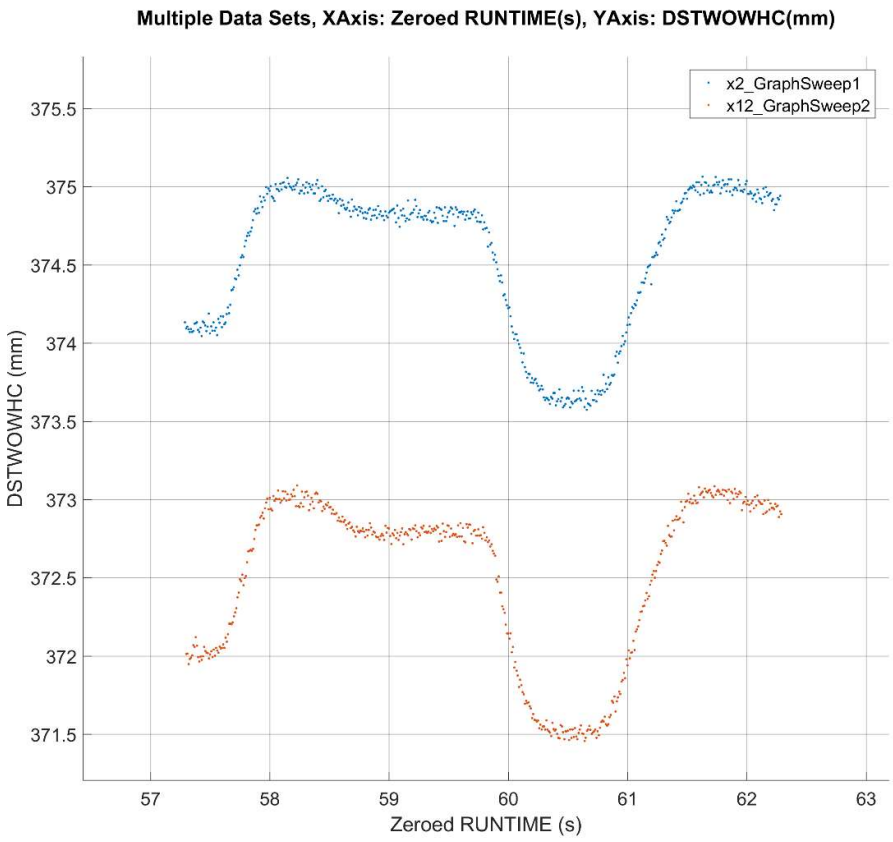

Figure 4.2.12-C. Distance ground to wheel centre of the middle of the five sweeps that make up Graph Sweeps 1 and 2.

Figure 4.2.12-C shows that the tyre has worn by around 2mm (difference between the two datasets on the Y Axis) during the test procedure, which explains the small differences in the tyre's performance between Graph Sweeps 1 and 2 presented in Figure 4.2.12-A. The original tread depth of these tyres is 5.6mm, with 1.6mm being the minimum required for the tyre to be road legal under UK law, hence the tyre has 4mm (5.6 – 1.6 = 4mm) of avaliable tread. At the end of this test procedure the tyre has only used 2mm of the avaliable 4mm of tread, meaning it was only 50% worn. This is well within the operating limits of the tyre. Therefore, any difference seen in the tyre's performance as a result of this wear is within the variation one would encounter when using the tyre on a road car and therefore within the usual operating range of the vehicle. For this reason it is acceptable for data of the small amount of variability to be included in the MF-Tyre 6.1 tyre model paramterisation process.

4.3 'GS2MF StaticLong'

The 'GS2MF StaticLong' test procedure is designed to gather longitudinal stiffness data that can be processed and used in conjunction with longitudinal slip data to determine the tyre's

longitudinal relaxation length. The test procedure is far simpler than the 'GS2MF FreeRolling' and 'GS2MF BrkDrv' tests. It features just one static longitudinal test that involves rolling the tyre forward at the test load with zero slip angle and camber angle, before bringing the tyre to a halt. While the tyre is locked in position, unable to rotate, the flat-trac's belt is slowly moved longitudinally. This effectively drags the tyre across the road surface for around 0.1m, although it is actually the road that moves rather than the tyre. As the road surface moves, the tyre's contact patch initially remains adhered to the surface whilst the sidewall deforms. During this period, longitudinal force builds up until the tyre loses traction and begins to slide across the surface, at this point the test ends. After this, the tyre is rolled forward again, allowing the deformation in the tyre's sidewall to relax before another test is commenced. In order to capture the load sensitivity, this same test is then repeated at six different vertical loads ranging from 0.4 to 1.4 times the tyre's nominal load. The six loads are then repeated at three inflation pressures to measure the pressure sensitivity. Ideally testing will be conducted at higher loads (up to around 2.0 times the nominal load to align with the 'FreeRolling' test) but at both SoVaMotion and Calspan, this causes the test surface to tear, invalidating the test. Instead the MF-Tyre 6.1 model which will be fitted to the data will be used to extrapolate to these higher loads. This will result in a slight reduction in accuracy in this region but such issues are common when constrained by the limitations of even the best available test equipment.

During each test, the tyre's longitudinal force as well as the distance travelled by the road way are measured. This data is not used directly in the MF-Tyre 6.1 model parametrisation, instead the data is first post-processed before it is used. The longitudinal force versus displacement is plotted and the tyre's longitudinal stiffness can be determined via a simple linear fit. This means that a single value is extracted from each test rather than the entire data set being used directly. A possible problem with this is that any small error in the testing or post processing can cause a significant change to the measured longitudinal stiffness which then causes a change to the predicted longitudinal relaxation length. To avoid this, each test is repeated four times during the test procedure and the longitudinal stiffness results are averaged. This means the procedure contains a total of 72 tests, made up of six loads at three inflation pressures (to measure the load and pressure sensitivity) and then all repeated four times (to average out potential errors). These tests are carried out on a static tyre which means there is minimal friction induced heat and therefore the tyre temperature remains constant throughout. For this reason, there is no need to allow time between each test for the tyre to cool, therefore the 72 tests can be conducted very quickly, in this case taking just 840s (14mins). The averaged results from these tests are shown in Figure 4.3-A.

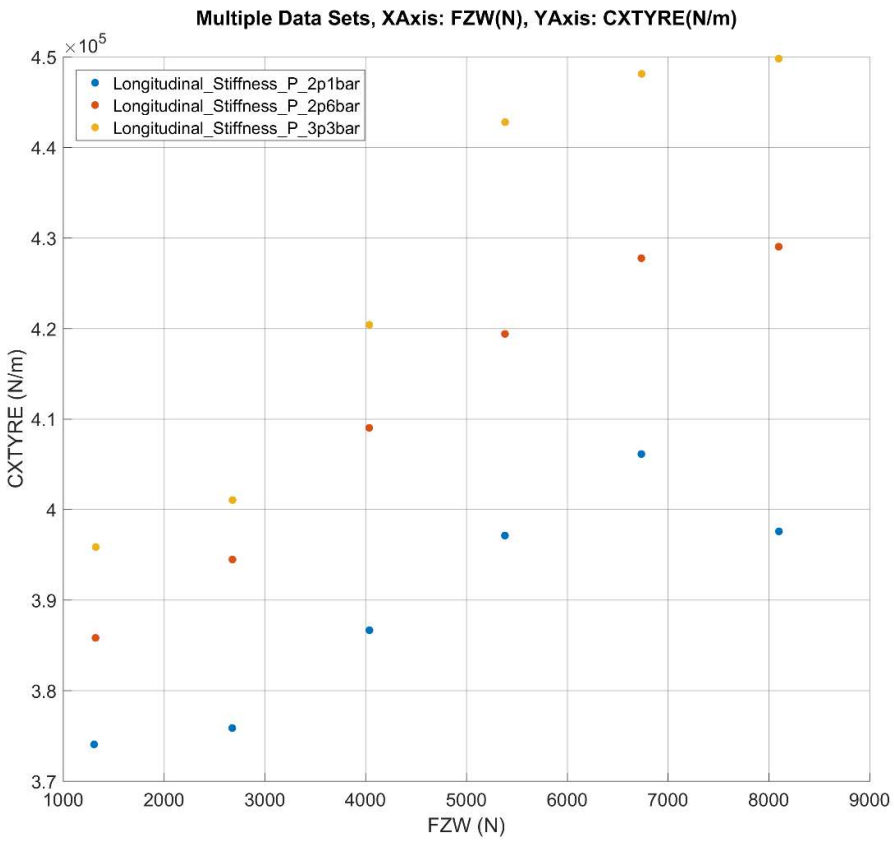

Figure 4.3-A. The averaged results of the longitudinal stiffness testing, where the longitudinal stiffness sensitivity to vertical load and inflation pressure can be observed.

Figure 4.3-A shows the averaged results from the static longitudinal stiffness testing. The results show that as expected the longitudinal stiffness increases with inflation pressure. Also shown is that the longitudinal stiffness increases with load, up until a point, after which it decreases with load when the tyre becomes overloaded. The point at which the tyre becomes overloaded is dependent on the inflation pressure. This is captured at the lower inflation pressure; however, at the middle and higher pressure, the overloading point seems to occur at loads above the tested range. Unfortunately testing into this load range is not possible given the limitations of the available test apparatus. This test limitation means that the resulting tyre model may not capture the reduction in longitudinal stiffness that occurs at higher loads, instead the modelled stiffness will continue to increase with load. As a result, this will adversely affect the accuracy of the modelled longitudinal relaxation length while running at these conditions. While not ideal, this will only have a minor effect on the overall tyre model. This is because the issue will only cause a reduction in accuracy, rather than a complete failure and it will only effect one tyre attribute, that being the longitudinal relaxation length. Furthermore, it will only occur at very specific load cases of running at high load while at high inflation pressure. Therefore, the overall effect

on the resulting tyre model will be minimal. This issue will occur in both GS2MF and the Square Matrix test procedure; however, both procedures could easily be modified with additional load cases added if the test apparatus were to be improved.

Once the average longitudinal stiffness results are obtained, they are used in the MF-Tyre 6.1 tyre model fitting process to calculate the longitudinal relaxation length. This is defined as the ratio of slip stiffness to longitudinal stiffness, where slip stiffness can be obtained using the steady state MF-Tyre 6.1 tyre model fitted using the 'GS2MF BrkDrv' data. Details of the longitudinal stiffness post processing can be found in Section 3.12.2 Longitudinal Relaxation Lengths, while details of the MF-Tyre 6.1 fitting process which uses this data can be found throughout Chapter 5.0 on GS2MF Fitting.

4.4 GS2MF versus Square Matrix Data Comparison

An attempt was made to directly compare the data generated using the GS2MF test procedure with data generated via Square Matrix testing. However, the GS2MF test procedure was not designed such that any sweep would necessarily match up with corresponding sweeps from the Square Matrix procedure. So, while in some cases a direct comparison was possible a more practical method is to build MF-Tyre 6.1 tyre models from the two data sets and compare the resulting models. Details of this can be found in Section 5.3 on GS2MF versus Square Matrix Model Comparison.

4.4.1 GS2MF versus Square Matrix, 'FreeRolling' Comparison

Directly comparing sweeps from the Square Matrix test to the 'GS2MF FreeRolling' test procedure is unfortunately not possible due to both the vertical loads and the slip angle rates being different throughout (shown in Figure 4.4.1-B). Instead, both data sets are used to parameterise MF-Tyre 6.1 tyre models and these models are then compared; this comparison can be found in section 5.3.1 'FreeRolling' Model Comparison.

The Square Matrix free rolling testing is split into two sections, HAS (High Angle Slip) and LAT (Lateral). The reason for the two tests is to avoid the compromise that exists due to the slip angle rate. This is where a 'high rate' allows testing to high slip angles with minimal wear but induces large amounts of on-centre mechanical hysteresis. Meanwhile, a 'low rate' overcomes the mechanical hysteresis problems but causes the tyre to overheat as it spends long periods of time at high slip angles. The two parts of the Square Matrix free rolling procedure are intended to address this compromise. Where the HAS procedure sweeps to +/-27° of slip angle at a rate of 12°/s, while the LAT procedure sweep to +/-15° of slip angle at a rate of 4°/s. A comparison between otherwise identical Square Matrix HAS and LAT test can be found in Figure 4.4.1-A.

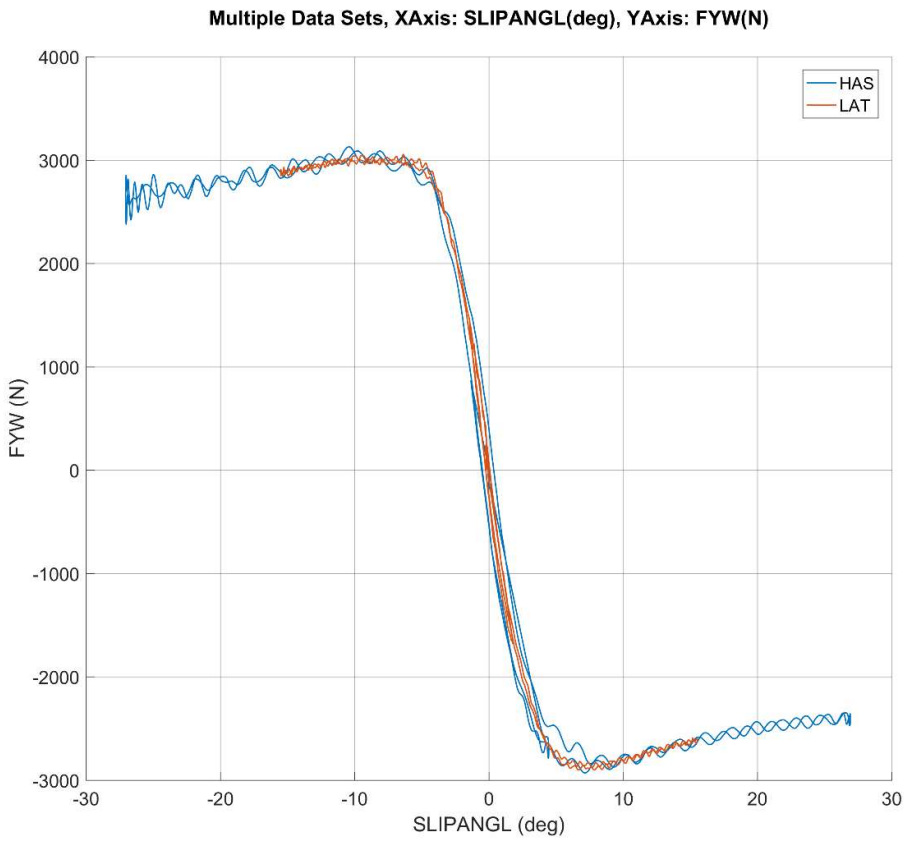

Figure 4.4.1-A. Lateral force versus slip angle for two otherwise identical HAS and LAT sweeps.

Figure 4.4.1-A shows the difference between the Square Matrix HAS and LAT tests. The intention of these different tests is that the LAT test can be used to parametrise the on-centre part of the MF-Tyre 6.1 tyre model, while the HAS test can be used to parameterise the high slip regions. This approach can work; however, it is also very inefficient as it requires both tests to be run, which doubles the required rig time. In GS2MF the variable rate sweep is used to overcome the slip rate compromise and it achieves this in such a way that only one sweep is required to gather both on-centre and high slip angle data, negating the need for two separate free rolling test procedures and hence increasing the test efficiency. The variable rate sweep is detailed in Section 3.6 on Variable Rate Sweep. However, this does mean that no Square Matrix and GS2MF sweeps are conducted at the same slip angle rates, making a direct comparison impossible.

Another factor that rules out a direct comparison between the Square Matrix and GS2MF data is that ‘GS2MF FreeRolling’ uses asymmetric loading (this is to better replicate a vehicles lateral

weight shift while cornering) that is not present in the Square Matrix testing. This means there are no similarly loaded sweeps that can be directly compared. This is shown in Figure 4.4.1-B.

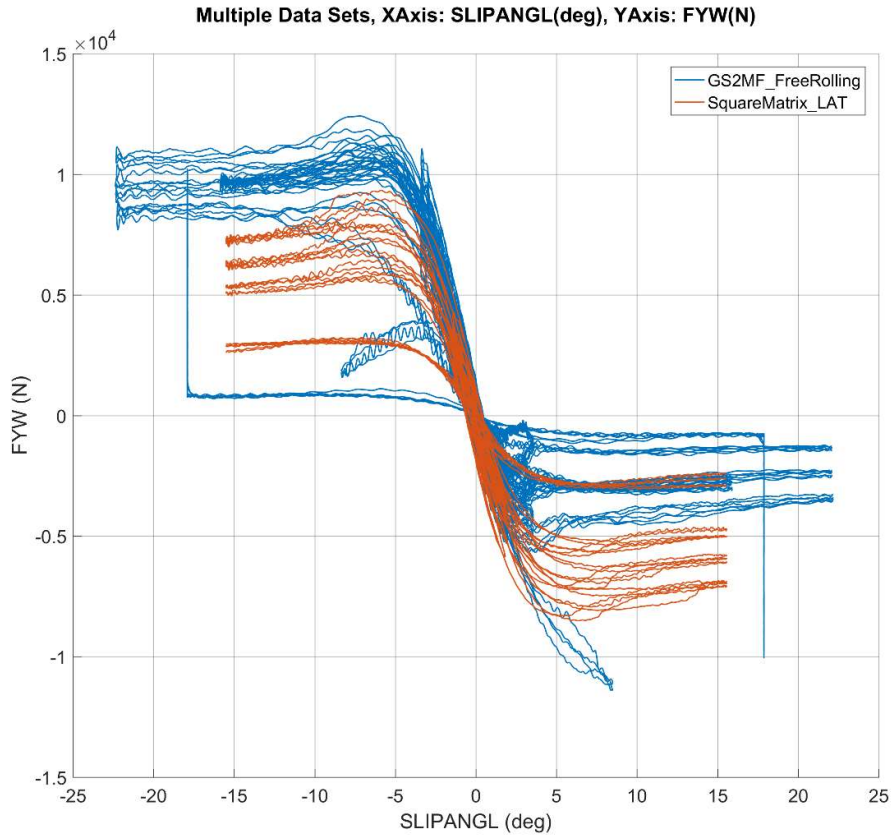

Figure 4.4.1-B. Comparison of lateral force versus slip angle for the force and moment section of 'GS2MF FreeRolling' and the Square Matrix LAT test.

Figure 4.4.1-B shows the difference between the 'GS2MF FreeRolling' and Square Matrix LAT test data. During the Square Matrix testing, the tyre generated similar lateral grip when steering to the left or the right, this is due to the left and right testing being conducted at the same vertical load. Conversely during the 'GS2MF FreeRolling' testing, the tyre generated more grip at negative slip angles (steering left), compared to positive slip angles (steering right). This is due to the asymmetric loading employed in GS2MF; where negative slip angle testing was conducted at vertical loads that were higher than those used in the Square Matrix testing, while positive slip angle testing was conducted at loads that were lower than the Square Matrix testing. This loading system makes GS2MF more accurate as it closer replicates the loading conditions of a real car; it also makes GS2MF more efficient is it avoids testing the tyre at load cases that are unachievable on a vehicle. However, it means that there are no sweeps that are comparable between the GS2MF and Square Matrix test procedures. The asymmetric loading system is described in Section 3.7 on Asymmetric Loading.

For these two reasons (different slip angle rates and different vertical loads) a comparison between the Square Matrix and 'GS2MF FreeRolling' data sets was not carried out. Instead MF-Tyre 6.1 tyre models were fitted to each data set. These tyre models could then both be solved at the same load cases and a meaningful comparison could be made between them. Furthermore, the ultimate objective of the two test procedures is to facilitate the parametrisation of representative MF-tyre 6.1 tyre models. Therefore, a comparison of the data would only be a mid-step towards the final delivery and comparison of the resulting tyre models. This tyre model comparison can be found in Section 5.3 on GS2MF versus Square Matrix Model Comparison.

4.4.2 GS2MF versus Square Matrix, 'BrkDrv' Comparison

When attempting to compare the data from 'GS2MF FreeRolling' with the equivalent Square Matrix tests, it was concluded that the load cases were too different and that no direct comparison was possible. This was due to the use of the variable rate sweep and asymmetric loading within GS2MF. The variable rate sweep is also used in 'GS2MF BrkDrv' but it has less of an effect on the resulting data compared to free rolling; furthermore, asymmetric loading is not used at all in GS2MF BrkDrv. Therefore, a comparison can be made by selecting two sweeps from the two test procedures that purely by chance, happen to have been conducted under similar load conditions. During these two sweeps the tyre is tested at the same 6,750N of vertical load, zero slip angle and zero camber. The only difference is in the slip ratios, where the Square Matrix test sweeps at 25%/s to peaks of +/-35%, while the GS2MF test sweeps at a variable rate to peaks of +/-25%. A comparison between these two sweeps is shown in Figure 4.4.2-A.

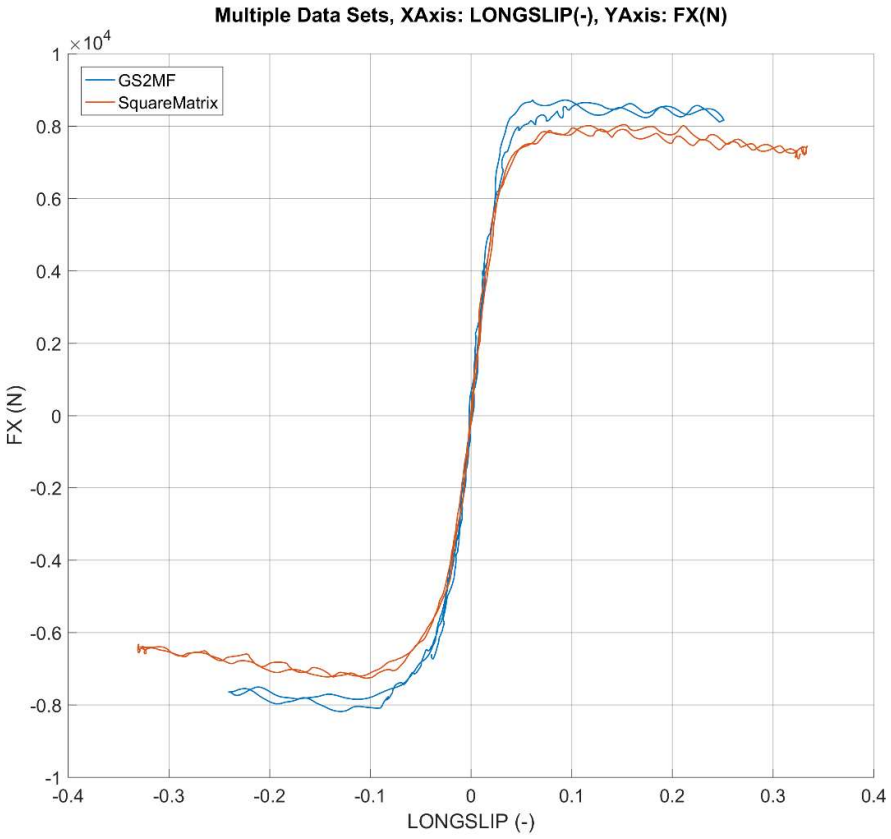

Figure 4.4.2-A. Comparison of a pure longitudinal sweep from 'GS2MF BrkDrv' with a similar sweep from the Square Matrix test procedure.

Figure 4.4.2-A shows that there is a surprisingly large difference of up to 13% (peak negative slip ratios of -7,000 and -8,000N) between the longitudinal force generated by the two similar sweeps from the 'GS2MF BrkDrv' and Square Matrix test procedures. Further analysis revealed that the tyre was running at very different temperatures during these two sweeps. During the GS2MF test sweep, the tyre surface temperature range was from 46 to 84°C, while during the Square Matrix test the tyre temperature range was 73 to 112°C, which accounts for the difference in tyre performance. The cause for this was traced back to the tyre reaching such high peak temperatures during the preceding Square Matrix sweep that the thermal pause system timed-out after 120s. This time-out feature is included in the thermal logic system to prevent a never-ending test, where the system waits for the tyre to return to a condition that is unobtainable, more details of this can be found in section 3.5 on Thermal Logic. As result of the time-out, heat continued to build up within the tyre while the Square Matrix procedure was run. This caused the tyre to overheat and thus generate less grip. Meanwhile the tyre used in GS2MF did not overheat and therefore generated more grip. This explains the difference in tyre performance shown in Figure 4.4.2-A.

The Square Matrix test could have been repeated with the time-out feature disabled; however, this would have been very costly to run due to the extensive rig time required while waiting for the tyre to cool down. Furthermore, this reveals an intrinsic problem with the Square Matrix test design, where the nature of the testing causes the tyre to generate a substantial amount of heat. This means that the temperature variation during each sweep induces significant variation in the resulting data. Since the MF-Tyre 6.1 tyre model does not include a thermal model with which to capture this temperature variation, it instead an uncontrolled variable which manifests as an inaccuracy between the model and the data. This worsens the accuracy of the resulting tyre model. Furthermore, due to the increased heat in the tyre a great deal of rig time is required to allow the tyre to cool to a steady baseline temperature between each sweep. This significantly increases the cost of the testing and reduces efficiency. GS2MF overcomes these problems by using the variable rate sweep to keep tyre temperatures much lower during each sweep. This reduces the variability of the tyre's performance during the test, which increases the accuracy of the resulting tyre model. Furthermore, the lower temperatures reduce the required cool down times after each sweep, leading to a further reduction in overall rig time and testing costs.

4.4.3 GS2MF versus Square Matrix, Rolling Radius Comparison

The GS2MF and Square Matrix Rolling Radius procedures are very similar; although in Square Matrix this forms a specific test, whilst in GS2MF the Rolling Radius testing is incorporated into 'GS2MF FreeRolling'. Both tests roll the tyre at zero slip angle and zero camber angle while changing the vertical load and forward velocity. In GS2MF, six vertical loads are used and three forward velocities, while in the Square Matrix test, five vertical loads are used and five forward velocities. It appears the five forward velocities are included in the Square Matrix test to better capture the tyre's centrifugal expansion as velocity increases. With data collected at five forward velocities a vertical stiffness model can be obtained which better replicated the vertical stiffness sensitivity to forward velocity. This is important for certain racing application; where an accurate model of the tyre's vertical stiffness is needed to better predict the cars ride height which can have a significant effect on the air flow under the car and hence its aerodynamic performance. However, road cars are typically far less sensitive to small changes is ride height, hence in GS2MF two of the five forward velocities were removed to reduce the overall test duration. This resulted in a 40% reduction in testing costs with no discernible effect on accuracy as the resulting data is virtually identical, shown in section 5.2.8 on Loaded Radius. If GS2MF were to be adapted for testing race car tyres, then these additional tests at higher velocities could easily be added. However, GS2MF is currently intended for testing road car tyres where these additional tests are not required, whereas the 40% reduction in Rolling Radius test duration is more desirable.

4.5 GS2MF versus Square Matrix Test Duration Comparison

A comparison between the test durations of the full GS2MF suite of tests compared to the Square Matrix testing reveals some significant differences between the two approaches. GS2MF in its entirety consists of three test procedures: 'GS2MF FreeRolling' which in this case took 4,080s to run, 'GS2MF BrkDrv' which took 2,875s and 'GS2MF StaticLong' which took 877s, totalling 7,832s of runtime. Each of these test procedures include testing at three inflation pressures so no repeated testing is required to capture pressure sensitivity. The 'GS2MF StaticLong' test causes very minimal tyre wear and hence the same tyre specimen can be used during the 'GS2MF FreeRolling' test; with a new tyre being needed for 'GS2MF BrkDrv'. This means that a total of two specimens are required. Mounting a new test tyre to the Calspan rig takes around 900s (15mins), meaning GS2MF requires a total of 1800s (2 × 900 = 1800s or 30min) of tyre change time. These test durations are detailed in Table 4.5-A.

GS2MF Test Procedure	**Description**	**Duration, s**
'GS2MF FreeRolling'	Free rolling component of GS2MF	4,080
'GS2MF BrkDrv'	Braking and driving component of GS2MF	2,875
'GS2MF StaticLong'	Static longitudinal components of GS2MF	877
	GS2MF Total Running Duration	*7,832*
Necessary tyre changes. (each takes 900s or 15mins)	'GS2MF StaticLong' and 'GS2MF FreeRolling' can be conducted on the same tyre, with 'GS2MF BrkDrv' needing a new tyre. Meaning two tyres in total.	1,800 (2 × 900 = 1,800)
Grand Total Test Duration	*GS2MF Grand Total Duration (including tyre changes and testing at three inflation pressures.*	*9,632*

Table 4.5-A. GS2MF test durations (including testing at three inflation pressures).

Table 4.5-A reveals that a full suite of GS2MF tests including tyre changes takes a total of 9632s, or two hours and 40 minutes of rig time to run and requires two tyre specimens. The test duration can change when testing different tyres as the thermal logic system will adjust the test duration based on however long is required for the test tyre to cool. A high-performance tyre will likely generate more grip and hence more friction and therefore more friction induced heat compared to lower performance tyre, this additional heat will take longer to cool which adds to the test duration. Furthermore, 900s is known to be the average time required to change a tyre when using the Calspan test rig.

The Square Matrix test procedure consists of five separate tests, these are: HAS which took 1,600s to run, LAT which took 1,523s, pure longitudinal testing at zero slip angle integrated with combined testing at -5° of slip angles took 2,504s, combined testing at slip angles of 2 and -2° took 2,524s and finally the Rolling Radius test took 799s. This comes to a total running duration of 8,950s. However, unlike GS2MF, the Square Matrix procedure only includes testing at one inflation pressure, which means all the tests need to be repeated three times, (once at each of the three required pressures) bringing the total running duration to 26,850s ($3 \times 8{,}950 = 26{,}850$s). This is essential to populate the pressure sensitivity capability in the MF-Tyre 6.1 tyre model that is to be parameterised from the test data. However, doing so not only triples the total running duration but also requires multiple additional tyre changes. All the Square Matrix Rolling Radius tests can be conducted on the same tyre specimen; as the tyre is running at zero slip through this test so there is minimal wear (one tyre for rolling radius). One HAS and one LAT test can be run on the same tyre specimen; these need to be repeated three times for the three inflation pressures. So far requiring four tyres in total, one for Rolling Radius and three for all HAS and LAT tests. Finally, six further tyres are required for the two longitudinal and combined tests each needing new tyres and these also need to be run three times, requiring six tyres. The means that the Square Matrix test requires a total of 10 tyre specimens, one for rolling radius, three for HAS and LAT and six for combined, totalling 10 tyres. These 10 tyre changes, each taking 900s (15mins) comes to 9,000s (two hours and 30 mins) in total. All the Square Matrix test durations are detailed in Table 4.5-B.

Square Matrix Test Procedure	**Description (All include only one inflation pressure)**	**Duration, s**
Square Matrix HAS	Square Matrix free rolling to high slip angles	1,600
Square Matrix LAT	Square Matrix free rolling to low slip angles	1,523
Square Matrix Combined, SA = 0 and -5°	Square Matrix combined longitudinal testing at slip angles of 0 and -5°	2,504
Square Matrix Combined, SA = 2 and -2°	Square Matrix combined longitudinal testing at slip angles of 2 and -2°	2,524
Rolling Radius	Rolling Radius and vertical stiffness testing	799
	Square Matrix Total Running Duration (For one inflation pressure only)	*8,950*
Three Inflation Pressures	Each test needs to be run three times to gather the inflation pressure sensitivity.	26,850 (3 × 8,950 = 26,850)
Necessary tyre changes. (each takes 900s or 15mins)	A total of 10 tyre changes are required.	9,000 (10 * 900 = 9,000)
Grand Total Test Duration	*Square Matrix Grand Total Duration (including tyre changes and testing at three inflation pressures.*	35,850

Table 4.5-B. Square Matrix test durations.

Table 4.5-A shows that a complete set of Square Matrix testing, including tyre changes, requires a total of 35,850s to run, or nine hours and 58 minutes and requires 10 tyre specimens. By contrast GS2MF required just 9,632s, or two hours and 40 minutes and only two tyre specimens. This means that GS2MF requires 73% less rig time than the Square Matrix test procedure. This is a very significant rig time saving and with most test rigs charging by the hour, this equates to a highly significant cost save and test efficiency gain.

4.6 Full GS2MF Procedure Conclusions

Overall, the comparison between the complete GS2MF and Square Matrix test procedures revealed some significant differences between the two. GS2MF proved to effectively regulate the tyre temperature, whereas the Square Matrix test regularly caused the tyre to overheat. This improvement in GS2MF was mainly achieved in two ways. Firstly, by using the variable rate sweep, which reduced the overall amount of sliding energy during each sweep thus reducing temperature build up. Secondly, with asymmetric loading which reduced the overall amount to testing to only load cases that were obtainable in a physical car. Together these reduce the

overall rig time and hence the testing costs. Both procedures used the thermal logic system to pause the test long enough for the tyre to return to a steady baseline temperature. Although this only proved effective in GS2MF as during Square Matrix testing the tyre reached such high temperatures that the thermal logic system timed-out. This improved temperature regulation of GS2MF leads to a more consistent tyre temperature during each sweep and hence less temperature induced variation in tyre performance. This temperature variation cannot be captured in the MF-Tyre 6.1 tyre model, therefore removing it is effectively eliminating unwanted noise and improving the models' ability to accurately represent the data.

A direct comparison between the GS2MF and Square Matrix data sets may have been interesting, unfortunately this was not possible in most cases due to the inherent differences in the test procedures. However, the ultimate purpose of both test procedure it to facilitate the parameterisation of MF-Tyre 6.1 tyre models. Therefore, a comparison of the resulting models is more relevant. This can be found in Section 5.3 GS2MF versus Square Matrix Model Comparison.

In general, GS2MF is shown to generate data with less thermal and mechanical hysteresis compared to Square Matrix testing, while also significantly reducing rig time. The grand total test duration of the Square Matrix procedure was almost 10 hours. This was reduced by 73% to just two hours and 40 minutes using GS2MF. With most test rigs charging by the hour, this equates to a very substantial cost saving and efficiency gain. Finally, GS2MF could gather all the required data for MF-Tyre 6.1 model parameterisation using just two tyre specimens, whereas the Square Matrix test required 10. This reduces the cost of both purchasing and shipping the test tyres to the test facility. Furthermore, in the automotive sector, most of this type of testing in conducted using prototype tyres, which are only manufactured in small batches. In such a situation, 10 tyre specimens were often not available meaning a Square Matrix test procedure could not be run at all. This problem is eased substantially with GS2MF where only two tyre specimens are required.

5.0 GS2MF Fitting

In this section, the MF-Tyre 6.1 fitting process is discussed. This includes details of the required pre-processing, data dissecting and checking the data itself, as well as using the data to determine some basic values required for the fitting process. After this, a complete and detailed example of fitting an MF-tyre 6.1 tyre model to GS2MF data is shown through every stage of the process. Finally, the resulting GS2MF derived tyre model is compared to an equivalent model of the same tyre parameterised using Square Matrix test data.

The scope of the project is to develop the GS2MF test procedure for use in MF-Tyre 6.1 model parameterisation; therefore, the scope of the project is constrained to the test procedure development and the model parameterisation is generally beyond this scope. However, the GS2MF test procedure is only valid if it can be used to parameterise an MF-Tyre 6.1 tyre model. For this reason, the following section is included to attest to the fact that GS2MF can indeed be used for this purpose. Furthermore, this section goes on to demonstrate how using GS2MF led to improvements in the resulting tyre model, compared to a similar model built from Square Matrix derived test data.

5.1 Data Pre-Processing

Data delivered straight from the test rig must be pre-processed before it can be used in model parameterisation. The data is delivered in TYDEX format with all channels and units named according to the TYDEX convention (van Oosten, Unrau, Riedel and Bakker, 1999). Once delivered, the data from the long test session is dissected into the different segments required at each stage of the fitting process. These segments are not necessarily the same as the technology components detailed throughout Section 4.0 on GS2MF Full Procedure; that section details how GS2MF is built up from various component technologies and assembled into a full test procedure. Instead these segments detail how after running GS2MF the resulting large dataset is dissected and used for various stages of the MF-Tyre 6.1 tyre model fitting process. After dissecting the data, it is checked to ensure that the tyre has not been excessively worn or overheated through the testing, which will cause its performance to change. If this occurs, the testing must be repeated using new tyre specimens. Once the data check is complete, the range of load cases the tyre model will be valid within is determined from the test data. Finally, the data is used to perform some basic calculations of nominal values required in the fitting process. All these stages are detailed in the forthcoming chapters.

5.1.1 Segment the Data

The ‘GS2MF FreeRolling’ and ‘GS2MF BrkDrv’ test procedures each take around one hour to run, depending on the variable length of the thermal pauses. Once the testing is complete and

the data is obtained, it needs to be cutup into the different segments. These separate segments of data are then used independently during the various stages of the model parameterisation process. Details of how the 'GS2MF FreeRolling' data is segmented are shown in Figure 5.1.1-A.

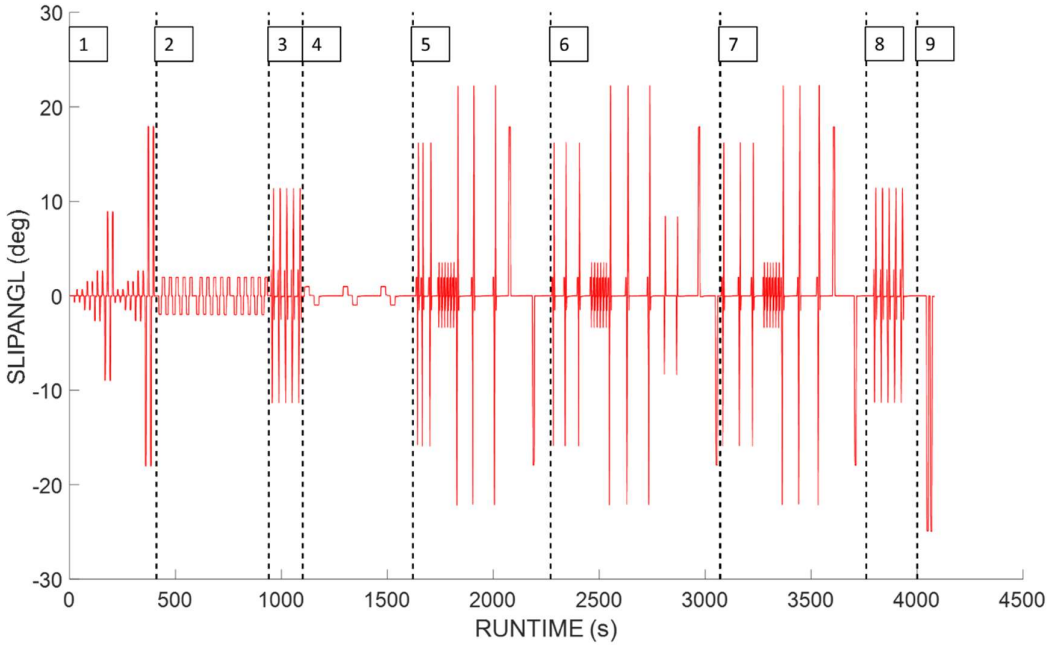

Figure 5.1.1-A. 'GS2MF FreeRolling' test procedure dissected into segments.

The different 'GS2MF FreeRolling' segments (as numbered in Figure 5.1.1-A) are summarised below. More details of the component technologies within these segments can be found in Section 3.0 on Technology Components.

1. Warmup. The warmup heats the tyre closer to its operating temperature and 'breaks in' the tyre to ensure consistent performance. This reduces the impact of temperature as a cause for error in the resulting tyre models. The data from this segment is not used in the MF-Tyre 6.1 fitting procedure.
2. Step-steer. Step-steer tests are performed to gather data pertaining to the tyre's lateral relaxation length under various load cases. This data is used in conjunction with the static longitudinal data to fit the transient components of the tyre model.
3. Graph Sweep 1. Graph Sweep 1 is conducted to establish the tyre's benchmark performance under optimal conditions (warm but only lightly worn). The tyre's performance during Graph Sweep 1 is compared with Graph Sweep 2 to check the quality of the data prior to fitting the tyre model (See Section 5.1.2 on Data Check). If the comparison of these Graph Sweeps is poor then the test needs to be repeated using new tyre specimens.

4. Cornering Stiffness and Vertical Stiffness. Cornering stiffness and vertical stiffness testing is conducted at three inflation pressures. The cornering stiffness data is used in conjunction with the force and moment data as part of the FY Pure and MZ Pure fits (See Section 5.2.1 on FY Pure and section 5.2.2 on MZ Pure). The vertical stiffness data is used twice; first to determine the tyre's Unloaded Radius prior to fitting the tyre model (See Section 5.1.4 on Base Calculations) and secondly in the Loaded Radius fitting (See Section 5.2.8 on Loaded Radius).
5. Force and Moment, Inflation Pressure 1. General force and moment testing is conducted at the lowest inflation pressure.
6. Force and Moment, Inflation Pressure 2. General force and moment testing is conducted at the middle inflation pressure with a few additional sweeps.
7. Force and Moment, Inflation Pressure 3. General force and moment testing is conducted at the highest inflation pressure; this is identical to the force and moment testing at the lowest pressure. Data from all three force and moment segments is used in the FY Pure and MZ Pure stages of the tyre model fitting, (See Section 5.2.1 on FY Pure and section 5.2.2 MZ Pure).
8. Graph Sweep 2. Graph Sweep 2 is a repeat of Graph Sweep 1; this allows data from these two sweeps to be compared and any change in tyre performance through the testing to be observed and the testing repeated if necessary (See Section 5.1.2 on Data Check).
9. Severe. Severe testing under high slip angles and cambers is conducted at the end so that the additional wear caused by these sweeps does not affect any other results. This data is also used to fit FY Pure and MZ Pure, (See Section 5.2.1 on FY Pure and section 5.2.2 on MZ Pure).

The 'GS2MF BrkDrv' data is handled slightly differently. It can be delivered from the test rig either as one full test procedure, including the warmup and thermal pauses. Alternatively, the warmup can be removed and the data cut into individual sweeps in order to post process the slip ratio channel, (See the Nomenclature on Calculated Channels). Figure 5.1.1-B shows an example of the latter and how the various segments are grouped in a similar way to the 'GS2MF FreeRolling' data.

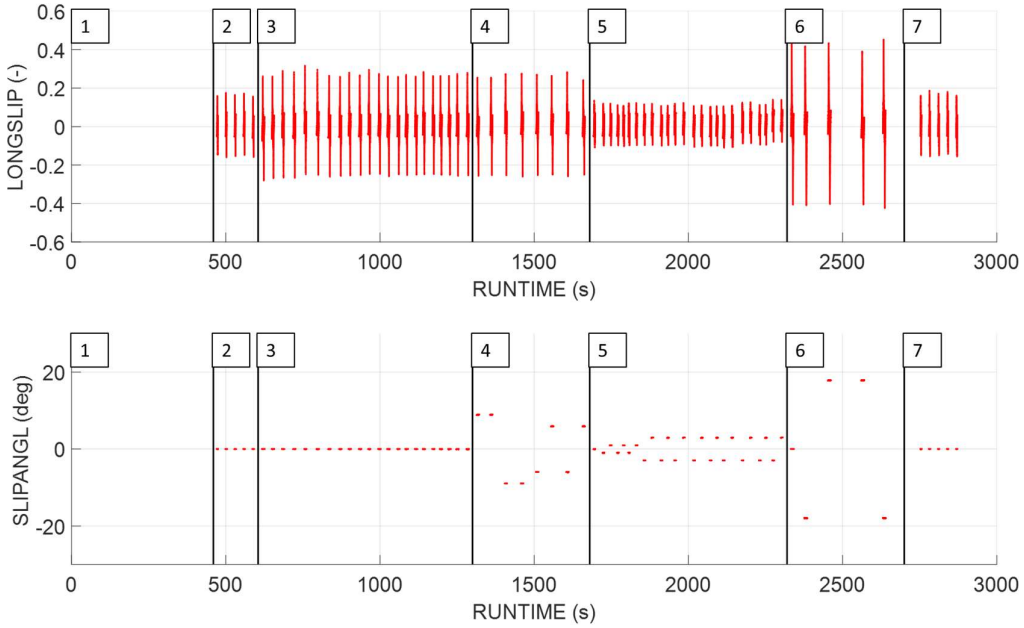

Figure 5.1.1-B. 'GS2MF BrkDrv' test procedure dissected into separate segments.

The different 'GS2MF BrkDrv' segments as numbered in Figure 5.1.1-B are summarised below:

1. Warmup (Not Shown). The warmup segment in the 'GS2MF BrkDrv' data is not shown, as it is removed as part of the test facilities data processing procedure; though it can be included if needed. However, the 'BrkDrv' warmup is identical to that used in 'FreeRolling' and serves the same purpose, that being to heat the tyre to its operating temperature and 'bed in' the tyre to ensure consistent performance. The warmup data is not used in any part of the MF-Tyre 6.1 fitting procedure.
2. Graph Sweep 1. As with the 'FreeRolling' data Graph Sweep 1 and 2 are compared to observe if the tyre performance has changed throughout the testing, (See Section 5.1.2 on Data Check).
3. Pure Longitudinal. In the MF-Tyre 6.1 fitting procedure, FXPure and Combined are both fitted together at the same time. Therefore, this pure longitudinal data is used in conjunction with the combined data. (See Section 5.2.3 on FX Pure and Combined).
4. Combined Medium Slip. The combined medium segment, tests the tyre in combined load cases where slip ratio is swept, while the tyre is held at a constant slip angle. Hence both combined longitudinal and lateral forces and moments are generated simultaneously. In this case the tyre is swept to a medium peak slip ratio of +/-0.25 while held at a medium slip angle of +/-9°. This is designed to represent a road vehicle during high slip vehicle dynamics manoeuvres and is used in all combined sections of the MF-Tyre fitting process, (See Section 5.2.3 on FX Pure and Combined).

5. Combined Low Slip. The second combined sweeps are carried out at lower slip ratios and slip angles to minimise wear on the tyre; in this segment, the tyre is swept to peak slip ratios of +/-0.1 while held at a medium slip angle of +/-3°. This data represents a vehicle close to every day driving conditions and is used in all combined sections of the MF-Tyre fitting process, (See Section 5.2.3 on FX Pure and Combined).
6. Combined High Slip. The third segment of combined sweeps, test the tyre to combined higher slip angles and slip ratios; these test the tyre under extreme handling conditions that are representative of a vehicle during a high slip manoeuvre. This segment causes the most wear to occur on the tyre hence it is placed at the end of the test procedure. Here the tyre is swept to peak slip ratio of +/-0.4 while held at a medium slip angle of +/-18°. This data is used in all combined sections of the MF-Tyre fitting process, (See Section 5.2.3 on FX Pure and Combined).
7. Graph Sweep 2. The data from Graph Sweep 2 is compared to Graph Sweep 1 to determine if the tyre has been excessively worn through the testing.

Once all the data is dissected appropriately it can be processed and analysed more easily. It also allows different segments of data to be used in different stages of the MF-Tyre 6.1 fitting process.

5.1.2 Data Check

Before any tyre model building is carried out, the GS2MF data is checked to ensure the tyre itself has not significantly changed as a result of the testing, this is done using the Graph Sweeps. These are the same series of five sweeps repeated at the start and end of the test procedure allowing any changes in the tyre's performance to be observed. If the Graph Sweep comparison reveals a significant change to the tyre's performance, then the test must be repeated using new tyre specimens. MF-Tyre 6.1 does not include a wear model or any capability of modelling that a tyre's performance can change throughout its life. Therefore, it is important to ensure that the tyre's performance remains as consistent as possible throughout the testing. This data check process is detailed in the forthcoming sections.

'FreeRolling' Data Check

Figure 5.1.2-A shows that in this case the lateral force performance of the tyre is very similar at the start (GraphSweep1) compared to the end (GraphSweep2) of the test procedure. The magnitude of peak grip at high load negative slip conditions has not changed at all and its only changed by 0.9% at the positive slip side (from -8,910N to – 8,990N).

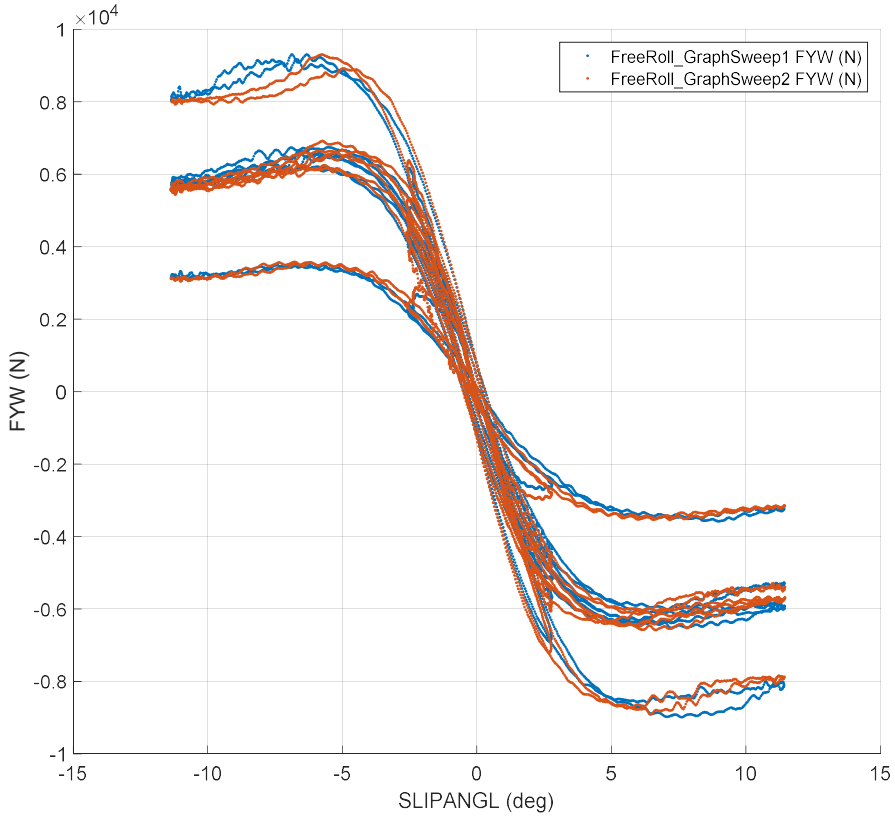

Figure 5.1.2-A. Comparison of 'GS2MF FreeRolling' GraphSweep1 and GraphSweep2, for Lateral Force, FYW (N) versus Slip Angle, SLIPANGL (°).

Figure 5.1.2-A shows that the location of the peaks has moved by a negligible 0.4° which is within the amplitude of the tyre vibration. It is also common to see a change in conering stiffness as a tyre wears, this is due to reduced flex that comes with lower tread blocks. However, this is not evident in this particular case. Overall, this demonstrates that the tyre's grip characteristics have not significantly changed as a result of the testing. At high loads and beyond the peak (the top left section of the data), there is a discrepency where the tyre generates less grip during GraphSweep2 compared to GraphSweep1, this is due to chatter where the tyre vibrates in the rig. This was visible during the testing. The chatter is caused by the lack of compliance in the test rig meaning tyre vibrations cannot be effectivly absorbed. When the tyre is mounted to a vehicle, the bushes and dampers in the suspension eliminate any form of chatter. However, modifying the test rig to be more compliant would severley reduce the accuracy and consistency of the measurement, this is therefore not a viable option. Instead, the presence of chatter, when it occurs, is typically accepted as a limitation of the testing. Fortuntely, it only effects very particular load cases and does not affect the whole dataset. Therefore, it has a minimal effect on the overall accuracy of the resulting tyre model. Unfortunatly the particular

load case at which chatter occurs is largely unpredictable, though it more commonly occurs at high load, high slip angle test cases. If chatter is found to occur at a particular load case then the only way to avoid it is to modify the test procedure such as to avoid testing altogether at the given load case. However, if data is required at that particualar load condition (such as in this case) then the chatter and associate slight reduction in accuracy cannot be avoided.

Figure 5.1.2-B compares the radius, defined as the distance from the ground to the wheel centre (DSTWOWHC) of the tyre during Graph Sweeps 1 and 2. In this case, radius was plotted aginst 'Zeroed RUNTIME', this is the standard runtime channel but zeroed at the start of each segment of the test, such that the two data sets line up with each other (see Nomincalture Section), allowing them to be compared more easily. The large changes in radii are due to the vertical load changing through the test and are hence expected. In this case the tyre radius has reduced by around 2.6mm (shown in 5.1.2-B). The original tread depth of these particular tyres is 5.6mm, however the law in the UK requires tyres to have a minimum tread depth of 1.6mm when used on public roads. GS2MF is designed to measure tyre performance for on road applications, so during testing the tyre should never wear down to below this legal minimum. This means that this particular tyre has 4mm (5.6 – 1.6 = 4mm) of avaliable tread. During this test 2.6mm of the avaliable 4mm of tread was used, meaning by the end of the test the tyre had 35% of its usable tread still remaining. This is well within the acceptable limits and normal operating conditions of the tyre. Therefore, this is demonstrating that the tyre was not excessivly worn as a result of the testing.

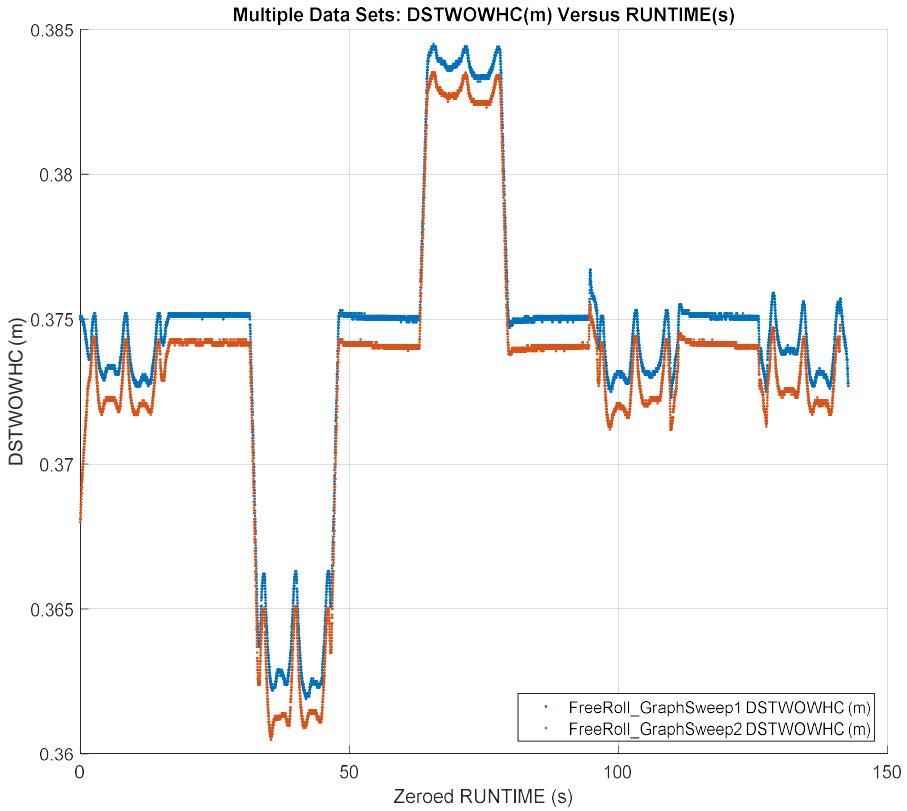

Figure 5.1.2-B. Comparison of 'GS2MF FreeRolling' GraphSweep1 and GraphSweep2, for Radius, DSTWOWHC (m) versus Zeroed RUNTIME (s).

Figure 5.1.2-C shows that the temperature profiles of Graph Sweeps 1 and 2 are almost indistinguishably similar to each other in the lower temperature regions. This suggests that the testing is highly repeatable and that the thermal control system is working effectivly. During the second peak, the temperatures differ by up to 9.1% (95.5 °C to 86.8 °C), while at every other peak the temperatures are typically within 5% of each other. Furthermore, the tyre cools between each sweep to almost identical temperatures. This demonstrates that during Graph Sweeps 1 and 2 the tyre is tested ender very similar themal conditions, suggesting the results are comparable.

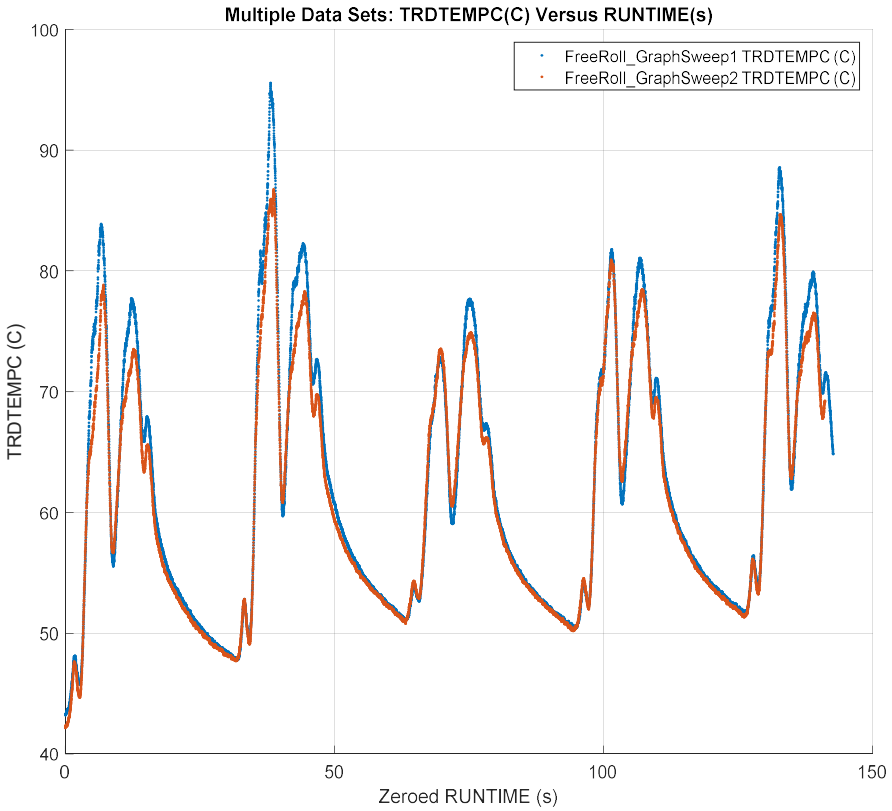

Figure 5.1.2-C. Comparison of 'GS2MF FreeRolling' GraphSweep1 and GraphSweep2, for Central Tread Temperature, TRDTEMPC (C) versus Zeroed RUNTIME (s).

Overall, the Graph Sweeps suggest that this 'GS2MF FreeRolling' data is of sufficient quality to use for model parameterisation. There is a small amount of chatter occuring under high load high slip angle conditions once the tyre is mildly worn, this is a characterisitc occationally observed with this particular tyre that cannot be avoided. However, the chatter is only slight and only occurs under one very specific load case and will likely have a minimal effect on the resulting tyre model. The wear is well within the tyre's limits and the temperature profiles of the Graph Sweeps are very similar. Therefore, this data can be used in the model parameterisation, this process is detialed in the forthcoming chapters.

'BrkDrv' Data Check

Figure 5.1.2-D shows the pure longitudinal performance of the tyre at the start of the 'GS2MF BrkDrv' test procedure (BrkDrv_GraphSweep1) compared to the end of the test procedure (BrkDrv_GraphSweep2). The plot shows that there is little difference between the two Graph Sweeps, meaning the tyre's pure longitudinal performance did not drastically change as a result of the testing. This suggests that testing has not excessivly damanged the tyre and the data is

suitable for model parameterisation. As the tyre wears, it is typical for its slip and cornering stiffness to increase, as the tread blocks become shorter they flex less, but in this case there is very little evidence of this in the data. Peak grip has changed by just 4.4% (from 11,400N to 10,900N), again suggesting that the data is suitable for model parmeterisation. If there were significant differences between the Graph Sweeps it would suggest that the tyre's performance had changed; likley as a result of excessive wear or overheating during the testing. This rarely occurs and in such a case, the test procedure would have to be modified and the rest repeated.

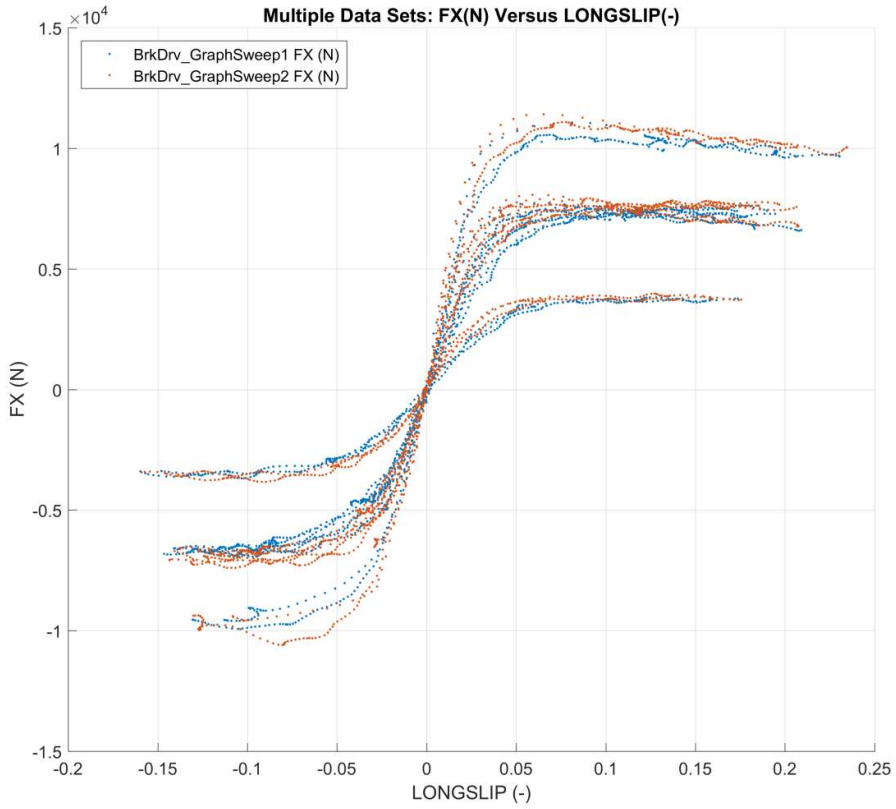

Figure 5.1.2-D. Comparison of 'GS2MF BrkDrv' GraphSweep1 and GraphSweep2, for Longitudinal Force, FX (N) versus Slip Ratio, LONGSLIP (-).

Figure 5.1.2-E shows a plot of tyre radius (distance from ground to wheel centre) against the zeroed runtime (zeroed such as to overlay to the two data sets that occure at different times in the test procedure). The plot shows that during the 'BrkDrv' test, the tyre has worn by just 2mm (Average difference between the two data sets on the Y axis). During the GS2MF FreeRollling test, the Graph Sweeps revealed 2.6mm of wear (shown in Figure 5.1.2-B). This 2.6mm was well within the limits of the tyre, that had 35% of its usable tread remaining before the tread depth was below the legal minimum for road use. The 'BrkDrv' test wore the tyre even less than

the ‘FreeRolling’ test and is well within the usual operating range of the tyre. It is therefore, not concerning to see this much wear over the course of the test procedure.

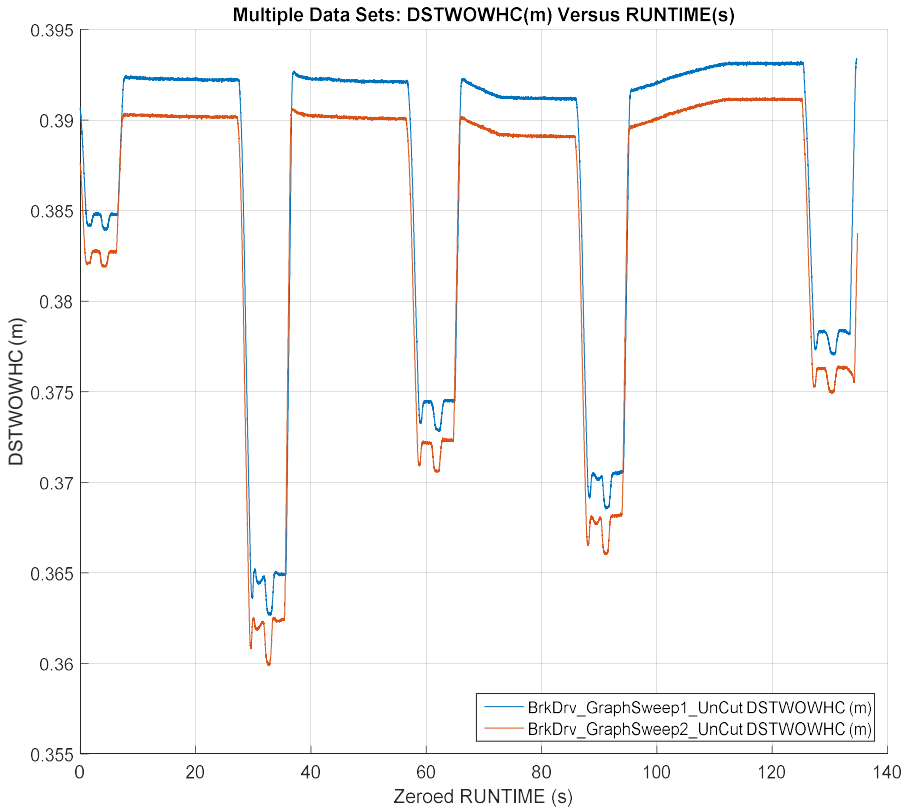

Figure 5.1.2-E. Comparison of ‘GS2MF BrkDrv’ GraphSweep1 and GraphSweep2, for Radius, DSTWOWHC (m) versus Zeroed RUNTIME (s).

Figure 5.1.2-F shows the thermal profile of the two data sets, this time looking at the central tyre tread temperature against zeroed time (zeroed such that they can be overlaid). The plot shows that the tyre operated under almost identical thermal conditions during the two Graph Sweeps. The maximum variation was less than 2°C and well within the expected variation of this type of testing. This therefore, shown that there is no concern regarding the temperature management during the two Graph Sweeps.

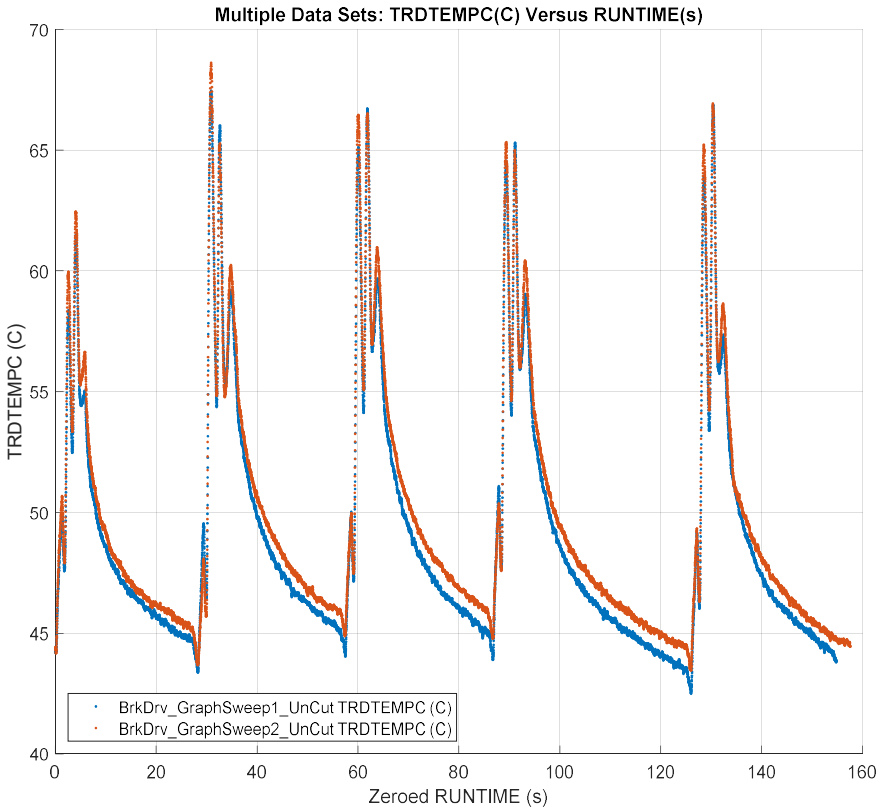

Figure 5.1.2-F. Comparison of 'GS2MF BrkDrv' GraphSweep1 and GraphSweep2, for Central Tread Temperature, TRDTEMPC (C) versus Zeroed RUNTIME (s).

Overall, the 'GS2MF BrkDrv' Graph Sweeps suggest that the testing has been sucesful and that the data output from the test should be suitable for paramterising MF-Tyre 6.1 models. This was demonstrated by the very consistent longitudinal force versus slip ratio sweeps, as well as the minimal amount of tyre wear and highly consistent temperatures during the test.

Temperature Profile Check

In the absence of a thermal modelling capability in MF-Tyre 6.1, it is important to ensure the tyre temperature remains as constant as possible, not just during the Graph Sweeps but throughout the test procedure. For this reason, a thermal check is performed before using the test data in the fitting process. If the tyre temperature is shown to trend up or down during the test, it will reduce the accuracy of the resulting tyre model which is unable to take temperature into account. To address this, a thermal logic control system is used to regulate the tyre's temperature as accurately as possible. This works by adjusting the length of the pauses between each sweep to allow the tyre to cool to a pre-set baseline temperature of 45°C (See Section 3.5 on Thermal Logic). The system avoids the temperature of the tyre creeping up or down during

the test, causing the tyre performance to change as a result. The temperature profile of the 'GS2MF FreeRolling' test procedure can be found in Figure 5.1.2-G.

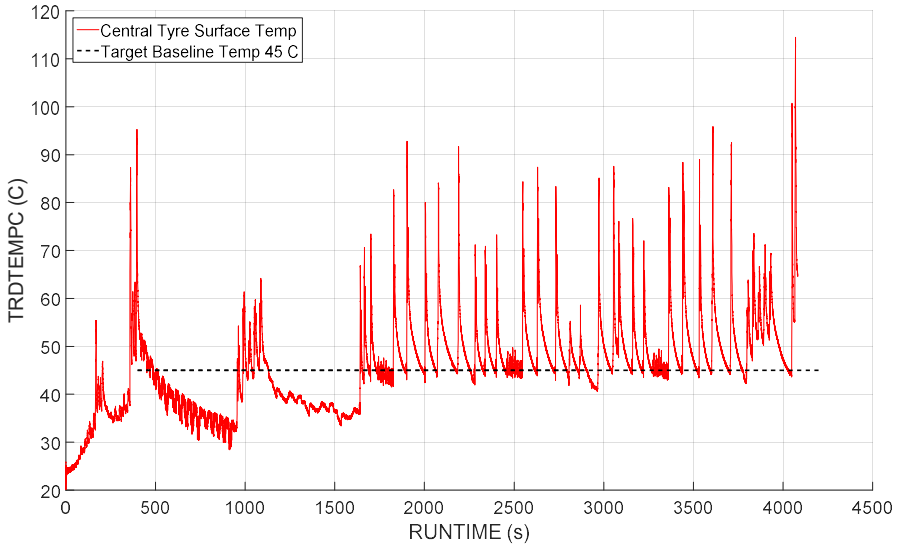

Figure 5.1.2-G. Temperature profile of 'GS2MF FreeRolling' data, Central Tread Temperature, TRDTEMPC (C) versus RUNTIME (s) along with the target baseline temperature.

Figure 5.1.2-G shows how the tyre temperature changes through the 'GS2MF FreeRolling' test procedure. In this case, the tyre is warmed appropriately during the warmup section; however, it then cools to around 35°C (10°C below the 'threshold') during the Step-Steer section. This is not ideal but cannot be avoided as the Step-Steer section is a very low energy part of the testing, where little heat is generated by the tyre. However, Graph Sweep 1 is placed after the low energy Step-Steer section in order to regain the heat in the tyre, which it does, quickly bringing the tyre back up the baseline temperature. After Graph Sweep 1 the tyre cools again during the low energy cornering stiffness and Loaded Radius section. Before again quickly regaining its temperature as the force and moment sweeps are run. After this point, each sweep of the force and moment section begins with the tyre at, or very close to the 45°C baseline temperature. Overall, this constant baseline temperature through the force and moment tests demonstrates a good thermal management of the tyre and the data is suitable for the parameterisation of the MF-tyre 6.1 tyre models.

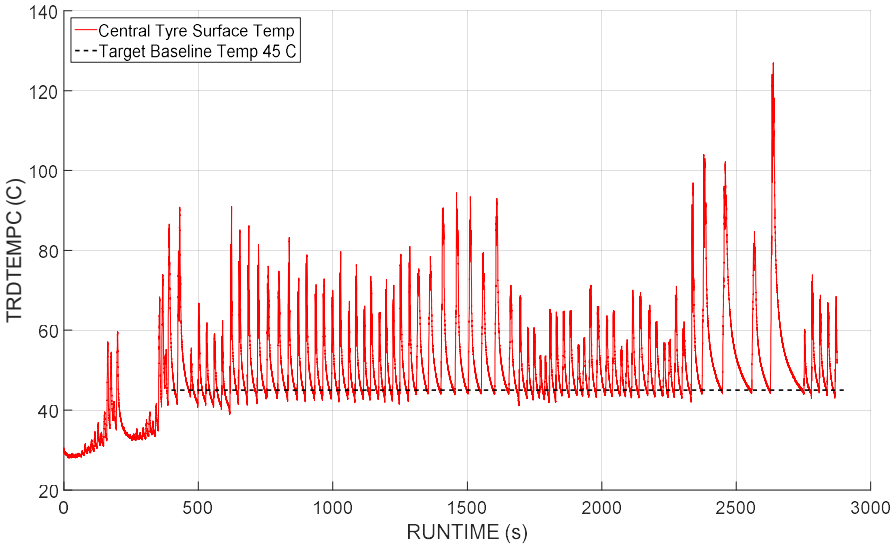

Figure 5.1.2-H. Temperature profile of 'GS2MF BrkDrv' Data, Central Tread Temperature, TRDTEMPC (C) versus RUNTIME (s) along with the target baseline temperature.

Figure 5.1.2-H shows the temperature profile of the 'GS2MF BrkDrv' test procedure. During this test, there were no regions where the tyre cooled significantly below the 45°C baseline temperature. Instead the warmup section heats the tyre appropriately and thereafter, the thermal logic control system correctly manages the pauses between each sweep. As a result, every sweep through the test procedure starts with the tyre at or very close to the 45°C baseline temperature; thus, ensuring the thermal consistency of the testing. This is critical to the consistency of the tyre performance and the accuracy of the resulting tyre model built from this dataset.

5.1.3 Valid Ranges

Before starting the MF-Tyre 6.1 fitting procedure, it is important to determine the range of load cases the resulting tyre model will be valid within. MF-Tyre 6.1 is an empirical model parameterised by fitting the model to test data. Typically, it is therefore unable to accurately replicate the performance of the tyre at load conditions beyond the tested range available in the data used in the models' parameterisation. The valid range of the resulting tyre model is therefore typically defined by the range of load cases at which the tyre is tested, as detailed below.

1. Slip Angle. The 'GS2MF FreeRolling' procedure tests the tyre to maximum slip angles of +/-25°, therefore the resulting tyre model will be valid with this range, which is sufficient for most vehicle dynamics simulations. In some cases, the tyre model can

output reasonable approximations beyond this range, however this cannot be guaranteed as the MF-Tyre 6.1 tyre model can often be unstable when extrapolating. Instead, if the model is required to correlate outside of this range then the test procedure will need to be modified to test at higher slip angles. Doing so is simple, but it will increase the sliding energy during the testing, as a result the tyre temperature will increase, leading to longer cool down times and ultimately a longer and more expensive overall test procedure.

2. Slip Ratio. The 'GS2MF BrkDrv' procedure tests the tyre to maximum slip ratios of +/-0.5, therefore the tyre model will be valid within this range. As with slip angle this range is suitable for the majority of vehicle dynamics simulations. It is also possible that the model will be representative outside of this range but this cannot be guaranteed. If the model is required to be valid outside of this range then the test procedure will need to be modified however doing so will result in additional heat build-up and wear in the tyre. Ultimately, this will result in the test procedure being more expensive to run.
3. Camber Angle. The 'GS2MF FreeRolling' procedure tests at camber angles up to +/-6°, meaning camber is valid within this range. As with slip angle and slip ratio, this is suitable for most vehicle dynamics simulations; extrapolating beyond this range is likely to be inaccurate but the test procedure could easily be modified to cover a wider range if required, but this will induce additional testing costs.
4. Inflation Pressure. The default GS2MF inflation pressures are 2.1, 2.6 and 3.3bar meaning the tyre model will be valid within the range of 2.1 to 3.3bar. Extrapolating beyond this range can be possible but it typically results in the model becoming mathematically unstable. However, these inflation pressures are only defaults and can be changed as necessary to suit the given application.
5. Vertical Load. The tested vertical load range is dependent on the ETRTO load rating of the tyre (ETRTO Standards Manual, 2017). The maximum tested load is three times the nominal load, with the nominal load being 65% of the tyre's ETRTO rating, (See Section 3.3 on Vertical Load Linked to Tyre Load Rating). In this example, a tyre of load rating 110 is tested which equates to a load range of 765N to 20,256N. However, the tyre's performance at zero load is predictable based on the assumption of zero lateral or longitudinal force and zero vertical load. So, the tyre model will be valid between 0 and 20,256N of vertical load. This is expected to be suitable for nearly all applications. A vehicle that exerts higher vertical loads than this will require a tyre with a higher load rating. As such the range of test loads will be recalculated from that higher load rating and the tyre will instead be tested at a suitably higher set of loads.
6. Forward Velocity. Only the Rolling Radius component of MF-Tyre 6.1 is sensitive to forward velocity while the force and moment prediction is not at all sensitive. As with

the inflation pressure the forward velocity used in GS2MF is not hard coded and instead can be changed to suit the application, for example sports car tyres may benefit from being tested at higher speeds. In this example, the tyre is tested at 8.3, 16.6 and 33.2m/s. However, the tyre performance is predictable close to zero forward velocities and MF-Tyre has functionality to avoid instabilities at very low speed. Therefore, the tyre model built from this data will provide representative force and moment predictions at any speed while the Rolling Radius will be valid between 0 and 33.2m/s. At any velocity beyond 33.2m/s the Rolling Radius output from the model will be equal to that at 33.2m/s, this ensures the models mathematical stability at any velocity. This means that for road car applications (where the lack of critical ground effect aerodynamics means the high-speed Rolling Radius is of little importance) the model can be extrapolated to higher velocities, making it suitable for most road car applications.

A summary of the valid range of a tyre model built from this particular data set can be found in Table 5.1.3-A.

Input	**Minimum**	**Maximum**
Slip Angle	-25°	25°
Slip Ratio	-0.5	0.5
Camber Angle	-6°	6°
Inflation Pressure	2.1bar	3.3bar
Vertical Load	0N	20,256N
Forward Velocity	0m/s	33.2m/s

Table 5.1.3-A. Valid range of a tyre model built from this specific data set.

5.1.4 Base Calculations

Before the fitting of an MF-Tyre 6.1 tyre model can begin, some basic calculations are required. All of these calculations are defined in the documentation that comes with the OptimumTire MF-Tyre fitting software developed by OptimumG, Denver CO. (OptimumTire, 2017). All calculations are carried out by simple analysis of the GS2MF data as described below:

1. Nominal Speed, V0. This is the forward velocity at which all the force and moment testing is carried out. In the case of GS2MF this is 16.6m/s (60kph).
2. Nominal Pressure, Pi0. This is the nominal pressure and is used as part of the pressure interpolation calculations within MF-Tyre 6.1. In the case of GS2MF, this is the middle inflation pressure used in the force and moment testing, 2.6bar.

3. Nominal Load, FZ0. This is the nominal load and is used within MF-Tyre 6.1 as part of the load sensitivity calculations. This is calculated as 65% of tyre's ETRTO load rating in Newtons (Reference: ETRTO Standards Manual, 2017).
   For example: A tyre with a load rating of 110, equates to 1,060kg using the ETRTO load rating look up table, or 10,399N (multiplying by acceleration due to gravity of 9.81m/s^2).
   65% of 10,399N = 6,759N
   Therefore, FZ0 for a tyre with a load rating of 110 will be 6,759N.
4. Static Unloaded Radius, R0. This is the tyre's Unloaded Radius which can be extracted from the 'GS2MF FreeRolling' data by extrapolating the Rolling Radius data down to zero vertical load. Within 'GS2MF FreeRolling' there are three Rolling Radius sections one corresponding to each of the three inflation pressures. A plot showing vertical load versus tyre radius for these three sections of data can be found in Figure 5.1.4-A.

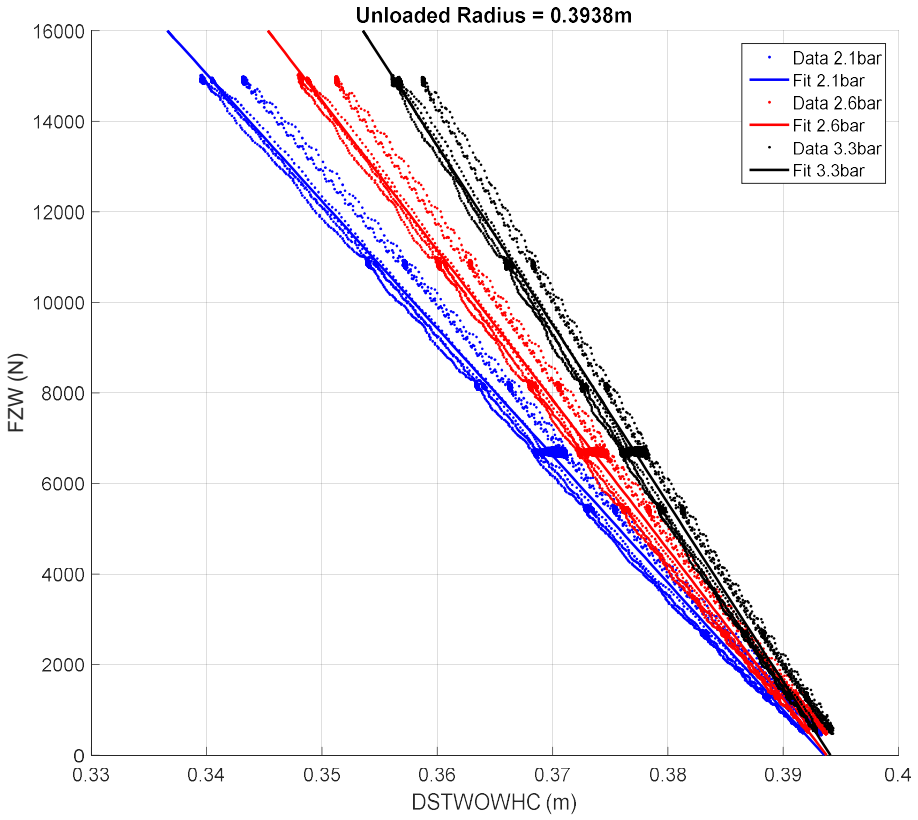

Figure 5.1.4-A. Vertical Load, FZW (N) versus Loaded Radius, DSTWOWHC (m); coloured by Inflation Pressure, P. Data is from 'GS2MF FreeRolling' Rolling Radius section divided into separate inflation pressures, linear fits are applied independently to each pressure and extrapolated to FZW = 0 where they converge on the Unloaded Radius of 0.3938m.

Figure 5.1.4-A shows the Loaded Radius data plotted separately for each pressure. A simple linear model is applied to each of the three data sets and extrapolated to zero vertical load. The radius at which these three lines cross zero vertical load can then be read from the plot, which correspond to the Unloaded Radius at each pressure. These three radii are very close to each other and the average of them is used as the single value for Unloaded Radius, R0. In this case is calculated to be 0.3938m, as shown in Table 5.1.4-A.

Calculating the Unloaded Radius from the rolling tyre data in this way is more accurate than attempting to measure it directly from the static tyre. This is because a direct static measurement could be influenced by many factors, such as the tyre not sitting perfectly on a section of the bead seat, or by the measurement equipment applying a small load (compressing the tyre) when there should be zero load. Furthmore, such tests would have to be conducted separately from the main force and moment testing, whereas these rolling tests can be integrated into the wider test procedure, increasing test efficiency.

Inflation Pressure, bar	**Unloaded Radius, m**
2.1	0.3936
2.6	0.3938
3.3	0.3941
R0, (Mean Unloaded Radius)	*0.3938*

Table 5.1.4-A. Results after extracting the Unloaded Radius from the 'GS2MF FreeRolling' data.

5.2 Force and Moment Fitting Process

Once the data has been checked, pre-processed and all the necessary initial calculations have been completed, the tyre model fitting process can begin. The main fitting process of MF-Tyre 6.1 consists of multiple steps, in this case carried out using the OptimumTire fitting software developed by OptimumG, Denver CO. The process is a compartmental curve fitting optimisation, where the coefficients for a specified portion of the MF-Tyre 6.1 tyre model are optimised such as to minimise the error between the modelled output and the test data. Various optimisation algorithms can be used to carry out the fitting; OptimumTire uses a genetic algorithm (Cabrera, Ortiz, Carabias and Simon, 2004). This algorithm is inspired by the process of natural selection, where each iteration includes various children, the best child is selected and characteristics from that child are used to propagate the next iteration. The exact details of the genetic algorithm used in this case are considered intellectual property protected by OptimumG. OptimumTire also uses the Least Squares (OptimumTire, 2017) approach as a means of judging the error between the model and the data. This process works by calculating the sum of the squares of the errors between the model and the data. Once calculated this sum-square-error is

then minimised by the optimisation algorithm such that the model attempts to represent the data with the minimum possible error.

The MF-Tyre 6.1 fitting is conducted in several stages each of which must be carried out in a specific order; this is because the coefficients from previous stages are carried forward into the subsequent stages. Furthermore, each stage of the optimisation process must be fitted to the appropriate data, which is detailed in Table 5.2-A.

Fitting Stage	Stage Name	Data Used
1	FY Pure	'FreeRolling'
2	MZ Pure	'FreeRolling'
3	FX Pure and Combined	'BrkDrv'
4	FY Combined	'BrkDrv'
5	MZ Combined	'BrkDrv'
6	MX Combined	'BrkDrv'
7	MY Combined	Rolling Resistance
8	Loaded Radius	Rolling Radius
9	Transients	StepSteer and Static Long

Table 5.2-A. Details of the MF-Tyre 6.1 fitting process and the appropriate data to be used for each stage.

The following sections go through a worked example of fitting a complete MF-Tyre 6.1 tyre model to GS2MF data. In each section plots are shown to demonstrate the quality of the model fitting to the test data. These plots are generated using OptimumTire which uses its own internal data channel naming convention; this naming convention is detailed in the nomenclature and differs from the TYDEX convention used elsewhere.

5.2.1 FY Pure

The first stage of fitting an MF-Tyre 6.1 tyre model is to perform a pure lateral fit. This stage fits a series of 42 coefficients to the free rolling test data and attempts to capture the pure lateral steering performance of the tyre. Following a successful completion of this stage the tyre model will accurately represent the lateral force generated by the tyre while under pure steering (without any braking or accelerating) conditions; and be sensitive to slip angle, vertical load, camber angle and inflation pressure. An example of a completed fit is shown in Figure 5.2.1-A.

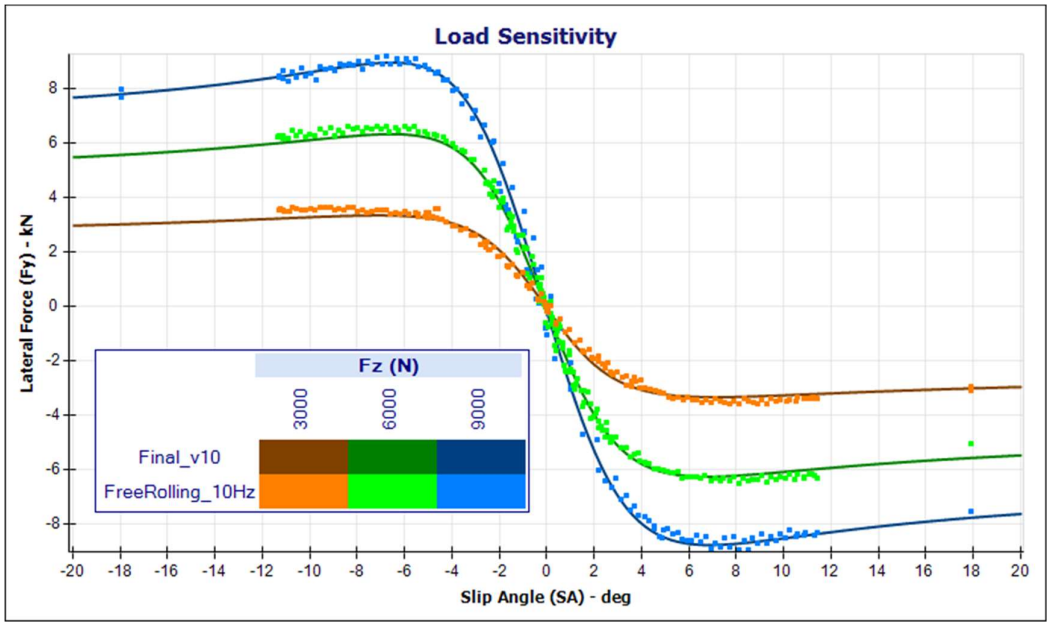

Figure 5.2.1-A. Model (Final_v9) and 'FreeRolling' Data (FreeRolling_10Hz) for Lateral Force, FY (kN) versus Slip Angle, SA (°); coloured by Vertical Load, FZ (N).

Figure 5.2.1-A is a plot of lateral force versus slip angle for both the GS2MF data (showing just three sweeps for clearer visulaization) and the overlayed tyre model. The regular data in the centre of the plot, between -11 and 11° of slip angle is from the force and moment variable rate sweeps present in GS2MF. The data points at -18 and 18° of slip angle are from the vertical load sweeps, these provide reduced data over a wide range of loads which improves the tyre models ability to accurately predict the tyre performance at high slip conditions. In this case the plot demonstrates that the tyre's model provides a very good representation of the data across the entire slip angle range and at each of the vertical loads. In this case the cornering stiffness is well captured, along with both the magnitude and location of the peaks. This is shown by the model accurately representing the regular force and moment data in the centre of the plot. Furthermore, the reduction in grip at high slip conditions is well captured by the MF-Tyre 6.1 tyre model. This is due to the model fitting being influenced by the vertical load sweep data at high slip angles. Overall the model shows a very good correlation to the test data across the full range of slip angles and three different vertical loads, in this case camber is zero and the inflation pressure is set to the nominal pressure of 2.6 bar.

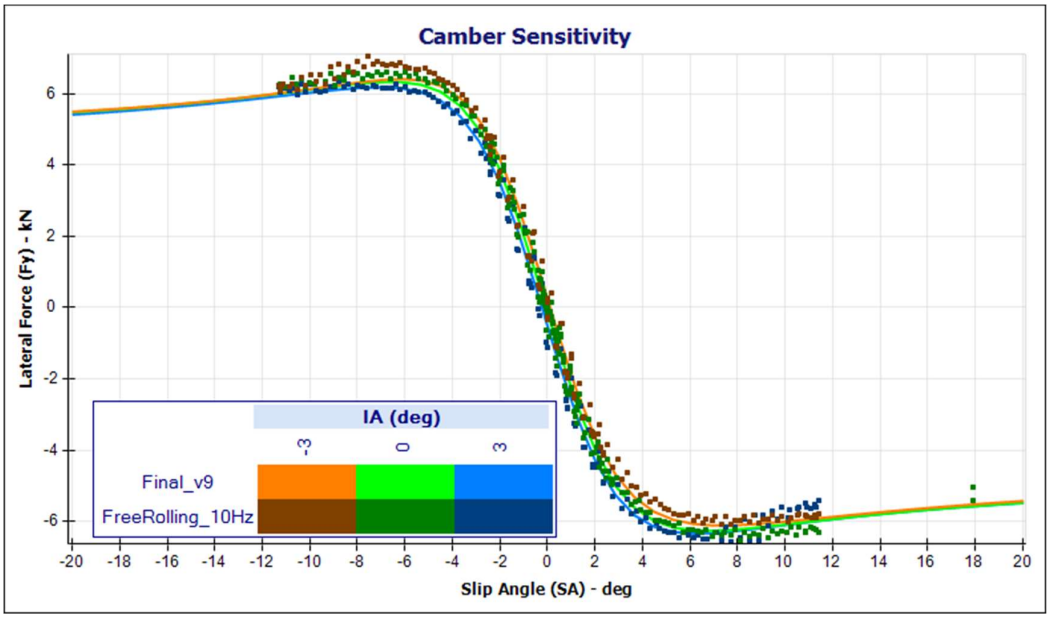

Figure 5.2.1-B. Model (Final_v9) and 'FreeRolling' Data (FreeRolling_10Hz) for Lateral Force, FY (kN) versus Slip Angle, SA (°); coloured by Camber Angle, IA (°).

Figure 5.2.1-B is another plot of lateral force versus slip angle, showing both the GS2MF test and the tyre model. As with Figure 5.2.1-A, the vertical load sweeps data at 18° of slip angle is also visible. The plot demonstrates the camber sentivity of the tyre model, which in this case is very slight. As the test data shows that this particular tyre is largely insentivite to camber, with peak grip only changing by around 700N across the 6° range of camber angles. This is typical of SUV tyres with high sidewall profiles such as the one used here. Nevertheless, this low sensitivity has been sucessfully captured by the tyre model which is consistently within around 200N, or 3.0% of the test data across the full range of slip angle. In this case the data is obtained at the nominal vertical load of 6,759N and inflation pressure remains at 2.6bar.

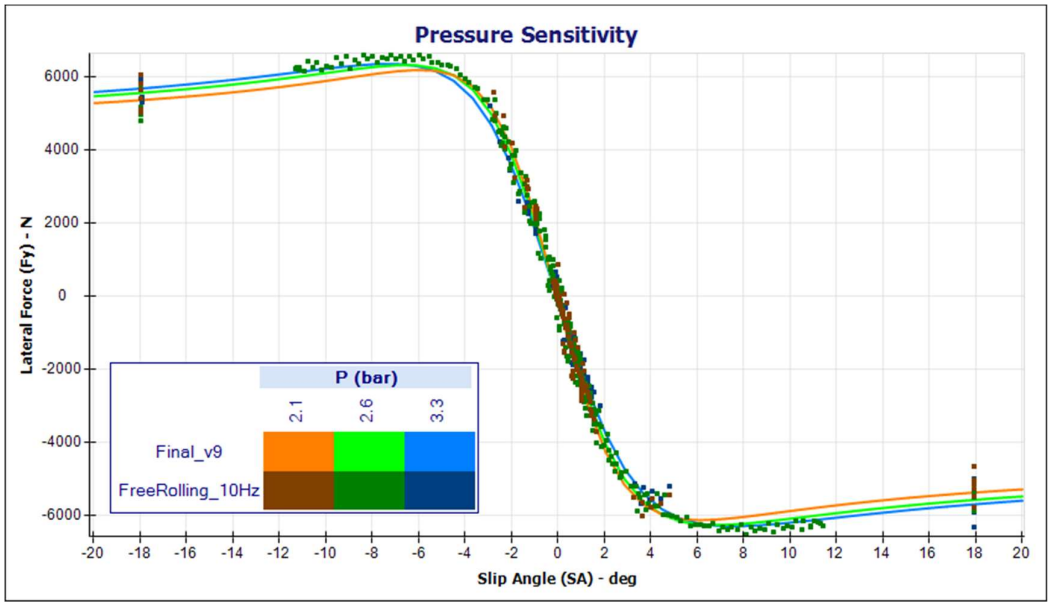

Figure 5.2.1-C. Model (Final_v9) and 'FreeRolling' Data (FreeRolling_10Hz) for Lateral Force, FY (N) versus Slip Angle, SA (°); coloured by Inflation Pressure, P (bar).

Figure 5.2.1-C shows that as with camber, the pressure sensitivity of this particular tyre is also very minimal, again this is captured by the tyre model. Figures 5.2.1-A/B and C all show the same data but filtered in different ways to highlight load, camber and pressure sensitivity. In this case, the filtering is such that vertical load sweeps at +/-18° of slip angle are more visible; however this filtering is only applied for visualisation and data comparison, no filters are applied during the model fitting where all data is used. In this case Figure 5.2.1-C shows a negligible change in lateral force as a result of inflation pressure. This is typical of an all-purpose SUV road car tyre such as this, which is engineered to be as consistent as possible under all conditions, rather than to maximise performance. The data at this stage is shown at zero camber and 6,759N of vertical load, both nominal conditions of the tyre model.

Overall, the model is demonstrated to accurately predict lateral force at a range of slip angles, vertical loads, camber angles and inflation pressures. Therefore, the pure lateral part of the modelling process is complete and the 42 coefficients optimised here can be carried forward into aligning torque fitting.

5.2.2 MZ Pure

Once the pure lateral fitting has been completed, stage two of the model building process is MZ pure. This stage is similar to FY Pure in that a successful fit will result in the tyre model being able to accurately predict MZ during pure steering manoeuvres and be sensitive to slip angle, vertical load, camber angle and inflation pressure. During this stage, the tyre model is fitted to

the same test data as used in the FY Pure fitting only now the MZ (aligning torque) data is used in place of FY. Due to unavoidable limitations in the testing equipment, this data is typically noisier than the lateral force data and as a result the accuracy of the fitting is often worse.

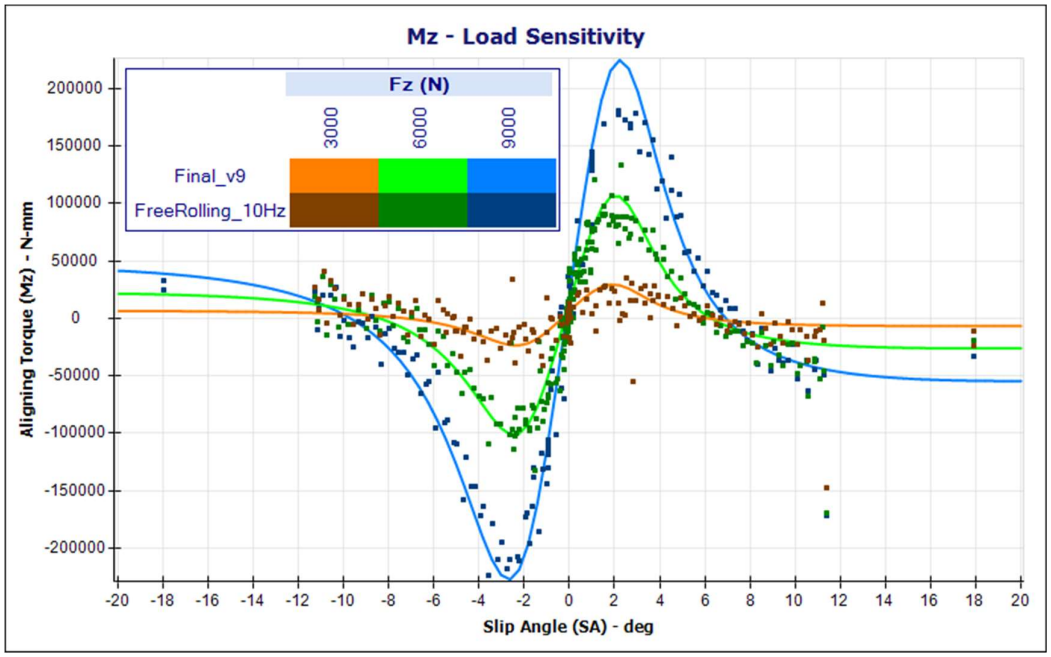

Figure 5.2.2-A. Model (Final_v9) and 'FreeRolling' Data (FreeRolling_10Hz) for Aligning Torque, MZ (N-mm) versus Slip Angle, SA (°); coloured by Vertical Load, FZ (N).

Figure 5.2.2-A shows the slip angle and load sensitivity of MZ pure has been captured in the model. Here the three solutions to the model, at the three vertical loads, each pass through the centre of the unavoidably noisy datasets. Noisy data such as this limits the potential accuracy of the resulting tyre model. However, in this case the plot shows that the tyre model can accurately predict MZ over a range of slip angles and vertical loads, while camber angle and inflation pressure are held at their nominal values.

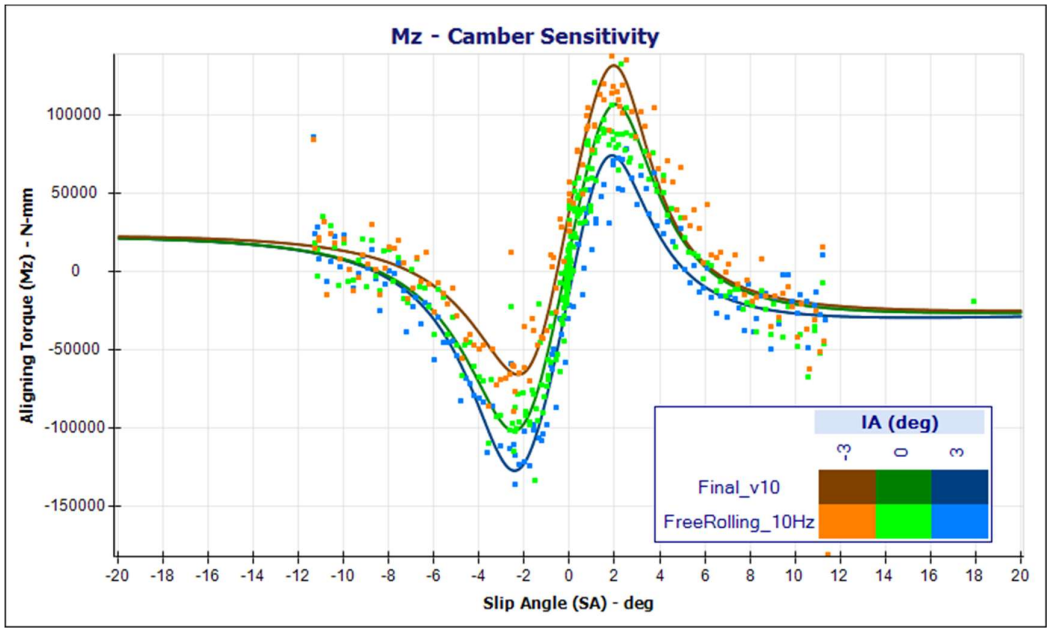

Figure 5.2.2-B. Model (Final_v9) and 'FreeRolling' Data (FreeRolling_10Hz) for Aligning Torque, MZ (N-mm) versus Slip Angle, SA (°); coloured by Camber Angle, IA (°).

Figure 5.2.2-B shows the tyre's MZ sensitivity to camber angle. Here, and comparing to Figure 5.2.1-B, it can be seen that MZ is more sensitive to changes in camber than FY. Again, the model accurately captures the tyre's camber sensitivity as shown in the test data.

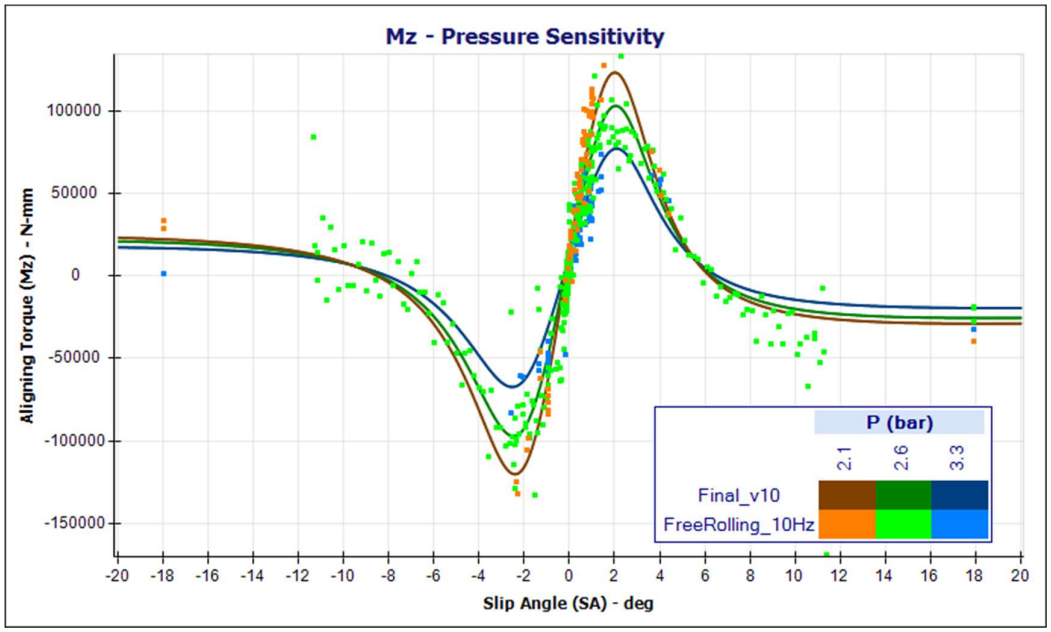

Figure 5.2.2-C. Model (Final_v9) and 'FreeRolling' Data (FreeRolling_10Hz) for Aligning Torque, MZ (N-mm) versus Slip Angle, SA (°); coloured by Inflation Pressure, P (bar).

Figure 5.2.2-C shows that the model has captured the tyre's pressure sensitivity and is able to accurately predict MZ over a range of slip angles and inflation pressures. With the MF-Tyre 6.1 model now parameterised to accurately represent MZ Pure over a range of slip angles, vertical loads, camber angles and inflation pressures, this stage of the fitting is complete. The FY Pure stage of the fitting has also been completed meaning the tyre model is now able to accurately represent lateral force and self-aligning torque over the tested range of load cases.

It can be valid to stop the fitting process at this stage and accept a model that is correlated for free rolling only. In vehicle dynamics simulations, this model can be used for any simulation where there is no throttle application or braking and the vehicle is in a pure free rolling condition. Since only free rolling data is used up until this stage of the fitting, accepting such a model will negate the need for 'BrkDrv' testing, leading to a significant cost reduction. However, a model that is valid for free rolling only is very restrictive, as the simulation of any manoeuvres that involve a throttle of brake input will be invalid. Therefore, the fitting process continues to capture the braking and driving performance of the tyre using the 'GS2MF BrkDrv' test data.

5.2.3 FX Pure and Combined

Once the pure lateral FY and MZ fits have been completed, the tyre's pure free rolling performance is fully captured within the model. The coefficients for these stages are then carried forward to be used in the next stages of the fitting process. In stage three, the FX pure longitudinal and combined coefficients are optimised to fit the 'BrkDrv' test data.

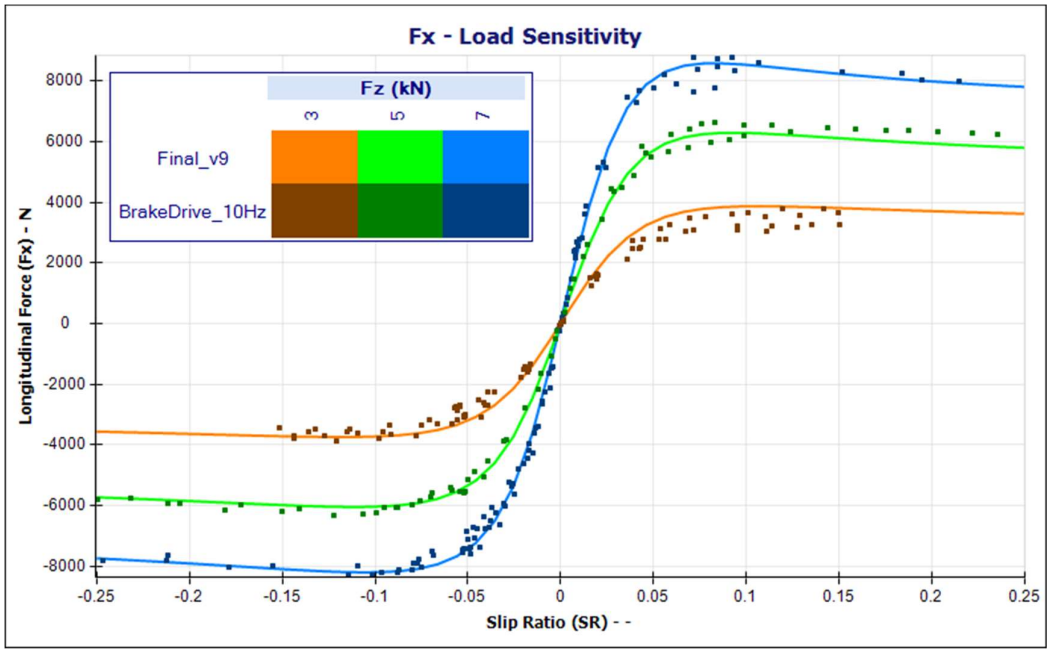

Figure 5.2.3-A. Model (Final_v9) and 'BrkDrv' Data (BrakeDrive_10Hz) for Longitudinal Force, FX (N) versus Slip Ratio, SR (-); coloured by Vertical Load, FZ (kN).

Figure 5.2.3-A shows the pure longitudinal performance of the tyre and its senitivity to vertical load. As with the pure lateral performance the MF-Tyre 6.1 model has accurately captured the longitudinal performance. All the peaks of the model are accurate to well within the range of noise in the test data, the same is true within the high slip regions beyond the peaks. Finally the slip stiffness section of the data is also well represented by the model. This demonstrates the model is able to estimate longitudinal force over a wide range of slip ratios and vertical loads.

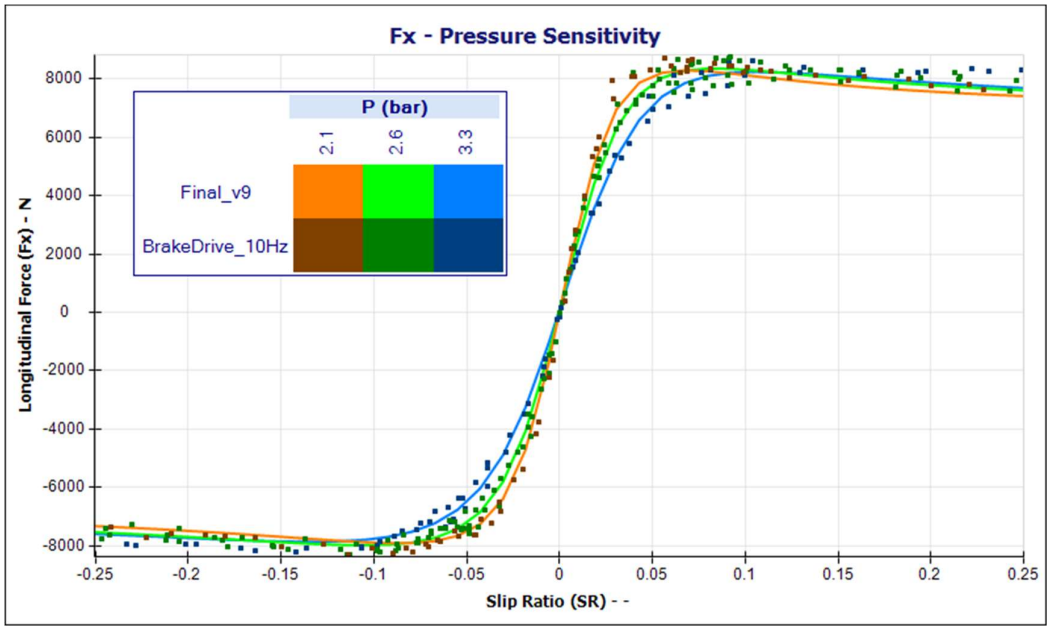

Figure 5.2.3-B. Model (Final_v9) and 'BrkDrv' Data (BrakeDrive_10Hz) for Longitudinal Force, FX (N) versus Slip Ratio, SR (-); coloured by Inflation Pressure, P (bar).

Figure 5.2.3-B shows that the FX Pure fit is accurate and is sensitive to changes in inflation pressure, this is demonstrated by the model continually matching the three datasets at the three tested inlation pressures. The model's peak grip magnitude is not sensitive to inflation pressure; however, the data also shows no change in the magnitude of the peaks. The slip ratio locations of the peaks does change as a result of the inflation pressure inducing a change in the tyre's contact patch dimentions. The data shows that at 2.1bar the positive peak occurs at a slip ratio of around 0.06 and the 3.3bar positive peak occurs at 0.1, a change of 67% which is captured accurately by the model. Furthermore, the slip stiffness changes significantly in the data, as can be seen in the low slip region, this is also precisely captured by the tyre model. This shows that overall the MF-tyre 6.1 tyre model has accurately captured the tyre's longitudinal inflation pressure sensitivity.

Only one coefficient is present within the MF-Tyre 6.1 tyre model to capture the FX and combined sensitivity to camber angle. This is due to the assumption that small camber angles have very little influence on a tyre's longitudinal behaviour. This is an unavoidable limitation in the MF-Tyre 6.1 tyre model; however, it is typically a valid assumption. As road cars normally use low camber angles anyway, meaning the already minimal influence of camber on longitudinal behaviour is reduced further. If camber angle increases significantly, such as in a roll over event, then the tyre's peak longitudinal grip characterisitcs will be affected. However, in such conditions the MF-Tyre 6.1 model will not be valid anyway as sidewall interactions and

radical changes to the contact patch shape amongst other phenomina are not taken into account. Therefore, the MF-Tyre 6.1 tyre model in its standard form for road car appliations is only valid for smaller camber angles of up to around 5-6°, depending on the test conditions and tyre construction. Within this range the tyre's longitudinal behaviour is almost completly unaffected by camber and for this reason a complex sensitivity is not included in MF-Tyre 6.1. The only exception being a special adaption of MF-Tyre 6.1 for motorcycle application which is outside the scope of this project.

At this stage all necessary longitudinal sensitivies are captured in the model on top of the already captured free rolling behaviour. The tyre model is now able to accurately predict lateral force and aligning torque under free rolling conditions and longitudinal force under braking and driving conditions. During the next stage of the fitting, the tyre model will be updated in order to predict FY under combined conditions.

5.2.4 FY Combined

After completing the pure and combined longitudinal fits as well as the pure lateral fits, the combined lateral fitting can be completed. Successful completion of this stage will complete all the force prediction fits, leading to a model able to predict both longitudinal and lateral forces under any load case within the tested range.

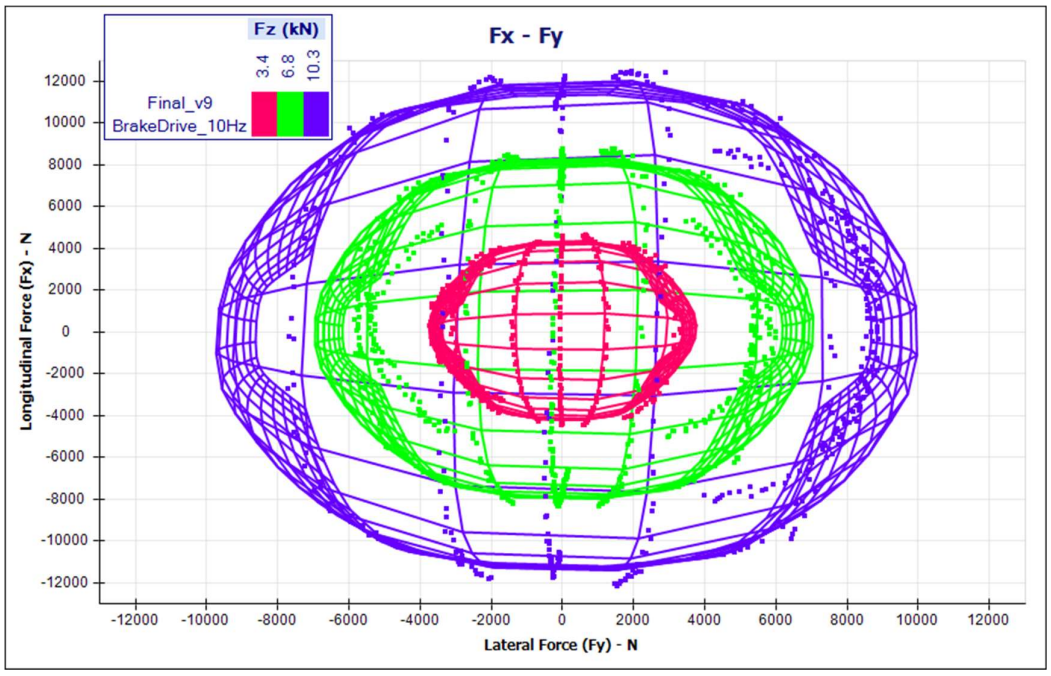

Figure 5.2.4-A. Model (Final_v9) and 'BrkDrv' Data (BrakeDrive_10Hz) for Longitudinal Force, FX (N) versus Lateral Force, FY (N); coloured by Vertical Load, FZ (kN).

Figure 5.2.4-A shows the full friction ellipse at three vertical loads, which can be plotted after completing the FX and FY combined fits. The full friction circle shows the wide-ranging tyre performance and is useful to confirm that the model fitting has converged on a realistic result. In some cases, the optimisation algorithm converges on a local minima which results in a square shaped friction ellipse. In such cases, the optimisation should be re-initiated and repeated. In this case the plot shows a good 'round shaped' friction ellipse, it is difficult to see how well the model matches the data, for that purpose a reduced friction ellipse is shown in Figure 5.2.4-B.

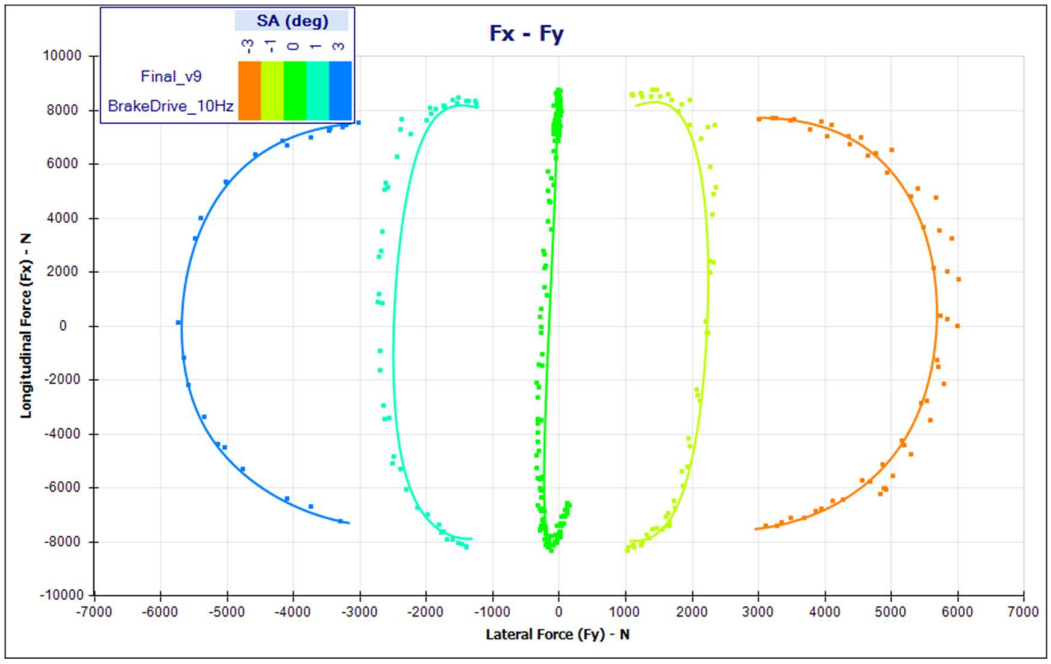

Figure 5.2.4-B. Model (Final_v9) and 'BrkDrv' Data (BrakeDrive_10Hz) for Longitudinal Force, FX (N) versus Lateral Force, FY (N); coloured by Slip Angle, SA (°).

Figure 5.2.4-B shows that the correlation between the tyre model and the test data under combined conditions. During this test, the tyre is held at a constant slip angle (slip angles of -3, -1, 0 +1 and +3° are shown) while slip ratio is swept between braking and accelerating. Such an experiment allows the tyre to be assessed under combined conditions where both longitudinal and lateral forces are observed at the same time. In this case, the tyre model shows a good correlation to the data throughout the shown tests, predicting both longitudinal and lateral force accurately and typically within the noise present in the data. In this case the model does not capture the 1° slip angle test condition as accurately as the other conditions. This is often the case when modelling a wide variety of different load conditions, where the model is typically good in some areas and worse in others. Overall, a compromise must be made where the model is reasonable across the required load conditions. At this stage, all the force prediction fits are

complete resulting in the tyre model being able to predict forces under all load cases within the valid range.

5.2.5 MZ Combined

Once all the forces have been modelled as well as MZ pure (Section 5.2.2 MZ Pure), the MZ combined stage of the MF-Tyre 6.1 fitting can be conducted. The fit does not perform well, as the data quality is poor. This is due to unavoidable limitations is the available test equipment where measuring a small MZ (maximum of around 450Nm) while at the same time measuring a large FX (maximum of around 8,000N) always results in a poor signal to noise ratio. This is shown in Figure 5.2.5-A.

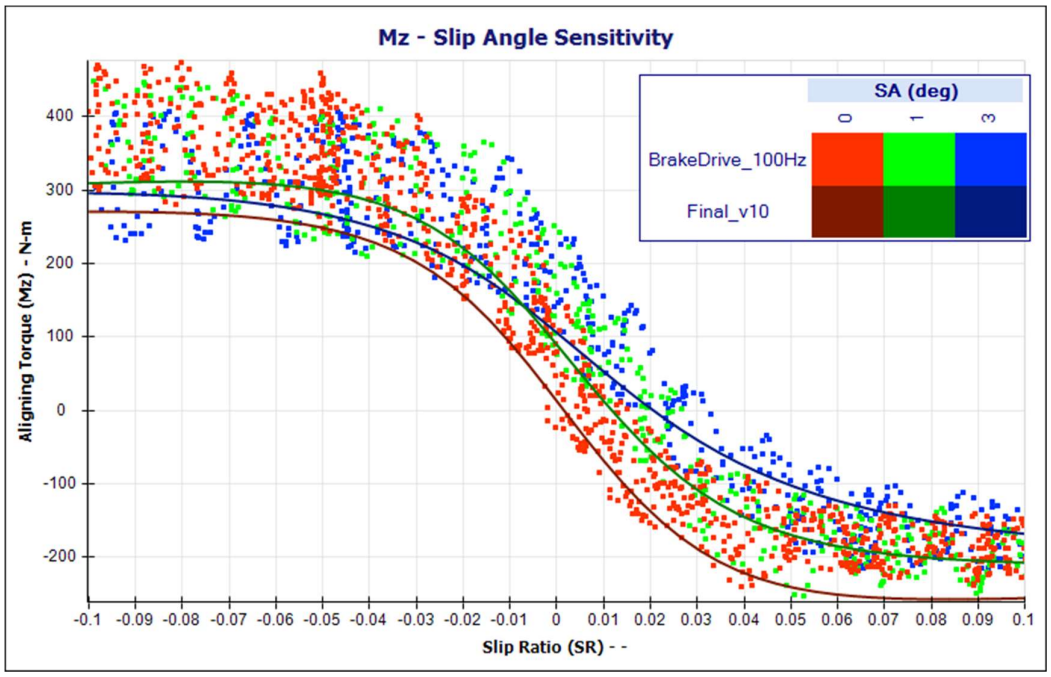

Figure 5.2.5-A. Model (Final_v10) and 'BrkDrv' Data (BrakeDrive_100Hz) for Combined MZ (N-m) versus Slip Ratio, SR (-); coloured by slip angle, SA (°).

Figure 5.2.5-A shows the MZ combined fit to the 'BrkDrv' test data. The large amount of noise can be observed across the entire data set but unfortunately this is unavoidable and it is present in data provided by all flat-trac rigs. As an example, the region of peak MZ for zero slip angle, (which occurs at close to -0.1 slip ratio and is coloured red in Figure 5.2.5-A), varies between around 300 and 470Nm about a mean of 385Nm. This equates to 85Nm of noise on a 385Nm signal, or 22% noise. This significant amount of noise makes it impossible for the model to achieve a good fit. However, this is a limitation of the test rig itself rather than the test procedure or model fitting process. This is evident as the same noise can be observed in the Square Matrix data and in GS2MF from either Calspan or SoVaMotion. With there being no

way of avoiding the signal noise, the only option is to accept the fit as is and move onto the next stage of the fitting process.

5.2.6 MX Combined

The MX combined fitting is the next stage of MF-Tyre 6.1 parameterisation process. As with the MZ combined there are limitations based on the noise in the test data, this is shown in Figure 5.2.6-A.

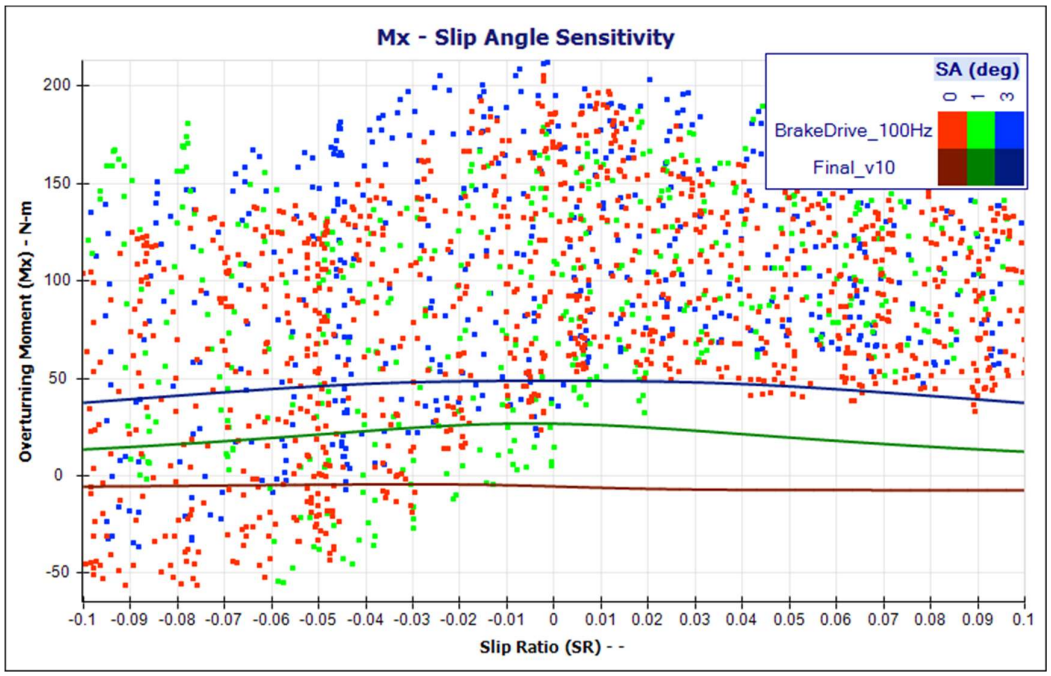

Figure 5.2.6-A. Model (Final_v10) and 'BrkDrv' Data (BrakeDrive_100Hz) for Overturning Moment MX (N-m) versus Slip Ratio, SR (-); coloured by Slip Angle, SA (°).

Figure 5.2.6-A shows that the 'BrkDrv' test data has an unusable level of noise on the MX channel. As with MZ this noise is a result of limitations in the available test equipment and cannot be avoided. An attempt was made to fit the MF-Tyre 6.1 tyre model to this data; however, as shown after the fitting was complete, the model remained insensitive to slip ratio. Therefore, the MX combined part of the fitting was instead fitted to the free rolling data, as shown in Figure 5.2.6-B. This effort addresses the issue to some degree, making the model sensitive to slip angle but not slip ratio. However, no further action can be taken to improve this in either GS2MF or Square Matrix testing. This prohibitively large amount of noise on the MX data during 'BrkDrv' testing is a known limitation of the Calspan rig, where this data was sourced; however, it is also typical of similar flat-trac rigs such as SoVaMotion. The issue is caused by a very slight misalignment of one of the beams that forms part of the instrumented head. The tiny misalignment changes with rotation, so with an accurate angle sensor and

additional testing the noise could potentially be measured and then reduced in post processing. However, while this forms part of Calspan's future development plan, it was not available at the time testing was conducted.

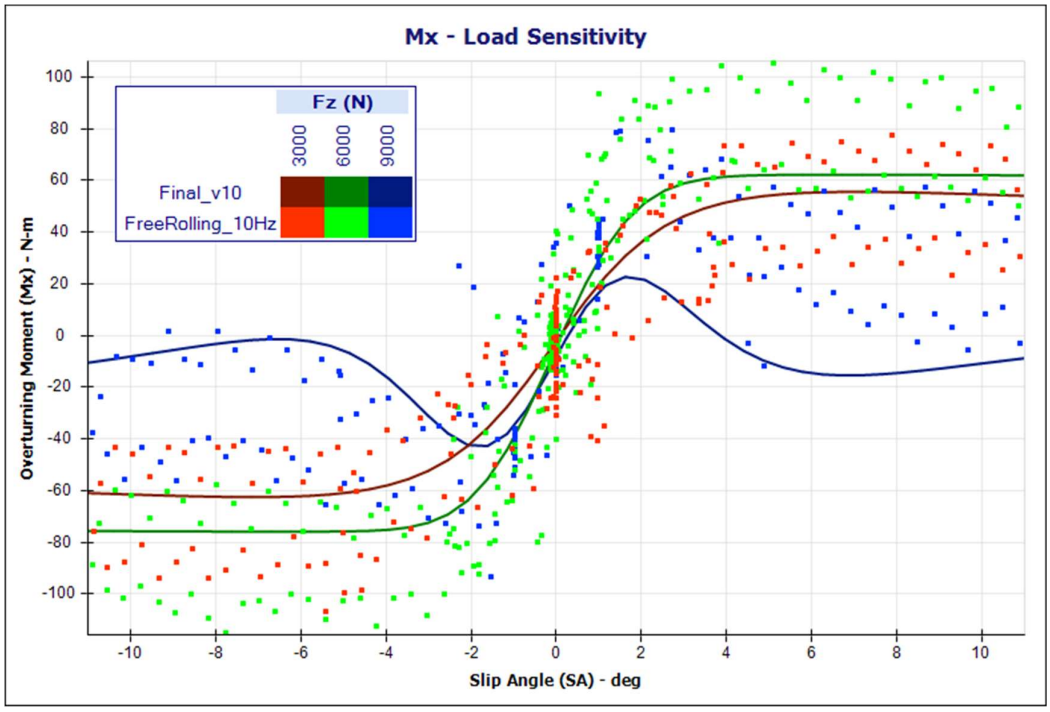

Figure 5.2.6-B. Model (Final_v10) and 'FreeRolling' Data (FreeRolling_10Hz) for Overturning Moment MX (N-m) versus Slip Angle, SA (°); coloured by Vertical Load, FZ (N).

Figure 5.2.6-B shows the MF-Tyre 6.1 model fitted to the free rolling test data. A large amount of noise is still visible in the data; however, this data has significantly less noise than the 'BrkDrv' data. This is a result of Calspan engineers reconfiguring the rig by removing the drive shaft that connects the instrumented hub to the drive motor. Doing so realigns the problematic sensor in the instrumented head, resulting in less noise on the MX channel but disabling the 'BrkDrv' capability. The improved data allows some trends, in this case sensitivity to load and slip angle, to be observed. These trends are also successfully captured in the model. This means the MX combined fit is effectively only MX pure, as there is no slip ratio resistivity due to the model being fitted to free rolling (zero slip ratio) test data. This is the best model sensitivity realistically achievable using the available data, regardless of the test procedure used.

5.2.7 MY Fitting

MY is the rolling resistance component of the MF-Tyre 6.1 tyre model. The rolling resistance of a tyre is extremely small compared to the other forces and moments a tyre can generate. Typically, a road car tyre will generate around 8N of rolling resistance force for every 1,000N

of vertical load applied to it. In order to measure such small forces, specialist rigs must be used in place of the large scale Calspan rig, used here. Rolling resistance rigs are usually drum rigs that are especially set up and calibrated to measure the extremely small rolling resistance forces and moments. As a result of their very precise calibration they are not often used for regular force and moment testing, such as steering or braking and driving. This is because the large forces generated by the tyre during such testing can cause the machine to lose its calibration. Conversely test rigs set up for regular force and moment testing (such as the Calspan rig) are not able to accurately measure the small rolling resistance forces generated by the tyre. As the signal is lost amongst the noise generated by the other, much larger forces being generated. For this reason, no rolling resistance testing is included as part of either the Square Matrix or the GS2MF test procedure and hence appropriate data was not available. As a result, the MY component of the MF-Tyre 6.1 fitting was not completed. The resulting tyre model will therefore be valid for force and moment based vehicle dynamics simulations, but will not be suitable for rolling resistance based simulations such as fuel consumption estimation which is outside of the project scope.

5.2.8 Loaded Radius

Once all the force and moment fitting is complete, the ancillary fits can be carried out. These are much simpler fits typically including only a few coefficients, in this case to model the effective rolling radius, Re, of the tyre.

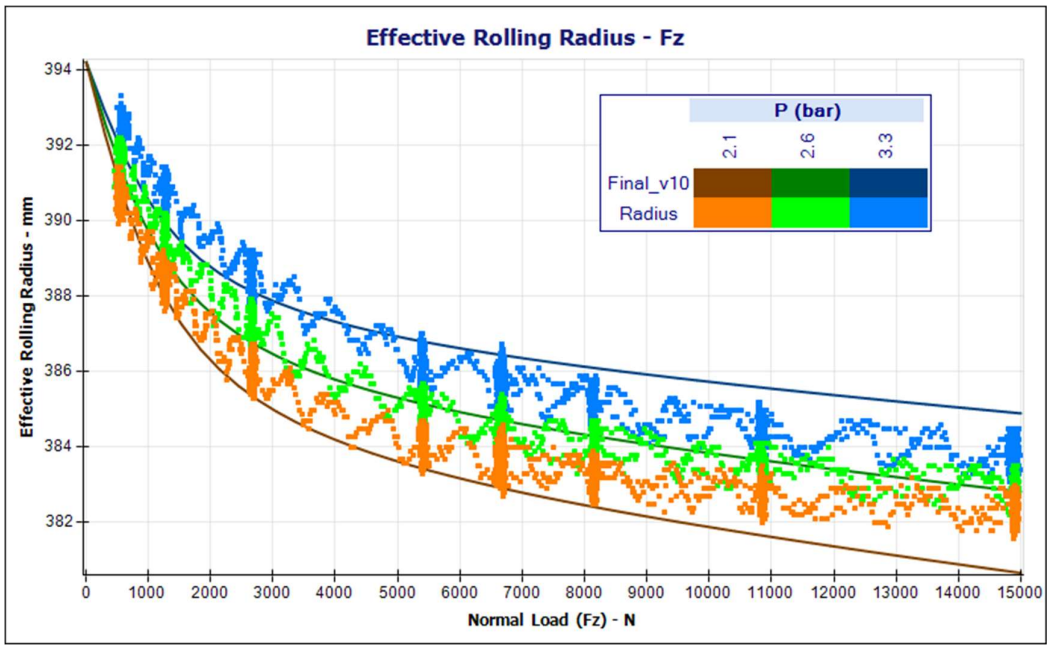

Figure 5.2.8-A. Model (Final_v10) and 'FreeRolling' Data (Radius) for Effective Rolling Radius, Re (mm) versus Vertical Load, FZ (N); coloured by Inflation Pressure, P (bar).

Figure 5.2.8-A shows the test data from the vertical stiffness section of the 'GS2MF FreeRolling' test procedure. The test involves rolling a tyre while the vertical load is stepped to eight different vertical loads. The data shows each of these steps (where the data is clustered) along with the transition between them. The testing is then repeated at three inflation pressures, which is also shown. Overlaid on Figure 5.2.8-A is the MF-Tyre 6.1 tyre model that was fitted to this test data. In this case the model is accurate to within around 1mm of the test data at all but the very highest test loads, where the accuracy is still around 1.5mm. This demonstrates a very good correlation to the test data at each of the three inflation pressures and across the entire range of vertical loads. The precise prediction of ride height is not critical for a road car application such as this as they do not have ground effect aerodynamic packages. If GS2MF were to be adapted for race car applications then additional load cases could be added to the test procedure to improve the model accuracy at high loads; however, this is outside the scope of this project.

5.2.9 Transients

The final stage of the MF-Tyre 6.1 fitting procedure is to complete the longitudinal and lateral stiffness fits which add the relaxation lengths into the tyre model. GS2MF uses two different methods of testing to acquire this data. For longitudinal, the stiffness is measured directly via static longitudinal testing; this is where the tyre is held, unable to rotate on the rig while being dragged longitudinally. Using this method, the longitudinal stiffness can be measured by dividing the longitudinal force data by the longitudinal displacement data. The tyre model is then fitted to this calculated longitudinal stiffness data, as shows in Figure 5.2.9-A.

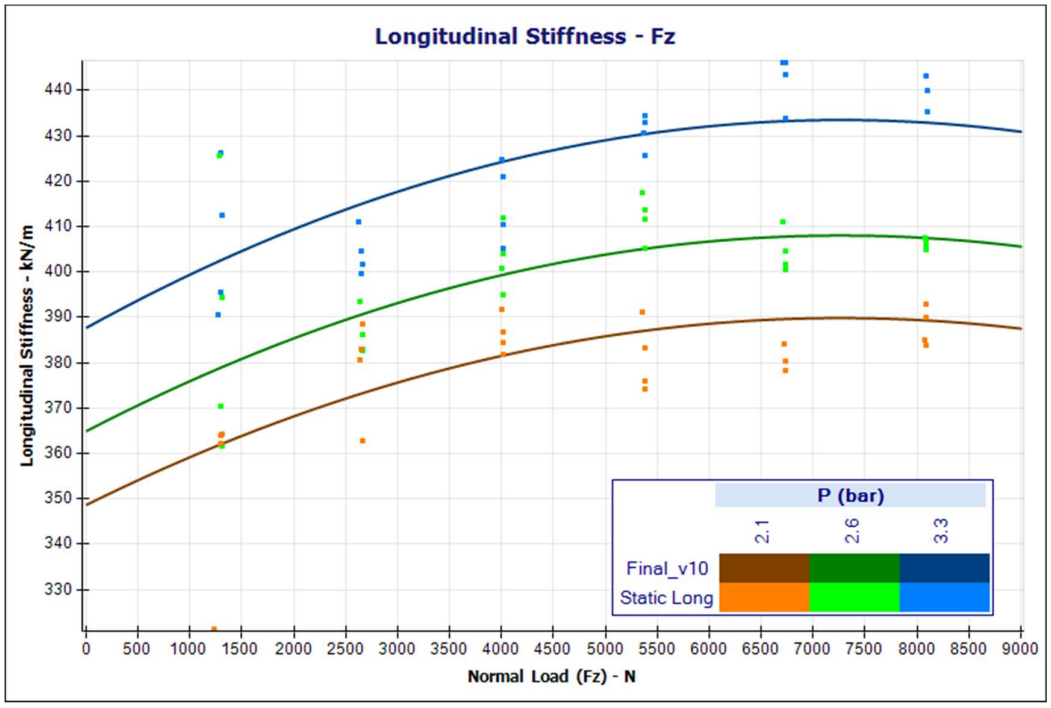

Figure 5.2.9-A. Model (Final_v10) and Static Longitudinal Data (Static Long) for Longitudinal Stiffness, Cx (kN/m) versus Vertical Load, FZ (N); coloured by Inflation Pressure, P (bar).

Figure 5.2.9-A shows that there is a lot of noise in the data, this due to a single value being extracted from each dataset as described in Section 4.3 'GS2MF StaticLong'. In order to reduce the noise, the fitting algorithm groups together and averages the repeated tests, thus minimising any test repeatability issues. As a result of this the tyre model can accurately estimate the longitudinal stiffness; as well as being able to capture both the vertical load and inflation pressure sensitivities.

Once the longitudinal stiffness is modelled (as shown in Figure 5.2.9-A) and the slip stiffness is captured within the FX Pure stage of the fitting; then the MF-Tyre 6.1 tyre model uses these to calculate the longitudinal relaxation length using Equation 5.2.9-A

$$\sigma_x = \frac{K_{xk}}{C_x}$$

Equation 5.2.9-A. Longitudinal relaxation length equation. Where σ_x is the longitudinal relaxation length, K_{xk} is the slip stiffness and C_x is the longitudinal stiffness (Besselink, Schmeitz and Pacejka, 2010).

The lateral stiffness testing is conducted differently to the longitudinal. In this case Step-Steer testing is conducted; this is where the tyre is rolled forward, stopped, then steered to a fixed slip

angle, after which the tyre is accelerated. This test means the lateral force build up over longitudinal distance travelled can be observed and the relaxation length can be measured directly from the data. The relaxation length is the distance travelled until the point at which the lateral force builds up to 63.3% of the saturated lateral force visible in the measurements, meaning it can be measured directly (Laptak, 2006). Using this data, the lateral stiffness can be calculated using Equation 5.2.9-B.

$$\sigma_y = \frac{K_{y\alpha}}{C_y}$$

Equation 5.2.9-B. Lateral relaxation length equation. Where σy is the lateral relaxation length, $K_{y\alpha}$ is the cornering stiffness and C_y is the lateral stiffness (Besselink, Schmeitz and Pacejka, 2010).

Once the lateral stiffness has been calculated using Equation 5.2.9-B the tyre model can be fitted to the data, as shown in Figure 5.2.9.-B.

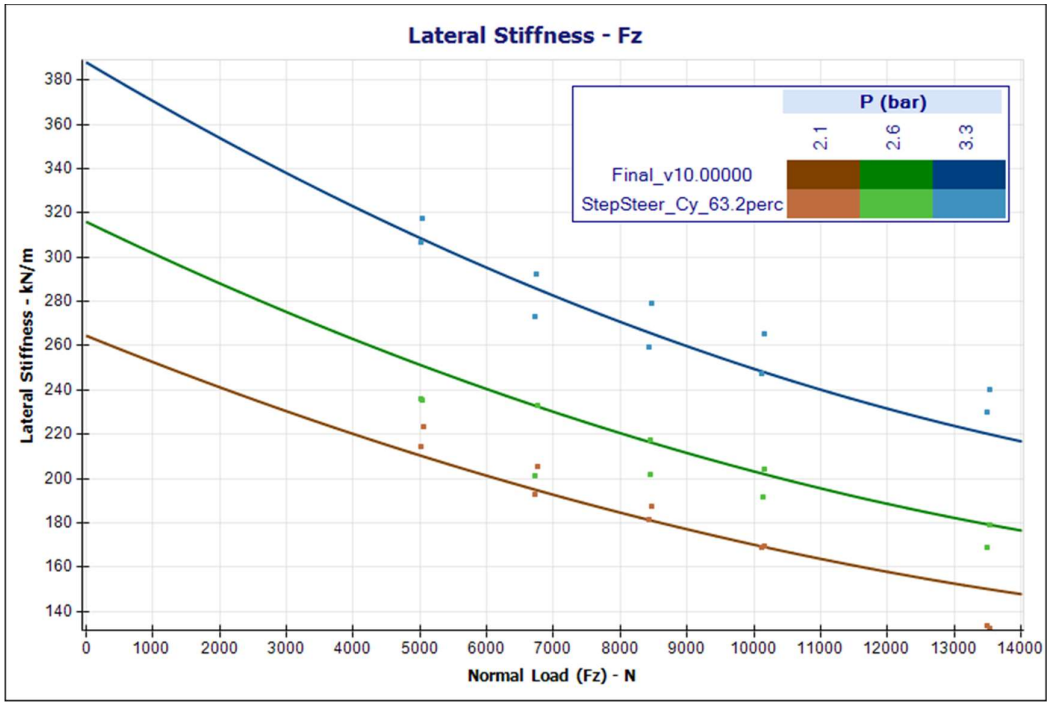

Figure 5.2.9-B. Model (Final_v10) and StepSteer Data (StepSteer_Cy_63.2perc) for Lateral Stiffness, Cy (kN/m) versus Vertical Load, FZ (N); coloured by Inflation Pressure, P (bar).

Figure 5.2.9-B shows that as with the longitudinal stiffness there is some noise in the data. However despite this, the model can accurately predict the lateral stiffness while also capturing its sensitivity to both vertical load and inflation pressure, leading to a good overall tyre model.

5.2.10 Analysis of results and quality of fit

Overall, the MF-Tyre 6.1 fitting process is a simple one to follow and providing all stages are followed correctly, a good quality Magic Formula tyre model can be output and used in vehicle dynamics simulations. The parameterisation process does highlight some limitations with the standard implementation of MF-Tyre 6.1. These include the fact that there is minimal camber

sensitivity included in longitudinal force prediction. Furthermore, the effects of tyre temperature and wear are not captured in the model. If they were, the model could correlate better under combined high slip high load conditions where the tyre heats up quickly. Such efforts could result in a tyre model that is more able to represent the data, leading to more accurate vehicle simulation. Finally, the fitting process highlighted some limitations with the test equipment where high levels of noise made the fitting more challenging in some areas and ultimately caused the tyre model to be less representative of the real tyre behaviour. It is unknown at this stage if development in this area could result in an improved rig design to overcome these limitations. However, this project focuses on the development of the GS2MF test procedure, therefore the developments of the tyre model and test rigs are outside of the projects' scope.

5.3 GS2MF versus Square Matrix Model Comparison

Once an MF-Tyre 6.1 tyre model had been parameterised using the GS2MF data, it was compared to a similar model of the same tyre construction that was built using data obtained using the Square Matrix test procedure. As mentioned in the data comparison section (See Section 4.4 on GS2MF versus Square Matric Data Comparison) a full Square Matrix test was not carried out as the test procedure is very inefficient and costly to run. Instead, a reduced Square Matrix test was run at one pressure (2.6bar) only. It is therefore invalid to compare the pressure sensitivity of these two models built from GS2MF and Square Matrix data, as the Square Matrix derived model is only valid at 2.6bar. Every other aspect of the tyre models should be comparable. However, also mentioned in the data comparison section, the Square Matrix 'BrkDrv' testing caused the tyre to generate so much heat that the rig's thermal pause system timed out, meaning the tyre did not properly cool between each sweep. As a result, some Square Matrix 'BrkDrv' sweeps started with the tyre temperature being above 90°C rather than the target baseline of 45°C. This overheated tyre data was used in the longitudinal sections of the Square Matrix model parameterisation. This means the Square Matrix derived tyre model is far less representative of the tyre's behaviour under normal operating conditions where the tyre will be much cooler. The comparison between the longitudinal performances of the two models in the forthcoming chapters highlights this limitation of the Square Matrix procedure. Theoretically, the Square Matrix testing could be repeated using increasing long pauses between each sweep to allow the tyre to fully cool. However, in practical terms this would greatly inflate the already extremely long and expensive test procedure, therefore running this test could not be justified.

5.3.1 'FreeRolling' Model Comparison

Figures 5.3.1-A shows a free rolling lateral force comparison between the MF-Tyre 6.1 tyre model parameterised using data obtained via the GS2MF test procedure (GS2MF Model),

against an equivalent tyre model parameterised using data obtained via the Square Matrix test procedure (SquareMatrix Model).

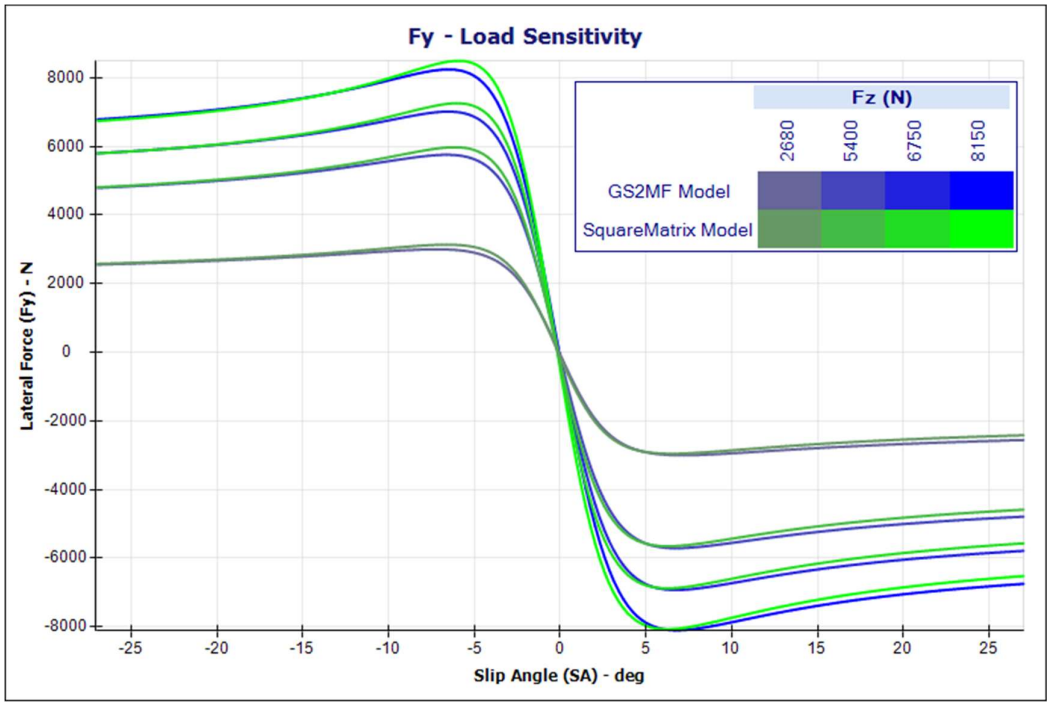

Figure 5.3.1-A. Model Comparison of GS2MF Model and SquareMatrix Model, for Lateral Force, FY (N) versus Slip Angle, SA (°); Showing load sensitivity.

Figure 5.3.1-A shows that the pure lateral load sensitivity of the two tyre models (one built from GS2MF data, the other build from Square Matrix data) are almost identical. The cornering stiffness of the two models is very close at lower slip angles. This deviated very slightly at higher slip angles where the Square Matrix model predicts slightly higher cornering stiffness than the GS2MF model. This leads to the Square Matrix model predicting marginally higher peak grip on the negative slip angle region. However even here, the models were within 2.5% of each other. The drop off after the peak of both models is very similar with the Square Matrix model predicting slightly lower grip in the high slip angle region on the positive side. Overall, these differences are minimal with both models performing similarly. This is expected as during the Square Matrix free rolling test the tyre ran hotter but did not overheat, meaning the data sets used to build the respective model are gathered while the tyre is under similar conditions.

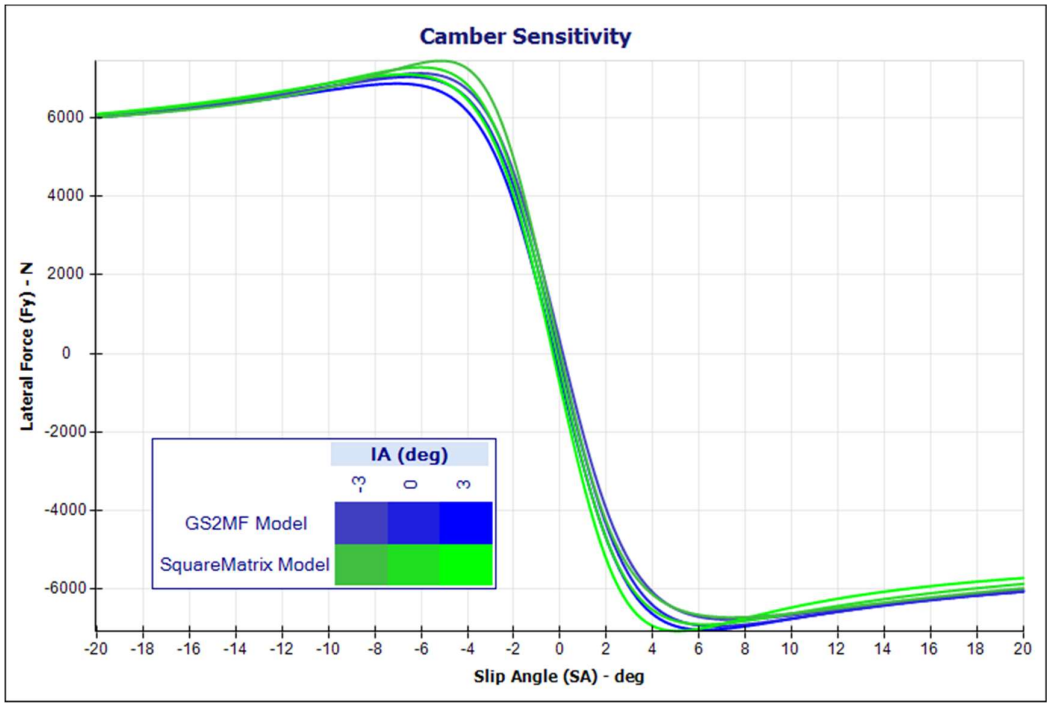

Figure 5.3.1-B. Model Comparison of GS2MF Model and SquareMatrix Model, for Lateral Force, FY (N) versus Slip Angle, SA (°); Showing camber sensitivity.

Figure 5.3.1-B shows that the camber sensitivity of the models is very slightly different; there being an increase in the cornering stiffness on the Square Matrix model compared to the GS2MF model. As with the load sensitivity comparison the differences are slight and the trends are very similar. This slight difference is likely due to the tyre generally running cooler during the GS2MF test as a result of the improved thermal tyre management. This cooler temperature is a more accurate representation of a tyre while in normal use on a road car. This cooler rubber will be slightly stiffer, hence resulting in the increased cornering stiffness compared to the Square Matrix derived tyre model. However, such a minimal variation is unlikely to have any discernible effect during vehicle simulation.

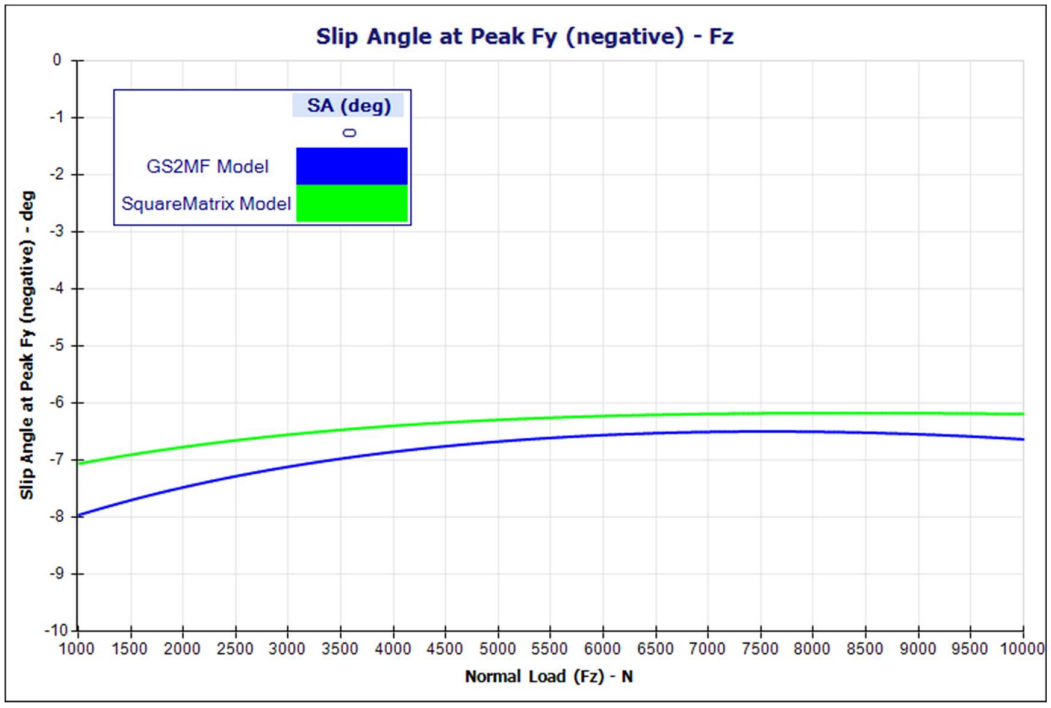

Figure 5.3.1-C. Model comparison of GS2MF Model and SquareMatrix Model, for Slip angle it which peak FY occurs (Negative, turning left), (°) versus Nominal Load, FZ (N).

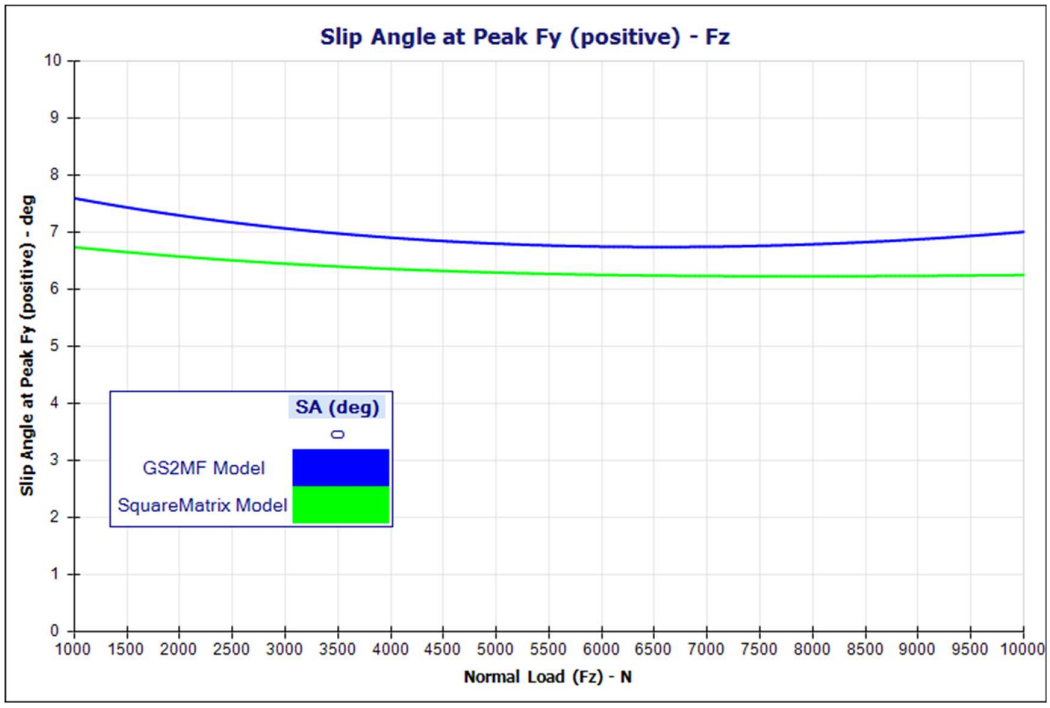

Figure 5.3.1-D. Model comparison of GS2MF Model and SquareMatrix Model, for Slip angle it which peak FY occurs (Positive, turning right), (°) versus Nominal Load, FZ (N).

Figures 5.3.1-C and 5.3.1-D show that the two models predict the tyre's peak grip to occur at slip angles within around 0.7° of each other, over a wide range of vertical loads. This is extremely close and the trends are similar in both the positive and negative slip angle regions. In all cases, the Square Matrix model predicts the peak grip to occur at slightly lower slip angles compared to the GS2MF. This could be due to the tyre running slightly hotter during Square Matrix testing and being slightly less stiff as a result, this leads to a reduced cornering stiffer and peak grip occurring at lower slip angles. However, the magnitude of the difference is small enough not to have any effect during vehicle simulations.

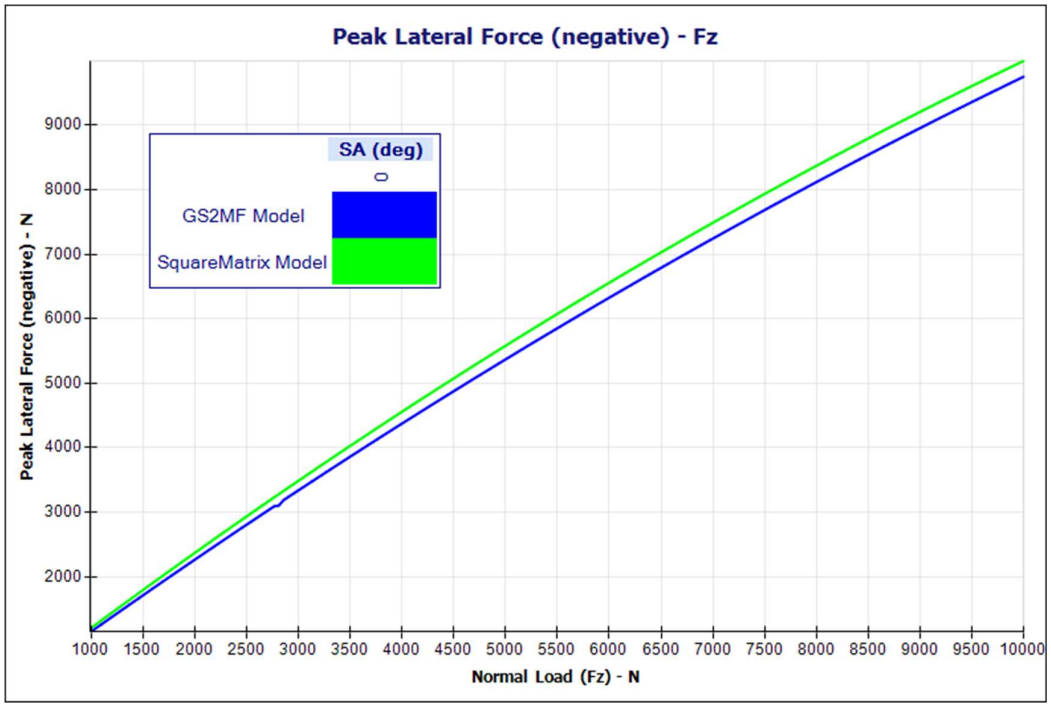

Figure 5.3.1-E. Model Comparison of GS2MF Model and SquareMatrix Model, for Magnitude of peak lateral force (Negative, turning left), (°) versus Nominal Load, FZ (N).

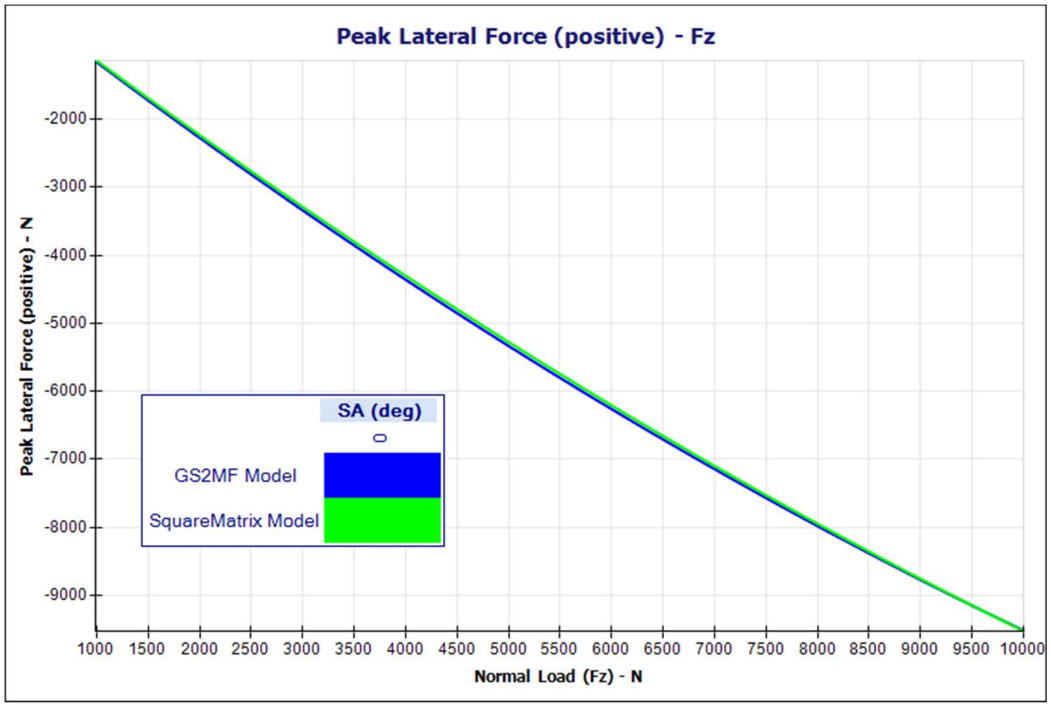

Figure 5.3.1-F. Model Comparison of GS2MF Model and SquareMatrix Model, for Magnitude of peak lateral force (Positive, turning right), (°) versus Nominal Load, FZ (N).

Figure 5.3.1-E and 5.3.1-F show that the two models' predictions of the peak grip magnitudes are extremely close. In the negative slip angle region, the peak lateral grip predictions are always within 1.5% of each other while the vertical load ranges from 1000-10,000N. In the positive slip angle region, the difference between the models is even less, at around 50N across the vertical load range. This is remarkably close considering the models are built from entirely different data sets and this will have no effect at vehicle level. Again, this demonstrates that the tyre model derived from GS2MF data is comparable to the one derived from the Square Matrix testing while being far less expensive to run.

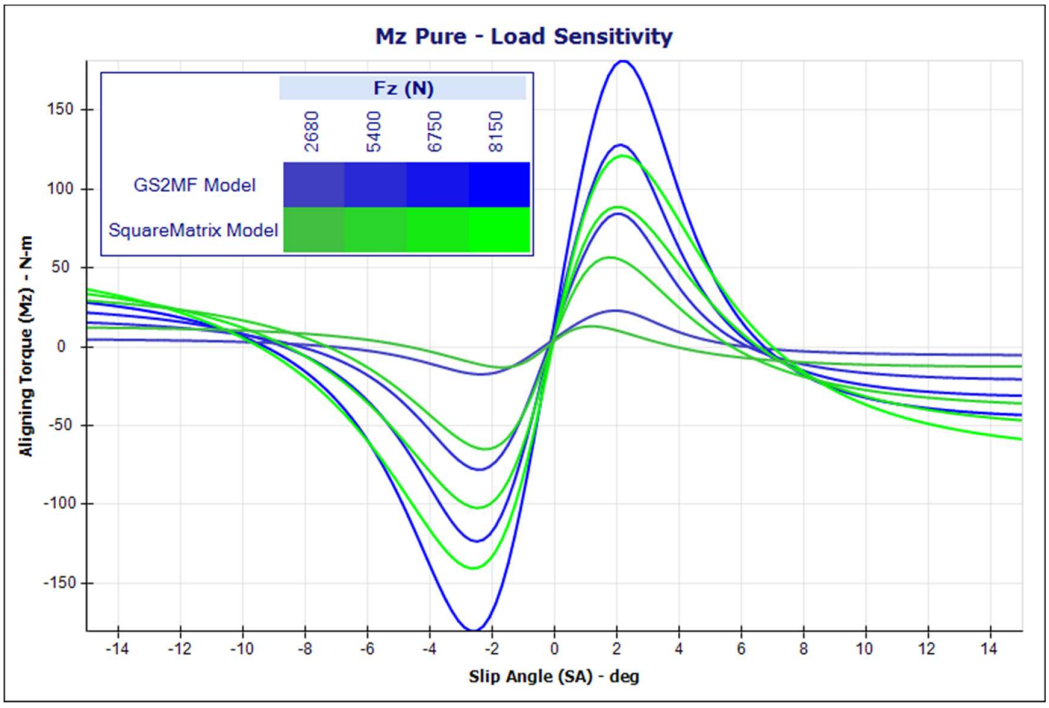

Figure 5.3.1-G. Model Comparison of GS2MF Model and SquareMatrix Model, for Aligning Torque, MZ, (Nm) versus Slip Angle, SA (°); showing load sensitivity.

Figure 5.3.1-G shows that the MZ pure trends between the two models are similar and the slip angle locations of the peaks are also similar; however, there are significant differences of up to 50% between the magnitudes of the MZ peaks predicted by the two models. This is due to the unavoidably high levels of noise shown in the MZ channels of both data sets. As a result of the noise, it is difficult for the optimisation algorithm to converge on an accurate fit from either data set. This therefore demonstrates a general limitation in the accuracy of either tyre model brought on by limitations in the test rig and data quality. However, the discrepancy is in the order of 50Nm of Mz, while the vertical load ranges from 2,680 to 8,150N. Therefore, in practical terms this is a very minor inaccuracy and is unaffected by using GS2MF rather than the Square Matrix test method.

The tyre models are not expected to be identical to each other as they are parameterised from two different data sets obtained using different test methods; however, they should perform similarly. This analysis demonstrates that in free rolling, the two models are very similar overall, with the cornering stiffness as well as magnitude and location of peak grip all correlating remarkably well. There is a small difference in the camber sensitivity between the two models, where the cornering stiffness increases more with camber in the Square Matrix model compared to the GS2MF. The only significant difference between the two models is the MZ output. However, this is ultimately due to the noise in the MZ channels of both data sets

used to parameterise the models, rather than a result of either test procedure. Overall, this means that the tyre model produced using GS2MF data is comparable to the equivalent model produced using the far most expensive Square Matrix data.

5.3.2 'BrkDrv' Model Comparison

Despite the overheating of the tyre during the 'BrkDrv' testing, a comparison of the longitudinal performances of the tyre models' was attempted. The Square Matrix test procedure does not define a baseline temperature or any use of a logic system to cool the tyre, which causes significant practical problems. Prior to running the test, estimated pauses can be added after each sweep to allow the tyre to cool. However, the length of these pauses depends on how hot the tyre gets during the preceding sweep. This peak temperature is dependent on the tyre's grip, with more grip resulting in more friction induced heat. However, the grip is the very attribute being measured and is hence not known before testing commences. Therefore, an iterative approach could be used, where the test is repeated several times and the pause lengths are tuned after each run to manage the temperature. However, this is extremely inefficient and costly to run, while also being impractical due to the number of physical tyres that are available. To avoid this, the thermal logic system was used, despite not explicitly being stated in the Square Matrix test procedure.

Even when using the thermal logic system, the Square Matrix test caused additional tyre overheating issues. This was because the procedure calls for the tyre to be tested under conditions of extremely high sliding energy, such as the combined high load high slip tests. During these tests, the tyre reaches very high temperatures and requires excessively long pauses to fully cool. This caused the thermal logic system to time out during the excessively long thermal pauses and trigger the next sweep before the tyre had fully cooled. The time out feature is included to avoid the scenario of a never-ending pause; where the system continually waits for an impossible condition to be met, such as the tyre reaching a temperature that is lower than the ambient temperature. During the Square Matrix testing, the tyre reached such high temperatures that the thermal logic system thought the specified 45°C baseline temperature would not be met and triggered the following sweep while the tyre was still above the baseline. Overall, this resulted in Square Matrix testing being conducted while the tyre was at higher temperatures than it was at during GS2MF testing. Unfortunately, despite continued and repeated efforts, this proved unavoidable without significantly altering the Square Matrix test itself, which would have invalidated the comparison. As a result, most of the forthcoming comparison between the Square Matrix and GS2MF derived tyre models show that the they are very different.

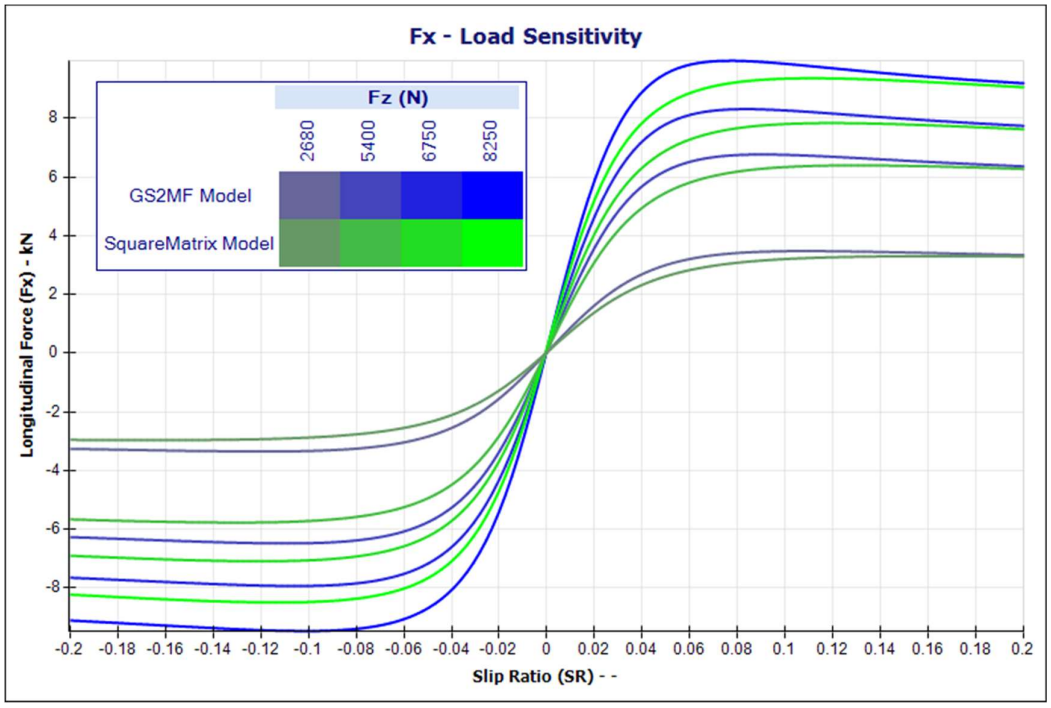

Figure 5.3.2-A. Model Comparison of GS2MF Model and SquareMatrix Model, for Longitudinal Force, FX, (N) versus Slip Ratio, SR (-); Showing load sensitivity.

Figure 5.3.2-A shows a pure longitudinal comparison between the tyre model parameterised using Square Matrix data and the model parameterised using GS2MF data. As expected, the results are very different with the Square Matrix derived tyre model predicting lower longitudinal forces compared to the GS2MF model. This is because the tyre had overheated during the Square Matrix 'BrkDrv' testing and was thus operating outside of its optimal thermal conditions and hence the tyre generated less grip. This reduction in grip was captured in the tyre model that was parameterised using this data.

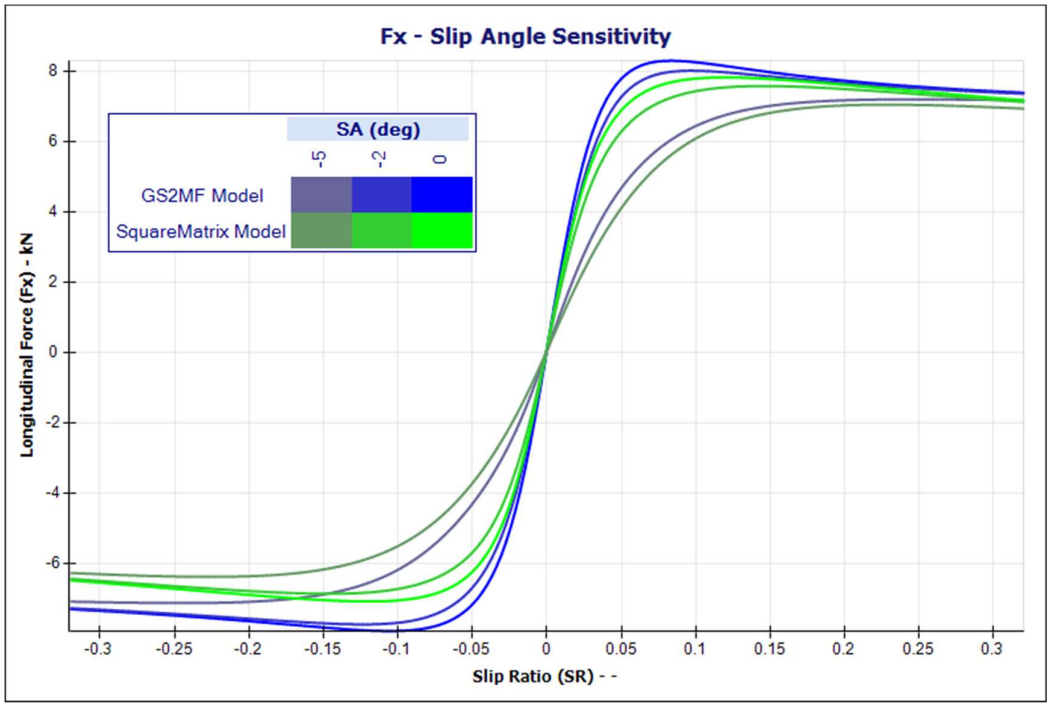

Figure 5.3.2-B. Model Comparison of GS2MF Model and SquareMatrix Model, for Longitudinal Force, FX, (N) versus Slip Ratio, SR (-); Showing slip angle sensitivity.

Figure 5.3.2-B shows how the two tyre models compare in combined longitudinal performance. Again, it can be seen that the Square Matrix model generates significantly less grip than the GS2MF model, due to the tyre overheating during the Square Matrix 'BrkDrv' testing.

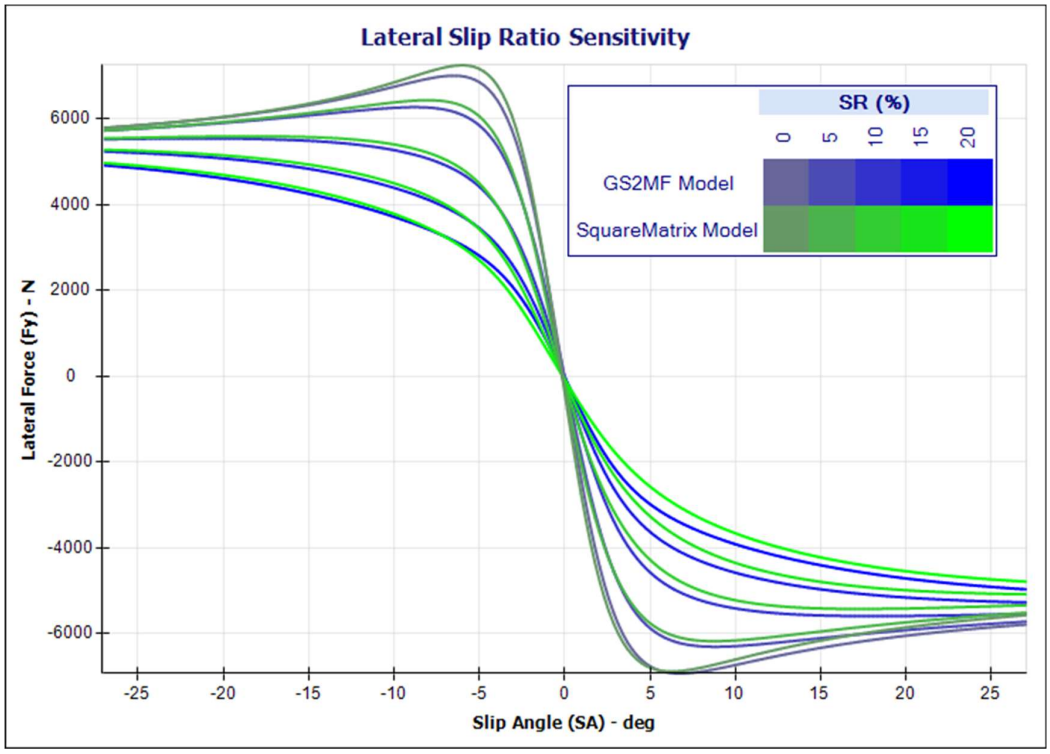

Figure 5.3.2-C. Model Comparison of GS2MF Model and SquareMatrix Model, for Lateral Force, FY, (N) versus Slip Angle, SA (°); Showing slip ratio sensitivity.

Figure 5.3.2-C shows how the tyre models compare under a combined slip condition, where the lateral force sensitive to slip angle can be observed while held at a given slip ratio. This is a load case where during either test procedure, the tyre experiences very high sliding energy and hence very high temperatures. Therefore, the tyre is hot during either test procedure and hence the problems with cooling the tyre during Square Matrix testing had less influence on the results. For this reason, the plot shows a reasonably good correlation between the two tyre models. In some cases, matching up perfectly and at worst being around 3% different in peak lateral force at -5° of slip angle and up to 15% different at +5° of slip angle. Generally, in the negative slip angle region, the two models are reasonably similar and in the positive slip angle region the models are still quite similar. However, the Square Matrix model is showing slightly less lateral force than the GS2MF model due to the overheating. Overall, this demonstrates a reasonable correlation in the lateral force sensitivity to slip ratio during combined slip conditions.

As discussed, the 'BrkDrv' performance of the two models under ideal conditions could not be assessed due to the tyre overheating during the Square Matrix 'BrkDrv' testing. However, despite this, there is some evidence that the tyre models would correlate if the tyre was cooler during the Square Matrix test. This is demonstrated in Figure 5.3.1-A where the lateral forces output by the two models are very similar to one another and again in the combined slip

comparison in Figure 5.3.2-C. However, the design of the Square Matrix test procedure is such that keeping the tyre cool is practically impossible without a vastly extended test to accommodate the extensive cool down times. Doing so would likely cause the resulting tyre models to be comparable. However, the excessively long Square Matrix test procedure would then be extremely expensive to run and was not within the budget of the project.

5.3.3 Model Comparison Summary

Overall, the two tyre models; one built from GS2MF data and the other built from Square Matrix data, perform similarly in some regions and differently in other regions. The pure lateral performance of the two models is generally similar with little difference between them. Cornering stiffness, as well as magnitude and location of peak grip are all very similar. There is a small difference in camber sensitivity and the aligning torque of the two models are different. However, this is likely due to the noise in both data sets and resulting poor quality fits, rather than being due to either test procedure. Conversely the assessment demonstrated that there are more noticeable differences between the longitudinal performances of the two models. As discussed, this is likely due to the tyre overheating during the Square Matrix testing. This could be resolved by further extending the pause times between each sweep to allow the tyre to cool; which will likely bring the Square Matrix data into line such that it matches the GS2MF data and hence the derived models are also likely to be comparable. However, while numerous attempts were made to aid the tyre cooling during Square Matrix testing without altering the test itself, such as using the thermal logic system and somewhat longer thermal pauses. Adding further pause times would significantly increase the already vastly inflated cost of Square Matrix testing as well as use up a significant portion of the available rig time. In practice, this is not practical due to time and cost.

'GS2MF FreeRolling' and 'GS2MF BrkDrv' required 6,955s (just under two hours) of rig time to run them both. While the four force and moment components of Square Matrix testing took a total of 8,151s (around two and a quarter hours) to run. However, the Square Matrix testing was run at a single inflation pressure only, whereas GS2MF testing includes three inflation pressures to allow for an improved MF-Tyre 6.1 tyre model with pressure interpolation. In order to acquire equivalent data to be comparable to GS2MF the Square Matrix test procedure would need to be repeated three times, once at each pressure. This will bring the total Square Matrix rig time up to 24,453s (around six and three-quarter hours). Further to that, additional thermal pauses need to be added to the Square Matrix test procedure to address the overheating issues, which further increase the test duration. Overall, GS2MF could gather all required data, suitable for parameterising comparable tyre models using 72% less rig time compared to Square Matrix testing. A more detailed brake down of the test durations can be found in Section 4.5 on GS2MF

versus Square Matrix Test Duration Comparison. In addition to the reduction on test duration, GS2MF is also shown to delivery higher quality data, this is largely due to the improved tyre temperature regulation compared to Square Matrix testing.

6.0 Conclusions and Future Work

6.1 Conclusions

The initial background research and literature review highlighted that there was a need for more published research material on tyre testing procedures and specifically test procedures for the parameterisation of Magic Formula tyre models. This has largely been addressed with the development and publication of GS2MF.

The procedure utilises several completely new and innovative methodologies while also building on other pre-existing ideas. The biggest breakthrough came from linking the rig testing more precisely to the load cases a tyre will be subjected to when mounted to a vehicle. This included linking the vertical load and slip angle conditions such that they match that of the right-side tyres on a car (these can later be mirrored to represent the left side tyres). As a result of this, several unnecessary sections of testing could be removed completely as they went into load conditions that were unobtainable in the real world; this led to an immediate reduction in the test duration and cost.

Another key breakthrough came when seeking to overcome the inherent compromise that exists when running slip angle or slip ratio sweeps at any constant slip rate. A fast slip rate results in excessive on-centre hysteresis meaning the stiffness cannot be accurately measured; while a slow slip rate results in the tyre spending prolonged periods of time at high slip conditions leading to excessive wear and temperature build-up, which then takes time to dissipate. This issue was comprehensively addressed using an innovative variable rate sweep. This sweep used a slow slip rate ('low rate') close to zero slip and a faster slip rate ('high rate') further from zero, resulting in low hysteresis throughout, as well as lower peak temperatures. These lower temperatures mean less time was required for the tyre to cool between sweeps, therefore increasing the overall test efficiency and reducing costs.

Several other key methodologies were also included in GS2MF. Such as a thermal logic system which holds the tyre at a zero-slip condition after each sweep for as long as required until the tyre cools to a predetermined baseline temperature. This ensures that every sweep begins with the tyre at the same temperature, reducing test variation. 'Graph Sweeps' are included in GS2MF, these are identical sweeps repeated at the start and end of the test to assess any change in the tyre itself as a result of the testing. Furthermore, additional components work to ensure the tyre is appropriately warmed up prior to testing, while other sections gather data pertaining to the tyre's longitudinal and lateral relaxation length as well as the vertical stiffness.

All these components and methodologies are compiled together to form the 'GS2MF FreeRolling', 'GS2MF BrkDrv' and 'GS2MF StaticLong' test procedures. Together, these tests gather all the data required to parameterise a fully populated MF-Tyre 6.1 tyre model. This includes free rolling, longitudinal and combined load cases both in steady state and inclusive of

relaxation lengths, vertical stiffness and inflation pressure variation. Pre-existing test procedures typically only cover some of these aspects of tyre modelling, often missing out the inflation pressure variation. This means that when the user wants to include the inflation pressure the whole test must be repeated three times (once at each pressure), significantly reducing test efficiency. GS2MF facilitates this by including testing at three pressures within the standard procedure. At vehicle level, this means inflation pressure tuning can be conducted more easily.

Also demonstrated is how the resulting GS2MF test data can successfully be used to parametrise a representative MF-tyre 6.1 tyre model. This parametrisation process follows similar steps regardless of the selected data set. With the demonstration shown using the commercially available OptimumTire fitting software from OptimumG, Denver CO; however, other MF-Tyre 6.1 parameterisation software could also be used.

Overall, GS2MF is shown to result in a full suite of test data using 73% less rig time than the presented Square Matrix test procedure. In most cases this equates to an equally large cost reduction. Furthermore, GS2MF achieves this with an increase in the general data quality above that of the Square Matrix data that often caused the tyre to overheat. This is demonstrated by the improved regulation of tyre temperature and the overall reduction in tyre wear, which reduces the test variation during the procedure. For real world engineering applications, this means that nearly four times more unique tyre models can be delivered using a given test budget. Alternatively, a given number of tyre models can be delivered at around 27% of the cost, compared to more traditional test methods. With test rigs being very expensive pieces of equipment to use, this represents a highly significant cost saving and overall efficiency gain resulting from the novel test procedures developed in this study.

6.2 Future Work

While the project is complete and GS2MF has reached a level of design maturity where it is valuable in a tyre engineering setting; there remains numerous potential ways to improve upon it.

1) The SoVaMotion flat-trac rig can run free rolling and brake drive tests without the need to reconfigure the rig. Whereas Calspan, must physically decouple the drive motor from the rig to ensure a pure free rolling test condition. The added flexibility of the SoVaMotion system means there does not need to be a distinct separation of the ‘GS2MF FreeRolling’ and ‘GS2MF BrkDrv’ test procedures. Instead, these could be integrated together to better manage the heat build-up and tyre wear. As a result, with additional research it might be possible to run just one test on one tyre to obtain all the necessary data. However, this new test could then only be run at SoVaMotion and not

Calspan, which could induce a risk management problem due to over reliance on any one test facility.

2) The comparison of GS2MF with an existing Square Matrix test procedure was not ideal due to the tyre overheating during the Square Matrix testing. This was realised at the time and thermal pauses were added to the Square Matrix test procedure in a partly successful attempt to address the issue. Due to its inefficient design, properly managing the tyre temperature would significantly inflate the already expensive Square Matrix testing costs and was hence not completed. With additional funds this testing could be carried out and a direct comparison of GS2MF versus Square Matrix would be possible. However, it remains difficult to justify the significant expense of running a knowingly inefficient test procedure simply to benchmark against an improved procedure.

3) The variable rate sweep analysis concluded that the optimal 'high rate' (that being the slip angle rate used in the fastest section of the sweep) was that of the highest rate possible on the available test equipment. It is therefore possible that the actual ideal rate is somewhere higher than what was tested. With improved test equipment, it would be possible to discover exactly what the optimal rate is. However, knowing this true optimal 'high rate' will be of minimal engineering value, as in practical applications the rate will remain limited by the capability of the available test equipment.

4) During the longitudinal variable rate analysis, it was concluded that the 'high rate' was limited by the tyre slipping on the rim. If this issue could be overcome (perhaps using adhesives or higher friction wheel bead designs), then a more efficient variable rate longitudinal sweep could be developed. This could facilitate the use of faster slip rates, leading to reduced time spend at high slip conditions, lower peak temperatures, shorter cool down times and thus increase test efficiency. However, any increase in test efficiency will need to be balanced against the increased cost and complexity of the unusual tyre mounting methods.

5) GS2MF was developed specifically for the MF-Tyre 6.1 tyre model, which is a non-thermal empirical tyre model. However, there are numerous thermal versions of the Magic Formula tyre model developed by various institutions around the world, such as Dr. George Mavros at Loughborough University (Mavros, 2017). It could be possible to add additional tests into GS2MF to obtain data pertaining to the thermal sensitivity of

the tyre. A GS2MF+T (plus thermal) could then be used to gather data to parameterise such thermal tyre models.

6) The GS2MF static longitudinal testing could only be run at relatively low vertical loads, this was due to the sand paper tearing during the test. Further research into the mounting of the sand paper using stronger adhesives or tougher backing material could facilitate the static longitudinal testing at higher loads. If successful, this would ultimately improve the high load accuracy of the longitudinal relaxation length in the resulting MF-Tyre 6.1 tyre model.

7) GS2MF has been developed specifically for road car applications. With further development, the procedure could be modified to better suit the acquisition of test data pertaining to other tyre applications, such as race car tyres or truck tyres. This was outside the scope of this project but could be included in the future.

8) The current Variable Rate Sweep steps between two distinct slip angle rates (the 'high rate' and the 'low rate') at a given threshold. This approach could be further developed into a 'Continually Varying Rate Sweep', where the transition between the high and low slip rates occurs smoothly. In such a sweep, the slip rate would change dynamically from close to 0°/s at 0 slip angle, to the highest possible slip rate at higher slip angles. Doing so may lead to further efficiency gains in both the 'FreeRolling' and 'BrkDrv' test procedures. An example of a Continually Variable Rate Sweep is shown in Figure 6.2-A.

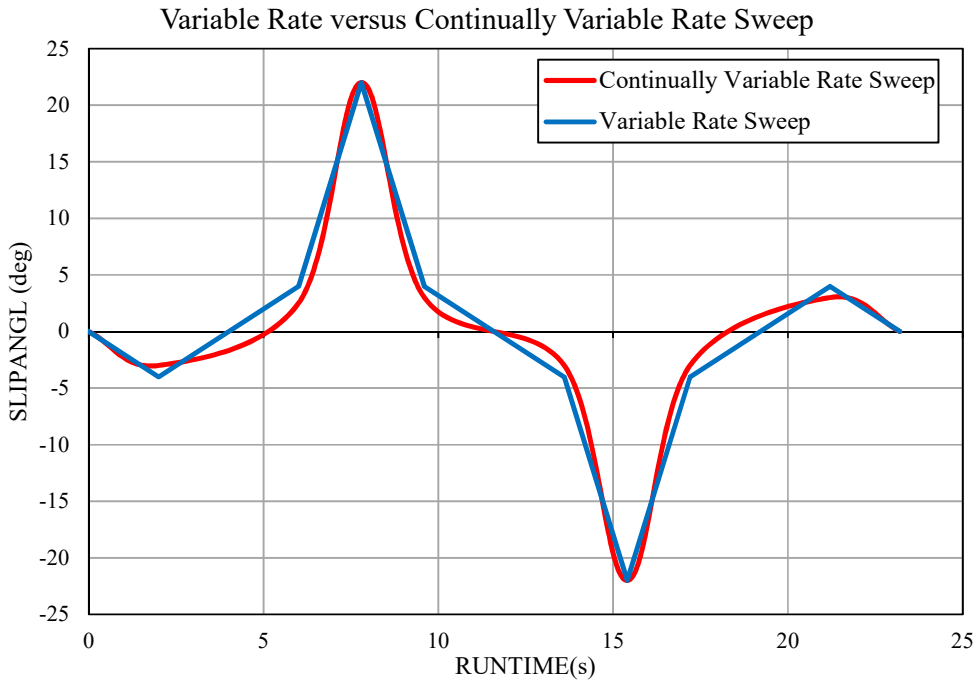

Figure 6.2-A. Comparison between the Variable Rate Sweep and a potential Continually Variable Rate Sweep.

References

Alagappan, V. A., Narasimha Rao, K. V. and Krishna Kumar, R. (2014). A comparison of various algorithms to extract Magic Formula tyre model coefficients for vehicle dynamics simulations. Vehicle System Dynamics: International Journal of Vehicle Mechanics and Mobility.

Arrigoni, S., Cheli, F., Gavardi, P. And Sabbioni, E. (2017). Influence of Tire Parameters on ABS Performance. Tire Science and Technology, TSTCA, Vol. 45, No. 2. pp.121-143.

Bakker, E., Nyborg, L. and Pacejka, H. B. (1987). Tyre modelling for use in vehicle dynamics studies. SAE Technical Paper 870421.

Bakker, E., Pacejka, H. B. and Lidner, L. (1989). A new tyre model with application in vehicle dynamics studies. SAE Technical Paper 890087.

Besselink, I. J. M., Schmeitz, A. J. C. and Pacejka, H. B. (2010). An improved magic formula/Swift tyre model that can handle inflation pressure changes. Vehicle System Dynamics: International Journal of Vehicle Mechanics and Mobility, 48:1. pp.337–352.

Best, M. C., (2010). IdentiFYing tyre models directly from vehicle test data using an extended Kalman filter. Vehicle System Dynamics: International Journal of Vehicle Mechanics and Mobility. 48:2, pp.171-187.

Bird, K., and Martin, J., (1973). The CALSPAN Tire Research Facility: Design, Development, and Initial Test Results. Society of Automotive Engineers, SAE Technical Paper 730582.

Blundell, M. (2000). The modelling and simulation of vehicle handling part 3: tyre modelling. Proc IMechE Part K: J Multi-body Dynamics, 214: pp.1–32.

Blundell, M. and Harty, D. (2006). Intermediate tyre model for vehicle handling simulation. Proc IMechE Part K: J Multi-body Dynamics, 221(1): pp.41–62.

Braghin, F., Cheli, F. and Sabbioni, E., (2007). Environmental effects on Pacejka's scaling factors. Vehicle System Dynamics: International Journal of Vehicle Mechanics and Mobility. 44:7, pp.547-568.

Braghin, F., Cheli, F. and Sabbioni, E., (2011). Identification of Tire Model Parameters Through Full Vehicle Experimental Tests. Journal of Dynamics Systems, Measurement, and Control. 133.

Buisson, J. (2006). Michelin indoor characterisation for handling applied to mathematical formulae. Aachener colloquium fahrzeug- und motorentechnik, Aachen, Germany.

Cabrera, J. A., Ortiz, A., Carabias, E. and Simon, A. (2004). An Alternative Method to Determine the Magic Tyre Model Parameters Using Genetic Algorithms. Vehicle System Dynamics: International Journal of Vehicle Mechanics and Mobility, 41:2, pp.109-127.

Cadiou, J. C., El Hadire, A. and Chikhi, F. (2004). Non-linear tyre forces estimation based on vehicle dynamics observation in a finite time. Proceedings of the Institution of Mechanical Engineers, Part D: Journal of Automobile Engineering, Vol 218, Issue 12. pp.1379–1392.

Calspan. (2016). Force and Moment Testing. [online]. Available at: http://www.calspan.com/services/tire-performance-testing/force-moment-testing/ [Accessed 16 Feb. 2016]

Calspan History. (2010). Calspan, History in Providing Independent Engineering Services. [online]. Available at: http://www.calspan.com/company/history/ [Accessed 1 Aug. 2017]

Camber Ridge. (2017). Camber Ridge Home Page. [online]. Available at: http://www.camberridge.com/ [Accessed 1 Aug. 2017]

The Contact Patch – Contact Patch. (2017). Book : The Contact Patch, C.2020 – The Contact Patch. [online] Available at: http://the-contact-patch.com/book/road/c2020-the-contact-patch [Accessed 28 Jul. 2017].

The Contact Patch – Introduction. (2017). Book : The Contact Patch, G.3000 – Introduction. [online] Available at: http://the-contact-patch.com/book/general/g3000-introduction [Accessed 8 Aug. 2017].

The Contact Patch – Rubber Tyres. (2017). Book : The Contact Patch, C.1610 – Rubber Tyres. [online] Available at: http://the-contact-patch.com/book/road/c1610-rubber-tyres [Accessed 28 Jul. 2017].

Coleman, T. F. and Li, Y. (1996). An Interior Trust Region Approach for Nonlinear Minimization Subject to Bounds. Society for Industrial and Applied Mathematics, (6:2). pp.418-445.

Conte, D., (2010). Tyre Parameter Identification from road tests on a complete vehicle. MSc. Delft University of Technology.
Delft-Tyre. (2017). Delft-Tyre All-in-one solution for tyre modelling. [online] Available at: https://www.tassinternational.com/delft-tyre [Accessed 3 Aug. 2017].

Durand-Gasselin, B., Dailliez, T., Mössner-Beigel, M., Knorr, S. and Rauh, J. (2010). Assessing the thermo-mechanical TaMeTirE model in offline vehicle simulation and driving simulator tests. Vehicle System Dynamics: International Journal of Vehicle Mechanics and Mobility, 48:S1, pp.211-229.

Ervin, R. D., MacAdam, C. C. (1981). *Truck tire traction. Final report.* Ann Arbor, Mich.: University of Michigan, Highway Safety Research Institute.

ETRTO Standards Manual. (2017). Standards Manual 2017, The European Tyre and Rim Technical Organisation.

Fiala, E. (1954). Lateral Forces on Rolling Pneumatic Tires. Zeitschrift V.D.I. 96, pp. 973-979.

FKA Flat-Trac IV CT plus. (2016). FKA FKA Flat-Trac IV CT plus. [pdf]. Aachen Germany: Forschungsgesellschaft Kraftfahrwesen mbH Aachen.

FKA Tyres in Motion. (2013). Driving Innovations. [pdf]. Aachen, Germany: Forschungsgesellschaft Kraftfahrwesen mbH Aachen.

Gallrein, A., Baecker, M., Burger, M. and Gizatullin, A. (2014). An advanced flexible realtime tire model and its integration into Fraunhofer's driving simulator. SAE paper 2014-01-861.

Gent, A., Walter, J. (2005). The Pneumatic Tire. Akron OH: National Highway Traffic Safety Administration.

Gipser, M. (1999). A new fast tire model for ride comfort simulations. Berlin, Germany: 14th European ADAMS users' conference, pp.1–11.

GM Corporate Newsroom. (2012). GM and Partners Burn Rubber to Improve Fuel Economy. [online]. Available at: https://media.gm.com/media/us/en/gm/home.detail.html/content/Pages/news/us/en/2012/Nov/1121_tire_research.html [Accessed 2 Aug. 2017]

Gnadler, R., Huinink, H., Frey, M., at al. (2005). Traction measurements on snow with internal drum test bench. ATZ Worldwide. Volume 107, Issue. pp.11–14.

Greßler, M., Gauterin, F., Hartmann, B. and Wies, B., (2007). Influencing factors on force transmission of tires on snow tracks. [pdf]. Karlsruhe, Germany: Karlsruhe Institute of Technology.

Guo, H., Bastien, C., Blundell, M. and Wood, G. (2014). Development of a detailed aircraft tyre finite element model for safety assessment. J Mater Des 2014; 53: pp.902–909.

IDIADA Tire Modeling. (2016). Tire Modeling MF and FTire model. [pdf]. Tarragona, Spain: IDIADA. Available at: http://www.applusidiada.com/en/service/Tyre_development-1340256099065 [Accessed 31 July. 2017].

IPG CarMaker. (2017). CarMaker: Virtual Testing of Automobiles and Light-Duty Vehicles. [online] Available at: https://ipg-automotive.com/products-services/simulation-software/carmaker/ [Accessed 3 Aug. 2017].

Jenniges, R. L., Zenk, J. E., and Maki, A. E., (2003). A New System for Force and Moment Testing of Light Truck Tires. Society of Automotive Engineers, SAE 2003-01-1272.

Karlsruhe Testing Facilities. (2017). Karlsruhe Testing Facilities Institute of Vehicle Systems Technology – FAST. [pdf]. Karlsruhe, Germany: Karlsruhe Institute of Technology.

Kasprzak, E., Lewis, K. and Milliken, D. (2006). Inflation Pressure Effects in the Nondimensional Tire Model. Society of Automotive Engineers, 2006-01-3607.

Kistler Wheel Force Transducers, (2016). Kistler Wheel Force Transducers and RoaDyn Wheel Force Sensors for Optimal Fatigue Strength. [online] Available at: https://www.kistler.com/bw/en/products/products-by-applications/durability-testing-products/ [Accessed 31 July. 2017].

Langer, W., and Potts, G., (1980). Development of a Flat Surface Tire Testing Machine. Society of Automotive Engineers, SAE Technical Paper 800245.

Laptak, B. (2006). Control Basics. In: B. Laptak, ed., Instrument Engineers' Handbook, Vol. 2: Process Control and Optimization, 4th Edition. Boca Raton, FL USA.

Lorenz, B., Persson, B. N. J., Fortunato, G., Giustiniano, M. and Baldoni, F. (2013). Rubber friction for tire tread compound on road surfaces. Journal of Physics: Condensed Matter, 25, 095007.

MATLAB Optimization Toolbox. (2017). Mathworks, MATLAB Optimisation Toolbox: Solve linear, quadratic, integer, and nonlinear optimization problems. [online] Available at: https://www.mathworks.com/products/optimization.html [Accessed 7 Aug. 2017].

Mavros, G. (2017). Advanced Thermo-Frictional Tyre Modelling for Vehicle Dynamics. IMechE Seminar on Ride and Handling, Birmingham, England.

Miller, S., Youngberg, B., Millie, A., Schweizer, P. and Gerdes, J. (2001). Calculating Longitudinal Wheel Slip and Tire Parameters Using GPS Velocity. Arlington, VA: American Control Conference, pp.25-27.

MSC Adams. (2017). Adams, The Multibody Dynamics Simulation Solution. [online] Available at: http://www.mscsoftware.com/product/adams [Accessed 3 Aug. 2017].

MTS Flat-Trac Classic. (2005). MTS Flat-Trac Classic Tire Test System. [pdf]. Eden Prairie, MN: MTS Systems Corporation. Available at: https://www.mts.com/cs/groups/public/documents/library/dev_003375.pdf [Accessed 2 Aug. 2017]

MTS Flat-Trac CT Plus. (2005). MTS Flat-Trac CT Plus Tire Test System. [pdf]. Eden Prairie, MN: MTS Systems Corporation. Available at: https://www.mts.com/cs/groups/public/documents/library/mts_006435.pdf [Accessed 2 Aug. 2017]

MTS Flat-Trac LTR. (2005). MTS Flat-Trac LTR Tire Test System. [pdf]. Eden Prairie, MN: MTS Systems Corporation. Available at:

https://www.mts.com/cs/groups/public/documents/library/dev_002224.pdf [Accessed 2 Aug. 2017]

MTS Flat-Trac Overview. (2005). Flat-Trac Tire Test Systems. [pdf]. Eden Prairie, MN: MTS Systems Corporation. Available at: https://www.mts.com/cs/groups/public/documents/library/dev_002227.pdf [Accessed 2 Aug. 2017]

MTS Flat-Trac SS. (2005). MTS Flat-Trac SS Tire Test System. [pdf]. Eden Prairie, MN: MTS Systems Corporation. Available at: https://www.mts.com/cs/groups/public/documents/library/dev_003377.pdf [Accessed 2 Aug. 2017]

MTS Measurement System. (2014). MTS Tire Rolling Resistance Measurement System, Supporting the Development of Tomorrow's Fuel-Efficient Tires. [pdf]. Eden Prairie, MN: MTS Systems Corporation.

M'gineering History of Tire Characterizing. (2016). History of Characterizing Tire Forces and Moments Applied to a Vehicle, by Marion Pottinger. [pdf]. Akron OH: M'gineering

Nelder, J. A. and Mead, R. (1965). A simplex method for function minimization. The Computing Journal, (7:4), pp. 308–313.

van Oosten, J. J. M., Augustin, M., Gnadler, R. and Unrau, H. J. (1998). Tire measurements, forces and moments. Workpackage 2: analysis of parameters influencing tyre test results. Darmstädter Reifencolloquium, Darmstad, Germany. ID: 362448.

Van Oosten, J. J. M. and Bakker, E. (1993). Determination of the Magic tyre Model Parameters. Vehicle System Dynamics: International Journal of Vehicle Mechanics and Mobility, 21, pp.19-29.

van Oosten, J. J. M., Savi, C., Augustin, M., Bouhet, O., Sommer, J and Colinot, J. P. (1999). Tire measurements forces and moments a new standard for steady state cornering tyre testing. EAEC congress on vehicle systems technology for the next century, Barcelona, Spain. paper STA99C209.

van Oosten, J. J. M., Unrau, H. J., Riedel, A. and Bakker, E. (1999). Standardization in Tire Modeling and Tire Testing TYDEX Workgroup, TIME Project. Tire Science and Technology, Vol. 27, No. 3. pp.188-202.

OptimumTire. (2017). OptimumG OptimumTire. [online] Available at: http://www.optimumg.com/software/optimumtire/ [Accessed 3 Aug. 2017].

Ortiz, A., Cabrera, J. A., Guerra, A. L. and Simon, A. (2006). An easy procedure to determine Magic Formula parameters: a comparative study between the starting value optimization technique and the IMMa optimization algorithm. Vehicle System Dynamics: International Journal of Vehicle Mechanics and Mobility, 44:9, pp.689-718

Pacejka, H. B. (1995). The role of tyre dynamic properties. The Netherlands: Seminar on smart vehicles. pp.55–68.

Pacejka, H. B. (2006). Tyre and vehicle dynamics. 2nd edition. Oxford: Butterworth–Heinemann.

Pacejka, H. B. and Bakker, E. (1992). The magic formula tyre model. Vehicle System Dynamics: International Journal of Vehicle Mechanics and Mobility, 21:1, pp.1-18.

Pacejka, H. B. and Besselink, I. J. M. (1997). Magic formula tyre model with transient properties. Vehicle System Dynamics: International Journal of Vehicle Mechanics and Mobility, 27. pp.145–155.

Pacejka, H. B. and Sharp, R. S. (1991). Shear force generation by pneumatic tyres in steady state conditions: a review of modelling aspects. Vehicle System Dynamics: International Journal of Vehicle Mechanics and Mobility, 20, pp.121–176.

Palkovics, L. and El-Gindy, M. (1993). Neural Network Representation of Tyre Characteristics: The Neuro-Tyre. International Journal of Vehicle Design. (14:5-6), pp. 563–591.

Phelps, R. L., Pelz, W., Pottinger, M. G. and Marshall, K. D. (1976). The Mathematical Characteristics of Steady State, Low Slip Angle Force and Moment Data. SAE Technical Paper 760031.

Pottinger, M., (1992). The Flat-Trac IIâ Machine, the State-of-the-Art in Tire Force and Moment Measurements. Tire Science and Technology, TSTCA, Vol. 20, No. 3. pp.132-153.

Pottinger, M., Marshall, K., and Arnold, G. (1976). Effects of Test Speed and Surface Curvature on Cornering Properties of Tires. SAE760029, SAE Transactions, Vol. 84, No. 6.

Rajapakshe, M. P., Gunaratne, M. and Kaw, A. K. (2010). Evaluation of LuGre Tire Friction Model with Measured Data on Multiple Pavement Surfaces. Tire Science and Technology, TSTCA, Vol. 38, No. 3. pp.213-227.

Rill, G. (2006). First Order Tire Dynamics. III European Conference on Computational Mechanics Solids, Structures and Coupled Problems in Engineering. Lisbon, Portugal.

Rill, G. (2013). TMeasy – The Handling Tire Model for all Driving Situations. Brazil: Proceedings of the XV International Symposium on Dynamic Problems of Mechanics.

RMOD-K 7. (2016). Measurement and Parameterdetermination of the Modeling System RMOD-K. [pdf]. Brandenburg , Germany: TH Brandenburg Faculity of Engineering.

Sharp, R. S. and Bettella, M. (2003). Tyre Shear Force and Moment Descriptions by Normalisation of Parameters and the ‘‘Magic Formula’’. Vehicle System Dynamics: International Journal of Vehicle Mechanics and Mobility, 39:1, pp.27-56.

Simulia SimPack. (2017). Simulia SimPack Multi-Body Simulation Software, Automotive Modules. [online] Available at: http://www.simpack.com/mbs-software-product-automotive.html [Accessed 3 Aug. 2017].

Smith, G. (2014) Advanced tire CAE. Tire Technology International 2014 Annual Showcase, pp.48.

Smith, G. (2016). Column: Gregory Smith on Tire Friction. Tire Technology International, July. pp64

Smith, G. and Blundell, M. (2016). A new efficient free-rolling tyre-testing procedure for the parameterisation of vehicle dynamics tyre models. Proceedings of the Institution of Mechanical Engineers, Part D: Journal of Automobile Engineering, Vol 231, Issue 10. pp.1435–1448.

Smithers Rapra. (2017). Smithers Rapra - Tire Industry Partnership to Provide Enhanced Force and Moment Testing at Ravenna, Ohio Laboratory. [online]. Available at: http://www.smithersrapra.com/news/2017/april/tire-industry-partnership-to-provide-enhanced-forc [Accessed 2 Aug. 2017]

SoVaMotion. (2014). SoVaMotion - Tire Testing Services. [online]. Available at: http://sovamotion.com/flat-belt.html [Accessed 2 Aug. 2017]

Storn, R. and Price, K. (1997). Differential Evolution – A Simple and Efficient Heuristic for Global Optimization over Continuous Spaces. Journal of Global Optimization, (11). pp.341-359.

Tass International, (2017). Tyre Testing Dedicated on-road test laboratory. [online] Available at: https://www.tassinternational.com/tyre-testing [Accessed 31 July. 2017].

TNO Equation Manual. (2010). MF-Tyre/MF-Swift 6.1.2 Equation Manual. [pdf] The Netherlands: TNO Automotive.

TNO Measurement Requirements. (2010). Measurement Requirements and TYDEX file generation for MF-Tyre/MF-Swift 6.1. [pdf] The Netherlands: TNO Automotive.

TRA. (2017). The Tire and Rim Association, Inc. [online] Available at: http://www.us-tra.org [Accessed 20 Dec. 2017].

Trevorrow, N. and Gearing, R. (2015). MuRiTyre: real time simulation of distributed contact patch forces, moments and temperatures. Guildford, United Kingdom: Proceedings of the 4th International Tyre Colloquium: tyre models for vehicle dynamics analysis. pp.41-49.

VI-Grade. (2017). VI-Grade Bridging the gap between testing and simulation. [online] Available at: https://www.vi-grade.com/ [Accessed 3 Aug. 2017].

Wei, T. and Dorfi, H. (2014). Tire Transient Lateral Force Generation: Characterization and Contribution to Vehicle Handling Performance. Tire Schience and Technology, (42,4). pp 263-289.

Winkler, C., (2017). UMTRI [email].

Yang, A. S. and Deb, S. (2009). Cuckoo search via Lévy flights. Proceedings; IEEEWorld Congress on nature & biologically inspired computing. pp. 210–214.